Institute of Veterinary Medicine

Nicolaus Copernicus University

Department of Basic and Clinical Sciences

Doctoral Thesis

Dietary effect of polyunsaturated fatty acids on the porcine liver by analyzing the differential gene expression and weighted gene co-expression network analysis of miRNA data in Polish Landrace and Polish Landrace x Duroc pigs

Wpływ wielonienasyconych kwasów tłuszczowych w diecie na wątrobę świń poprzez analizę zróżnicowanej ekspresji genów oraz analizę sieci ważonej koekspresji genów danych miRNA u świń rasy polskiej białej zwisłouchej i krzyżówki polskiej białej zwisłouchej z duroc

Mateusz Sachajko

Ph.D. thesis under the supervision of:
Prof. dr hab. n. wet. Chandra S. Pareek
Department of Basic and Clinical Sciences
Institute of Veterinary Medicine
Nicolaus Copernicus University, Poland

Assistant supervision of:
dr hab. Anna Sławińska, prof. UMK
Department of Basic and Clinical Sciences
Institute of veterinary medicine
Nicolaus Copernicus University

Toruń, 2023

Acknowledgments

The author would like to express his gratitude to prof. Haja Kadarmideen, TU, Denmark, prof. dr hab. Mariusz Pierzchała, co-supervisor, dr hab. Anna Slawinska, prof. UMK, and supervisor prof. dr hab. Chandra Shekhar Pareek for their critical reading and insights.

Table of content

Abstract (ENG)

Thesis title: Dietary effect of polyunsaturated fatty acids on the porcine liver by analyzing the differential gene expression and weighted gene co-expression network analysis of miRNA data in Polish Landrace and Polish Landrace x Duroc pigs.

Background: The objective of the research is to investigate how omega-6 and omega-3 polyunsaturated fatty acids (PUFA) affect liver transcriptome activity in pigs. The study aims to analyze the alterations in hepatic gene expression, co-expression and metabolic pathways linked to pig genotype. Although the impact of these fatty acids on potential health outcomes has been settled, their action on the whole transcriptome level remains unclear. The researchers plan to vary the pigs' diet with different amounts of omega-6 and omega-3 PUFAs and then use RNA sequencing to examine changes in liver gene expression. By exploring how dietary omega-6 and omega-3 PUFAs affect the transcriptome and gene co-expression in pigs, the study could provide valuable information for understanding the health effects of these fatty acids and optimizing pig nutrition and production.

Methods: The NGS based small RNA sequencing (miRNA-Seq) of porcine liver transcriptome was performed on 6 Polish Landrace (PL) pigs, and 6 PL x Duroc (PLxDuroc) pigs using MiSeq Illumina platform (ICNT, UMK, Torun). The miRNA-Seq reads were mapped onto the miRBase v.22 using miRDeep2 was used. MiRDeep. Six differentially expressed miRNA (DE-miRNA) genes comparisons analysis between diets (n=2) and breeds (n=2) were performed to identify the upregulated and downregulated DE-miRNA genes of porcine liver. The co-expression analysis of porcine hepatic miRNA was performed using weighted gene co-expression network analysis (WGCNA) R/Bioconductor R package. The biological interactions between gene networks and metabolic pathways of DE miRNA genes were performed using ClueGO v 2.2.0 Cytoscape v. 3.1.0 software, and the GO-BiologicalProcess-EBI-UniProt-GOA database for human genes.

Results: Using MiSeq illumina platform, the NGS experiment generated 12 fastq files of porcine liver miRNA reads, ranging from lowest number of 135842 and highest number of 4018483 sequence reads. The lowest and highest GC content were 46% and 49%. Mapping results revealed the matrix of 535 miRNAs reads for 12 samples which were later utilized in DEGs and WGCNA analysis of porcine liver transcriptome representing Polish Landrace (PL) purebred and Polish Landrace x Duroc (PLxDuroc) crossbred pigs. The miRNA DEGs experiment was divided into four groups representing, control diet and PUFAs diets in PL pigs, and control diet and PUFAs diets in PLxDoruc pigs. A total of six miRNA DEGs comparisons were performed. In first comparison between control and PUFAs diets of PLxDuroc pigs, 1256 DE-miRNA transcript were identified that commonly sheared in both control vs PUFAs diets of PLxDuroc pigs. By comparing the control vs PUFAs diets in PLxDuroc pigs, 13 significant ($p < 0.05$), 5 upregulated ($log2FC > 2$) and 10 downregulated ($log2FC > 5$) DE-MiRNA transcripts were identified. In the Second comparison between control diets of PL and PLxDuroc, 1060 breed-specific DE-miRNA transcript were identified that commonly sheared in control diet of both PL and PLxDuroc pigs. By comparing the control vs PUFAs diets in PLxDuroc pigs, 10 significant ($p < 0.05$), 21 upregulated ($log2FC > 3$) and 31 downregulated ($log2FC > 5$) DE-MiRNA transcripts were identified. In the third comparison between control diet of PLxDuroc pigs and PUFAs diet of PL pigs, 1380 DE-miRNA transcript were identified that commonly sheared in both control and PUFAs diets of PL and PLxDuroc pigs. By comparing the control diet of PLxDuroc vs PUFAs diet in PL pigs, 54 significant ($p < 0.05$), 29 upregulated ($log2FC > 2$) and 64 downregulated ($log2FC > 5$) DE-MiRNA transcripts were identified. In the fourth comparison between control diet of PL pigs and PUFAs diet of PLxDuroc pigs, 696 DE-miRNA transcripts were identified that commonly sheared in both control and PUFAs diets of PL and PLxDuroc pigs. by comparing the control diet of PL pigs vs PUFAs diet in PLxDuroc pigs, 56 significant ($p < 0.05$), 5 upregulated ($log2FC > 2$) and 10 downregulated ($log2FC > 5$) DE-MiRNA transcripts were identified. In the fifth comparison between PUFAs diets of PL and PLxDuroc pigs, 986 DE-miRNA transcript were identified that commonly sheared the PUFAs diets in both PL and PLxDuroc pigs. by comparing the PUFAs diets between PL vs PLxDuroc pigs, 27 significant ($p < 0.05$), 5 upregulated ($log2FC > 2$) and 10 downregulated ($log2FC > 5$) DE-MiRNA transcripts were identified. In the sixth comparison between control vs PUFAs diets of PL pigs, 1019 diet-specific DE-miRNA transcript were identified that commonly sheared in both control vs PUFAs diets of PL pigs. By comparing the control vs PUFAs diets in PL pigs, 34 significant ($p < 0.05$), 29 upregulated ($log2FC > 2$) and 27 downregulated ($log2FC > 5$) DE-MiRNA transcripts were identified.

In WGCNA analysis, a total of 94 miRNAs counts were normalized using the "varinaceStabilizingTransformation" function from DESeq2 library, and soft threshold power $\beta=18$ was established to construct the gene network type of Topological Overlap Matrix (TOM). Basing on the TOM the co-expressed miRNA with the highest interconnection were clustered into the modules which were represented by different colors. In WGCNA analysis, a total of 9 trait-associated modules that are significantly associated with the measured phenotypic traits were identified in PL and PLxDoruc pigs namely, meat color (a*), shoulder

subcutaneous fat thickness, conductivity 24 hours post mortem (PE24), and ashes, respectively. Trait-wise, large set of co-expressed miRNA of porcine liver were identified in these trait-associated significant modules (9, 7 ,2, and 8) affected by PUFAs diets in PL and PLxDoruc pigs. The mapping of fixed target miRNA genes result revealed that identified 44 miRNAs (out of 94 miRNA) had a 6719 statistically significant target genes with the target score >90. The highest number of target genes were found in ssc-miR-30e-5p (520) in magenta module, followed by ssc-miR-30b-5p (518) in pink module, and ssc-miR-30c-5p (518) in yellow module. The lowest number of target genes were found for ssc-miR-126-3p and ssc-miR-423-3p (1 each) in purple and brown modules.

Based on the identified trait-specific modules, the GO/pathway analysis were performed using the GO-BiologicalProcess-EBI-UniProt-GOA database for human genes. ClueGO analysis identified the highest number of GO/pathway specific term associated with miRNAs' target genes in green module (90). The second highest number of GO/pathway specific term were observed for target genes of yellow miRNAs (88). The lowest number of GO/pathway specific term were found for miRNAs' targets from clustered in modules: purple (16), turquoise (14), brown (6), and magenta (4).

Conclusions: Porcine hepatic miRNA gene expression profile database developed during the study will allow further investigation of relations between miRNA expression and porcine phenotypic traits. The study indicated the differences in miRNA expression between the types of diet and breeds. Furthermore, discovered modules in WGCNA show the strong interconnection between co-expressed miRNAs. Hub genes of discovered miRNAs clusters can be considered as predicted miRNA genes associated with PE24, meat color, Shoulder subcutaneous fat thickness, and ashes. Additionally, co-expressed miRNAs indirectly affect other functional pathways by regulation of it's target genes. Discovered target genes for miRNA clusters play significant roles in biological functions such as: i) muscle organ development, ii) different cellular processes and developments, iii) system development, iv) metabolic processes, v) muscle tissue development.

Keywords: fatty acids, PUFA, pig, liver, NGS, RNA-Seq, transcriptome, miRNA, DEG, WGCNA, bioinformatics

Abstract (PL)

Tytuł pracy: Wpływ wielonienasyconych kwasów tłuszczowych w diecie na wątrobę świń poprzez analizę zróżnicowanej ekspresji genów oraz analizę sieci ważonej koekspresji genów danych miRNA u świń rasy polskiej białej zwisłouchej i krzyżówki polskiej białej zwisłouchej z duroc.

Wprowadzenie: Celem pracy było określenie wpływu kwasów tłuszczowych omega-6 i omega-3 na profil transkryptomu w wątrobie świń, oraz charakterystyka interakcji w ekspresji genów w wątrobie, określenie jej zależności od genotypu świń oraz jej wpływu na szlaki metaboliczne. Choć potencjalny zdrowotny wpływ WNKT został ustalony, to ich oddziaływanie na na ekspresje genów na poziomie całego transkryptomu wciąż dostarczyć może niowych cennych informacji, dotyczących indukowanej przez nie regulacji ekspresji genów. Dla potrzeb niniejszych badań wykorzystano świnie zróżnicowane pod względem rasy oraz zastosowano wzbogaconą i zróżnicowaną pod względem ilości i stosunku kwasów tłuszczowych omega-6 i omega-3 paszę. Po uboju na pobranych próbkach wątroby przeprowadzono sekwencjonowanie RNA, które miało na celu ogreślenie globalnych zmian w ekspresji genów. Uzyskane wyniki posłużyły do bioinformatycznego opracowania wpływu diety omega-6 i omega-3 na transkryptom w tym koekspresję genów w wątrobie u świń, które to dostarczyło nowych cennych informacji charakteryzujących potencjalny wpływ wielonienasyconych kwasów tłuszczowych na prawidłowe funkcje wątroby a tym samym stan zdrowia zwierząt, oraz optymalizację żywienia i poprawę efektywności produkcji świń.

Metodyka: Na bazie danych pochodzących z sekwencjonowania micro RNA (miRNA-Seq) z wątroby świń rasy Polish Landrace (PL) (n=6) i Landrace x Duroc (PLxDuroc) (n=6) przeprowadzono analizę sieci ważonej koekspresji genów (WGCNA). Do sekwencjonowania miRNA-Seq wykorzystano platformę MiSeq Illumina (ICNT, UMK, Toruń), zmapowanie odczytów wykonano z wykorzystaniem oprogramowania miRDeep2 i bazy danych miRBase w wersji 22. W ramach analizy zróżnicowanej ekspresji miRNA (DE-miRNA) wykonano 6 porównań, pomiędzy dietami (kontrolna i wzbogacona w PUFA) i rasami (PL i PLxDuroc) identyfikujacymi miRNA o zwiększonej i o zmniejszonej ekspresji w wątrobie świń w zależności od rasy i diety. Następnie za pomocą pakietu R/Bioconductor WGCNA wykonano analizę ważonej koekspresji genów. Natomiast przy użyciu oprogramowania ClueGO v 2.2.0 Cytoscape v.3.1.0 oraz bazy danych GO-BiologicalProcess-EBI-UniProt-GOA dla ludzkich genów, scharakeryzowano interakcje biologiczne między sieciami genów a szlakami metabolicznymi genów miRNA.

Wyniki: W ramach eksperymentu NGS z wykorzystaniem platformy MiSeq illumina wygenerowano 12 plików fastq z sekwencjami miRNA w wątrobie świń. Długości odczytów wynosiły od 135 842 do 401 8483 w sekwencji. Najniższa i najwyższa zawartość GC wynosiła odpowiednio 46% i 49%. Wyniki mapowania ujawniły macierz 535 miRNA dla 12 próbek zmapowanych odczytów, które następnie wykorzystano w analizie DEGs i WGCNA transkryptomu wątroby świń rasy PL i mieszańców PLxDuroc. Badanie zróżnicowanej ekspresji miRNA zostało podzielone na cztery grupy, reprezentujące dietę kontrolną i diety wzbogacone w PUFA u świń PL oraz dietę kontrolną i diety wzbogacone w PUFA u świń PLxDuroc. Wykonano łącznie sześć porównań miRNA DEGs. W pierwszym porównaniu między dietą kontrolną a dietą PUFAs u świń PLxDuroc zidentyfikowano 1256 transkryptów miRNA o zróżnicowanej ekspresji, które były wspólne dla obu grup. Porównując dietę kontrolną i dietę PUFAs u świń PLxDuroc, zidentyfikowano 13 istotnie statystycznych ($p < 0,05$) transkryptów miRNA o zróżnicowanej ekspresji, w tym 5 o zwiększonej ekspresji ($log2FC > 2$) i 10 o obniżonej ($log2FC > 5$). W drugim porównaniu między dietami kontrolnymi PL i PLxDuroc zidentyfikowano 1060 transkryptów miRNA o zróżnicowanej ekspresji, charakterystycznych dla rasy, które były wspólne dla obu grup. Porównując dietę kontrolną i dietę PUFAs u świń PLxDuroc, zidentyfikowano 10 istotnie statystycznych ($p < 0,05$) transkryptów miRNA o zróżnicowanej ekspresji, w tym 21 o wyższej ekspresji ($log2FC > 3$) i 31 o niższej ($log2FC > 5$). W trzecim porównaniu między dietą kontrolną świń PLxDuroc a dietą PUFAs świń PL, zidentyfikowano 1380 transkryptów miRNA o zróżnicowanej ekspresji, które wspólnie występowały zarówno w diecie kontrolnej, jak i w diecie PUFAs dla świń PL i PLxDuroc. Porównując dietę kontrolną świń PLxDuroc z dietą PUFA u świń PL, zidentyfikowano 54 statystycznie istotne transkrypty miRNA o zróżnicowanej ekspresji ($p < 0,05$), 29 o podwyższonej ($log2FC > 2$) i 64 obniżonej ($log2FC > 5$) ekspresji. W czwartym porównaniu między dietą kontrolną świń PL a dietą PUFAs świń PLxDuroc zidentyfikowano 696 transkryptów miRNA o zróżnicowanej ekspresji, które wspólnie występowały zarówno w diecie kontrolnej, jak i w diecie wzbogaconej o PUFA dla świń PL i PLxDuroc. Porównując dietę kontrolną świń PL z dietą wzbogaconą o PUFA u świń PLxDuroc, zidentyfikowano 56 statystycznie istotnych transkryptów miRNA o zróżnicowanej ekspresji ($p < 0,05$), 5 o podwyższonej ($log2FC > 2$) i 10 o obniżonej ($log2FC > 5$) ekspresji. W piątym porównaniu między dietami wzbogaconymi w PUFA świń PL i PLxDuroc zidentyfikowano 986 transkryptów miRNA o zróżnicowanej ekspresji, które wspólnie występowały w dietach PUFA zarówno u świń rasy PL i PLxDuroc. Porównując diety wzbogacone w PUFA pomiędzy świniami PL vs PLxDuroc, 27 statystycznie istotnych transkryptów o

zróżnicowanej ekspresji zostało zidentyfikowanych ($p < 0,05$), 5 o podwyższonej ekspresji ($log2FC > 2$) i 10 o obniżonej($log2FC > 5$) ekspresji. W szóstym porównaniu diety kontrolnej z dietą wzbogaconą w PUFA u świń PL, zidentyfikowano 1019 transkryptów miRNA o zróżnicowanej ekspresji, które występowały w diecie kontrolnej i diecie wzbogaconej w PUFA u świń PL. Porównując dietę kontrolną z PUFAs u świń PL, zidentyfikowano 34 statystycznie istotne transkrypty miRNA o zróżnicowanej ekspresji ($p < 0,05$), 29 o podwyższonej ($log2FC > 2$) i 27 o obniżonej ($log2FC > 5$) ekspresji.

W analizie WGCNA, odczyty dla 94 miRNA zostały znormalizowane przy użyciu funkcji „varianceStabilizingTransformation" z biblioteki DESeq2, a zmienna moc progowa została ustalona na poziomie $\beta=18$ w celu skonstruowania sieci genów typu Topological Overlap Matrix (TOM). Na podstawie TOM, miRNA ulegające koekspresji o najwyższych zależnościach, zostały zgrupowane w moduły, które reprezentowane są przez kolory. W analizie WGCNA zidentyfikowano łącznie 9 modułów związanych z cechami, które są istotnie związane z badanymi cechami fenotypowymi. Ponadto, analiza wewnątrz modułowa dla MEM (miRNA w modułach o danym kolorze) zidentyfikowała cztery cechy fenotypowe istotnie zależne od diety PUFAs u świń PL i PLxDuroc: kolor mięsa (a*), grubość tłuszczu podskórnego w łopatce, przewodność 24 godziny post mortem (PE24) i popiół. Z cechami istotnie statystycznie, skorelowana jest inna liczba wykrytych modułów (9, 7, 2, 8). Mapowanie targetów miRNA ujawniło, że zidentyfikowane 44 miRNA (z 94 miRNA) miały 6719 statystycznie targety z wynikiem docelowym >90. Największą liczbę targetów w ssc-miR-30e-5p (520) w module o kolorze magenty, następnie ssc-miR-30b-5p (518) w module o kolorze różowym i ssc-miR-30c-5p (518) w module o kolorze żółtym. Najmniej genów docelowych znaleziono dla ssc-miR-126-3p i ssc-miR-423-3p (po 1) w modułach o kolorach fioletowym i brązowym.

Na podstawie zidentyfikowanych modułów istotnie skorelowanych z cechami fenotypowymi przeprowadzono analizę GO/pathway z wykorzystaniem bazy GO-BiologicalProcess-EBI-UniProt-GOA dla genów ludzkich. Analiza ClueGO zidentyfikowała najwyższą liczbę funkcji GO/szlaków powiązanych z targetami modułów miRNA w module o kolorze zielonym (90). Drugą najwyższą liczbę funkcji GO/szlaków wykryto dla targetów miRNA modułu zółtego. Najniższa liczbę funkcji GO/szlaków powiązanych z targetami, wykryto dla modułów: fioletowego (16), turkusowego (14), brązowego (6) i magenty (4).

Wnioski: Opracowana w trakcie badań baza danych profilu ekspresji genów miRNA wątroby świń może zostać wykorzystana do dalszych badań nad zależnościami pomiędzy ekspresją miRNA a cechami użytkowymi świń. Przeprowadzone badania wskazały na zróżnicowaną ekspresję miRNA pomiędzy typami diety i rasami. Ponadto, moduły/grupy zidentyfikowane w analizie WGCNA wskazują na silne powiązania pomiędzy ekspresją miRNA. miRNA będące węzłami klastrów można uznać za kandydujące geny miRNA związane z PE24, barwą mięsa, grubością podskórnego tłuszczu łopatki i popiołem. Dodatkowo, miRNA ulegające koekspresji wpływają pośrednio na inne szlaki funkcjonalne, poprzez regulację ich targetów. Zidentyfikowane geny docelowe dla klastrów miRNA odgrywają znaczącą rolę w takich funkcjach biologicznych, jak i) rozwój układu mięśniowego, ii) procesy rozwoju komórki, iii) procesy rozwoju organizmu, iv) procesy metaboliczne, v) rozwój tkanki mięśniowej.

Słowa kluczowe: kwasy tłuszczowe, PUFA, świnie, wątroba, sekwencjonowanie nowej generacji, sekwencjonowanie RNA, transkryptom, miRNA, DEG, WGCNA, bioinformatyka

1. Introduction

Lipids are the dietary source of fatty acids (FAs) in supplementary diet experiments in pigs. Lipids play a key role in the cell membrane structure and biological functions, as well as in the transcriptional regulation of physiological processes (**Eshak et al., 2018; Moghadasian and Shahidi, 2017**). Lipids are molecules of hydrophobic nature and are an important source of metabolic energy. They also play an important role in the membrane permeability barrier by acting as a structural matrix **(Elmadfa and Kornsteiner, 2009; Moghadasian and Shahidi, 2017**). Lipids delivered in diets contribute not only to energy supply, cell structure, and gene expression levels, but also play the important role in several physiological processes and biological processes associated with the health benefits in humans (health of meat consumers) and meat production in domestic animals.

Dietary lipids are comprised of the fatty acids (FAs) and cholesterol. The FAs differ in length of the carbon chains, which influences their physicochemical properties. Based on the presence or absence of the double bonds between the carbon molecules, FAs are divided into three main classes: saturated FAs (SFAs: palmitic acid, myristic acid, and lauric acid), monounsaturated FAs (MUFAs: ω-9 oleic acid (OA), and polyunsaturated FAs (PUFAs). As part of the complex lipid molecules, the FAs are the basic structure of lipids such as fats and phospholipids, which are stored in adipose tissue as triacyloglycerides, and are the predominant dietary source of FAs (**Moghadasian and Shahidi, 2017; Petrovic and Arsic, 2016**).

The most common SFAs found in plant and animal tissues are those with a linear chain of 12 to 18 carbons, with palmitic acid (C16:0) being the most abundant and found in most plant oils, fish oil, and in the body fat of some animals. The most common SFAs in the diets are stearic acid (C18:0), myristic acid (C14:0), and lauric acid (C12:0) (**Eshak et al., 2018; Moghadasian and Shahidi, 2017**). In humans, stearic acid is important and related to the cholesterol levels. The studies revealed that the stearic acid contributes to reducing the cholesterol levels in human blood (**Monsma and Ney, 1993**). The feed intake of myristic acid in the human diet improves long-chain n-3 levels, which contributes to the improved cardiovascular system (**Dabadie et al., 2005**). Studies revealed that a small amount of the myristic acid is metabolized by the liver in the form of triglycerides (**Dayrit, 2015**).

The PUFAs have two or more double bonds in their aliphatic chain. They include two important families (essential groups), i.e., the omega-3 (or n-3 or ω-3), and the omega-6 (or n-6 or ω-6) FAs, which have to be obtained through the diet because they cannot be synthetized by the

human enzymes. Among ω-3 FAs, linolenic acid (ALA; 18:3 ω-3) is mostly contained in plants (i.e., flaxseed, canola, soybean, nuts, walnuts, chia seeds, etc.), while eicosapentaenoic acid (EPA; 20:5 ω-3) and docosahexaenoic acid (DHA; 22:6 ω-3) are present mostly in fish, seafood, and marine algae (**Baker et al., 2016; Moghadasian and Shahidi, 2017; Wood et al., 2008 Bork et al., 2020; Caterina, 2011**). Among ω-6 FAs, linoleic acid (LA; 18:2 ω-6) is provided by the seed oils, soybean, nuts, and cereals, while arachidonic acid (ARA; 20:4 ω-6) is found in the poultry meat and eggs **(Al-Khalaifah et al. 2020)**. Land-based food chain is dominated by a higher LA than ALA. These two essential FAs initiate ω-6 and ω-3 series, which have a different impact on the inflammatory response.

Both SFA and PUFAs have been recognized as molecules regulating a variety of functions in the cell, such as serving as a source of energy, being a vital component of the cell membranes, and acting as signaling molecules, which regulate different processes, including gene expression. Despite being essential for maintaining homeostasis in animal organisms, a lack of enzymes responsible for endogenous synthesis of the omega-6 and omega-3 FAs by the mammals necessitates their constant dietary intake. Hence they are referenced to as essential fatty acids (EFAs) **(Simopoulos, 2001; El-Badry et al., 2007)**. The omega-6 linoleic acid (LA) and omega-3 α linolenic acid (ALA) are critical EFAs, since they are exclusively delivered from the diets as their only source. They are at the beginning of conversion pathways for long-chain omega-6 and omega-3 PUFAs as their precursors. Long-chain PUFAs (LC-PUFAs) are supplied most of all with the diets. They can also be metabolized from dietary precursors, LA and ALA, but the efficiency of conversion in mammals is very low.

The importance of adding and enriching products with specific levels of healthier PUFAs diet are highly influenced by consumers. For example, the oils used in the pig diets are palm oil, fish oil, sunflower oil, linseed oil, canola oil **(Souza et al., 2020)**, and soybean oil **(Fanalli et al., 2022)**. The oil blends supplemented in the diets have been tested in experiments aimed to improve performance, composition, and deposition of FAs, as well as carcass characteristics, carcass yield, meat marbling, enrichment of bacon and loin with omega-9 and stearic acid, **(Souza et al., 2020)**. For example, the inclusion of 3% soybean oil or canola oil in pig diets reduced loin shear force and increased oleic acid content in the intramuscular fat **(Almeida et al., 2021)**. Furthermore, the supplementation of the pigs' diets with 1.5 or 3% soybean oil influenced the differential expression of the genes related to inflammation, immune processes, pathways associated with oxidative stress, type 2 diabetes, and metabolic dysfunction in the growing and finishing phases **(Fanalli et al., 2022)**.

The experimental pig breed Landrace is a relatively modern breed and one of the most widely distributed breeds in the world, which has high lean meat content and is known for producing high-quality pork **(Vidal et al.)**, whereas, the experimental pig breed Duroc pig is a typical lean breed which are the predominate Terminal sire used in the world; it excels for meat quality and eating characteristics, such as high percentage of IMF (marbling) and high pH value **(Lonergan et al. 2001)**.

1.1. Dissertation‘s research hypothesis

1. Nutritional properties of the dietary omega-3 and omega-6 PUFAs control hepatic gene expression through a series of physiological, biochemical and metabolic mechanisms.

2. Based on the literature studies, we hypothesized that using pig as an animal model, omega-3 and omega-6 PUFAs supplementary healthy diet with high efficiency of metabolic action can be utilized to identify novel porcine hepatic miRNA gene profile. In this dissertation, pig as a proven animal model for digestive system health study was utilized.

3. Nutrigenomics studies involving comprehensive transcriptome investigations on standard (control) and health-promoting (PUFAs) diets in pig animal model will provide new insights on mammalian gut health, hepatoprotective mechanism, and present novel research findings, such as identification of the potential candidate genes (CGs) for animal production and human health, and the metabolic pathways based on the gene networks interactions.

4. Contrast between breeds used in the experiment will generate the differentially expressed miRNA gene profiles in porcine liver and advanced bioinformatics analysis of miRNA data will help to elucidate factors determining the potential putative miRNA genes in context to health and animal production.

1.2. Review of the literature related to the doctoral dissertation

1.2.1. PUFA diets and multiple tissue (internal vital organs) gene expression

The PUFAs are considered essential for both humans and animals as they cannot be made either de novo or from other FAs endogenously. The dietary effects of PUFAs were investigated in several different internal organs such as liver, muscle, spleen, heart, etc. **(Ito et al. 2013, Frayn et al. 2006, Wang et al. 2013, Panov et al. 2014)**. Studies show that for FA metabolism, there is interdependency between liver-intestine-heart (Ito et al. 2013), liver-adipose-**muscle (Frayn et al. 2006)**, liver-adipose-testes **(Wang et al. 2013)** and across the CNS **(Panov et al. 2014)**.

Studies suggested the presence of a metabolic network whose activity is shaped by several factors such as dietary intake. Thus, the dietary effects of supplementing PUFAs not only imply that several organs can be affected simultaneously but also that there are general, systemic effects dependent on the inter-organ traffic. Furthermore, the questions of which PUFAs diets have what effect(s) and where, whether unintended or undesired effects can be avoided, and how rapidly and specifically the desired effect can be achieved on the target organ remain unresolved. In literatures, several studies dealt with the dietary effects of supplementary diets including n-3 and n-6 polyunsaturated FA (PUFA) on the porcine liver and other metabolic organs were investigated.

1.2.2. Pig as animal model in supplementary diet oriented studies

In general, supplementary diet-oriented studies were carried out in Pig, chicken and laboratory rodents. The domestic pigs (*Sus scrofa*) are considered animal models for nutrigenomics and metabolomics researches **(Doreau and Chilliard, 1997; Lunney, 2007; Pan et al., 2021)**, because it shares anatomical, morphological, physiological and metabolic similarities with humans **(Bassols et al., 2014; Pan et al., 2021)**. Moreover, the domestic pigs also have high homology and chromosome structure with the human genome compared to other animal species **(Pan et al., 2021; Schook et al., 2015).**

1.2.3. Role of porcine metabolic organ liver in health and pork production

The pig (*Sus scrofa*) is an important agricultural animal, utilized as a cost-effective source of meat (pork) for human consumption (**Lo et al. 1992, Tummaruk et al. 2001**). Because of their anatomical, physiological, and genetic similarities to humans, and their high level of fat deposition, pigs represent a suitable animal model for use in the study of human health obesity and energy metabolism **(Houpt et al. 1979)** and animal production. The investigated pig breed, Landrace is a typical lean-type western breed, which has been intensively selected to increase lean meat production and reduce fat deposition **(Rauw et al. 1998)**, as well as supplementary diet-oriented studies. In most of the supplement diet studies, the effects of healthy diets in context to animal health as well as, to improve meat quality and metabolism in pigs are always an immediate area of research focus. The liver is the largest digestive gland and most important metabolic organ, which plays key roles in the regulation of appetite, body weight, and several metabolic processes **(Fam et al. 2012)**. In pigs, the de novo synthesis of PUFAs and cholesterol, and fatty acid oxidation mainly occur in the liver **(Duran-Montge et al. 2009, Munoz et al.**

2013, Burgess et al. 2011). Hence, the liver is suitable tissue to study the dietary effect of PUFA healthy diets to understand the molecular mechanisms of fat metabolism in pigs.

In this dissertation, key metabolic organ Liver is targeted to study microRNA (miRNA) profiling of porcine liver to understand this metabolic mechanism and miRNA gene regulations **(Nakanishi et al. 2009, Esau et al. 2006, Li et al. 2011).** miRNAs are important regulators in gene expression which play key roles in biological processes such as cell proliferation and differentiation **(McKenna et al. 2010)**, and pathogenesis and disease **prevention (Meng et al. 2014)**. Several studies showed the regulation of miR-122 has been associated with lipid metabolism and liver diseases **(Christine et al. 2006, Sharda and Kalpana, 2015)**. The study showed that the Mir-224-5p directly targets early growth response 2 (EGR2) and acyl-CoA synthetase long-chain family member (ACSL4), which is a novel negative regulator of adipocyte differentiation through post-transcription regulation of EGR2 during early adipogenesis and regulates fatty acid metabolism at terminal differentiation through ACSL4 **(Peng et al. 2013)**. In another study, the MiR-130 and miR-27 suppress adipogenesis by inhibiting peroxisome proliferator-activated receptor γ (PPARγ) expression **(Eun Kyung et al. 2011, Qun et al. 2009).**

1.2.4. HT-NGS technologies and miRNA-Seq

High-throughput (HT) technology such as next-generation genome sequencing (NGS) **(Pareek et al. 2011)** of transcriptome (mRNA-Seq, miRNA-seq) is presently an efficient suitable method in order to identify diet-induced changes in the transcriptome of a biological tissue **(Szostak et al. 2016)**. In recent year, several studies have investigated the effects of plant-derived bioactive compounds, polyphenols, synthetic antioxidants etc. on gene expression in swine and other model organism, such as chicken and laboratory animals **(Azorín-Ortuño et al. 2011, Fiesel et al. 2014, Zhang et al. 2015, Gessner et al. 2017, Liu et al. 2016).** It is worth noting that healthy diet of PUFAs can have a positive role in human and animal metabolism showing a positive effect against health **(Oh et al. 2010, De Groote et al. 2012, Hussain et al.2016, Kim et al. 2016)**, and in pig production (growth and performance trait). However, most of the diet induced studies have been investigated mainly in rodents and only scarcely in farm animals **(Fiesel et al. 2014, Lipinski et al. 2017, Szostak et al. 2016, Szostak, 2020)**. In pigs, the few studies reported in literature evidenced that diet induced studies may influence the expression of genes involved in lipid metabolism, inflammation and extracellular matrix remodeling **(Azorín-Ortuño et al. 2011, Fiesel et al. 2014, Gessner et al. 2017)**.

1.2.5. Importance of PUFAs diet in context to lipid metabolism in liver

Several studies based on the diet induced changes to modify the fatty acid profile of porcine liver and other tissues by enhancing PUFAs contents in daily feed intake. Most of the studies on PUFAs supplemented pig diets (viz., linseed, rapeseed, sea buckthorn, pomace cakes/oils/meals) resulted in an increase in n-3 PUFA content and a decrease in the n-6/n-3 fatty acid ratio in intramuscular fat **(Juarez et al. 2010, Nurnberg et al. 2015, Skugor et al. 2019, Tretola et al. 2019)**. However, in contrast, sunflower seed/oil/meal supplemented diets revealed an increase in n-6 PUFA content in pig muscle tissues **(Realini et al. 2010).** In daily food intake, the proportion of n-6/n-3 polyunsaturated fatty acid (PUFA) plays an important role in regulating lipid metabolism. PUFAs, especially the n-3 and n-6 series PUFAs, play a major role in the body's lipid metabolism, gene expression regulation, and fatty acid composition of animal products **(Yu 2012, Gao et al. 2013)**. Because n-6 and n-3 series PUFAs cannot be converted into each other and have to be taken in through food, the balancing of the n-6/n-3 PUFA ratio has attracted much attention in improving human/animal health by controlling inflammation and metabolic diseases **(Sobol et al. 2015, Caiyan et al. 2019, Michelle et al. 2020, Yue et al. 2021).** The previous studies showed that n-3 and n-6 PUFA in diets regulate the lipid deposition and oxidation in human and animals, thereby affecting the composition of fatty acids in **tissues (Hill et al. 1993, Couet et al. 1997, Newman et al. 2002, Ebrahimi et al. 2018)**. Several investigations into gene expression as it relates to lipid metabolism were conducted in swine, chickens, and geese, among other animals **(Bee et al. 2001, Corino et al. 2005, Schmid et al. 2006, Jiang et al. 2010)**. In recent study, supplementary diet with n-3 PUFA in pig is utilized as a strategy to obtain healthier meat products containing more unsaturated FAs and a lower n-6/n-3 ratio, in view of the general concern on the high consumption of saturated FAs from red meat, which may increase the risk of disease **(WHO, 2013)**. Moreover, several studies showed that supplementing farm animal diets with functional ingredients such as antioxidants can improve the nutritional quality of meat products by reducing lipid oxidation **(Wood et al. 2004, Lahucky et al. 2005, Niculita et al. 2007, Kawecka et al. 2013, Morel et al. 2013, Pieszka et al. 2017)**, however, comprehensive knowledge of the dietary effects of these supplements at the molecular level is poorly known **(Oczkowicz et al. 2016).**

1.2.6. Micro-RNAs

MicroRNAs (miRNAs) are short non-coding RNAs about 19 to 25 nt in length (~22 nucleotides) which play important roles in post-transcriptional regulation by mRNA cleavage and/or translational repression or in another word, regulate gene expression at the post-transcriptional level via translational inhibition or mRNA degradation **(Ambros 2004, Carrington et al. 2003, Bartel 2004)**; The emerging evidence has demonstrate that miRNAs play a direct critical role in liver and indirect role in skeletal muscle biology, however, little is known about the difference in miRNAs expression profiles in porcine liver **(Ambros 2004).**

The miRNAs are involved in almost every biological process, including cell growth and differentiation **(McKenna et al. 2010)**, pathogenesis and disease prevention **(Lund 2010)**. In mammals, differentiation of miRNA expression profiles has been well characterized **(Shivdasani et al. 2006)** to delineate the miRNA transcriptomes of different tissues **(McKenna et al. 2010, McDaneld et al. 2009, Xie et al. 2011)**. In pigs, miRNAs expression profiling studies have been reported to play a pivotal part in regulating the liver and skeletal muscle and adipose tissues development **(Shen et al. 2022, Hu et al. 2022, Herrera et al. 2022)**. In past studies, at least 24,521 miRNAs have been identified in 206 species, including viruses, plants, and animals **(Kozomara et al. 2014)**. However, the biological functions and precise regulatory mechanisms of most miRNAs remain unclear. In recent studies, the miRNA expression profiling was used to investigate the correlation between miRNA expression patterns and target miRNA, and to identify potential interactions between miRNAs and mRNAs **(Huang et al. 2007, Tang et al. 2015, Li et al. 2012).**

In pigs, miRNAs have been reported to play important roles in the regulation of fat deposition and energy metabolism. For example, identified MiR-181a was shown to accelerate the accumulation of lipid droplets and increase the amount of triglycerides by binding to its target, tumor necrosis factor-α (TNF-α) **(Li et al. 2013)**, whereas, MiR-302a was found to be a negative regulator of adipocyte differentiation via interaction with the 3′-UTR of peroxisome proliferator activated receptor gamma (PPARγ) mRNA **(Wang et al. 2011).**

The majority of diet induced studies in domestic animals have investigated the effects of dietary factors on the mean expression of messenger RNAs (mRNAs) **(Szostak et al. 2016, Benitez et al. 2017),** whereas the potential consequences of nutrition on the expression profiles of microRNAs (miRNAs) and long intergenic non-coding RNAs (lincRNAs) have not been

explored in depth and/or have not been fully elucidated yet **(Ayuso et al. 2015, Jia et al. 2016, Munoz et al. 2018).**

In recent years, there has been an increased interest in the use of different sources of lipids and their fatty acid profile in animal production and human health, because of the important role of this macromolecule on animals' production efficiency and animal health, which is directly related to human health. In this dissertation, we investigated the main role of dietary fatty acids PUFAs on animal and human health using miRNA-seq HT-NGS sequencing. Our main goal of this dissertation was to reflect on the role of dietary PUFAs as a functional component present in foods of animal and plant origin. The present dissertation was carried out to identify the putative microRNA genes of porcine liver to understand the biological processes that PUFAs can modulate and affect health and animal production. In this dissertation, First, analysis of differentially expressed of MicroRNA in porcine liver was performed. In second analysis, a co-expression network analysis approach to elucidate potential regulatory interactions between expressed miRNAs genes as well as to investigate the relationship between gene co-expression modules and phenotypic records related to meat quality and fatty acid composition traits was investigated.

2. Dissertations' research objective and goals

Main aim of the present dissertation was to investigate the effect of dietary omega-6 and omega-3 PUFAs on porcine microRNA gene expression in liver transcriptome, and to identify the physiological and molecular processes associated with differentially expressed (DE) microRNA genes (upregulated and downregulated) and co-expression network (WGCNA) at whole hepatic transcriptomic level in Polish Landrace purebred pigs (PL) as well as PL x Duroc crossbred pigs (PLxDuroc). The genome-wide microRNA expression in the porcine liver was assessed using the miRNA-seq approach of the NGS method. The porcine hepatic transcriptomes changed by omega-6 and omega-3 PUFAs dietary supplements feeding were compared to outcomes of standard diets.

In this dissertation, the DEGs and WGCNA analysis of porcine hepatic microRNA-seq data were carried out to achieve the following research objective tasks:

- To generate the hepatic MicroRNA gene expression profile FASTq data set of the PL purebred and the PLxDuroc crossbred (submission: to NCBI resource database, after the PhD dissertation).
- To align and map the miRNA-Seq reads of hepatic gene expression data of PL purebred and the PL x Duroc crossbred to the *Sus scrofa* reference genome.

  Analysis of DEGs of porcine MicroRNA: by Six miRNA-DEGs comparisons
- To identify the differentially expressed microRNA gene-transcripts (miRNA DEGs-transcripts) within PL purebred by comparing the standard (control) diet versus supplementary diet enriched with omega-6 and omega-3 fatty acids (PUFAs) on the liver transcriptome.
- To identify the miRNA DEGs-transcripts within PLxDuroc crossbred by comparing the standard (control) diet versus supplementary diet enriched with omega-6 and omega-3 fatty acids (PUFAs) on the liver transcriptome.
- To identify the miRNA DEGs-transcripts in pigs fed with standard (control) diet by comparing between the PL purebred versus PLxDuroc crossbred liver transcriptome.
- To identify the miRNA DEGs-transcripts in pigs fed with omega-6 and omega-3 fatty acids (PUFAs) supplementary diet by comparing between the PL purebred versus PLxDuroc crossbred liver transcriptome.

  miRNA WGCNA analysis:
- To identify co-expressed miRNAs

- To find correlation between co-expressed miRNAs and phenotypic traits
- To identify the miRNA expression profile and the targeted hub genes in trait-specific detected modules affected by PUFAs diets in PL and PLxDuroc pigs.
- To identify the trait associated miRNA genes of significance (GS) affected by PUFAs diets in PL and PLxDuroc pigs.
- To identify hepatic miRNA target genes expression networks and metabolic pathways in trait-specific modules affected by PUFAs diets in PL and PLxDuroc pigs.

3. Materials and methods

3.1. Animals

In this dissertation, 12 pigs representing Polish Landrace (PL) purebred (n=6), and PL x Duroc crossbred (n=6) were investigated in the NGS-based miRNA experiment. However, the feeding experiment was carried out previously by Szostak et al. (2016), and the PhD dissertation of Szostak, A. (2020). In this dissertation, we did not perform the feeding experiment, but we utilized the feeding experiment of Szostak et al. (2016), and Szostak (2020), to categorized the two experimental healthy and control dietary group of PUFAs in both PL and PLxDuroc pigs. A detailed description of feeding experiment is presented in Figure 1 **(Szostak et al. 2016, Szostak, 2020)**.

3.2. Feeding experiment pertaining to fatty acid profiling of porcine liver of previous study

The feeding experiment pertaining to fatty acid profiling of porcine liver was carried out previously and were according to previous studies of Szostak et al. 2016, and Szostak, 2020. In this dissertation, the feeding experimental data of purebred PL (n=6) and PLxDuroc (n=6) crossbreed female pigs were utilized as investigated in previous study of Szostak et al. (2016), Szostak, (2020) to investigate the effect of omega-6 and omega-3 PUFAs supplementation on the porcine hepatic fatty acids miRNA profile. The laboratory procedures of fatty acid profiling of porcine liver including lipid extraction, Gas chromatography and statistical analysis on fatty acids phenotypic data, were also according to the previous studies of Szostak et al. 2016, and Szostak, (2020). In this dissertation, the experimental design of the feeding experiment pertaining to fatty acid profiling of porcine liver according to previous study of Szostak et al. 2016, Szostak, (2020) is illustrated in Figure 1.

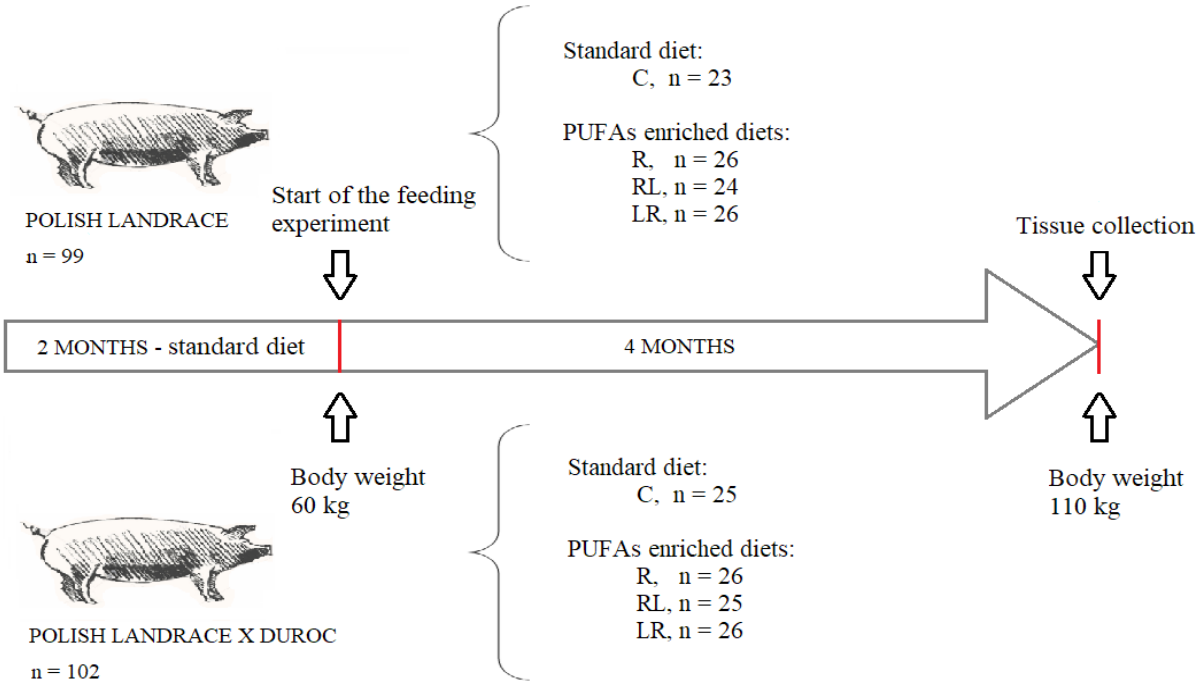

Figure 1. The scheme of the feeding experiment. C – control diet; R – standard diet plus 2% of rapeseed oil; RL – standard diet plus 2% of rapeseed oil + 1% of linseed oil; LR – standard diet plus 1% of rapeseed oil + 2% of linseed oil. (Szostak et al. 2016, Szostak, 2020)

3.3. Experimental design of NGS-based miRNA-Seq experiment

The NGS-based miRNA-Seq experiment was carried out to investigate the porcine liver microRNA.

- Two major bioinformatics analysis were conducted in the NGS experiment.
    - DEGs experiment to investigate the differentially expressed (DE) porcine liver microRNA in PL and PLxDuroc pigs.
    - WGCNA experiment to investigate the co-expression of porcine liver microRNA in PL and PLxDuroc pigs.

3.3.1. Study design

In the NGS based miRNA-seq experiment, a MiSeq Illumina NGS platform was utilized to sequence the microRNA of porcine liver transcriptome (miRNA-Seq) in purebred PL (n=6) and crossbred PLxDuroc (n=6) pigs.

Based on the previous study **(Szostak et al. 2016, Szostak, 2020)**, we categorized two dietary groups (Fig. 1), standard (control) diet, and PUFAs-enriched diet to carried out the NGS-based miRNA-seq experiment. According to Szostak studies, the PUFAs-enriched dietary group,

which effectively affected omega-6/omega-3 ratio in the liver of both pig breeds was classified as PUFAs-enriched diet (LR, referred further as PUFAs-enriched diet) was enriched both with LA and ALA including 660 mg of LA in 100 g of fodder and 64 mg ALA in 100 g of fodder, whereas the control diet contained 268 mg of LA and 25 mg of ALA in 100 g of fodder.

Both control and PUFAs-enriched diets were isoenergetic, with ME=12.86 MJ/kg and ME=13.51 MJ/kg of dry matter, respectively, and isoproteic with crude protein percentages rate 15.66% and 15.65%, appropriately. Total fat content was 1.78% for the control diet and 4.72% for the PUFAs-enriched diet. The threshold value of < 7 for low and > 7 for high omega-6/omega-3 fatty acids ratio was used in this study. In this NGS based miRNA-Seq experiment, the comparison of miRNA gene expression profiles (DEGs) and WGCNA analysis were performed for the control versus PUFAs-enriched dietary groups for each breed. The selection of liver samples for NGS (n=12) was based on fatty acid profiles as described above in order to compare hepatic transcriptomes characterized by low (control groups) with high (PUFAs-enriched diet groups) omega-6/omega-3 fatty acids ratio in both purebred and crossbred pigs. The number of liver samples used in the NGS experiment was 3 per diet group for PL purebred and 3 per diet group for PLxDuroc crossbred using MiSeq Illumina platform.

3.3.2. Laboratory procedures of NGS based miRNA-Seq experiment for PL purebred and PLxDuroc crossbred pigs using the MiSeq Illumina platform

The laboratory procedures of NGS based miRNA sequencing experiments for both purebred and crossbred pig liver transcriptome are described in the following sub-sections, as below.

3.3.2.1. RNA Extraction

The total RNA was extracted from 20 mg of liver samples (n=12) of PL purebred and PLxDuroc crossbred pigs using RNeasy Lipid Tissue Mini Kit (Qiagen, Hilden, Germany) following the manufacturer's instructions. The concentration and purity of RNA were measured using NanoDrop spectrophotometer (Thermo Scientific, USA). RNA integrity number (RIN) was assessed by Bioanalyzer 2100 and RNA 6000 Nano kit (Agilent Technologies, Inc., Santa Clara, CA, USA). The high-quality extracts (RIN≥7) were used for miRNA libraries preparation.

3.3.2.2. miRNA libraries preparation

The construction of cDNA libraries was performed using Illumina TruSeq miRNA Sample Prep Kit v2 (Illumina, San Diego CA, USA).

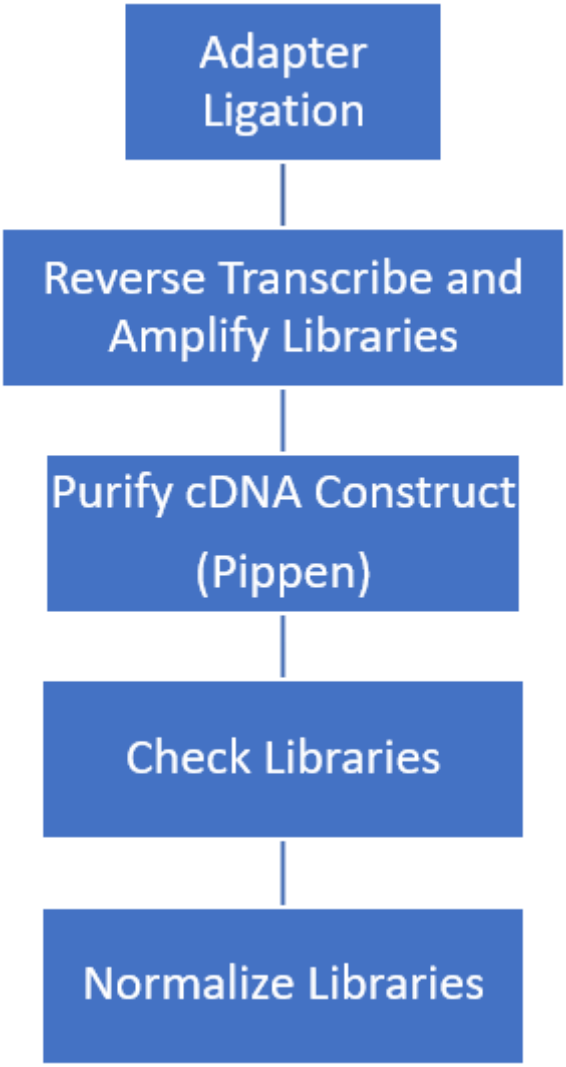

Figure 2. Workflow (Illumina TruSeq miRNA Sample Prep Kit v2)

3.3.2.3. Adapter Ligation

The construction of cDNA libraries was started with 1ug of Total RNA to initiate the illumina library preparation protocol using ligation buffer (HML), RNA 3' adapter, RNA 5' adapter, stop solution and ultra pure water.

3.3.2.4. 3' Adapter Ligation

Adapter ligation reaction was performed using by incubating the RNA 3' Adapter (RA3), total RNA and nuclease free H2O at 70˚C in a thermal cycler, followed by the ligation mix reaction using ligation Buffer (HML), RNase Inhibitor and T4 RNA Ligase 2 deletion mutant. After that the samples were transferred to thermal cycler and incubated at 28˚C for 1 hr. While in the thermal cycler, 1ul of Stop Solution was added to each sample, then incubation continued for 15 min. at 28C. After that, samples were transferred to ice.

3.3.2.5. 5’ Adapter Ligation

Before starting this step, thermal cycler was pre-warmed to 70˚C by initiating cycler profile, followed by Aliquoting (1.1 x N µl) of the RNA 5’ Adapter (RA5) into a 200ul nuclease-free tube. The adapter was incubated in thermal cycler at 70˚C for 2.5 min. On ice, 10mM ATP was added to the aliquoted RNA 5’ Adapter tube and mixed. After that T4 RNA Ligase was added to the aliquoted RNA 5’ Adapter mix and mixed. Later 3ul of 5’ Adapter mix were transferred to the 3’ Adapter reaction for a total of 14ul and mixed on ice. 5’ Adapter reaction was incubated for 1 hour at 28˚C.

3.3.2.6. Reverse Transcription and Amplification

This step was started by removing the Illumina consumables and thaw on ice. 25mM dNTP Mix was diluted by mixing with ultra pure H_2O in 1:1 ratio. 1ul of solution were used per sample. Master mix of RT was prepared by mixing 6ul of 5’ & 3’ adapter ligated RNA with 1ul of RNA RT Primer. Later the samples were incubated at 70˚C for 2.5 min. When finished the were immediately placed on ice. To each sample 5.5ul of the RT Master mix were added for a total volume of 12.5ul and for 1 hour at 50˚C. Indexing list for all samples based on the RNA PCR Primer Index (RPI X) that were used was prepared. To each RT sample the 2ul of appropriate RPI X were added. Then the PCR Master mix were prepared by mixing 8.5ul of pure H2O, 25ul of PCR Mix (PML) and 2ul of RNA PCR Primer. The solution was placed on ice.

PCR Master Mix was added to each RT sample and placed on ice. Later the samples were moved to the thermal cycler and following program were run to Amplify samples:

- 1 cycle of 98˚C → 30 seconds
- 11 cycles of:
    - 98˚C → 10 seconds
    - 60˚C → 30 seconds
    - 72˚C → 15 seconds
- 1 cycle of 72˚C → 10 minutes
- 4˚C → hold

Validation of cDNA was performed by using 1ul of each sample on an Agilent High Sensitivity DNA Chip. The amplified cDNA constructs were stored at -25˚C until ready to perform purification.

3.3.2.7. Purify cDNA Construct using Pippen

The purification and size selection was performed using the Sage Pippin Prep 3% Cassettes Dye-Free (Cat# CDF3010). Before start purification, Pippin Prep loading solution was left at Room Temperature for 30 min. To capture the mature miRNA without adapter the Insert Size Target (IST) was set as 22bpA. PIWI-interacting RNAs, miRNAs and regulatory small RNAs were captured by setting IST as 30bpB and Pippin Run capture size as 150bpC. To the adaptor sequence the Pippin Run capture size was set as 150bpC.

Pippin cassette was prepared according to the manual instructions. All buffer from elution well was removed and replaced with 40ul of electrophoresis buffer to validate the quality of cassette.

After the quality was confirmed 10ul of water and 20ul of RT Pippin Prep loading solution were added and mixed with every sample. Samples prepared this way, were loaded into the cassettes wells in volume of 40ul per well, 2 times per sample. Prepared cassette was used to run the analysis with parameters mentioned above.

After the run samples were collected and moved into the separates tubes.

The final clean-up of cDNA library was performed using the Qiagen MinElute PCR Purification Kit. EtOH was added to the wash buffer PE. 400ul of PB buffer was mixed with 80ul of Pippin Prep Elute and with the wash buffer with addition of PE. The elution was placed in a MinElute column and centrifuged for 1 minute at 13,000 RPM at RT. Finally, the samples were moved to tubes and placed on ice, and the validation of the library was performed using the DNA 1000 or High Sensitivity DNA to check the size, purity, and concentration of the library.

3.3.3. NGS miRNA sequencing using MiSeq

Normalization and quality control (QC) of libraries: First, the library concentration to 2nM was normalized using Tris-HCl 10 mM (pH 8.5). The QC procedures were performed using the 30 µl Qiagen EB and 1µl of prepared library sample on Agilent Bioanalyzer (1000 DNA chip). After validation of libraries, KAPA quantification with samples in TSP1 plate was performed.

Denaturation of libraries: The denaturation of libraries was performed by adding 5 µl 0.2 N NaOH to the 2nM diluted library (5 µl). After vortexing and centrifuging at 280 × g for 1 minute, the diluted libraries were incubated at room temperature for 5 minutes. finally, 990 µl prechilled HT1 was added to the tube containing denatured library.

Denaturation of PhiX Control: The denaturation of Phix control was performed by adding 5 µl 0.2 N NaOH to the 2nM Phix library (5 µl). After vortexing and centrifuging at 280 × g for 1 minute, the diluted Phix libraries were incubated at room temperature for 5 minutes. Finally, MiSeq NGS sequencing was performed by loading both normalized diluted libraries (594 µl 570 µl) and the diluted PhiX control (6 µl 30 µl) onto the reagent cartridge, and put on to the MiSeq illumina sequencer.

3.3.4. Pre-processing of the miRNA-Seq data

The NGS experiment yielded miRNA-Seq data using MiSeq Illumina platform. The MiSeq FASTq miRNA-Seq data of both breeds of pig will be submitted after the publication of the Ph.D. dissertation to NCBI GEO database (https://www.ncbi.nlm.nih.gov/geo) and NCBI SRA database (https://www.ncbi.nlm.nih.gov/sra).

FastQC software was used for quality control of 12 fastq files with porcine miRNA reads. FastQC is a bioinformatics used for a quality control of raw sequencing data. It summarizes read quality by position and provides information about base sequence quality, length distribution of reads, levels of duplication, overrepresented sequences, adapter and Kmer content **(Brown J. et al., 2017).**

The output of such analysis is presented in the form of human readable report which summarize all the mentioned parameters.

From 12 fastqc files obtained during the NGS all samples had zero sequences with poor quality. Every sample had a sequence length from 35 to 51 bases. Sample with the lowest number of total sequences was 3R1.fastq with 135842 total sequences. The largest number of total sequences was present in 1R2.fastq, which had 4018483 total sequences. The lowest GC content were found in the 21R2.fastq sample with 46%. The highest content of GC bases was 49% which was present in samples 1R2.fastq, 4R3.fastq and 9R3.fastq (Table 1).

Table 1. Base statistics of FastQC quality control analysis. **Filename:** name of the fastq file input. **Sample:** sample id; **Diet:** Animal diet. C – standard diet, T – treated group, fed with diet enriched with PUFA acids; **Breed:** Breed of the animal. P – polish landrace, PxD – Polish Landrace and Duroc crossbreed; **Total sequences:** number of reads in file; **Poor quality sequences**: number of sequences with poor quality; **Sequence length:** Length of reads present in the sample; **GC Content [%]:** amount of G and C bases in the reads in percents.

Filename	Sample	Diet	Breed	Total sequences	Poor quality sequences	Sequence length	GC content [%]
1R1.fastq.gz	1R1_PxD_ctrl	C	PxD	1990353	0	35-51	47
1R2.fastq.gz	1R2_PxD_ctrl	C	PxD	4018483	0	35-51	49
2R1.fastq.gz	2R1_PxD_treat	T	PxD	315868	0	35-51	47
3R1.fastq.gz	3R1_P_ctrl	C	P	135842	0	35-51	47
3R2.fastq.gz	3R2_PxD_ctrl	C	PxD	1703333	0	35-51	47
4R1.fastq.gz	4R1_PxD_treat	T	PxD	3410675	0	35-51	47
4R3.fastq.gz	4R3_PxD_treat	T	PxD	826995	0	35-51	49
9R3.fastq.gz	9R3_P_treat	T	P	1383595	0	35-51	49
20R3.fastq.gz	20R3_P_treat	T	P	1949792	0	35-51	48
21R2.fastq.gz	21R2_P_treat	T	P	541104	0	35-51	46
30R2.fastq.gz	30R2_P_ctrl	C	P	194906	0	35-51	47
32R3.fastq.gz	32R3_P_ctrl	C	P	1335600	0	35-51	47

3.3.5. Post-processing of the miRNA-Seq data: miRNA mapping and reads counting

Good quality of reads allowed to skip the trimming part of NGS data preparation. The next step was to map obtained reads to the reference genome. For a reference genome, hairpin and mature sequences of porcine was used.

The sequences were extracted from miRBase v.22 **(Grifith-Jones S. et al., 2007; Kozomara A. et al., 2010)**. To map the reads from fastq files mapper.pl module of miRDeep2 was used. MiRDeep is the bioinformatics tool that allow to identify novel and known miRNAs from NGS data. It is able to parse reads data in such formats as a fastq or fasta. It is able to collapse the reads and clip the 3' adapters. Furthermore, miRDeep introduces the variety of parameters that allow the user to perform, suitable for the use case, NGS data preparation **(Friedlander M. R. et al., 2011).**

Mapping reads were performed for all 12 fastq files. The parameters used was "-l 18" which defines the seed region of a read to the first 18 bases in the sequence. Parameter "-m 5" was set which means only reads that do not map more than five times to the reference genome were kept. The rest of the parameters were set to default. The output of this step was the fasta file with mapped reads.

The second feature of miRDeep2 software is the quantifier module. The module maps the sequences to predefined hairpin and mature forms of miRNA, and determines the number of read counts. A read is assumed to represent a sequenced mature miRNA if it falls within the same position on the precursor, plus 2 nt upstream and 5 nt downstream **(Friedlander M. R. et al., 2011)**. The above mentioned feature was used to establish the number of reads for mature miRNAs. The reads generated in previous step was used as an input. As the results the matrix of 535 miRNAs reads for 12 samples were obtained which was later used in miRNA-DEG and WGCNA analysis.

3.3.6. Bioinformatic analysis of miRNA-Seq data of porcine liver transcriptome

After sequencing 12 fasta files were obtained, each for every animal. The Illumina pipeline was used for image acquisition and base-calling. Files were controlled to make sure only the reads with the highest quality would be used in the DEG and WGCNA analyses. After ensuring the quality of reads, they mapped to the reference genome and then counted.

Log2 counts normalization was used for the DEG analysis, while the Variance stabilization counts were used to normalize counts for WGCNA analysis **(Langfelder P., 2008).**

The DEG analysis was performed to investigate the differentially expressed genes between different groups of animals. The differentially expressed genes were investigated within the breeds in the same diet group and outside the breed. The same was performed between breeds with the consideration of diet and without the diet.

The WGCNA analysis was performed to analyze the co-expression of miRNA. MiRNAs were clustered into modules, which later were correlated with the phenotypic traits of the samples. MiRNA in modules with statistical significance were used to identify the target genes. Later, for the target genes with the most robust score, functional pathways were created.

The whole workflow of analysis is present in the figure 3.

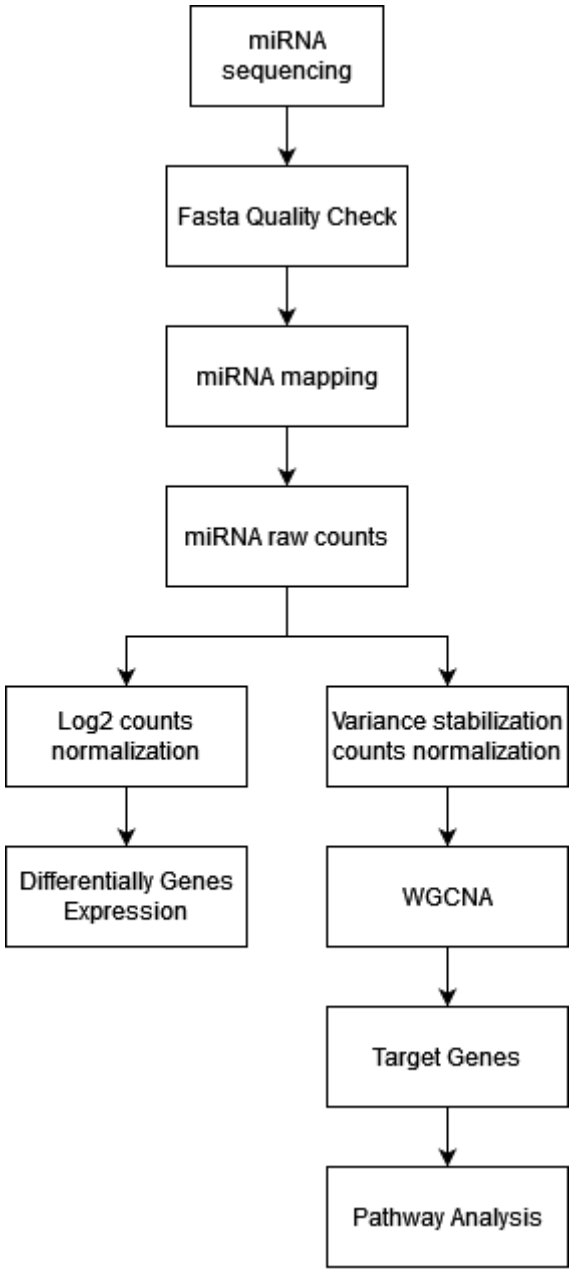

Figure 3. High level pipeline of bioinformatics analysis of miRNA-Seq data of porcine liver transcriptome.

3.3.7. DEG analysis

The DEG analysis was performed for 12 samples which were divided into 4 groups, according to the experiment design. Two diet groups within two different breeds (Table 2).

Table 2. Groups in DEG analysis. **Group:** The ID of a group; **Diet:** Group diet. Control – is standard diet, **experimental –** diet enriched in PUFA acids; **Breed –** PLxD **–** Polish Landrace x Duroc crossbred. PL – Polish Landrace pure breed.

Group	Diet	Breed
I	Control	PLxD
II	Experimental	PLxD
III	Control	PL
IV	Experimental	PL

In total 6 comparisons were performed to find the DEGs between groups.

- I vs II – diet comparison within the PLxDuroc crossbred.
- I vs III – comparison between PLxDuroc crossbred and PL pure breed, both groups fed with standard diet.
- I vs IV – comparison between PLxDuroc crossbred fed with standard diet with the PL pure breed fed with experimental diet.
- II vs III – comparison between PLxDuroc crossbred fed with experimental diet with the PL purebred fed with standard diet.
- II vs IV – comparison between PLxDuroc crossbred and PL pure breed, both groups fed with experimental diet.
- III vs IV – diet comparison within the PL pure breed.

After the quality control (1.4.4. Pre-processing of the miRNA-Seq data section) the fastq files were imported as raw read counts matrix were the i^{th} row and the j^{th} column tells how many reads were assigned to the transcript in a sample. To achieve that the R tximport package was used, with 12 fastq files as an input and, with "type" parameter set as "salmon" (**Soneson C. et al. 2015**).

Salmon is a bioinformatic tool, which requires fastq files and reference genome from the transcript quantification from RNA-seq data **(Soneson C. et al., 2015).**

Later the DESeq2 library was used to normalize the count matrix with log2 transformation which minimizes differences between samples for rows with small counts. The parameter used

as factor in the analysis design was the experimental group. Finally, the upregulated and down regulated transcript were identified based on the log2 fold change generated by the DESeq2 library **(Love M. I. et al., 2014).** Additionally, p-values and adjusted p-values were calculated for transcripts in each comparison. For p-value the Wald test was used and for the adjusted p-values False Discovery Rate (FDR) was used.

Transcripts with adjusted p-value > 0.05 were excluded from the comparison.

3.3.8. WGCNA Analysis

WGCNA analysis were performed for 12 samples. For all samples from 4 experimental groups one Co-expression network were created. Group, breed and diet information were added to the samples phenotypic traits to find the potential correlation between detected modules and breed, diet type or experimental group.

The matrix of raw counts of miRNAs per sample were used as an input for the WGCNA analysis. MiRNAs were placed in rows and samples in columns. Initially the matrix contained counts for 535 distinct miRNAs for 12 samples (section: 1.4.5. Post-processing of the miRNA-Seq data: miRNA mapping and reads counting)

Firstly, miRNAs with zero counts in each sample were filtered. Later, miRNAs with low number of counts were discarded from further analysis. The filtered data were normalized with the varianceStabilizingTransformation function from R DESeq2 library **(Anders S. et al., 2010; Langfelder P. et al., 2008).**

Before network construction, the miRNA expression profile was clustered and visualized in the form of dendrogram. Euclidian distance was used to show the difference between samples. Furthermore, the heatmap for phenotype was generated to compare the quantitative traits between the samples **(Horvath S. et al., 2008).**

Later, the soft-thresholding power β was established **(Zhang B. et al., 2005).**

After that, the co-expression network was constructed using the normalized miRNAs counts, and discovered earlier soft-thresholding power β **(Horvath S. et al., 2006)**. The co-expression network identified correlated miRNAs and clustered them into modules. Each module is represented by a module eigengene (ME), which is the first principal component of the expression values of all genes in the module **(Yip A. et al. 2007)**.

Each module was correlated with the phenotypic trait. Modules specific to the trait was chosen by the p-value (≥ 0.05) **(Langfelder P., 2008)**.

3.3.9. Finding Target Genes

For miRNAs in modules discovered in WGCNA analysis the target genes were identified. miRDB, an online database with miRNA target predictions, were used to find the target genes. The database contains information about the target genes and its' target genes score. Target gene score is the parameter describing how much a miRNA is related to the gene. The higher the score, the bigger relation of miRNA to a target gene **(Liu W. et al., 2019).**

The discovered target genes were filtered out leaving only the genes with the genes target score higher than 90.

3.3.10. Pathway analysis

After discovering the target genes for miRNAs clustered into the modules, the pathway analysis for these target genes were performed with Cytoscape ClueGo v2.5.9 software **(Binde G. et al., 2009).**

The GO/pathway analysis was performed using the GO-BiologicalProcess-EBI-UniProt-GOA database for human genes **(Barrel D. et al., 2009)**. Every functional group pathway discovered were filtered out if the p-value after Bonferroni correction was less than 0.05.

In the end the pathways and functional groups were generated for each module miRNAs' target genes.

4. Results

4.1. DEGs analysis of miRNA-Seq of porcine liver representing PL purebred and PLxDuroc crossbred pigs

In general, the experiment was divided into four groups, control diet and PUFAs diets in PL pigs, and Control diet and PUFAs diets in PLxDuroc pigs. For each group control diet PLxDuroc, PUFA diet PLxDuroc, control diet PL and PUFA diet PL, miRNA transcripts were identified in.

In this dissertation, six DEGs comparisons were performed and results of each DEGs comparison is described in the following sub-sections.

4.1.1. Identification of DE-miRNA transcripts in liver transcriptome by comparing the control vs PUFAs diets in PLxDuroc pigs

By comparing the control vs PUFAs diets in PLxDuroc pigs, 3921 (Control) and 1840 (PUFAs) diet-specific DE-miRNA transcript identified in PLxDuroc pigs. Furthermore, a total of 1256 DE-miRNA transcript were identified that commonly shared in both control vs PUFAs diets of PLxDuroc pigs (Fig. 4).

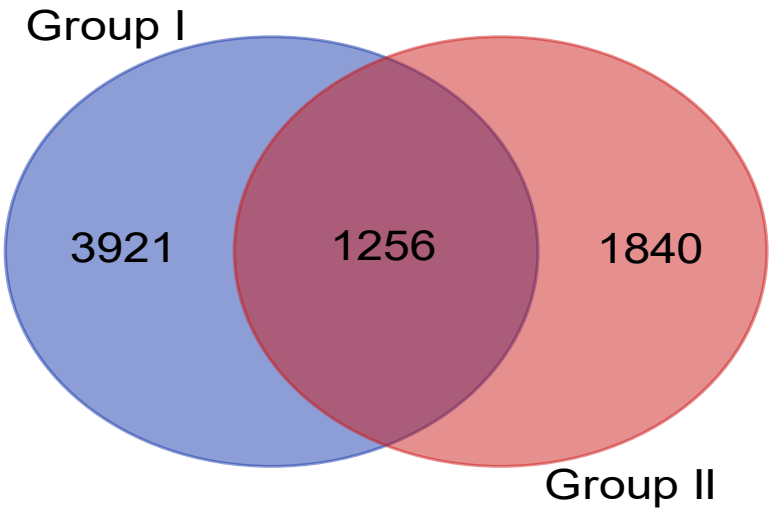

Figure 4. Comparison between the control vs PUFAs diets in PLxDuroc pigs. **Group I –** PLxDuroc crossbred, control**; Group II –** PLxDuroc, PUFA Diet

4.1.1.1. Identification of DE-miRNA transcripts ($p < 0.05$) in liver transcriptome by comparing between the control and PUFAs diets in PLxDuroc pigs

By comparing the control vs PUFAs diets in PLxDuroc pigs, results revealed the identification of 13 diet-specific DE-miRNA transcripts with significant cutoff values of $p \leq 0.05$ (Table 3). Using the BioMart ensembl (https://www.ensembl.org/biomart/martview/), 5 annotated DE-miRNA transcript namely: small nucleolar RNA, C/D box 123, microRNA 10a, ssc-mir-141, ssc-mir-103-2 and LncRNA NSSSCT00000041574, respectively, and 8 unannotated transcripts (ENSSSCT00000048121.1, ENSSSCT00000044507.1, ENSSSCT00000054955.1, ENSSSCT00000038143.1, ENSSSCT00000039582.1, ENSSSCT00000043911.1, ENSSSCT00000039714.1, ENSSSCT00000056391.1) were identified (Table 3).

Table 3. Identification of differentially expressed upregulated miRNA-transcripts (miRNA DETs) of porcine liver by comparing normal and PUFA diets in PL pigs. **Ensembl ID** – ensemble transcript stable ID; **I vs II p-value** – p-value; **I vs II adj p-value** – adjusted p-value; **Chr** – Chromosome/scaffold name; **Start** – transcript start (bp); **End** – transcript end (bp); **TL** – transcript length (including UTRs and CDS); **TT** – Transcript type

Ensembl ID	I vs II p-value	I vs II adj p-value	Gene stable ID version	Transcript stable ID version	Gene description	Chr	Start	End	TL	Gene name	Transcript name	TT	Source
ENSSSCT00000020853.2	0.01561	0.90353	ENSSSCG00000019258.2	ENSSSCT00000020853.2	small nucleolar RNA C/D box 123	16	72793462	72793531	70	SNORD123	SNORD123-201	snoRNA	ensembl
ENSSSCT00000020865.2	0.03905	0.90353	ENSSSCG00000019270.2	ENSSSCT00000020865.2	microRNA 10a	12	24833627	24833730	104	MIR10A	MIR10A-201	miRNA	ensembl
ENSSSCT00000022420.2	0.02472	0.90353	ENSSSCG00000020795.3	ENSSSCT00000022420.3	ssc-mir-141	5	63757578	63757642	65	ssc-mir-141	ssc-mir-141.1-201	miRNA	ensembl
ENSSSCT00000024011.2	0.03666	0.90353	ENSSSCG00000022382.3	ENSSSCT00000024011.3	ssc-mir-103-2	17	31808836	31808920	85	ssc-mir-103-2	ssc-mir-103-2.1-201	miRNA	ensembl
ENSSSCT00000041574.1	0.02172	0.90353	ENSSSCG00000038150.3	ENSSSCT00000041574.2	Novel transcript	10	28893934	28995455	2903			lncRNA	ensembl
ENSSSCT00000048121.1	0.03974	0.90353	unannotated	ENSSSCT00000048121.1									
ENSSSCT00000044507.1	0.03992	0.90353	unannotated	ENSSSCT00000044507.1									
ENSSSCT00000054955.1	0.04459	0.90353	unannotated	ENSSSCT00000054955.1									
ENSSSCT00000038143.1	0.04466	0.90353	unannotated	ENSSSCT00000038143.1									
ENSSSCT00000039582.1	0.04505	0.90353	unannotated	ENSSSCT00000039582.1									
ENSSSCT00000043911.1	0.04609	0.90353	unannotated	ENSSSCT00000043911.1									
ENSSSCT00000039714.1	0.04723	0.90353	unannotated	ENSSSCT00000039714.1									
ENSSSCT00000056391.1	0.04881	0.90353	unannotated	ENSSSCT00000056391.1									

4.1.1.2. Identification of upregulated DE-miRNA transcripts (FC > 2) in liver transcriptome by comparing the control vs PUFAs diets in PLxDuroc pigs

By comparing the control vs PUFAs diets in PLxDuroc pigs, results revealed the identification of 5 diet-specific upregulated DE-miRNA transcripts with log2FC > 2 in liver transcriptome (Table 4). Using the BioMart ensemble (https://www.ensembl.org/biomart/martview/), 3 annotated DE-miRNA transcripts namely: ssc-mir-451, lncRNA ENSSSCT00000062744, and lncRNA ENSSSCT00000029220, respectively, and two unannotated transcripts (ENSSSCT00000059159.1 and ENSSSCT00000059587.1) were identified (Table 4).

Table 4. Identification of differentially expressed upregulated miRNA-transcripts (miRNA DETs) of porcine liver by comparing normal and PUFA diets in PL pigs. **Ensembl ID** – ensemble transcript stable ID; **log2FC** – Log2 Fold change between group I and II; **Chr** – Chromosome/scaffold name; **Start** – transcript start (bp); **End** – transcript end (bp); **TL** – transcript length (including UTRs and CDS); **TT** – Transcript type

Ensembl ID	log2FC	Gene stable ID	Gene description	Chr	Start	End	TL	Gene name	Transcript name	TT	Source
ENSSSCT00000062744.1	3.276574955	ENSSSCG00000036117.3	Novel Transcript	10	66741325	66971746	2449			lncRNA	ensembl
ENSSSCT00000020949.3	2.249110848	ENSSSCG00000019354.3	ssc-mir-45	12	45088808	45088872	65	ssc-mir-451	ssc-mir-451.1-201	miRNA	ensembl
ENSSSCT00000029220.2	2.208091128	ENSSSCG00000027476.2	Novel Transcript	17	50961554	50961643	90			snoRNA	ensembl
ENSSSCT00000059159.1	3.453811938	Unannotated									
ENSSSCT00000059587.1	2.416692138	Unannotated									

4.1.1.3. Identification of downregulated DE-miRNA transcripts (FC > 5) in liver transcriptome by comparing the control vs PUFAs diets in PLxDuroc pigs

By comparing the control vs PUFAs diets in PLxDuroc pigs, results revealed the identification of 10 diet-specific downregulated DE-MiRNA transcripts with log2FC > 5 in liver transcriptome (Table 5). Using the BioMart ensembl (https://www.ensembl.org/biomart/martview/), four annotated DE-MiRNA transcript namely: U1 spliceosomal RNA, microRNA 10b, ssc-mir-141, and small nucleolar RNA, C/D box 38A, respectively, and six unannotated transcripts (ENSSSCT00000046899.1, ENSSSCT00000039008.1, ENSSSCT00000053425.1, ENSSSCT00000059663.1, ENSSSCT00000043911.1, and ENSSSCT00000040067.1) were identified (Table 5).

Table 5. Identification of differentially expressed upregulated miRNA-transcripts (miRNA DETs) of porcine liver by comparing normal and PUFA diets in PL pigs. **Ensembl ID** – ensemble transcript stable ID; **log2FC** – Log2 Fold change between group I and II; **Chr** – Chromosome/scaffold name; **Start** – transcript start (bp); **End** – transcript end (bp); **TL** – transcript length (including UTRs and CDS); **TT** – Transcript type

Ensembl ID	log2FC	Gene stable ID version	Gene description	Chr	Start	End	TL	Gene name	Transcript name	TT	Source (transcript)
ENSSSCT00000020974.2	-5.02585976	ENSSSCG00000019379.3	U1 spliceosomal RNA	13	84724484	84724640	157	U1	U1.11-201	snRNA	ensembl
ENSSSCT00000021537.2	-5.54591568	ENSSSCG00000019942.3	microRNA 10b	15	81951636	81951736	101	MIR10B	MIR10B-201	miRNA	ensembl
ENSSSCT00000022420.2	-5.69251869	ENSSSCG00000020795.3	ssc-mir-141	5	63757578	63757642	65	ssc-mir-141	ssc-mir-141.1-201	miRNA	ensembl
ENSSSCT00000058720.1	-5.69233134	ENSSSCG00000032021.1	small nucleolar RNA C/D box 38A	6	166551345	166551414	70	SNORD38A	SNORD38A-201	snoRNA	ensembl
ENSSSCT00000046899.1	-21.9564784	unannotated									
ENSSSCT00000039008.1	-6.07082843	unannotated									
ENSSSCT00000053425.1	-5.88610975	unannotated									
ENSSSCT00000059663.1	-5.55143519	unannotated									
ENSSSCT00000043911.1	-5.38093081	unannotated									
ENSSSCT00000040067.1	-5.00781694	unannotated									

4.1.2. Identification of DE-miRNA transcripts in liver transcriptome by comparing the control diets between PL vs PLxDuroc pigs

By comparing the control diets between PL vs PLxDuroc pigs, 4117 (PLxDuroc) and 1803 (PL) breed-specific DE-miRNA transcript identified in pigs fed with control diet (Fig. 5). Furthermore, a total of 1060 breed-specific DE-miRNA transcript were identified that commonly sheared in both PL and PLxDuroc pigs (Fig. 5).

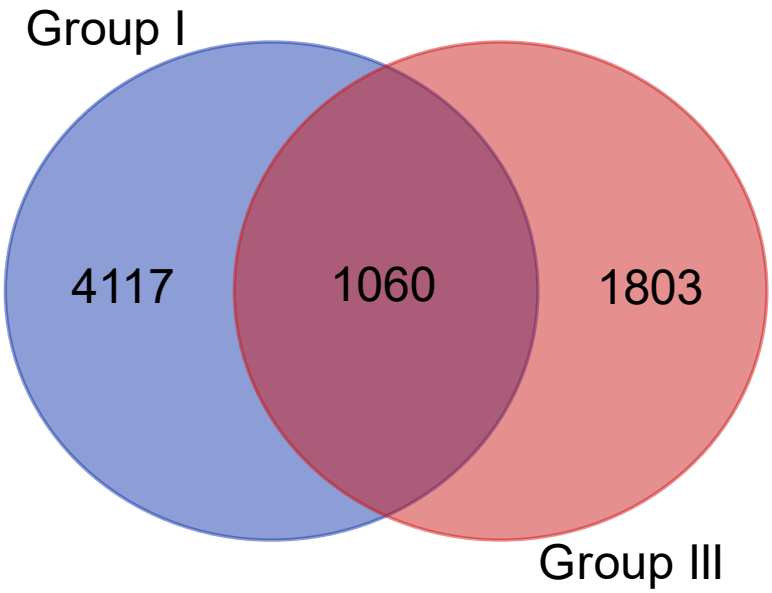

Figure 5. Comparison between the control vs PUFAs diets in PLxDuroc pigs. **Group I –** PLxDuroc crossbred, control diet**; Group III –** PL, control diet.

4.1.2.1. Identification of DE-miRNA transcripts ($p<0.05$) in liver transcriptome by comparing control diets between PL vs PLxDuroc pigs

By comparing the control diets between PL vs PLxDuroc pigs, results revealed the identification of 10 breed-specific DE-miRNA transcripts with significant cutoff values of $p<0.05$ (Table). Using the BioMart ensembl (https://www.ensembl.org/biomart/martview/), 6 annotated DE-MiRNA transcript namely: ssc-let-7f-2, ssc-let-7f-1, ssc-mir-143, ENSSSCG00000018071, ENSSSCG00000018077, and ENSSSCG00000018681 respectively, and 4 unannotated transcripts (ENSSSCT00000046577.1, ENSSSCT00000040180.1, ENSSSCT00000047143.1, and ENSSSCT00000055613.1) were identified (Table 6).

Table 6. Identification of differentially expressed upregulated miRNA-transcripts (miRNA DETs) of porcine liver by comparing normal and PUFA diets in PL pigs. **Ensembl ID** – ensemble transcript stable ID; **I vs III p-value** – p-value; **I vs III adj p-value** – adjusted p-value; **Chr** – Chromosome/scaffold name; **Start** – transcript start (bp); **End** – transcript end (bp); **TL** – transcript length (including UTRs and CDS); **TT** – Transcript type

Ensembl ID	Gene stable ID	I vs III p-value	Gene description	Chr	Start	End	TL	Gene name	Transcript name	TT	Source (transcript)
ENSSSCT00000019666.3	ENSSSCG00000018071	0.007200227	ENSSSCG00000018071	MT	6203	6270	68			mt_tRNA	RefSeq
ENSSSCT00000019672.1	ENSSSCG00000018077	0.00937213	ENSSSCG00000018077	MT	8135	8202	68			mt_tRNA	RefSeq
ENSSSCT00000020115.3	ENSSSCG00000018520	0.000778278	ssc-let-7f-2	3	43466027	43466133	107	ssc-let-7f-2	ssc-let-7f-2.1-201	miRNA	ensembl
ENSSSCT00000020276.4	ENSSSCG00000018681	0.002246212	ENSSSCG00000018681	11	60735343	60735449	107			miRNA	ensembl
ENSSSCT00000020693.2	ENSSSCG00000019098	0.002303096	ssc-let-7f-1	X	46303245	46303327	83	ssc-let-7f-1	ssc-let-7f-1.1-201	miRNA	ensembl
ENSSSCT00000020760.3	ENSSSCG00000019165	0.003419449	ssc-mir-143	2	150578738	150578817	80	ssc-mir-143	ssc-mir-143.1-201	miRNA	ensembl
ENSSSCT00000046577.1	unannotated	0.005387195									
ENSSSCT00000040180.1	unannotated	0.005398672									
ENSSSCT00000047143.1	unannotated	0.006424363									
ENSSSCT00000055613.1	unannotated	0.009973114									

4.1.2.2. Identification of upregulated DE-miRNA transcripts (logFC > 3) in liver transcriptome by comparing the control diets between PL vs PLxDuroc pigs

By comparing the control diets between PL vs PLxDuroc pigs, results revealed the identification of 21 breed-specific upregulated DE-miRNA transcripts with FC > 3 in liver transcriptome (Table 7). Using the BioMart ensembl (https://www.ensembl.org/biomart/martview/), 9 annotated DE-miRNA transcript namely: microRNA 1282, U6 spliceosomal, Small nucleolar RNA SNORD116, ENSSSCG00000018077, ENSSSCG00000039286, ENSSSCG00000032483, ENSSSCG00000039268, ENSSSCG00000035331, and ENSSSCG00000036117, respectively, and 12 unannotated transcript ENSSSCT00000041092.1, ENSSSCT00000057013.1, ENSSSCT00000049656.1, ENSSSCT00000056393.1, ENSSSCT00000042903.1, ENSSSCT00000050593.1, ENSSSCT00000037492.1, ENSSSCT00000049792.1, ENSSSCT00000064915.1, ENSSSCT00000064750.1, ENSSSCT00000047143.1 and ENSSSCT00000040180.1) were identified (Table 7).

Table 7. Identification of differentially expressed upregulated miRNA-transcripts (miRNA DETs) of porcine liver by comparing normal and PUFA diets in PL pigs. **Ensembl ID** – ensemble transcript stable ID; **log2FC** – log2 Fold change between group I and III; **Chr** – Chromosome/scaffold name; **Start** – transcript start (bp); **End** – transcript end (bp); **TL** – transcript length (including UTRs and CDS); **TT** – Transcript type

Ensembl ID	log2FC	p-value	**Gene stable ID**	**Gene description**	**Chr**	**Start**	**End**	**TL**	**Gene name**	**Transcript name**	**TT**	**Source (transcript)**
ENSSSCT00000019672.1	3.502546994	0.00937213	ENSSSCG00000018077	ENSSSCG00000018077	MT	8135	8202	68			mt_tRNA	RefSeq
ENSSSCT00000020329.2	3.173449047	0.22275245	ENSSSCG00000018734	microRNA 1282	1	127766052	127766152	101	MIR1282	MIR1282-201	miRNA	ensembl
ENSSSCT00000022233.2	3.207250426	0.03767249	ENSSSCG00000020638	U6 spliceosomal RNA	4	58090164	58090267	104	U6	U6.329-201	snRNA	ensembl
ENSSSCT00000037189.3	3.629978109	0.02592897	ENSSSCG00000039286	ENSSSCG00000039286	5	73909240	73947423	2198			lncRNA	ensembl
ENSSSCT00000037621.3	3.014362724	0.08139447	ENSSSCG00000032483	ENSSSCG00000032483	4	940756	944661	2754			lncRNA	ensembl
ENSSSCT00000039323.3	3.134332673	0.06504123	ENSSSCG00000039268	ENSSSCG00000039268	8	46865920	46919752	1035			lncRNA	ensembl
ENSSSCT00000056470.1	3.09302165	0.12454135	ENSSSCG00000032033	Small nucleolar RNA SNORD116	AEMK02000602.1	42147	42239	93	SNORD116	SNORD116.1-201	snoRNA	ensembl
ENSSSCT00000057520.3	3.809907726	0.04825643	ENSSSCG00000035331	ENSSSCG00000035331	7	21176239	21182879	1784			lncRNA	ensembl
ENSSSCT00000062744.1	3.905206918	0.09574000	ENSSSCG00000036117	ENSSSCG00000036117	10	66741325	66971746	2449			lncRNA	ensembl
ENSSSCT00000041092.1	3.037759109	#N/D!	unannotated									
ENSSSCT00000057013.1	3.049778412	0.09049127	unannotated									
ENSSSCT00000049656.1	3.241973781	#N/D!	unannotated									
ENSSSCT00000056393.1	3.314992089	0.13798700	unannotated									
ENSSSCT00000042903.1	3.340446188	0.20889735	unannotated									
ENSSSCT00000050593.1	3.34143079	#N/D!	unannotated									
ENSSSCT00000037492.1	4.002283283	0.04370786	unannotated									
ENSSSCT00000049792.1	4.244729369	0.06896438	unannotated									
ENSSSCT00000064915.1	4.522474774	0.05466698	unannotated									
ENSSSCT00000064750.1	4.7608977	0.16816444	unannotated									
ENSSSCT00000047143.1	5.580962764	0.00642436	unannotated									
ENSSSCT00000040180.1	5.684571203	0.00539867	unannotated									

4.1.2.3. Identification of downregulated DE-miRNA transcript (FC > 2) in liver transcriptome by comparing the control diets between PL vs PLxDuroc pigs

by comparing the control diets between PL vs PLxDuroc pigs, results revealed the identification of 31 breed-specific downregulated DE-miRNA transcripts with log2FC > 5 in liver transcriptome (Table 8). Using the BioMart ensembl (https://www.ensembl.org/biomart/martview/), 14 annotated DE-MiRNA transcript namely: small nucleolar RNA, C/D box 112, U6 spliceosomal RNA, small nucleolar RNA, C/D box 54, ssc-mir-136, U1 spliceosomal RNA, ssc-let-7f-2, small nucleolar RNA, H/ACA box 20, small nucleolar RNA, H/ACA box 2C, ssc-mir-141, small nucleolar RNA, C/D box 107, Small nucleolar RNA SNORD116, U6 spliceosomal RNA, ENSSSCG00000035515, ENSSSCG00000031490, respectively, and 17 unannotated transcript (ENSSSCT00000048787.1, ENSSSCT00000044470.1, ENSSSCT00000059234.1, ENSSSCT00000064244.1, ENSSSCT00000057418.1, ENSSSCT00000041898.1, ENSSSCT00000042319.1, ENSSSCT00000056747.1, ENSSSCT00000051585.1, ENSSSCT00000049825.1, ENSSSCT00000049537.1, ENSSSCT00000044245.1, ENSSSCT00000045339.1, ENSSSCT00000049874.1, ENSSSCT00000049643.1, ENSSSCT00000057057.1, and ENSSSCT00000039008.1) were identified (Table 8).

Table 8. Identification of differentially expressed upregulated miRNA-transcripts (miRNA DETs) of porcine liver by comparing normal and PUFA diets in PL pigs. **Ensembl ID** – ensemble transcript stable ID; **log2FC** – Log2 Fold change between group I and II; **Chr** – Chromosome/scaffold name; **Start** – transcript start (bp); **End** – transcript end (bp); **TL** – transcript length (including UTRs and CDS); **TT** – Transcript type

Ensembl ID	log2FC	p-value	Gene stable ID	Gene description	Chr	Start	End	TL	Gene name	Transcript name	TT	Source (transcript)
ENSSSCT00000019774.2	-5.21603253	0.08216197	ENSSSCG00000018179	small nucleolar RNA C/D box 112	7	121724050	121724126	77	SNORD112	SNORD112-201	snoRNA	ensembl
ENSSSCT00000019880.2	-4.37950432	0.21433404	ENSSSCG00000018285	U6 spliceosomal RNA	4	92165299	92165400	102	U6	U6.23-201	snRNA	ensembl
ENSSSCT00000019948.2	-5.22621465	0.04839383	ENSSSCG00000018353	small nucleolar RNA C/D box 54	4	75762686	75762750	65	SNORD54	SNORD54-201	snoRNA	ensembl
ENSSSCT00000020014.2	-4.40851250	0.08914159	ENSSSCG00000018419	ssc-mir-136	7	121711325	121711414	90	ssc-mir-136	ssc-mir-136.1-201	miRNA	ensembl
ENSSSCT00000020050.2	-4.84847018	0.20697745	ENSSSCG00000018455	U1 spliceosomal RNA	8	120190361	120190527	167	U1	U1.2-201	snRNA	ensembl
ENSSSCT00000020115.3	-4.96201507	0.00077827	ENSSSCG00000018520	ssc-let-7f-2	3	43466027	43466133	107	ssc-let-7f-2	ssc-let-7f-2.1-201	miRNA	ensembl
ENSSSCT00000020200.2	-4.22918564	0.06416887	ENSSSCG00000018605	small nucleolar RNA H/ACA box 20	1	7599025	7599157	133	SNORA20	SNORA20-201	snoRNA	ensembl
ENSSSCT00000022128.3	-5.12513341	#N/D!	ENSSSCG00000020533	small nucleolar RNA H/ACA box 2C	5	79282507	79282645	139	SNORA2C	SNORA2C-201	snoRNA	ensembl
ENSSSCT00000022420.3	-4.40653843	0.08638438	ENSSSCG00000020795	ssc-mir-141	5	63757578	63757642	65	ssc-mir-141	ssc-mir-141.1-201	miRNA	ensembl
ENSSSCT00000028380.2	-4.39095029	0.27808810	ENSSSCG00000026614	small nucleolar RNA C/D box 107	AEMK02000602.1	104436	104509	74	SNORD107	SNORD107-201	snoRNA	ensembl
ENSSSCT00000041769.1	-4.92190299	0.11325550	ENSSSCG00000035515	ENSSSCG00000035515	7	121818448	121818520	73			snoRNA	ensembl
ENSSSCT00000050921.1	-4.39095029	0.27808810	ENSSSCG00000062880	Small nucleolar RNA SNORD116	AEMK02000602.1	15296	15389	94	SNORD116	SNORD116.16-201	snoRNA	ensembl
ENSSSCT00000056785.1	-4.18773944	0.16358412	ENSSSCG00000031490	ENSSSCG00000031490	7	121812892	121812964	73			snoRNA	ensembl
ENSSSCT00000059934.1	-4.39095029	0.27808810	ENSSSCG00000039011	U6 spliceosomal RNA	AEMK02000389.1	31513	31614	102	U6	U6.526-201	snRNA	ensembl
ENSSSCT00000048787.1	-4.39095638	0.27808744	unannotated									
ENSSSCT00000044470.1	-4.39095029	0.27808810	unannotated									
ENSSSCT00000059234.1	-4.39095029	0.27808810	unannotated									
ENSSSCT00000064244.1	-4.39095029	0.27808810	unannotated									
ENSSSCT00000057418.1	-4.39095029	0.27808810	unannotated									
ENSSSCT00000041898.1	-4.39095029	0.27808810	unannotated									
ENSSSCT00000042319.1	-4.39095029	0.27808810	unannotated									
ENSSSCT00000056747.1	-4.39095029	0.27808810	unannotated									
ENSSSCT00000051585.1	-4.39095029	0.27808810	unannotated									
ENSSSCT00000049825.1	-4.39095029	0.27808810	unannotated									
ENSSSCT00000049537.1	-4.39095029	0.27808810	unannotated									
ENSSSCT00000044245.1	-4.39095029	0.27808810	unannotated									
ENSSSCT00000045339.1	-4.39095029	0.27808810	unannotated									
ENSSSCT00000049874.1	-4.39095029	0.27808810	unannotated									
ENSSSCT00000049643.1	-4.39095029	0.27808810	unannotated									
ENSSSCT00000057057.1	-4.39094437	0.27808875	unannotated									
ENSSSCT00000039008.1	-4.39088591	0.27809515	unannotated									

4.1.3. Identification of DE-miRNA transcripts in liver transcriptome by comparing the control diet in PLxDuroc vs PUFAs diet in PL pigs

By comparing the control diet in PLxDuroc vs PUFAS diet in PL pigs, 3797 (Control diet in PLxDuroc) and 1801 (PUFAs diet in PL) diet-specific DE-miRNA transcript identified in PL and PLxDuroc pigs (Fig. 6). Furthermore, a total of 1380 diet-specific DE-miRNA transcript were identified that commonly sheared in both control and PUFAs diets in PL and PLxDuroc pigs (Fig. 6).

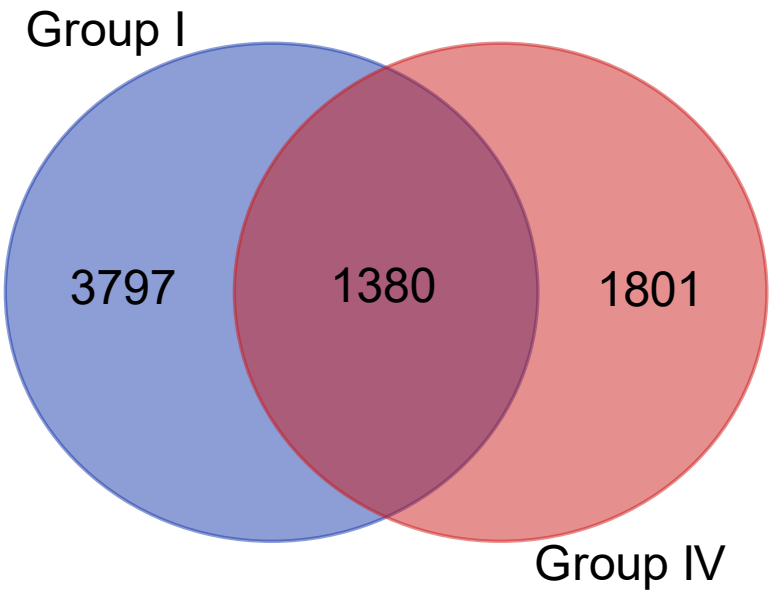

Figure 6. Comparison between the control diet in PLxDuroc vs PUFAs diets in PL pigs. **Group I –** PLxDuroc crossbred, control**; Group IV –** PLxDuroc, PUFA Diet

4.1.3.1. Identification of DE-miRNA transcripts ($p<0.05$) in liver transcriptome by comparing the control diet of PLxDuroc vs PUFAs diet in PL pigs.

By comparing the control diet of PLxDuroc vs PUFAs diet in PL pigs, results revealed the identification of 54 diet- and breed-specific DE-miRNA transcripts with significant cutoff values of $p < 0.01$ and $p < 0.05$ (Table 9 - 10). Using the BioMart ensembl (https://www.ensembl.org/biomart/martview/), 2 ($p < 0.01$) and 31 ($p < 0.05$) diet- and breed-specific annotated DE-MiRNA transcript namely: ssc-let-7f-1, and microRNA 22 ($p < 0.01$) and ssc-mir-425, ssc-mir-30c-1, ssc-mir-, microRNA 148a, small nucleolar RNA, H/ACA box 12, ssc-mir-191, ssc-mir-30d, ssc-mir-133a-1, ssc-mir-186, microRNA 142, ssc-mir-143, microRNA let-7g, microRNA 27b, ssc-let-7d, ssc-mir-16-1, ssc-mir-28, ssc-mir-122, microRNA let-7i, ssc-mir-194a, ssc-mir-30a, ssc-mir-101-2, ssc-mir-26a, ssc-mir-103-2,

microRNA 151a, ssc-mir-215, ENSSSCG00000018062, ENSSSCG00000018068, ENSSSCG00000018073, ENSSSCG00000018681, ENSSSCG00000039990, and ENSSSCG00000031914 ($p < 0.05$), respectively, were identified. Moreover, a total of 18 ($p < 0.05$) diet-specific unannotated transcript (ENSSSCT00000062826.1, ENSSSCT00000049859.1, ENSSSCT00000043456.1, ENSSSCT00000063347.1, ENSSSCT00000050810.1, ENSSSCT00000039582.1, ENSSSCT00000024894.2, ENSSSCT00000023227.2, ENSSSCT00000056553.1, ENSSSCT00000051609.1, ENSSSCT00000022223.2, ENSSSCT00000029616.2, ENSSSCT00000046107.1, ENSSSCT00000040324.1, ENSSSCT00000046058.1, ENSSSCT00000039038.1, ENSSSCT00000042113.1, and ENSSSCT00000039872.1, respectively) were identified (Table 9 - 10).

Table 9. Identification of differentially expressed upregulated miRNA-transcripts (miRNA DETs) of porcine liver by comparing normal and PUFA diets in PL pigs. Presented miRNA with p-value < 0.01. **Ensembl ID** – ensemble transcript stable ID; **log2FC** – Log2 Fold change between group I and II; **Chr** – Chromosome/scaffold name; **Start** – transcript start (bp); **End** – transcript end (bp); **TL** – transcript length (including UTRs and CDS); **TT** – Transcript type

Ensembl ID	Log2FC	p-value adjusted	Gene stable ID version	Gene description	Chr	Start	End	TL	Gene name	Transcript name	TT	Source (transcript)
ENSSSCG00000019098	-2.262978102	0.008716514	ENSSSCT00000020693.2	ssc-let-7f-1	X	46303245	46303327	83	ssc-let-7f-1	ssc-let-7f-1.1-201	miRNA	ensembl
ENSSSCG00000031748	-2.147353025	0.004506389	ENSSSCT00000046577.2	microRNA 22	12	47913326	47913419	94	MIR22	MIR22-201	miRNA	ensembl
unannotated	6.66751383	0.000446703	ENSSSCT00000063905.1									
unannotated	2.230530373	0.000823643	ENSSSCT00000050925.1									
unannotated	2.319194007	0.008646417	ENSSSCT00000039099.1									

Table 10. Identification of differentially expressed upregulated miRNA-transcripts (miRNA DETs) of porcine liver by comparing normal and PUFA diets in PL pigs. Presented miRNA with p-value < 0.05. **Ensembl ID** – ensemble transcript stable ID; **log2FC** – Log2 Fold change between group I and II; **Chr** – Chromosome/scaffold name; **Start** – transcript start (bp); **End** – transcript end (bp); **TL** – transcript length (including UTRs and CDS); **TT** – Transcript type

Ensembl ID	log2FC	p-value adjusted	Gene stable ID (p<0.05)	Gene description	Chr	Start	End	TL	Gene name	Transcript name	TT	Source (transcript)
ENSSSCT00000019657.1	-2.170362	0.047324111	ENSSSCG00000018062	ENSSSCG00000018062	MT	2206	2273	68			Mt_tRNA	RefSeq
ENSSSCT00000019663.3	-2.697284	0.017706877	ENSSSCG00000018068	ENSSSCG00000018068	MT	5017	5086	70			Mt_tRNA	RefSeq
ENSSSCT00000019668.1	-2.465368	0.049076238	ENSSSCG00000018073	ENSSSCG00000018073	MT	6379	6444	66			Mt_tRNA	RefSeq
ENSSSCT00000019768.3	-3.739476	0.013720204	ENSSSCG00000018173	ssc-mir-425	13	31654994	31655073	80	ssc-mir-425	ssc-mir-425.1-201	miRNA	ensembl
ENSSSCT00000019802.3	-3.922796	0.029564371	ENSSSCG00000018207	ssc-mir-30c-1	6	170426781	170426860	80	ssc-mir-30c-1	ssc-mir-30c-1.1-201	miRNA	ensembl
ENSSSCT00000019805.3	-2.119032	0.028019034	ENSSSCG00000018210	ssc-mir-126	AEMK02000682.1	1108695	1108767	73	ssc-mir-126	ssc-mir-126.1-201	miRNA	ensembl
ENSSSCT00000019872.3	-2.405713	0.026747417	ENSSSCG00000018277	microRNA 148a	18	46415202	46415281	80	MIR148A	MIR148A-201	miRNA	ensembl
ENSSSCT00000019978.2	2.1200580	0.026758951	ENSSSCG00000018383	small nucleolar RNA, H/ACA box 12	14	111359360	111359505	146	SNORA12	SNORA12-201	snoRNA	ensembl
ENSSSCT00000020161.3	-2.256421	0.014660912	ENSSSCG00000018566	ssc-mir-191	13	31655484	31655563	80	ssc-mir-191	ssc-mir-191.1-201	miRNA	ensembl
ENSSSCT00000020276.4	-2.219665	0.011205949	ENSSSCG00000018681	ENSSSCG00000018681	11	60735343	60735449	107			miRNA	ensembl
ENSSSCT00000020352.3	-1.955000	0.023743222	ENSSSCG00000018757	ssc-mir-30d	4	6948669	6948747	79	ssc-mir-30d	ssc-mir-30d.1-201	miRNA	ensembl
ENSSSCT00000020385.2	2.5169494	0.018185814	ENSSSCG00000018790	ssc-mir-133a-1	17	61904781	61904883	103	ssc-mir-133a-1	ssc-mir-133a-1.1-201	miRNA	ensembl
ENSSSCT00000020660.2	-2.193726	0.024637267	ENSSSCG00000019065	ssc-mir-186	6	141943328	141943409	82	ssc-mir-186	ssc-mir-186.1-201	miRNA	ensembl
ENSSSCT00000020733.3	-2.050597	0.033185346	ENSSSCG00000019138	microRNA 142	12	34609364	34609468	105	MIR142	MIR142-201	miRNA	ensembl
ENSSSCT00000020760.3	-2.130760	0.017186437	ENSSSCG00000019165	ssc-mir-143	2	150578738	150578817	80	ssc-mir-143	ssc-mir-143.1-201	miRNA	ensembl
ENSSSCT00000020901.3	-2.286415	0.021137228	ENSSSCG00000019306	microRNA let-7g	13	34406130	34406225	96	MIRLET7G	MIRLET7G-201	miRNA	ensembl
ENSSSCT00000020954.3	-1.987847	0.024333662	ENSSSCG00000019359	microRNA 27b	10	27079954	27080056	103	MIR27B	MIR27B-201	miRNA	ensembl
ENSSSCT00000020959.2	-3.618200	0.048770558	ENSSSCG00000019364	ssc-let-7d	3	43468501	43468596	96	ssc-let-7d	ssc-let-7d.1-201	miRNA	ensembl
ENSSSCT00000020984.2	-3.203531	0.046306663	ENSSSCG00000019389	ssc-mir-16-1	13	100083329	100083405	77	ssc-mir-16-1	ssc-mir-16-1.1-201	miRNA	ensembl

ENSSSCT00000020999.2	-2.253747	0.014018277	ENSSSCG00000019404	ssc-mir-28	13	126282167	126282252	86	ssc-mir-28	ssc-mir-28.1-201	miRNA	ensembl
ENSSSCT00000021167.3	-2.117796	0.035587867	ENSSSCG00000019572	ssc-mir-122	1	162329767	162329860	94	ssc-mir-122	ssc-mir-122.1-201	miRNA	ensembl
ENSSSCT00000021422.3	-2.167010	0.026509586	ENSSSCG00000019827	microRNA let-7i	5	27252787	27252894	108	MIRLET7I	MIRLET7I-201	miRNA	ensembl
ENSSSCT00000021501.2	-2.124642	0.019146796	ENSSSCG00000019906	ssc-mir-194a	2	7285466	7285541	76	ssc-mir-194a	ssc-mir-194a.1-201	miRNA	ensembl
ENSSSCT00000021536.2	-2.111111	0.018062523	ENSSSCG00000019941	ssc-mir-30a	1	51412827	51412933	107	ssc-mir-30a	ssc-mir-30a.1-201	miRNA	ensembl
ENSSSCT00000021585.2	-2.365269	0.039637699	ENSSSCG00000019990	ssc-mir-101-2	6	147330890	147330972	83	ssc-mir-101-2	ssc-mir-101-2.1-201	miRNA	ensembl
ENSSSCT00000023905.2	-1.965158	0.026180792	ENSSSCG00000022286	ssc-mir-26a	5	23112744	23112827	84	ssc-mir-26a	ssc-mir-26a.1-201	miRNA	ensembl
ENSSSCT00000024011.3	-3.290555	0.024745683	ENSSSCG00000022382	ssc-mir-103-2	17	31808836	31808920	85	ssc-mir-103-2	ssc-mir-103-2.1-201	miRNA	ensembl
ENSSSCT00000025885.3	-2.18620	0.027234919	ENSSSCG00000024238	microRNA 151a	4	2849038	2849130	93	MIR151A	MIR151A-201	miRNA	ensembl
ENSSSCT00000040236.3	1.8886537	0.024749165	ENSSSCG00000039990	ENSSSCG00000039990	13	152248627	152295769	2486			lncRNA	ensembl
ENSSSCT00000046476.3	1.5860745	0.034097196	ENSSSCG00000031914	ENSSSCG00000031914	14	13229780	13240405	852			lncRNA	ensembl
ENSSSCT00000049008.1	-2.791388	0.032584931	ENSSSCG00000032560	ssc-mir-215	10	9704606	9704701	96	ssc-mir-215	ssc-mir-215.1-201	miRNA	ensembl
ENSSSCT00000062826.1	4.7708617	0.010388091	unannotated									
ENSSSCT00000049859.1	1.9646971	0.014519884	unannotated									
ENSSSCT00000043456.1	-4.056081	0.014719998	unannotated									
ENSSSCT00000063347.1	2.5725798	0.020518812	unannotated									
ENSSSCT00000050810.1	1.7835080	0.025943942	unannotated									
ENSSSCT00000039582.1	-4.336406	0.026502097	unannotated									
ENSSSCT00000024894.2	2.250147621	0.027756657	unannotated									
ENSSSCT00000023227.2	-5.089176	0.030735734	unannotated									
ENSSSCT00000056553.1	2.5314647	0.030828481	unannotated									
ENSSSCT00000051609.1	1.4253057	0.034223131	unannotated									
ENSSSCT00000022223.2	2.2482338	0.035920076	unannotated									
ENSSSCT00000029616.2	-5.583481	0.040849982	unannotated									
ENSSSCT00000046107.1	1.6143178	0.04599256	unannotated									
ENSSSCT00000040324.1	1.9668737	0.046350388	unannotated									
ENSSSCT00000046058.1	1.6575070	0.047100893	unannotated									
ENSSSCT00000039038.1	1.7077664	0.048533077	unannotated									
ENSSSCT00000042113.1	1.5293331	0.049003247	unannotated									
ENSSSCT00000039872.1	2.3277681	0.049185613	unannotated									

4.1.3.2. Identification of upregulated DE-miRNA transcripts (log2FC > 2) in liver transcriptome by comparing the control diet of PLxDuroc vs PUFAs diet in PL pigs

By comparing the control diet of PLxDuroc vs PUFAs diet in PL pigs, results revealed the identification of 29 upregulated DE-MiRNA transcripts with log2FC > 2 in liver transcriptome (Table 11). Using the BioMart ensembl (https://www.ensembl.org/biomart/martview/), 9 annotated DE-miRNA transcript namely: microRNA 1282, small nucleolar RNA, H/ACA box 12, ssc-mir-133a-1, U6 spliceosomal RNA , ssc-mir-155, U6 spliceosomal RNA, U6 spliceosomal RNA, ENSSSCG00000018225, and ENSSSCG00000035331, respectively, and 20 unannotated transcript (ENSSSCT00000020408.2, ENSSSCT00000025157.2, ENSSSCT00000050925.1, ENSSSCT00000021961.2, ENSSSCT00000022223.2, ENSSSCT00000024894.2, ENSSSCT00000039099.1, ENSSSCT00000020921.2, ENSSSCT00000047143.1, ENSSSCT00000056553.1, ENSSSCT00000063347.1, ENSSSCT00000059834.1, ENSSSCT00000052342.1, ENSSSCT00000063950.1, ENSSSCT00000025078.2, ENSSSCT00000051559.1, ENSSSCT00000059587.1 ENSSSCT00000062826.1, ENSSSCT00000056949.1, and ENSSSCT00000063905.1) were identified (Table 11).

Table 11. Identification of differentially expressed upregulated miRNA-transcripts (miRNA DETs) of porcine liver by comparing the control diet of PLxDuroc vs PUFAs diet in PL pigs. Selected transcripts with log2FC > 2 **Ensembl ID** – ensemble transcript stable ID; **log2FC** – Log2 Fold change between group I and II; **Chr** – Chromosome/scaffold name; **Start** – transcript start (bp); **End** – transcript end (bp); **TL** – transcript length (including UTRs and CDS); **TT** – Transcript type

Ensembl ID	log2FC	p-value adjusted	Gene stable ID	Gene description	Chr	Start	End	TL	Gene name	Transcript name	TT	Source (transcript)
ENSSSCT00000020329.2	3.648752	0.234124	ENSSSCG00000018734	microRNA 1282	1	127766052	127766152	101	MIR1282	MIR1282-201	miRNA	ensembl
ENSSSCT00000019820.2	2.323375	0.49813	ENSSSCG00000018225	ENSSSCG00000018225	9	26158697	26158827	131			snoRNA	ensembl
ENSSSCT00000019978.2	2.120058	0.026759	ENSSSCG00000018383	small nucleolar RNA, H/ACA box 12	14	111359360	111359505	146	SNORA12	SNORA12-201	snoRNA	ensembl
ENSSSCT00000020385.2	2.516949	0.018186	ENSSSCG00000018790	ssc-mir-133a-1	17	61904781	61904883	103	ssc-mir-133a-1	ssc-mir-133a-1.1-201	miRNA	ensembl
ENSSSCT00000020657.2	2.082108	0.056327	ENSSSCG00000019062	U6 spliceosomal RNA	2	69197569	69197671	103	U6	U6.99-201	snRNA	ensembl
ENSSSCT00000020749.3	2.143319	0.464264	ENSSSCG00000019154	ssc-mir-155	13	189138822	189138902	81	ssc-mir-155	ssc-mir-155.1-201	miRNA	ensembl
ENSSSCT00000022125.2	2.037631	0.482179	ENSSSCG00000058894	U6 spliceosomal RNA	X	75488261	75488367	107	U6	U6.754-201	snRNA	ensembl
ENSSSCT00000027003.2	2.232472	0.064079	ENSSSCG00000055929	U6 spliceosomal RNA	5	55478031	55478134	104	U6	U6.676-201	snRNA	ensembl
ENSSSCT00000054465.3	2.852777	#N/D!	ENSSSCG00000035331	ENSSSCG00000035331	7	21176243	21182724	2020			lncRNA	ensembl
ENSSSCT00000020408.2	2.036363	0.657456	unannotated									
ENSSSCT00000025157.2	2.117941	0.371386	unannotated									
ENSSSCT00000050925.1	2.23053	0.000824	unannotated									
ENSSSCT00000021961.2	2.242655	0.460273	unannotated									
ENSSSCT00000022223.2	2.248234	0.03592	unannotated									
ENSSSCT00000024894.2	2.250148	0.027757	unannotated									
ENSSSCT00000039099.1	2.319194	0.008646	unannotated									
ENSSSCT00000020921.2	2.416789	0.185806	unannotated									
ENSSSCT00000047143.1	2.461678	0.244381	unannotated									
ENSSSCT00000056553.1	2.531465	0.030828	unannotated									
ENSSSCT00000063347.1	2.57258	0.020519	unannotated									
ENSSSCT00000059834.1	2.728193	0.219813	unannotated									
ENSSSCT00000052342.1	2.878616	0.259508	unannotated									
ENSSSCT00000063950.1	3.426546	0.109273	unannotated									
ENSSSCT00000025078.2	3.700408	0.053652	unannotated									
ENSSSCT00000051559.1	3.995612	0.143606	unannotated									
ENSSSCT00000059587.1	4.741247	0.08885	unannotated									
ENSSSCT00000062826.1	4.770862	0.010388	unannotated									
ENSSSCT00000056949.1	4.892946	#N/D!	unannotated									
ENSSSCT00000063905.1	6.667514	0.000447	unannotated									

4.1.3.3. Identification of downregulated DE miRNA transcript (log2FC > 3) in liver transcriptome by comparing the control diet of PLxDuroc vs PUFAs diet in PL pigs

by comparing the control diet of PLxDuroc vs PUFAS diet in PL pigs, results revealed the identification of 64 downregulated DE-MiRNA transcripts with log2FC > 5 in liver transcriptome (Table 12). Using the BioMart ensembl (https://www.ensembl.org/biomart/martview/), 36 annotated DE-MiRNA transcript namely: U6 spliceosomal RNA, ssc-mir-130b, ssc-mir-136, ssc-mir-219a, U6 spliceosomal RNA, U6 spliceosomal RNA, U2 spliceosomal RNA, ssc-mir-708, U2 spliceosomal RNA, small nucleolar RNA, H/ACA box 69, U6 spliceosomal RNA, U6 spliceosomal RNA, Small nucleolar RNA SNORA70, Small nucleolar RNA SNORA70, U6 spliceosomal RNA, U5 spliceosomal RNA, U6 spliceosomal RNA, U6 spliceosomal RNA, Metazoan signal recognition particle RNA, U6 spliceosomal RNA, U6 spliceosomal RNA, ssc-mir-4334, U6 spliceosomal RNA, U6 spliceosomal RNA, ssc-mir-9799, U6 spliceosomal RNA, U6 spliceosomal RNA, ENSSSCG00000057125, ENSSSCG00000018786, ENSSSCG00000019847, ENSSSCG00000019918, ENSSSCG00000020125, ENSSSCG00000020432, ENSSSCG00000023632, ENSSSCG00000024747, and ENSSSCG00000055545, respectively, and 28 unannotated transcript (ENSSSCT00000046899.1, ENSSSCT00000020452.2, ENSSSCT00000021063.2, ENSSSCT00000021498.2, ENSSSCT00000021699.2, ENSSSCT00000021705.2, ENSSSCT00000021831.3, ENSSSCT00000022114.2, ENSSSCT00000023227.2, ENSSSCT00000024557.2, ENSSSCT00000029616.2, ENSSSCT00000039008.1, ENSSSCT00000039582.1, ENSSSCT00000041365.1, ENSSSCT00000043456.1, ENSSSCT00000043911.1, ENSSSCT00000046567.1, ENSSSCT00000050647.1, ENSSSCT00000050667.1, ENSSSCT00000052855.1, ENSSSCT00000055839.1, ENSSSCT00000056288.1, ENSSSCT00000056883.1, ENSSSCT00000058490.1, ENSSSCT00000061253.1, ENSSSCT00000063310.1, ENSSSCT00000066098.1 and ENSSSCT00000066284.1) were identified (Table 12).

Table 12. Identification of differentially expressed upregulated miRNA-transcripts (miRNA DETs) of porcine liver by comparing the control diet of PLxDuroc vs PUFAs diet in PL pigs. Transcript presented with log2FC > 3. **Ensembl ID** – ensemble transcript stable ID; **log2FC** – Log2 Fold change between group I and II; **Chr** – Chromosome/scaffold name; **Start** – transcript start (bp); **End** – transcript end (bp); **TL** – transcript length (including UTRs and CDS); **TT** – Transcript type

Ensembl ID	log2FC	p-value adjusted	Gene stable ID	Gene description	Chr	Start	End	TL	Gene name	Transcript name	TT	Source (transcript)
ENSSSCT00000019716.2	-5.02104	0.197536	ENSSSCG00000057125	ENSSSCG00000057125	12	25130795	25130924	130			snoRNA	ensembl
ENSSSCT00000019907.2	-4.01996	0.378226	ENSSSCG00000018312	U6 spliceosomal RNA	6	106859293	106859400	108	U6	U6.27-201	snRNA	ensembl
ENSSSCT00000019955.3	-4.01884	0.312927	ENSSSCG00000018360	ssc-mir-130b	14	50245041	50245120	80	ssc-mir-130b	ssc-mir-130b.1-201	miRNA	ensembl
ENSSSCT00000020014.2	-4.01445	0.167489	ENSSSCG00000018419	ssc-mir-136	7	121711325	121711414	90	ssc-mir-136	ssc-mir-136.1-201	miRNA	ensembl
ENSSSCT00000020217.3	-4.01969	0.360523	ENSSSCG00000018622	ssc-mir-219a	7	25250839	25250921	83	ssc-mir-219a	ssc-mir-219a.1-201	miRNA	ensembl
ENSSSCT00000020263.3	-4.18577	0.120359	ENSSSCG00000018668	U6 spliceosomal RNA	6	161246086	161246189	104	U6	U6.62-201	snRNA	ensembl
ENSSSCT00000020379.2	-4.03585	0.358941	ENSSSCG00000018784	U6 spliceosomal RNA	15	122061852	122061956	105	U6	U6.69-201	snRNA	ensembl
ENSSSCT00000020381.2	-4.01969	0.360523	ENSSSCG00000018786	ENSSSCG00000018786	7	74812197	74812311	115			snoRNA	ensembl
ENSSSCT00000020418.2	-4.8342	0.284058	ENSSSCG00000018823	U2 spliceosomal RNA	6	23691605	23691795	191	U2	U2.4-201	snRNA	ensembl
ENSSSCT00000020794.3	-4.03081	0.279697	ENSSSCG00000019199	ssc-mir-708	9	13780171	13780250	80	ssc-mir-708	ssc-mir-708.1-201	miRNA	ensembl
ENSSSCT00000020873.2	-4.44487	0.126447	ENSSSCG00000019278	U2 spliceosomal RNA	15	111627482	111627671	190	U2	U2.7-201	snRNA	ensembl
ENSSSCT00000021195.2	-4.24366	0.350533	ENSSSCG00000019600	small nucleolar RNA, H/ACA box 69	X	98178787	98178918	132	SNORA69	SNORA69-201	snoRNA	ensembl
ENSSSCT00000021227.2	-4.24366	0.350533	ENSSSCG00000019632	U6 spliceosomal RNA	17	22408021	22408123	103	U6	U6.172-201	snRNA	ensembl
ENSSSCT00000021442.3	-4.8342	0.284058	ENSSSCG00000019847	ENSSSCG00000019847	4	83219154	83219230	77			snoRNA	ensembl
ENSSSCT00000021511.2	-4.52213	0.31799	ENSSSCG00000019916	U6 spliceosomal RNA	9	49760031	49760133	103	U6	U6.207-201	snRNA	ensembl
ENSSSCT00000021513.2	-4.52272	0.267221	ENSSSCG00000019918	ENSSSCG00000019918	5	79284695	79284826	132			snoRNA	ensembl
ENSSSCT00000021608.2	-4.68472	0.262609	ENSSSCG00000020013	Small nucleolar RNA SNORA70	9	61345532	61345667	136	SNORA70	SNORA70.6-201	snoRNA	ensembl
ENSSSCT00000021670.2	-4.16427	0.298634	ENSSSCG00000020075	Small nucleolar RNA SNORA70	15	2450542	2450675	134	SNORA70	SNORA70.7-201	snoRNA	ensembl
ENSSSCT00000021720.2	-4.20599	0.115313	ENSSSCG00000020125	ENSSSCG00000020125	13	48132610	48132742	133			snoRNA	ensembl
ENSSSCT00000022027.2	-4.5224	0.292838	ENSSSCG00000020432	ENSSSCG00000020432	12	25108081	25108314	234			snoRNA	ensembl
ENSSSCT00000022059.2	-4.01996	0.378226	ENSSSCG00000020464	U6 spliceosomal RNA	1	158527034	158527127	94	U6	U6.303-201	snRNA	ensembl
ENSSSCT00000022121.2	-4.01997	0.378225	ENSSSCG00000020526	U5 spliceosomal RNA	2	17831977	17832090	114	U5	U5.6-201	snRNA	ensembl
ENSSSCT00000022203.2	-4.78261	0.06808	ENSSSCG00000020608	U6 spliceosomal RNA	6	20154524	20154624	101	U6	U6.323-201	snRNA	ensembl
ENSSSCT00000022205.3	-4.34654	0.259498	ENSSSCG00000020610	U6 spliceosomal RNA	16	57867823	57867925	103	U6	U6.324-201	snRNA	ensembl
ENSSSCT00000025263.2	-4.36085	0.132625	ENSSSCG00000023632	ENSSSCG00000023632	3	23095003	23095132	130			snoRNA	ensembl
ENSSSCT00000026453.2	-4.24367	0.350532	ENSSSCG00000024747	ENSSSCG00000024747	3	13452692	13452840	149			snoRNA	ensembl
ENSSSCT00000027370.3	-4.01969	0.360523	ENSSSCG00000025642	Metazoan signal recognition particle RNA	18	22167311	22167423	113	Metazoa_SRP	Metazoa_SRP.8-201	misc_RNA	ensembl
ENSSSCT00000028256.3	-4.7514	0.292801	ENSSSCG00000026500	U6 spliceosomal RNA	12	47766011	47766112	102	U6	U6.389-201	snRNA	ensembl
ENSSSCT00000029363.3	-5.33242	0.235347	ENSSSCG00000027605	U6 spliceosomal RNA	6	51930973	51931076	104	U6	U6.397-201	snRNA	ensembl
ENSSSCT00000032301.2	-4.01925	0.167991	ENSSSCG00000030434	ssc-mir-4334	15	121399612	121399680	69	ssc-mir-4334	ssc-mir-4334.1-201	miRNA	ensembl
ENSSSCT00000041125.1	-4.01997	0.378225	ENSSSCG00000055545	ENSSSCG00000055545	7	121799539	121799613	75			snoRNA	ensembl
ENSSSCT00000055921.1	-4.5224	0.292838	ENSSSCG00000032635	U6 spliceosomal RNA	16	1106372	1106479	108	U6	U6.441-201	snRNA	ensembl

ENSSSCT00000057130.1	-4.33134	0.062615	ENSSSCG00000040068	U6 spliceosomal RNA	9	73156794	73156870	77	U6	U6.541-201	snRNA	ensembl
ENSSSCT00000060402.1	-4.01969	0.360523	ENSSSCG00000038318	ssc-mir-9799	16	36738809	36738895	87	ssc-mir-9799	ssc-mir-9799.1-201	miRNA	ensembl
ENSSSCT00000064226.2	-4.34016	0.339013	ENSSSCG00000036162	U6 spliceosomal RNA	10	5007234	5007336	103	U6	U6.496-201	snRNA	ensembl
ENSSSCT00000065173.1	-4.24272	0.312186	ENSSSCG00000040492	U6 spliceosomal RNA	3	45631441	45631543	103	U6	U6.547-201	snRNA	ensembl
ENSSSCT00000046899.1	-20.5603	#N/D!	unannotated									
ENSSSCT00000020452.2	-4.01921	0.332667	unannotated									
ENSSSCT00000021063.2	-4.52213	0.31799	unannotated									
ENSSSCT00000021498.2	-4.10327	0.324555	unannotated									
ENSSSCT00000021699.2	-4.01921	0.332667	unannotated									
ENSSSCT00000021705.2	-4.01997	0.378225	unannotated									
ENSSSCT00000021831.3	-4.01997	0.378225	unannotated									
ENSSSCT00000022114.2	-4.01997	0.378225	unannotated									
ENSSSCT00000023227.2	-5.08918	0.030736	unannotated									
ENSSSCT00000024557.2	-4.52213	0.31799	unannotated									
ENSSSCT00000029616.2	-5.58349	0.04085	unannotated									
ENSSSCT00000039008.1	-7.78496	0.080569	unannotated									
ENSSSCT00000039582.1	-4.33641	0.026502	unannotated									
ENSSSCT00000041365.1	-4.24367	0.350532	unannotated									
ENSSSCT00000043456.1	-4.05608	0.01472	unannotated									
ENSSSCT00000043911.1	-4.36164	0.146277	unannotated									
ENSSSCT00000046567.1	-4.83172	0.240678	unannotated									
ENSSSCT00000050647.1	-4.34015	0.339014	unannotated									
ENSSSCT00000050667.1	-4.08797	0.101115	unannotated									
ENSSSCT00000052855.1	-4.83172	0.240678	unannotated									
ENSSSCT00000055839.1	-4.01996	0.378226	unannotated									
ENSSSCT00000056288.1	-4.34654	0.259498	unannotated									
ENSSSCT00000056883.1	-4.24367	0.350532	unannotated									
ENSSSCT00000058490.1	-4.08155	0.060625	unannotated									
ENSSSCT00000061253.1	-4.71342	0.280583	unannotated									
ENSSSCT00000063310.1	-4.14989	0.125658	unannotated									
ENSSSCT00000066098.1	-4.24124	0.320583	unannotated									
ENSSSCT00000066284.1	-4.24366	0.350533	unannotated									

4.1.4. Identification of DE miRNA transcripts in liver transcriptome by comparing the control diet in PL pigs vs PUFAs diet in PLxDuroc pigs

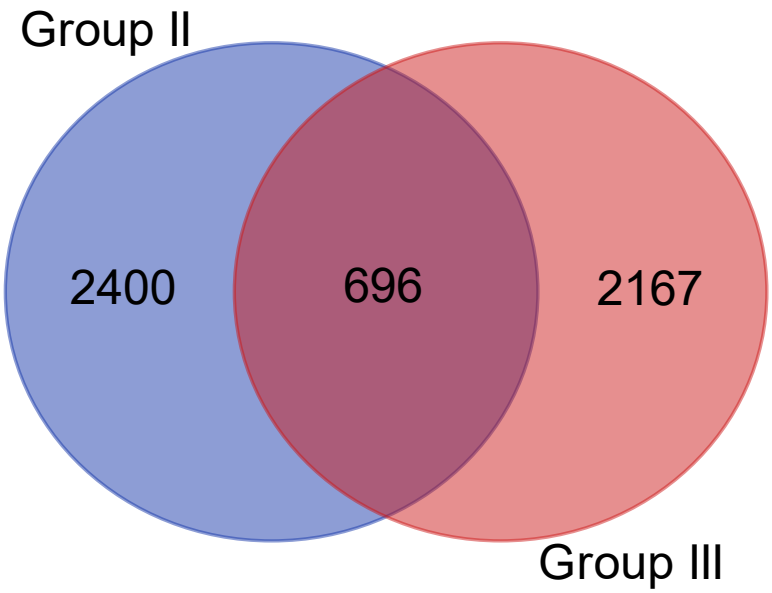

Figure 7. Comparison between the control diet in PL pigs vs PUFAs diet in PLxDuroc pigs. **Group II –** PLxDuroc, PUFA Diet; **Group III –** PL, control diet.

By comparing the control diet in PL pigs vs PUFAS diet in PLxDuroc pigs, 2400 (Control diet in PL) and 2167 (PUFAs diet in PLxDuroc) DE-miRNA transcript identified in PL and PLxDuroc pigs (Fig. 6). Furthermore, a total of 696 DE-miRNA transcript were identified that commonly sheared in both control and PUFAs diets in PL and PLxDuroc pigs (Fig. 6).

4.1.4.1. Identification of DE-miRNA transcripts ($p < 0.05$) in liver transcriptome by comparing the control diet in PL pigs vs PUFA diet in PLxDuroc pigs

By comparing the control diet in PL pigs vs PUFAs diet in PLxDuroc pigs, results revealed the identification of 56 DE-miRNA transcripts with significant cutoff values of $p < 0.05$ (Table 13). Using the BioMart ensembl (https://www.ensembl.org/biomart/martview/), 37 annotated DE-MiRNA transcript namely: ssc-mir-21, ssc-let-7f-1, ssc-mir-143, ssc-mir-378-2, microRNA 22, ENSSSCG00000018681, ENSSSCG00000039286, ENSSSCG00000032483 ENSSSCT00000040180, ENSSSCT00000047143 (all $p < 0.01$), small nucleolar RNA, C/D box 49A, ssc-let-7f-2, ssc-mir-221, ssc-mir-181a-2, Small nucleolar RNA Z195/SNORD33/SNORD32 family, small nucleolar RNA, C/D box 104, small nucleolar RNA, C/D box 45A, Small nucleolar RNA SNORD24, U12 minor spliceosomal RNA, Small nucleolar RNA SNORD42, ssc-let-7a-1, ssc-mir-101-2, U6 spliceosomal RNA, microRNA

26b, Small nucleolar RNA SNORD30, Small nucleolar RNA SNORD96 family, Small nucleolar RNA SNORD27, Small nucleolar RNA SNORD58, ENSSSCG00000018067, ENSSSCG00000018085, ENSSSCG00000018746, ENSSSCG00000027476, ENSSSCG00000039268, ENSSSCG00000038150, ENSSSCG00000040158, ENSSSCG00000038924, and ENSSSCG00000035331, respectively, and 19 unannotated transcript (ENSSSCT00000020179.3, ENSSSCT00000037492.1, ENSSSCT00000039452.1, ENSSSCT00000039920.1, ENSSSCT00000042978.1, ENSSSCT00000044673.1, ENSSSCT00000045294.1, ENSSSCT00000048121.1, ENSSSCT00000049792.1, ENSSSCT00000049975.1, ENSSSCT00000052705.1, ENSSSCT00000053008.1, ENSSSCT00000053796.1, ENSSSCT00000056393.1, ENSSSCT00000056706.1, ENSSSCT00000059464.1, ENSSSCT00000060513.1, ENSSSCT00000064785.1, and ENSSSCT00000064915.1) were identified (Table 13).

Table 13. Identification of differentially expressed upregulated miRNA-transcripts (miRNA DETs) of porcine liver by comparing normal and PUFA diets in PL pigs. **Ensembl ID** – ensemble transcript stable ID; **I vs III p-value** – p-value; **I vs III adj p-value** – adjusted p-value; **Chr** – Chromosome/scaffold name; **Start** – transcript start (bp); **End** – transcript end (bp); **TL** – transcript length (including UTRs and CDS); **TT** – Transcript type

Ensembl ID	log2FC	p-value adjusted	Gene stable ID	Gene description	Chr	Start	End	TL	Gene name	Transcript name	TT	Source (transcript)
ENSSSCT00000020150.2	-2.767269866	0.00176622	ENSSSCG00000018555	ssc-mir-21	12	36065267	36065358	92	ssc-mir-21	ssc-mir-21.1-201	miRNA	ensembl
ENSSSCT00000020276.4	-2.776271596	0.00157564	ENSSSCG00000018681	ENSSSCG00000018681	11	60735343	60735449	107			miRNA	ensembl
ENSSSCT00000020693.2	-2.807111244	0.00145344	ENSSSCG00000019098	ssc-let-7f-1	X	46303245	46303327	83	ssc-let-7f-1	ssc-let-7f-1.1-201	miRNA	ensembl
ENSSSCT00000020760.3	-2.703578431	0.00161818	ENSSSCG00000019165	ssc-mir-143	2	150578738	150578817	80	ssc-mir-143	ssc-mir-143.1-201	miRNA	ensembl
ENSSSCT00000030019.2	-4.645754442	0.00843320	ENSSSCG00000028234	ssc-mir-378-2	12	36947443	36947510	68	ssc-mir-378-2	ssc-mir-378-2.1-201	miRNA	ensembl
ENSSSCT00000037189.3	4.517427521	0.00964350	ENSSSCG00000039286	ENSSSCG00000039286	5	73909240	73947423	2198			lncRNA	ensembl
ENSSSCT00000037621.3	4.942934806	0.00728843	ENSSSCG00000032483	ENSSSCG00000032483	4	940756	944661	2754			lncRNA	ensembl
ENSSSCT00000046577.2	-2.419465447	0.0010416	ENSSSCG00000031748	microRNA 22	12	47913326	47913419	94	MIR22	MIR22-201	miRNA	ensembl
ENSSSCT00000040180.1	6.220646333	0.00413205	ENSSSCT00000040180.1	ENSSSCT00000040180								
ENSSSCT00000047143.1	8.078133136	0.00018454	ENSSSCT00000047143.1	ENSSSCT00000047143								
ENSSSCT00000019662.1	-2.704793402	0.04550025	ENSSSCG00000018067	ENSSSCG00000018067	MT	4943	5015	73			mt_tRNA	RefSeq
ENSSSCT00000019680.1	2.660062536	0.04790463	ENSSSCG00000018085	ENSSSCG00000018085	MT	11000	11068	69			mt_tRNA	RefSeq
ENSSSCT00000020051.2	-4.221569048	0.03279744	ENSSSCG00000018456	small nucleolar RNA, C/D box 49A	12	59133725	59133795	71	SNORD49A	SNORD49A-201	snoRNA	ensembl
ENSSSCT00000020115.3	-3.431178191	0.04273265	ENSSSCG00000018520	ssc-let-7f-2	3	43466027	43466133	107	ssc-let-7f-2	ssc-let-7f-2.1-201	miRNA	ensembl
ENSSSCT00000020293.2	-3.943998388	0.01826282	ENSSSCG00000018698	ssc-mir-221	X	40571068	40571137	70	ssc-mir-221	ssc-mir-221.1-201	miRNA	ensembl
ENSSSCT00000020341.2	-3.784932123	0.03704792	ENSSSCG00000018746	ENSSSCG00000018746	13	124584327	124584395	69			snoRNA	ensembl
ENSSSCT00000020429.3	-1.873914853	0.03890090	ENSSSCG00000018834	ssc-mir-181a-2	1	265497249	265497328	80	ssc-mir-181a-2	ssc-mir-181a-2.1-201	miRNA	ensembl
ENSSSCT00000020543.2	-4.157981832	0.03628083	ENSSSCG00000025540	Small nucleolar RNA Z195/SNORD33/SNORD32 family	6	54567160	54567240	81	SNORD33	SNORD33.1-201	snoRNA	ensembl
ENSSSCT00000020789.2	-3.761676095	0.04944999	ENSSSCG00000019194	small nucleolar RNA, C/D box 104	12	14867961	14868029	69	SNORD104	SNORD104-201	snoRNA	ensembl
ENSSSCT00000020885.2	-4.015388502	0.03412846	ENSSSCG00000019290	small nucleolar RNA, C/D box 45A	6	137532264	137532346	83	SNORD45A	SNORD45A-201	snoRNA	ensembl
ENSSSCT00000021207.2	-4.324164093	0.04812325	ENSSSCG00000019612	Small nucleolar RNA SNORD24	9	116147907	116147988	82	SNORD24	SNORD24.1-201	snoRNA	ensembl
ENSSSCT00000021363.2	3.738089399	0.03016138	ENSSSCG00000019768	U12 minor spliceosomal RNA	5	6174022	6174171	150	U12	U12.2-201	snRNA	ensembl
ENSSSCT00000021378.2	-4.356976473	0.0354446	ENSSSCG00000019783	Small nucleolar RNA SNORD42	12	44957658	44957724	67	SNORD42	SNORD42.1-201	snoRNA	ensembl
ENSSSCT00000021393.3	-2.156717422	0.0429646	ENSSSCG00000019798	ssc-let-7a-1	9	49152586	49152665	80	ssc-let-7a-1	ssc-let-7a-1.1-201	miRNA	ensembl
ENSSSCT00000021585.2	-2.976462713	0.01017812	ENSSSCG00000019990	ssc-mir-101-2	6	147330890	147330972	83	ssc-mir-101-2	ssc-mir-101-2.1-201	miRNA	ensembl
ENSSSCT00000022233.2	3.889596672	0.02332865	ENSSSCG00000020638	U6 spliceosomal RNA	4	58090164	58090267	104	U6	U6.329-201	snRNA	ensembl
ENSSSCT00000024283.2	-2.042156662	0.02541765	ENSSSCG00000022650	microRNA 26b	15	120453406	120453490	85	MIR26B	MIR26B-201	miRNA	ensembl
ENSSSCT00000025292.2	-4.292613164	0.0179882	ENSSSCG00000023669	Small nucleolar RNA SNORD30	2	8921535	8921604	70	SNORD30	SNORD30.1-201	snoRNA	ensembl
ENSSSCT00000025348.2	-3.603631144	0.0490911	ENSSSCG00000023739	Small nucleolar RNA SNORD96	2	57281755	57281833	79	SNORD96	SNORD96.1-201	snoRNA	ensembl

ENSSSCT00000029220.2	-4.857099984	0.01390021	ENSSSCG00000027476	ENSSSCG00000027476	17	50961554	50961643	90			snoRNA	ensembl
ENSSSCT00000030080.2	-3.61296361	0.03988472	ENSSSCG00000028290	Small nucleolar RNA SNORD27	2	8920141	8920216	76	SNORD27	SNORD27.1-201	snoRNA	ensembl
ENSSSCT00000032070.2	-3.986071318	0.04360912	ENSSSCG00000030194	Small nucleolar RNA SNORD58	1	99045184	99045247	64	SNORD58	SNORD58.3-201	snoRNA	ensembl
ENSSSCT00000039323.3	4.456611529	0.0152377	ENSSSCG00000039268	ENSSSCG00000039268	8	46865920	46919752	1035			lncRNA	ensembl
ENSSSCT00000041574.2	2.749067145	0.03422188	ENSSSCG00000038150	ENSSSCG00000038150	10	28893934	28995455	2903			lncRNA	ensembl
ENSSSCT00000044072.1	-4.115916794	0.04462300	ENSSSCG00000040158	ENSSSCG00000040158	9	116148144	116148205	62			snoRNA	ensembl
ENSSSCT00000049986.3	3.755328578	0.03867069	ENSSSCG00000038924	ENSSSCG00000038924	2	18618271	18726355	698			lncRNA	ensembl
ENSSSCT00000057520.3	5.177258208	0.01153114	ENSSSCG00000035331	ENSSSCG00000035331	7	21176239	21182879	1784			lncRNA	ensembl
ENSSSCT00000020179.3	-4.356141239	0.03818228	unannotated									
ENSSSCT00000037492.1	5.168103278	0.01482833	unannotated									
ENSSSCT00000039452.1	4.279096775	0.02796752	unannotated									
ENSSSCT00000039920.1	3.753070401	0.02106667	unannotated									
ENSSSCT00000042978.1	3.344662416	0.02459289	unannotated									
ENSSSCT00000044673.1	3.12449284	0.03044528	unannotated									
ENSSSCT00000045294.1	4.624551848	0.03836832	unannotated									
ENSSSCT00000048121.1	3.340881576	0.02127210	unannotated									
ENSSSCT00000049792.1	6.130751855	0.01328847	unannotated									
ENSSSCT00000049975.1	3.492584354	0.03102767	unannotated									
ENSSSCT00000052705.1	5.199483615	0.02341131	unannotated									
ENSSSCT00000053008.1	4.432647924	0.01814656	unannotated									
ENSSSCT00000053796.1	-3.2556102	0.04261189	unannotated									
ENSSSCT00000056393.1	4.901919392	0.04018439	unannotated									
ENSSSCT00000056706.1	3.33791513	0.02638116	unannotated									
ENSSSCT00000059464.1	3.488113151	0.03327652	unannotated									
ENSSSCT00000060513.1	2.814464813	0.01546186	unannotated									
ENSSSCT00000064785.1	3.144504553	0.03150255	unannotated									
ENSSSCT00000064915.1	6.247008421	0.01236864	unannotated									

4.1.4.2. Identification of upregulated DE-miRNA transcripts (log2FC > 2) in liver transcriptome by comparing the control diet in PL pigs vs PUFA diet in PLxDuroc pigs

By comparing the control diet in PL pigs vs PUFAs diet in PLxDuroc pigs, results revealed the identification of 16 upregulated DE-miRNA transcripts with log2FC > 2 in liver transcriptome. Using the BioMart ensembl (https://www.ensembl.org/biomart/martview/), 16 annotated DE-miRNA transcript namely: small nucleolar RNA, C/D box 49A, small nucleolar RNA, H/ACA box 20, small nucleolar RNA, H/ACA box 68, Small nucleolar RNA Z195/SNORD33/SNORD32 family, small nucleolar RNA, C/D box 45A, Small nucleolar RNA SNORD24, Small nucleolar RNA SNORD42, Small nucleolar RNA Z195/SNORD33/SNORD32 family, small nucleolar RNA, H/ACA box 2C, Small nucleolar RNA SNORD30, small nucleolar RNA, C/D box 99, ssc-mir-378-2, ENSSSCG00000019135, ENSSSCG00000027476, ENSSSCG00000040158, and ENSSSCT00000020179, respectively, were identified (Table 14).

Table 14. Identification of differentially expressed upregulated miRNA-transcripts (miRNA DETs) of porcine liver by comparing normal and PUFA diets in PL pigs. Presented transcripts with log2FC > 2. **Ensembl ID** – ensemble transcript stable ID; **log2FC** – Log2 Fold change between group I and III; **Chr** – Chromosome/scaffold name; **Start** – transcript start (bp); **End** – transcript end (bp); **TL** – transcript length (including UTRs and CDS); **TT** – Transcript type

ensembl Transcript stable ID	log2FC	p-value adjusted	Gene stable ID	Gene description	Chr	Start	end	TL	Gene name	Transcript name	TT	Source (transcript)
ENSSSCT00000020051.2	-4.22157	0.032797	ENSSSCG00000018456	small nucleolar RNA, C/D box 49A	12	59133725	59133795	71	SNORD49A	SNORD49A-201	snoRNA	ensembl
ENSSSCT00000020200.2	-4.08676	0.114717	ENSSSCG00000018605	small nucleolar RNA, H/ACA box 20	1	7599025	7599157	133	SNORA20	SNORA20-201	snoRNA	ensembl
ENSSSCT00000020280.2	-4.39565	#N/D!	ENSSSCG00000018685	small nucleolar RNA, H/ACA box 68	2	59893333	59893465	133	SNORA68	SNORA68-201	snoRNA	ensembl
ENSSSCT00000020543.2	-4.15798	0.036281	ENSSSCG00000025540	Small nucleolar RNA Z195/SNORD33/SNORD32 family	6	54567160	54567240	81	SNORD33	SNORD33.1-201	snoRNA	ensembl
ENSSSCT00000020730.2	-4.13141	0.067696	ENSSSCG00000019135	ENSSSCG00000019135	1	54632246	54632315	70			snoRNA	ensembl
ENSSSCT00000020885.2	-4.01539	0.034128	ENSSSCG00000019290	small nucleolar RNA, C/D box 45A	6	137532264	137532346	83	SNORD45A	SNORD45A-201	snoRNA	ensembl
ENSSSCT00000021207.2	-4.32416	0.048123	ENSSSCG00000019612	Small nucleolar RNA SNORD24	9	116147907	116147988	82	SNORD24	SNORD24.1-201	snoRNA	ensembl
ENSSSCT00000021378.2	-4.35698	0.035445	ENSSSCG00000019783	Small nucleolar RNA SNORD42	12	44957658	44957724	67	SNORD42	SNORD42.1-201	snoRNA	ensembl
ENSSSCT00000021469.2	-4.7093	#N/D!	ENSSSCG00000028483	Small nucleolar RNA Z195/SNORD33/SNORD32 family	6	54566454	54566537	84	SNORD33	SNORD33.2-201	snoRNA	ensembl
ENSSSCT00000022128.3	-5.46287	#N/D!	ENSSSCG00000020533	small nucleolar RNA, H/ACA box 2C	5	79282507	79282645	139	SNORA2C	SNORA2C-201	snoRNA	ensembl
ENSSSCT00000025292.2	-4.29261	0.017988	ENSSSCG00000023669	Small nucleolar RNA SNORD30	2	8921535	8921604	70	SNORD30	SNORD30.1-201	snoRNA	ensembl
ENSSSCT00000029029.2	-4.15911	0.056603	ENSSSCG00000027280	small nucleolar RNA, C/D box 99	6	85593936	85594009	74	SNORD99	SNORD99-201	snoRNA	ensembl
ENSSSCT00000029220.2	-4.8571	0.0139	ENSSSCG00000027476	ENSSSCG00000027476	17	50961554	50961643	90			snoRNA	ensembl
ENSSSCT00000030019.2	-4.64575	0.008433	ENSSSCG00000028234	ssc-mir-378-2	12	36947443	36947510	68	ssc-mir-378-2	ssc-mir-378-2.1-201	miRNA	ensembl
ENSSSCT00000044072.1	-4.11592	0.044623	ENSSSCG00000040158	ENSSSCG00000040158	9	116148144	116148205	62			snoRNA	ensembl
ENSSSCT00000020179.3	-4.35614	0.038182	ENSSSCT00000020179.3	ENSSSCT00000020179								

4.1.4.3. Identification of downregulated DE-miRNA transcripts (log2FC > 2) in liver transcriptome by comparing the control diet in PL pigs vs PUFAs diet in PLxDuroc pigs

By comparing the control diet in PL pigs vs PUFAs diet in PLxDuroc pigs, results revealed the identification of 26 downregulated DE-miRNA transcripts with log2FC > 2 in liver transcriptome (Table 15). Using the BioMart ensembl (https://www.ensembl.org/biomart/martview/), 6 annotated DE-MiRNA transcript namely: microRNA 10b, U2 spliceosomal RNA, ENSSSCG00000039286, ENSSSCG00000032483, ENSSSCG00000039268, and ENSSSCG00000035331, respectively, and 20 unannotated transcript (ENSSSCT00000021768.2, ENSSSCT00000037492.1, ENSSSCT00000039452.1, ENSSSCT00000040180.1, ENSSSCT00000041092.1, ENSSSCT00000043006.1, ENSSSCT00000043469.1, ENSSSCT00000045294.1, ENSSSCT00000046899.1, ENSSSCT00000047143.1, ENSSSCT00000047849.1, ENSSSCT00000049792.1, ENSSSCT00000050593.1, ENSSSCT00000052705.1, ENSSSCT00000053008.1, ENSSSCT00000056041.1, ENSSSCT00000056393.1, ENSSSCT00000060831.1, ENSSSCT00000064750.1, and ENSSSCT00000064915.1) were identified (Table 15).

Table 15. Identification of differentially expressed downregulated miRNA-transcripts (miRNA DETs) of porcine liver by comparing normal and PUFA diets in PL pigs. Transcript presented with log2FC > 2. **Ensembl ID** – ensemble transcript stable ID; **log2FC** – Log2 Fold change between group I and II; **Chr** – Chromosome/scaffold name; **Start** – transcript start (bp); **End** – transcript end (bp); **TL** – transcript length (including UTRs and CDS); **TT** – Transcript type

Ensembl id	log2FC	p-value adjusted	Gene stable ID	Gene description	Chr	Start	End	TL	Gene name	Transcript name	Transcript type	Source (transcript)
ENSSSCT00000021537.3	4.421655	#N/D!	ENSSSCG00000019942	microRNA 10b	15	81951636	81951736	101	MIR10B	MIR10B-201	miRNA	ensembl
ENSSSCT00000037189.3	4.517428	0.009644	ENSSSCG00000039286	ENSSSCG00000039286	5	73909240	73947423	2198			lncRNA	ensembl
ENSSSCT00000037621.3	4.942935	0.007288	ENSSSCG00000032483	ENSSSCG00000032483	4	940756	944661	2754			lncRNA	ensembl
ENSSSCT00000039323.3	4.456612	0.015238	ENSSSCG00000039268	ENSSSCG00000039268	8	46865920	46919752	1035			lncRNA	ensembl
ENSSSCT00000051313.1	4.45725	0.081902	ENSSSCG00000063550	U2 spliceosomal RNA	12	19671184	19671374	191	U2	U2.104-201	snRNA	ensembl
ENSSSCT00000057520.3	5.177258	0.011531	ENSSSCG00000035331	ENSSSCG00000035331	7	21176239	21182879	1784			lncRNA	ensembl
ENSSSCT00000021768.2	4.477067	0.071344	unannotated									
ENSSSCT00000037492.1	5.168103	0.014828	unannotated									
ENSSSCT00000039452.1	4.279097	0.027968	unannotated									
ENSSSCT00000040180.1	6.220646	0.004132	unannotated									
ENSSSCT00000041092.1	4.534729	#N/D!	unannotated									
ENSSSCT00000043006.1	4.210782	0.085893	unannotated									
ENSSSCT00000043469.1	4.39828	0.076481	unannotated									
ENSSSCT00000045294.1	4.624552	0.038368	unannotated									
ENSSSCT00000046899.1	33.05073	#N/D!	unannotated									
ENSSSCT00000047143.1	8.078133	0.000185	unannotated									
ENSSSCT00000047849.1	4.265206	0.055883	unannotated									
ENSSSCT00000049792.1	6.130752	0.013288	unannotated									
ENSSSCT00000050593.1	5.767864	#N/D!	unannotated									
ENSSSCT00000052705.1	5.199484	0.023411	unannotated									
ENSSSCT00000053008.1	4.432648	0.018147	unannotated									
ENSSSCT00000056041.1	4.45725	0.081902	unannotated									
ENSSSCT00000056393.1	4.901919	0.040184	unannotated									
ENSSSCT00000060831.1	4.45725	0.081902	unannotated									
ENSSSCT00000064750.1	6.706665	0.068173	unannotated									
ENSSSCT00000064915.1	6.247008	0.012369	unannotated									

4.1.5. Identification of DE-miRNA transcripts in liver transcriptome by comparing the PUFAs diets between PL vs PLxDuroc pigs

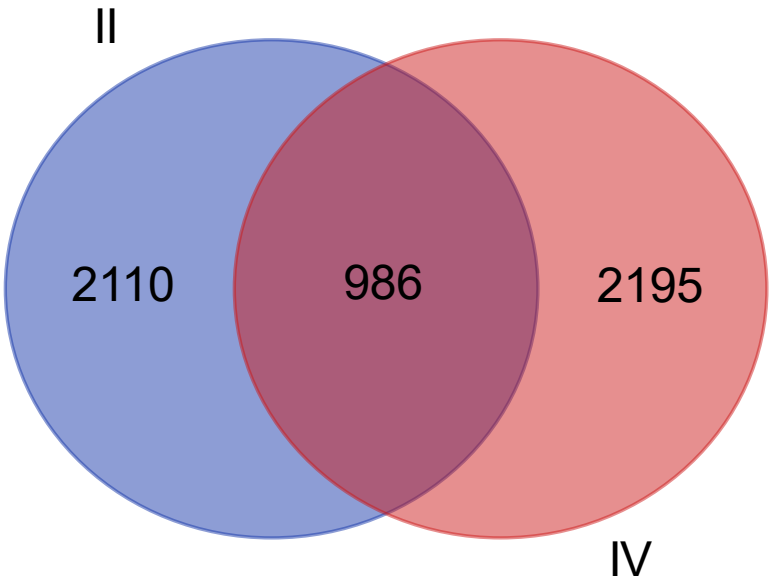

Figure 8. Comparison between the control vs PUFAs diets in PLxDuroc pigs. Group II – PLxDuroc, PUFA diet; Group IV - PL, PUFA diet

By comparing the PUFAs diets between PL vs PLxDuroc pigs, 2110 (PLxDuroc) and 2195 (PL) diet-specific DE-miRNA transcript identified in PL and PLxDuroc pigs (Fig. 7). Furthermore, a total of 986 diet specific DE-miRNA transcript were identified that commonly sheared the PUFAs diets in both PL and PLxDuroc pigs (Fig. 7).

4.1.5.1. Identification of DE-miRNA transcripts ($p > 0.05$) in liver transcriptome by comparing the PUFAs diets between PL vs PLxDuroc pigs

By comparing the PUFAs diets between PL vs PLxDuroc pigs, results revealed the identification of 27 PUFAs-diet-specific DE-MiRNA transcripts with significant cutoff values of $p < 0.05$ (Table 16). Using the BioMart ensembl (https://www.ensembl.org/biomart/martview/), 19 annotated DE-MiRNA transcript namely: microRNA 148a, ssc-let-7a-2, ssc-mir-21, ssc-mir-133a-1, ssc-let-7f-1, microRNA 142, ssc-mir-143, ssc-mir-451, microRNA 27b, ssc-mir-30e, ssc-mir-122, ssc-mir-101-2, ssc-mir-26a, microRNA 26b, ssc-mir-378-2, microRNA 22, ENSSSCG00000018077, ENSSSCG00000018681, and ENSSSCG00000033576, respectively, and 8 unannotated transcript (ENSSSCT00000039099.1, ENSSSCT00000047143.1, ENSSSCT00000050925.1,

ENSSSCT00000051609.1, ENSSSCT00000059159.1, ENSSSCT00000062826.1, ENSSSCT00000063347.1, and ENSSSCT00000063905.1) were identified (Table 16).

Table 16. Identification of differentially expressed miRNA-transcripts (miRNA DETs) of porcine liver by comparing normal and PUFA diets in PL pigs. Presented transcripts with adjusted p-value < 0.05. **Ensembl ID** – ensemble transcript stable ID; **I vs II p-value** – p-value; **I vs II adj p-value** – adjusted p-value; **Chr** – Chromosome/scaffold name; **Start** – transcript start (bp); **End** – transcript end (bp); **TL** – transcript length (including UTRs and CDS); **TT** – Transcript type

Ensembl ID	log2FC	p-value adjusted	Gene stable ID	Gene description	Chr	Start	End	TL	Gene name	Transcript name	Transcript type	Source (transcript)
ENSSSCT00000019672.1	-2.917474732	0.046577	ENSSSCG00000018077	ENSSSCG00000018077	MT	8135	8202	68			Mt_tRNA	RefSeq
ENSSSCT00000019872.3	-2.387514181	0.03808	ENSSSCG00000018277	microRNA 148a	18	46415202	46415281	80	MIR148A	MIR148A-201	miRNA	ensembl
ENSSSCT00000019914.3	-3.411428048	0.023298	ENSSSCG00000018319	ssc-let-7a-2	3	43465667	43465758	92	ssc-let-7a-2	ssc-let-7a-2.1-201	miRNA	ensembl
ENSSSCT00000020150.2	-2.566466769	0.008043	ENSSSCG00000018555	ssc-mir-21	12	36065267	36065358	92	ssc-mir-21	ssc-mir-21.1-201	miRNA	ensembl
ENSSSCT00000020276.4	-2.627394338	0.006636	ENSSSCG00000018681	ENSSSCG00000018681	11	60735343	60735449	107			miRNA	ensembl
ENSSSCT00000020385.2	2.380462163	0.035175	ENSSSCG00000018790	ssc-mir-133a-1	17	61904781	61904883	103	ssc-mir-133a-1	ssc-mir-133a-1.1-201	miRNA	ensembl
ENSSSCT00000020693.2	-2.737150094	0.004664	ENSSSCG00000019098	ssc-let-7f-1	X	46303245	46303327	83	ssc-let-7f-1	ssc-let-7f-1.1-201	miRNA	ensembl
ENSSSCT00000020733.3	-2.965141797	0.018466	ENSSSCG00000019138	microRNA 142	12	34609364	34609468	105	MIR142	MIR142-201	miRNA	ensembl
ENSSSCT00000020760.3	-2.523240725	0.008231	ENSSSCG00000019165	ssc-mir-143	2	150578738	150578817	80	ssc-mir-143	ssc-mir-143.1-201	miRNA	ensembl
ENSSSCT00000020949.3	-3.613241904	0.033347	ENSSSCG00000019354	ssc-mir-451	12	45088808	45088872	65	ssc-mir-451	ssc-mir-451.1-201	miRNA	ensembl
ENSSSCT00000020954.3	-2.164070735	0.024671	ENSSSCG00000019359	microRNA 27b	10	27079954	27080056	103	MIR27B	MIR27B-201	miRNA	ensembl
ENSSSCT00000021088.3	-2.254299557	0.029706	ENSSSCG00000019493	ssc-mir-30e	6	170429841	170429920	80	ssc-mir-30e	ssc-mir-30e.1-201	miRNA	ensembl
ENSSSCT00000021167.3	-2.802098917	0.010657	ENSSSCG00000019572	ssc-mir-122	1	162329767	162329860	94	ssc-mir-122	ssc-mir-122.1-201	miRNA	ensembl
ENSSSCT00000021585.2	-3.13156831	0.014038	ENSSSCG00000019990	ssc-mir-101-2	6	147330890	147330972	83	ssc-mir-101-2	ssc-mir-101-2.1-201	miRNA	ensembl
ENSSSCT00000023905.2	-2.030579438	0.031554	ENSSSCG00000022286	ssc-mir-26a	5	23112744	23112827	84	ssc-mir-26a	ssc-mir-26a.1-201	miRNA	ensembl
ENSSSCT00000024283.2	-2.032000963	0.041167	ENSSSCG00000022650	microRNA 26b	15	120453406	120453490	85	MIR26B	MIR26B-201	miRNA	ensembl
ENSSSCT00000030019.2	-4.156607409	0.027157	ENSSSCG00000028234	ssc-mir-378-2	12	36947443	36947510	68	ssc-mir-378-2	ssc-mir-378-2.1-201	miRNA	ensembl
ENSSSCT00000046577.2	-2.704945336	0.000938	ENSSSCG00000031748	microRNA 22	12	47913326	47913419	94	MIR22	MIR22-201	miRNA	ensembl
ENSSSCT00000050260.2	-2.747361809	0.039582	ENSSSCG00000033576	ENSSSCG00000033576	5	3396405	3396486	82			miRNA	ensembl
ENSSSCT00000039099.1	2.007933874	0.034404	unannotated									
ENSSSCT00000047143.1	4.958848166	0.025753	unannotated									
ENSSSCT00000050925.1	2.129042481	0.00277	unannotated									
ENSSSCT00000051609.1	1.428121508	0.048361	unannotated									
ENSSSCT00000059159.1	-4.718395349	0.033859	unannotated									
ENSSSCT00000062826.1	5.960585114	0.002014	unannotated									
ENSSSCT00000063347.1	2.412368268	0.04335	unannotated									
ENSSSCT00000063905.1	6.861946885	0.000469	unannotated									

4.1.5.2. Identification of upregulated DE-miRNA transcripts (log2FC > 2) in liver transcriptome by comparing PUFAs diets between PL vs PLxDuroc pigs

By comparing the PUFAs diets between PL vs PLxDuroc pigs, results revealed the identification of 15 diet-specific upregulated DE-MiRNA transcripts with log2FC > 2 in liver transcriptome (Table 17). Using the BioMart ensembl (https://www.ensembl.org/biomart/martview/), 6 diet-specific annotated DE-miRNA transcript namely: ssc-mir-378-1, ssc-mir-129b, microRNA 10b, ssc-mir-141, small nucleolar RNA, C/D box 38A, and ENSSSCG00000035331, respectively, and 9 diet-specific unannotated transcript (ENSSSCT00000062826.1, ENSSSCT00000063016.1, ENSSSCT00000063905.1, ENSSSCT00000020834.2, ENSSSCT00000037728.1, ENSSSCT00000047143.1, ENSSSCT00000051559.1, ENSSSCT00000053425.1, and ENSSSCT00000056949.1) were identified (Table 17).

Table 17. Identification of differentially expressed upregulated miRNA-transcripts (miRNA DETs) of porcine liver by comparing the PUFAs diets between PL vs PLxDuroc. Presented transcripts with log2FC > 2. **Ensembl ID** – ensemble transcript stable ID; **log2FC** – Log2 Fold change between group I and II; **Chr** – Chromosome/scaffold name; **Start** – transcript start (bp); **End** – transcript end (bp); **TL** – transcript length (including UTRs and CDS); **TT** – Transcript type

Ensembl	log2FC	p-value adjusted	**Gene stable ID**	**Gene description**	**Chr**	**Start**	**End**	**TL**	**Gene name**	**Transcript name**	**TT**	**Source (transcript)**
ENSSSCT00000020296.3	4.119773	0.259447	ENSSSCG00000018701	ssc-mir-378-1	2	150825865	150825944	80	ssc-mir-378-1	ssc-mir-378-1.1-201	miRNA	ensembl
ENSSSCT00000020421.3	4.244023	0.317806	ENSSSCG00000018826	ssc-mir-129b	18	20157213	20157296	84	ssc-mir-129b	ssc-mir-129b.1-201	miRNA	ensembl
ENSSSCT00000021537.3	5.352338	#N/D!	ENSSSCG00000019942	microRNA 10b	15	81951636	81951736	101	MIR10B	MIR10B-201	miRNA	ensembl
ENSSSCT00000022420.3	4.135064	0.180662	ENSSSCG00000020795	ssc-mir-141	5	63757578	63757642	65	ssc-mir-141	ssc-mir-141.1-201	miRNA	ensembl
ENSSSCT00000054465.3	6.793628	#N/D!	ENSSSCG00000035331	ENSSSCG00000035331	7	21176243	21182724	2020			lncRNA	ensembl
ENSSSCT00000058720.1	4.134938	0.393345	ENSSSCG00000032021	small nucleolar RNA, C/D box 38A	6	166551345	166551414	70	SNORD38A	SNORD38A-201	snoRNA	ensembl
ENSSSCT00000062826.1	5.960585	0.002014	unannotated									
ENSSSCT00000063016.1	4.18894	0.211019	unannotated									
ENSSSCT00000063905.1	6.861947	0.000469	unannotated									
ENSSSCT00000020834.2	4.001157	0.21268	unannotated									
ENSSSCT00000037728.1	4.4535	0.143405	unannotated									
ENSSSCT00000047143.1	4.958848	0.025753	unannotated									
ENSSSCT00000051559.1	5.311728	0.064135	unannotated									
ENSSSCT00000053425.1	4.328716	0.366727	unannotated									
ENSSSCT00000056949.1	6.221025	#N/D!	unannotated									

4.1.5.3. Identification of downregulated DE-miRNA transcripts (log2FC > 2) in liver transcriptome by comparing the PUFAs diets between PL vs PLxDuroc pigs

By comparing the PUFAs diets between PL vs PLxDuroc pigs, results revealed the identification of 22 diet-specific downregulated DE-MiRNA transcripts with log2FC > 2 in liver transcriptome (Table 18). Using the BioMart ensembl (https://www.ensembl.org/biomart/martview/), 17 diet-specific annotated DE-miRNA transcript namely: ssc-let-7a-2, microRNA 99b, microRNA 129-2, ssc-mir-451, Small nucleolar RNA SNORA70, Small nucleolar RNA SNORD24, microRNA 199b, Small nucleolar RNA SNORD83, ssc-mir-101-2, small nucleolar RNA, H/ACA box 2C, ssc-mir-378-2, Small nucleolar RNA SNORD36, Small nucleolar RNA SNORD116, ENSSSCG00000027476, ENSSSCG00000018229, ENSSSCG00000018942, and ENSSSCG00000036117, respectively, and 5 diet-specific unannotated transcript (ENSSSCT00000029616.2, ENSSSCT00000037207.1, ENSSSCT00000039186.1, ENSSSCT00000043456.1, and ENSSSCT00000059159.1) were identified (Table 18).

Table 18. Identification of differentially expressed downregulated miRNA-transcripts (miRNA DETs) of porcine liver by comparing the PUFAs diets between PL vs PLxDuroc pigs. Presented transcripts with log2FC > 2 **Ensembl ID** – ensemble transcript stable ID; **log2FC** – Log2 Fold change between group I and II; **Chr** – Chromosome/scaffold name; **Start** – transcript start (bp); **End** – transcript end (bp); **TL** – transcript length (including UTRs and CDS); **TT** – Transcript type

Ensembl ID	log2FC	p-value adjusted	Gene stable ID	Gene description	Chr	Start	End	TL	Gene name	Transcript name	TT	Source (transcript)
ENSSSCT00000019824.2	-3.08354	0.091964	ENSSSCG00000018229	ENSSSCG00000018229	9	116148715	116148792	78			snoRNA	ensembl
ENSSSCT00000019914.3	-3.41143	0.023298	ENSSSCG00000018319	ssc-let-7a-2	3	43465667	43465758	92	ssc-let-7a-2	ssc-let-7a-2.1-201	miRNA	ensembl
ENSSSCT00000020330.3	-3.10146	0.155781	ENSSSCG00000018735	microRNA 99b	6	58332205	58332284	80	MIR99B	MIR99B-201	miRNA	ensembl
ENSSSCT00000020537.2	-3.08848	0.216388	ENSSSCG00000018942	ENSSSCG00000018942	9	116147558	116147623	66			snoRNA	ensembl
ENSSSCT00000020716.3	-3.38637	0.114723	ENSSSCG00000019121	microRNA 129-2	2	18724213	18724304	92	MIR129-2	MIR129-2-201	miRNA	ensembl
ENSSSCT00000020949.3	-3.61324	0.033347	ENSSSCG00000019354	ssc-mir-451	12	45088808	45088872	65	ssc-mir-451	ssc-mir-451.1-201	miRNA	ensembl
ENSSSCT00000021160.2	-3.36496	0.238029	ENSSSCG00000019565	Small nucleolar RNA SNORA70	11	45234930	45235068	139	SNORA70	SNORA70.5-201	snoRNA	ensembl
ENSSSCT00000021207.2	-3.11358	0.202589	ENSSSCG00000019612	Small nucleolar RNA SNORD24	9	116147907	116147988	82	SNORD24	SNORD24.1-201	snoRNA	ensembl
ENSSSCT00000021339.2	-3.57908	0.32643	ENSSSCG00000019744	microRNA 199b	1	268691502	268691610	109	MIR199B	MIR199B-201	miRNA	ensembl
ENSSSCT00000021375.2	-3.03339	0.164381	ENSSSCG00000019780	Small nucleolar RNA SNORD83	7	23668175	23668252	78	SNORD83	SNORD83.2-201	snoRNA	ensembl
ENSSSCT00000021585.2	-3.13157	0.014038	ENSSSCG00000019990	ssc-mir-101-2	6	147330890	147330972	83	ssc-mir-101-2	ssc-mir-101-2.1-201	miRNA	ensembl
ENSSSCT00000022128.3	-3.45353	#N/D!	ENSSSCG00000020533	small nucleolar RNA, H/ACA box 2C	5	79282507	79282645	139	SNORA2C	SNORA2C-201	snoRNA	ensembl
ENSSSCT00000029220.2	-3.12206	0.156137	ENSSSCG00000027476	ENSSSCG00000027476	17	50961554	50961643	90			snoRNA	ensembl
ENSSSCT00000030019.2	-4.15661	0.027157	ENSSSCG00000028234	ssc-mir-378-2	12	36947443	36947510	68	ssc-mir-378-2	ssc-mir-378-2.1-201	miRNA	ensembl
ENSSSCT00000053894.1	-3.23044	0.139423	ENSSSCG00000037405	Small nucleolar RNA SNORD36	1	272964782	272964854	73	SNORD36	SNORD36.2-201	snoRNA	ensembl
ENSSSCT00000056470.1	-3.6337	0.114838	ENSSSCG00000032033	Small nucleolar RNA SNORD116	AEMK02000602.1	42147	42239	93	SNORD116	SNORD116.1-201	snoRNA	ensembl
ENSSSCT00000062744.1	-4.59347	0.099067	ENSSSCG00000036117	ENSSSCG00000036117	10	66741325	66971746	2449			lncRNA	ensembl
ENSSSCT00000029616.2	-3.61497	0.216695	unannotated									
ENSSSCT00000037207.1	-3.44623	0.278302	unannotated									
ENSSSCT00000039186.1	-3.44256	0.341637	unannotated									
ENSSSCT00000043456.1	-3.14684	0.099547	unannotated									
ENSSSCT00000059159.1	-4.7184	0.033859	unannotated									

4.1.6. Identification of DE-miRNA transcripts in liver transcriptome by comparing the control vs PUFAs diets in PL pigs

By comparing the control vs PUFAs diets in PL pigs, 1844 (Control) and 2162 (PUFAs) diet-specific DE-miRNA transcript identified in PL pigs (Fig. 8). Furthermore, a total of 1019 diet-specific DE-miRNA transcript were identified that commonly sheared in both control vs PUFAs diets of PL pigs (Fig. 8).

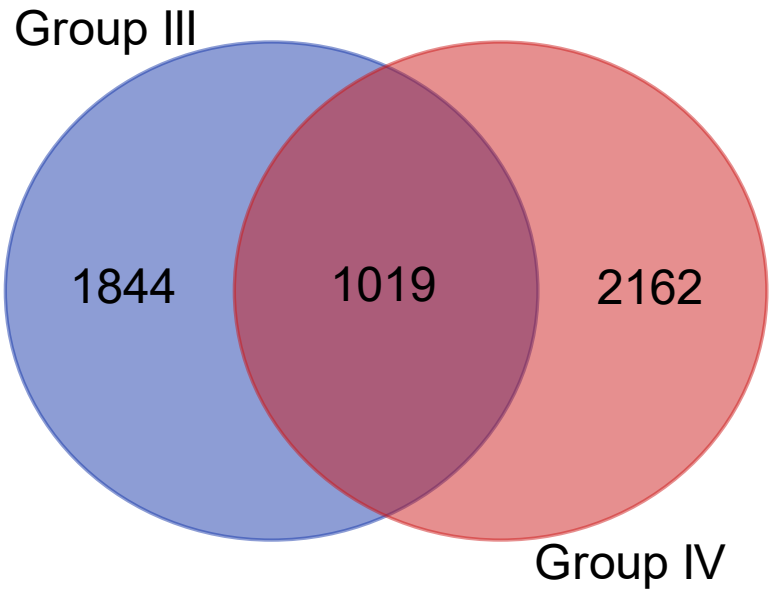

Figure 9. Comparison between the control vs PUFAs diets in PL pigs. **Group III –** PL, control**; Group IV –** PL, PUFA Diet

4.1.6.1. Identification of DE-miRNA transcripts ($p < 0.05$) in liver transcriptome by comparing the control vs PUFAs diets in PL pigs

By comparing the control vs PUFAs diets in PL pigs, results revealed the identification of 34 diet-specific DE-miRNA transcripts with significant cutoff values of $p < 0.05$ (Table 19). Using the BioMart ensembl (https://www.ensembl.org/biomart/martview/), 16 diet-specific annotated DE-MiRNA transcript namely: U12 minor spliceosomal RNA, U6 spliceosomal RNA, ENSSSCG00000018077, ENSSSCG00000039286, ENSSSCG00000040330, and ENSSSCG00000035331, (all $p < 0.01$), ssc-mir-214, ssc-mir-181a-1, small nucleolar RNA, C/D box 37, Small nucleolar RNA SNORD116, ENSSSCG00000018073, ENSSSCG00000018085, ENSSSCG00000032483, ENSSSCG00000039268, ENSSSCG00000038924, and ENSSSCG00000037794 (all $p < 0.05$), respectively, and 18 diet-specific unannotated transcript (ENSSSCT00000037492.1, ENSSSCT00000040180.1,

ENSSSCT00000050925.1, ENSSSCT00000063905.1, ENSSSCT00000020968.2, ENSSSCT00000024894.2, ENSSSCT00000025078.2, ENSSSCT00000025229.2, ENSSSCT00000043491.1, ENSSSCT00000043594.1, ENSSSCT00000049792.1, ENSSSCT00000049859.1, ENSSSCT00000051559.1, ENSSSCT00000053008.1, ENSSSCT00000056706.1, ENSSSCT00000057013.1, ENSSSCT00000062826.1, and ENSSSCT00000064915.1) were identified (Table 19).

Table 19. Identification of differentially expressed miRNA-transcripts (miRNA DETs) of porcine liver by comparing the control vs PUFAs diets in PL pigs. Presenting transcripts with adjusted p-value < 0.05. **Ensembl ID** – ensemble transcript stable ID; **I vs II p-value** – p-value; **I vs II adj p-value** – adjusted p-value; **Chr** – Chromosome/scaffold name; **Start** – transcript start (bp); **End** – transcript end (bp); **TL** – transcript length (including UTRs and CDS); **TT** – Transcript type

Ensembl ID	log2FC	p-value adjusted	Gene stable ID	Gene description	Chr	Start	End	TL	Gene name	Transcript name	TT	Source (transcript)
ENSSSCT00000019672.1	-4.651549918	0.002562	ENSSSCG00000018077	ENSSSCG00000018077	MT	8135	8202	68			mt_tRNA	RefSeq
ENSSSCT00000021363.2	-4.99162682	0.005599	ENSSSCG00000019768	U12 minor spliceosomal RNA	5	6174022	6174171	150	U12	U12.2-201	snRNA	ensembl
ENSSSCT00000022233.2	-4.55450709	0.008727	ENSSSCG00000020638	U6 spliceosomal RNA	4	58090164	58090267	104	U6	U6.329-201	snRNA	ensembl
ENSSSCT00000037189.3	-5.276999266	0.004366	ENSSSCG00000039286	ENSSSCG00000039286	5	73909240	73947423	2198			lncRNA	ensembl
ENSSSCT00000055228.3	-2.542014321	0.007985	ENSSSCG00000040330	ENSSSCG00000040330	14	26611666	26621558	3205			lncRNA	ensembl
ENSSSCT00000057520.3	-6.582343309	0.002944	ENSSSCG00000035331	ENSSSCG00000035331	7	21176239	21182879	1784			lncRNA	ensembl
ENSSSCT00000019668.1	-2.886846654	0.033012	ENSSSCG00000018073	ENSSSCG00000018073	MT	6379	6444	66			mt_tRNA	RefSeq
ENSSSCT00000019680.1	-2.977233893	0.038613	ENSSSCG00000018085	ENSSSCG00000018085	MT	11000	11068	69			mt_tRNA	RefSeq
ENSSSCT00000020353.3	-3.581646456	0.039942	ENSSSCG00000018758	ssc-mir-214	9	114527990	114528101	112	ssc-mir-214	ssc-mir-214.1-201	miRNA	ensembl
ENSSSCT00000021317.2	-4.271349994	0.03196	ENSSSCG00000019722	ssc-mir-181a-1	10	21696653	21696756	104	ssc-mir-181a-1	ssc-mir-181a-1.1-201	miRNA	ensembl
ENSSSCT00000031566.2	-4.466517552	0.015801	ENSSSCG00000029719	small nucleolar RNA, C/D box 37	2	74749611	74749675	65	SNORD37	SNORD37-201	snoRNA	ensembl
ENSSSCT00000037621.3	-4.850827507	0.013159	ENSSSCG00000032483	ENSSSCG00000032483	4	940756	944661	2754			lncRNA	ensembl
ENSSSCT00000039323.3	-4.269678663	0.027868	ENSSSCG00000039268	ENSSSCG00000039268	8	46865920	46919752	1035			lncRNA	ensembl
ENSSSCT00000049986.3	-3.915273345	0.042725	ENSSSCG00000038924	ENSSSCG00000038924	2	18618271	18726355	698			lncRNA	ensembl
ENSSSCT00000056470.1	-5.522628038	0.01638	ENSSSCG00000032033	Small nucleolar RNA SNORD116	AEMK02000602.1	42147	42239	93	SNORD116	SNORD116.1-201	snoRNA	ensembl
ENSSSCT00000059046.3	-3.247177001	0.029529	ENSSSCG00000037794	ENSSSCG00000037794	Y	7814378	7827973	5086			lncRNA	ensembl
ENSSSCT00000037492.1	-6.06944286	0.007557	unannotated									
ENSSSCT00000040180.1	-6.777448078	0.003945	unannotated									
ENSSSCT00000050925.1	2.172906531	0.002111	unannotated									
ENSSSCT00000063905.1	6.403637962	0.001088	unannotated									
ENSSSCT00000020968.2	-2.994311048	0.037112	unannotated									
ENSSSCT00000024894.2	2.243387814	0.038123	unannotated									
ENSSSCT00000025078.2	4.379370668	0.0293	unannotated									
ENSSSCT00000025229.2	-3.328536196	0.022238	unannotated									
ENSSSCT00000043491.1	-3.999053524	0.048878	unannotated									
ENSSSCT00000043594.1	-4.496376191	0.038382	unannotated									
ENSSSCT00000049792.1	-6.51668266	0.015959	unannotated									
ENSSSCT00000049859.1	1.803393294	0.034517	unannotated									
ENSSSCT00000051559.1	5.605743904	0.049225	unannotated									
ENSSSCT00000053008.1	-4.308987988	0.029926	unannotated									
ENSSSCT00000056706.1	-3.720484906	0.016889	unannotated									
ENSSSCT00000057013.1	-4.791368929	0.020755	unannotated									
ENSSSCT00000062826.1	4.801441496	0.013605	unannotated									
ENSSSCT00000064915.1	-6.345020307	0.020181	unannotated									

4.1.6.2. Identification of upregulated DE-miRNA transcripts (log2FC > 2) in liver transcriptome by comparing the control vs PUFAs diets in PL pigs

By comparing the control vs PUFAs diets in PL pigs, results revealed the identification of 29 diet-specific upregulated DE-miRNA transcripts with log2FC > 2 in liver transcriptome (Table 20). Using the BioMart ensembl (https://www.ensembl.org/biomart/martview/), 13 diet-specific annotated DE-MiRNA transcript namely: small nucleolar RNA, C/D box 112, ssc-mir-24-1, U1 spliceosomal RNA, small nucleolar RNA, C/D box 113-8, Small nucleolar RNA SNORD18, ssc-mir-30c-2, Small nucleolar RNA SNORD28, ENSSSCG00000020451, ENSSSCG00000035515, ENSSSCG00000061501, ENSSSCG00000037773, ENSSSCG00000035331, and ENSSSCG00000034303, respectively, and 16 diet-specific unannotated transcript (ENSSSCT00000020430.2, ENSSSCT00000020921.2, ENSSSCT00000021165.2, ENSSSCT00000025078.2, ENSSSCT00000037728.1, ENSSSCT00000047221.1, ENSSSCT00000049767.1, ENSSSCT00000051559.1, ENSSSCT00000052244.1, ENSSSCT00000053804.1, ENSSSCT00000057339.1, ENSSSCT00000059587.1, ENSSSCT00000059834.1, ENSSSCT00000062826.1, ENSSSCT00000063905.1, and ENSSSCT00000063950.1) were identified (Table 20).

Table 20. Identification of differentially expressed upregulated miRNA-transcripts (miRNA DETs) of porcine liver by comparing the control vs PUFAs diets in PL pigs. Transcripts with log2FC > 2 are presented. **Ensembl ID** – ensemble transcript stable ID; **log2FC** – Log2 Fold change between group I and II; **Chr** – Chromosome/scaffold name; **Start** – transcript start (bp); **End** – transcript end (bp); **TL** – transcript length (including UTRs and CDS); **TT** – Transcript type

Ensembl ID	log2FC	p-value adjusted	Gene stable ID	Gene description	Chr	Start	End	TL	Gene name	Transcript name	TT	Source (transcript)
ENSSSCT00000019774.2	4.503774258	0.219737	ENSSSCG00000018179	small nucleolar RNA, C/D box 112	7	121724050	121724126	77	SNORD112	SNORD112-201	snoRNA	ensembl
ENSSSCT00000019809.2	3.05757386	0.282896	ENSSSCG00000018214	ssc-mir-24-1	2	65308453	65308524	72	ssc-mir-24-1	ssc-mir-24-1.1-201	miRNA	ensembl
ENSSSCT00000020050.2	3.29107388	0.476733	ENSSSCG00000018455	U1 spliceosomal RNA	8	120190361	120190527	167	U1	U1.2-201	snRNA	ensembl
ENSSSCT00000020513.2	3.483008454	0.225765	ENSSSCG00000018918	small nucleolar RNA, C/D box 113-8	7	121781156	121781230	75	SNORD113-8	SNORD113-8-201	snoRNA	ensembl
ENSSSCT00000020521.2	3.482915862	0.224961	ENSSSCG00000018926	Small nucleolar RNA SNORD18	1	164477549	164477618	70	SNORD18	SNORD18.1-201	snoRNA	ensembl
ENSSSCT00000021115.2	4.469660677	0.077674	ENSSSCG00000019520	ssc-mir-30c-2	1	51383782	51383861	80	ssc-mir-30c-2	ssc-mir-30c-2.1-201	miRNA	ensembl
ENSSSCT00000022046.2	3.276922195	0.317634	ENSSSCG00000020451	ENSSSCG00000020451	13	103709223	103709367	145			snoRNA	ensembl
ENSSSCT00000030924.2	3.687557352	0.246832	ENSSSCG00000029095	Small nucleolar RNA SNORD28	2	8920524	8920599	76	SNORD28	SNORD28.2-201	snoRNA	ensembl
ENSSSCT00000041769.1	4.017545716	0.288286	ENSSSCG00000035515	ENSSSCG00000035515	7	121818448	121818520	73			snoRNA	ensembl
ENSSSCT00000042931.1	3.289797247	0.444171	ENSSSCG00000061501	ENSSSCG00000061501	7	121838822	121838893	72			snoRNA	ensembl
ENSSSCT00000046892.1	3.289797247	0.444171	ENSSSCG00000037773	ENSSSCG00000037773	7	121821063	121821134	72			snoRNA	ensembl
ENSSSCT00000054465.3	6.502552145	#N/D!	ENSSSCG00000035331	ENSSSCG00000035331	7	21176243	21182724	2020			lncRNA	ensembl
ENSSSCT00000062677.1	4.501677611	0.138408	ENSSSCG00000034303	ENSSSCG00000034303	AEMK02000452.1	7774	7846	73			snoRNA	ensembl
ENSSSCT00000020430.2	3.950819669	0.188555	unannotated									
ENSSSCT00000020921.2	3.234899929	0.089997	unannotated									
ENSSSCT00000021165.2	3.281833529	0.347977	unannotated									
ENSSSCT00000025078.2	4.379370668	0.0293	unannotated									
ENSSSCT00000037728.1	4.501543218	0.136006	unannotated									
ENSSSCT00000047221.1	3.289797247	0.444171	unannotated									
ENSSSCT00000049767.1	3.289797247	0.444171	unannotated									
ENSSSCT00000051559.1	5.605743904	0.049225	unannotated									
ENSSSCT00000052244.1	3.289797247	0.444171	unannotated									
ENSSSCT00000053804.1	3.289797247	0.444171	unannotated									
ENSSSCT00000057339.1	3.289797247	0.444171	unannotated									
ENSSSCT00000059587.1	3.556341281	0.232927	unannotated									
ENSSSCT00000059834.1	3.109057932	0.191874	unannotated									
ENSSSCT00000062826.1	4.801441496	0.013605	unannotated									
ENSSSCT00000063905.1	6.403637962	0.001088	unannotated									
ENSSSCT00000063950.1	3.094278296	0.180054	unannotated									

4.1.6.3. Identification of dowregulated DE-miRNA transcript (log2FC > 2) in liver transcriptome by comparing the control vs PUFAs diets in PL pigs

By comparing the control vs PUFAs diets in PLxDuroc pigs, results revealed the identification of 27 diet-specific downregulated DE-miRNA transcripts with log2FC > 2 in liver transcriptome (Table 21). Using the BioMart ensembl (https://www.ensembl.org/biomart/martview/), 12 diet-specific annotated DE-miRNA transcript namely: ssc-mir-181a-1, U12 minor spliceosomal RNA, U6 spliceosomal RNA, small nucleolar RNA, C/D box 37, Small nucleolar RNA SNORD116, U6 spliceosomal RNA, ENSSSCG00000018077, ENSSSCG00000039286, ENSSSCG00000032483, ENSSSCG00000039268, ENSSSCG00000035331, and ENSSSCG00000036117, respectively, and 15 diet-specific unannotated transcript (ENSSSCT00000037492.1, ENSSSCT00000040180.1, ENSSSCT00000041092.1, ENSSSCT00000042667.1, ENSSSCT00000043006.1, ENSSSCT00000043469.1, ENSSSCT00000043594.1, ENSSSCT00000046899.1, ENSSSCT00000049792.1, ENSSSCT00000050564.1, ENSSSCT00000050593.1, ENSSSCT00000053008.1, ENSSSCT00000057013.1, ENSSSCT00000064750.1 and ENSSSCT00000064915.1) were identified (Table 21).

Table 21. Identification of differentially expressed downregulated miRNA-transcripts (miRNA DETs) of porcine liver by comparing the control vs PUFAs diets in PL pigs. Transcriptome with log2FC > 2 were presented. **Ensembl ID** – ensemble transcript stable ID; **log2FC** – Log2 Fold change between group I and II; **Chr** – Chromosome/scaffold name; **Start** – transcript start (bp); **End** – transcript end (bp); **TL** – transcript length (including UTRs and CDS); **TT** – Transcript type

Ensembl ID	log2FC	p-value adjusted	Gene stable ID	Gene description	Chr	Start	End	TL	Gene name	Transcript name	TT	Source (transcript)
ENSSSCT00000019672.1	-4.651549918	0.002561999	ENSSSCG00000018077	ENSSSCG00000018077	MT	8135	8202	68			mt_tRNA	RefSeq
ENSSSCT00000021317.2	-4.271349994	0.031959749	ENSSSCG00000019722	ssc-mir-181a-1	10	21696653	21696756	104	ssc-mir-181a-1	ssc-mir-181a-1.1-201	miRNA	ensembl
ENSSSCT00000021363.2	-4.99162682	0.005599493	ENSSSCG00000019768	U12 minor spliceosomal RNA	5	6174022	6174171	150	U12	U12.2-201	snRNA	ensembl
ENSSSCT00000022233.2	-4.55450709	0.008726714	ENSSSCG00000020638	U6 spliceosomal RNA	4	58090164	58090267	104	U6	U6.329-201	snRNA	ensembl
ENSSSCT00000031566.2	-4.466517552	0.015800935	ENSSSCG00000029719	small nucleolar RNA, C/D box 37	2	74749611	74749675	65	SNORD37	SNORD37-201	snoRNA	ensembl
ENSSSCT00000037189.3	-5.276999266	0.004366377	ENSSSCG00000039286	ENSSSCG00000039286	5	73909240	73947423	2198			lncRNA	ensembl
ENSSSCT00000037621.3	-4.850827507	0.013159246	ENSSSCG00000032483	ENSSSCG00000032483	4	940756	944661	2754			lncRNA	ensembl
ENSSSCT00000039323.3	-4.269678663	0.027867692	ENSSSCG00000039268	ENSSSCG00000039268	8	46865920	46919752	1035			lncRNA	ensembl
ENSSSCT00000056470.1	-5.522628038	0.016380195	ENSSSCG00000032033	Small nucleolar RNA SNORD116	AEMK02000602.1	42147	42239	93	SNORD116	SNORD116.1-201	snoRNA	ensembl
ENSSSCT00000057130.1	-4.279833496	0.087805188	ENSSSCG00000040068	U6 spliceosomal RNA	9	73156794	73156870	77	U6	U6.541-201	snRNA	ensembl
ENSSSCT00000057520.3	-6.582343309	0.002944448	ENSSSCG00000035331	ENSSSCG00000035331	7	21176239	21182879	1784			lncRNA	ensembl
ENSSSCT00000062744.1	-5.222101534	0.05541608	ENSSSCG00000036117	ENSSSCG00000036117	10	66741325	66971746	2449			lncRNA	ensembl
ENSSSCT00000037492.1	-6.06944286	0.007557247	unannotated									
ENSSSCT00000040180.1	-6.777448078	0.00394547	unannotated									
ENSSSCT00000041092.1	-4.826996435	#N/D!	unannotated									
ENSSSCT00000042667.1	-4.088847055	0.079463289	unannotated									
ENSSSCT00000043006.1	-4.198300226	0.115792453	unannotated									
ENSSSCT00000043469.1	-4.427266022	0.099190418	unannotated									
ENSSSCT00000043594.1	-4.496376191	0.038381756	unannotated									
ENSSSCT00000046899.1	-31.65455649	#N/D!	unannotated									
ENSSSCT00000049792.1	-6.51668266	0.015958885	unannotated									
ENSSSCT00000050564.1	-4.028166627	0.179149923	unannotated									
ENSSSCT00000050593.1	-6.197573786	#N/D!	unannotated									
ENSSSCT00000053008.1	-4.308987988	0.029925617	unannotated									
ENSSSCT00000057013.1	-4.791368929	0.020755463	unannotated									
ENSSSCT00000064750.1	-7.844685732	0.053947604	unannotated									
ENSSSCT00000064915.1	-6.345020307	0.020180595	unannotated									

4.2. WGCNA analysis of miRNA-Seq of porcine liver representing PL purebred and PLxDuroc crossbred pigs

4.2.1. Design of the WGCNA R script

The WGCNA analysis were performed for 12 samples. For all samples from 4 experimental groups one Co-expression network were created. Group, breed and diet information were added to the samples phenotypic traits to find the potential correlation between detected modules and breed, diet type or experimental group.

The more detailed steps of co-expression network are described in further sections.

4.2.2. Raw expression data preparation and normalization

The matrix of raw counts of miRNAs per sample were used as an input for the WGCNA analysis. MiRNAs were placed in rows and samples in columns. Initially the matrix contained counts for 535 distinct miRNAs for 12 samples.

Firstly, miRNAs with zero counts in each sample were filtered out and were not used in the analysis leaving 226 miRNAs.

The next step was to filter the miRNAs with low number of counts. WGCNA method is sensitive for the samples with low counts numbers which generates statistical noise giving false correlation based on zeros (source: WGCNA package documentation). If the miRNA had a number of counts equal to 0 in ≥ 6 samples, it was removed from the analysis. After applying this filter, 94 of miRNAs were left and used in the analysis.

The counts for 94 miRNAs were normalized using the varinaceStabilizingTransformation function from DESeq2 library. Argument blind were set to “True”, and fit type was set to “local” to obtain the most robust normalization (Anders S. et al., 2010). Prepared data were used further, in WGCNA analysis.

4.2.3. Phenotypic traits description

In WGCNA analysis a total of 34 phenotypic traits were investigated and correlated with identified modules. The investigated traits were connected with the Body growth, meat color, component of meat, content of PUFA acids and other, general meat parameters. The full list of used traits can be found in the table 23 with the abbreviation.

4.2.3.1. Body growth connected traits

The body growth traits used in the analysis are: Body weight at end of fattening, daily gains, Carcass weight, meatiness, backfat thickness, Shoulder subcutaneous fat thickness.

The body weight in kilograms at end of fattening is the final weight of a pig by the end of process of feeding a pig with a diet. Daily gains are the average amount of weight in grams that a pig gained over a 24-hour period. Carcass weight of a pig refers to the weight of the pig's body after it has been slaughtered and processed, excluding the internal organs and head. Meatiness is the proportion of muscle tissue in percentages compared to other tissues such as bone, fat and connective tissue in a pig body. Backfat thickness is a measure of the amount of fat located in the subcutaneous layer of an animal's back. Shoulder subcutaneous fat thickness refers to the thickness of the layer of fat that lies immediately under the skin of the shoulder area of a pig. This trait was measured in mm.

4.2.3.2. Meat color

The meat color parameters investigated in the analysis were L*, a*, b*

The L* parameter in the CIELAB color system is used to describe the lightness or darkness of a color. L* value indicates the extent to which the meat appears light or dark. A higher L* value indicates a lighter color, while a lower L* value indicates a darker color.

In the case of meat, the a* parameter is used to describe the redness of the meat. A higher "a*" value indicates a more intense red color, while a lower a* value indicates a less intense red color.

The "b*" parameter in the CIELAB color system is used to describe the yellow-blue chroma of a color. In the context of meat color, the b* value indicates the extent to which the meat appears yellow or blue. A positive b* value indicates a yellowish color, while a negative b* value indicates a bluish color.

4.2.3.3. Meat components content

The content of fat, protein, ash and dry matter in meat were investigated in the WGCNA analysis.

Fat content in meat refers to the amount of fats present in the tissue. It contributes to the flavor, tenderness, and juiciness of the meat. The fat content was expressed as percentage of the total sample weight.

The protein content as the percentage of total weight of the sample.

Ash content in meat is a measure of the inorganic mineral content of the meat, including elements such as calcium, phosphorus, magnesium, potassium, and sodium. The ash content of meat was expressed as a percentage of the total weight of the sample.

Dry matter describes the total weight of a sample of food material of the water has been removed. It represents the portion of the sample that is made up of the actual food components, such as carbohydrates, proteins, fats, minerals, and vitamins, rather than water.

4.2.3.4. PUFA acids content

In the analysis the content of PUFA acids were analyzed. It included the content of the Lauric Acid, Myristic Acid, Palmitic Acid, Palmitoleic Acid, Stearic Acid, Oleic Acid, Elaidic Acid, Vaccenic Acid, Linoleic Acid, Alpha-Linolenic Acid, Arachidonic Acid, Eicosapentaenoic Acid and Docosahexaenoic Acid. All the mentioned were presented as the percentage content in the liver tissue.

Table 22. The list of PUFA acids included in the WGCNA analysis

Chemical Formula	Full Name	Abbreviation
C12:0	Lauric Acid	LA
C13:0	Myristic Acid	MA
C14:0	Myristoleic Acid	MOA
C16:0	Palmitic Acid	PA
C16:1	Palmitoleic Acid	POA
C18:0	Stearic Acid	SA
C18:1n9	Oleic Acid	OA
C18:1n7	Vaccenic Acid	VA
C18:2n6	Linoleic Acid	LA
C18:3n3	alpha-Linolenic Acid	ALA
C20:4n6	Arachidonic Acid	AA
C20:5n3	Eicosapentaenoic Acid	EPA
C22:6n3	Docosahexaenoic Acid	DHA

Furthermore, the cumulated content of n-3 and n-6 PUFA were investigated.

The n-3 trait is the sum of percentages content of alpha-Linolenic Acid, Eicosapentaenoic Acid, and Docosahexaenoic Acid. The n-6 trait is the sum of percentages of Linoleic Acid and Arachidonic Acid. The n-6/n-3 trait is the ratio of n-6 content to the n-3 acids content.

PUFA trait is the sum of percentage content of all Polyunsaturated Fatty Acids included in the trait list (Linoleic Acid, alpha-Linolenic Acid, Arachidonic Acid, Eicosapentaenoic Acid, Docosahexaenoic Acid).

MUFA trait is the sum of percentage content of all Monounsaturated Fatty Acid acids included in the trait list (Palmitoleic Acid, Oleic Acid, Vaccenic Acid).

SFA traits is the sum of percentage content of all Saturated Fatty Acid included in the trait list (Lauric Acid, Myristic Acid, Myristoleic Acid, Palmitic Acid, Stearic Acid).

PUFA/SFA is the ratio of PUFA to the SFA.

4.2.3.5. Other meat parameters

Other meat parameters included in the analysis were water holding capacity, drip loss, pH 45 minutes postmortem and conductivity 24 hours post mortem.

Water holding capacity is a measure of the ability of meat to retain its juiciness and tenderness during cooking and storage. It is represented by the percentage of water retained in the meat after processing.

Drip loss is the leakage and loss of water, iron and proteins during processing. It is represented as the percentage of weight loss during the process.

pH 45 minutes post mortem is the measurement of pH meat after the dead, where the pH = 7.0 is neutral, lower pH indicates acidity and the higher pH the more alkaline the meat is.

Conductivity 24 hours post mortem is the measurement of electrical conductivity in meat 24 hours after death. It provides an indication of the state of rigor mortis. It is measured in Siemens per meter (S/m).

4.2.4. Clustering dendrogram and heatmap of the investigated phenotypic trait associated with each pigs

Before network construction and module detection, 12 liver transcriptome from PLxDuroc crossbred (group-I: Control: with standard diet and group-II: treated with PUFAs-enriched diet including standard diet + linseed oil + rapeseed oil diets) and PL purebred (group-III: Control: with standard diet and group-IV: treated with PUFAs-enriched diet including standard diet + linseed oil + rapeseed oil diets) pigs were clustered and visualized in a heatmap to define how the body growth related (BW) trait (Table 1) corelated to the sample dendrogram (Fig. 10).

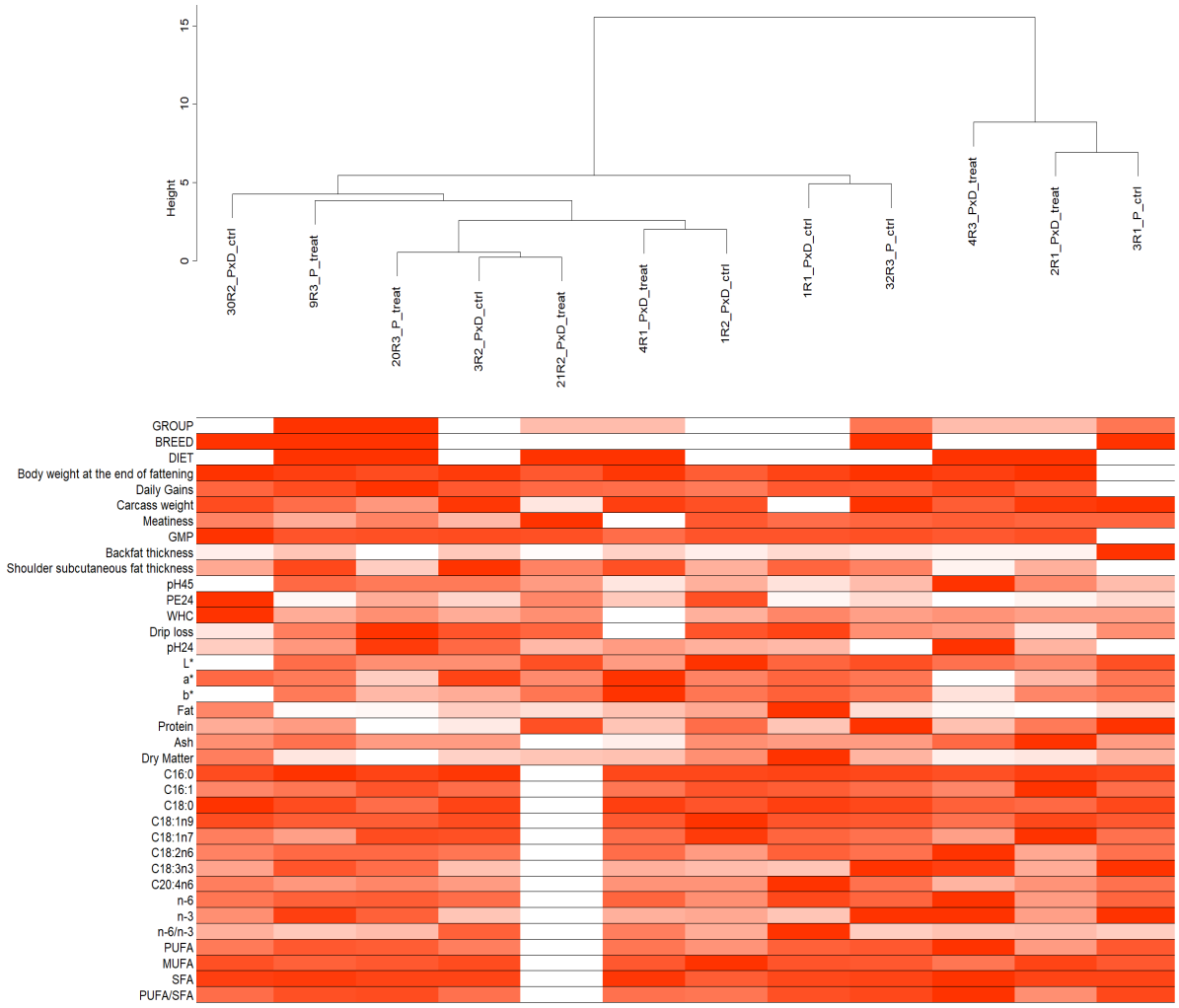

Figure 10. Clustering dendrogram of samples based on their Euclidean distance and heatmap of the investigated phenotypic trait associated with each pig.

Table 23. List of investigated phenotypic traits in WGCNA analysis of PL purebred and PLxDuroc crossbred pigs

Trait	Abbreviation
Body growth related at end of fattening	**BWF**
Daily gains	**DG**
Body growth related	**BW**
Meatiness	**M**
GMP	**GMP**
Backfat thickness	**BFT**
Shoulder subcutanesous fat thickness	**SSFT**
pH 45 min post mortem	**PH45**
Conductivity 24 hours post mortem	**PE24**
Water Holding Capacity	**WHC**
Drip loss	**DL**
pH 24 hours post mortem	**PH24**
L* - meat color	**L***
a* - meat color	**a***
b* - meat color	**b***
Fat	**FAT**
Protein	**Pr**
Ash	**ASH**
Dry matter	**DM**
C16:0	**C16:0**
C16:1	**C16:1**
C18:0	**C18:0**
C18:1n9	**C18:1n9**
C18:1n7	**C18:1n7**
C18:2n6	**C18:2n6**
C18:3n3	**C18:3n3**
C20:4n6	**C20:4n6**
n-6	**n-6**
n-3	**n-3**
n-6/n-3	**n-6/n-3**
PUFA	**PUFA**
MUFA	**MUFA**
Saturated Fatty Acid	**SFA**
PUFA/SFA	**PUFA/SFA**

4.2.5. Selecting and choosing the soft-thresholding power: analysis of network topology

The first step of WGCNA co-expression analysis was to establish soft threshold power β. Since it was impossible to reach R2 ≥ 0.8 (Fig. 11), soft thresholding power β was set for 18 as suggested in WGCNA documentation. Probable reason for high β, was because of low number of liver transcriptome (WGCNA documentation suggests at least 15 samples) and low number of miRNAs used in the analysis.

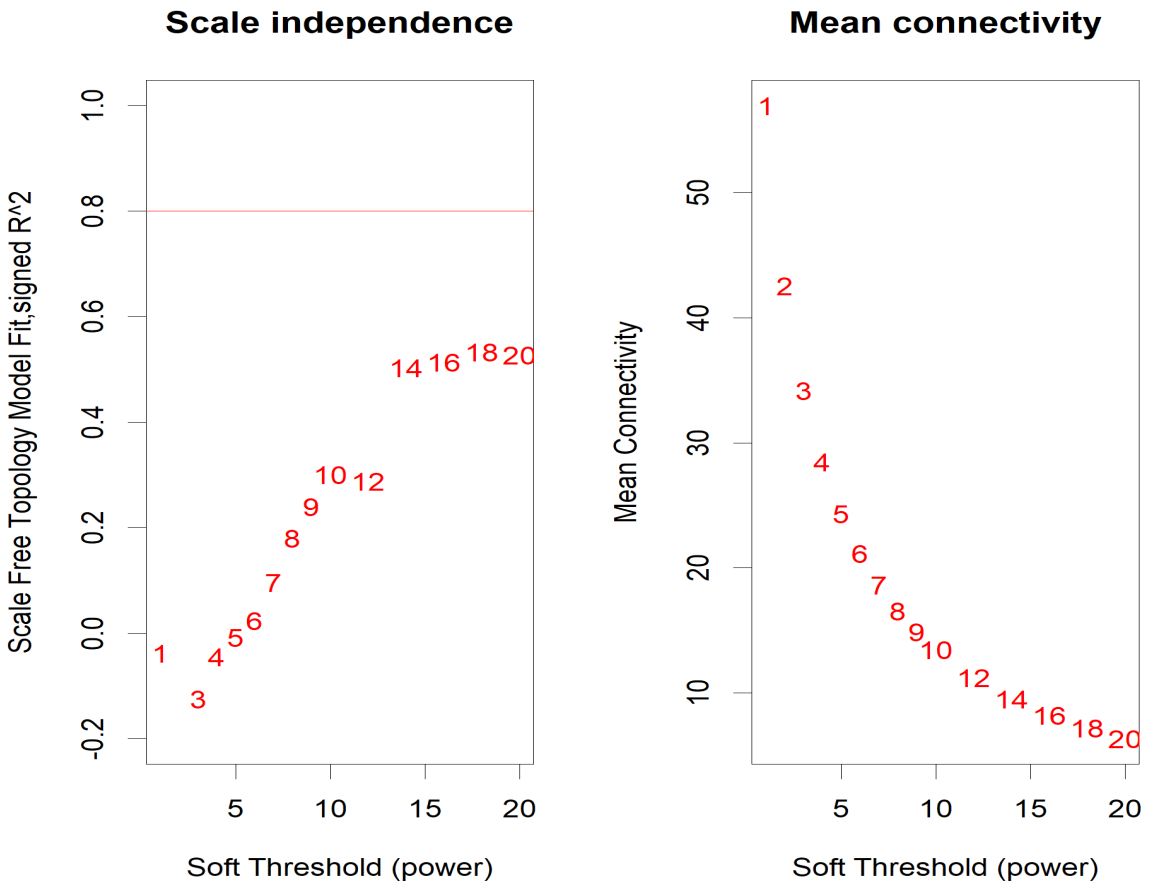

Figure 11. Determination of network topology for various soft-thresholding power in porcine liver transcriptome using WGCNA. (a) The left panel plot displays the scale-free topology fit index (y-axis) as a function of the various soft-thresholding powers (β) (x-axis). (b) The right panel plot displays the mean connectivity (degree, y-axis) as a function of the various soft-thresholding powers (x-axis).

4.2.6. Co-expression network construction and module detection.

The blockwiseModules function from WGCNA library was used to create the gene network. To create the most robust gene network type of Topological Overlap Matrix (TOM) and type of network was set as "signed" and bidweight midcorrelation was used.

The hierarchical agglomerative clustering was constructed considering the 1-TOM as a distance to identify the groups of trait-associated co-expressed miRNAs. Modules of co-expressed miRNAs were then determined by using the dynamic tree cut procedure with a minimum module size cut-off of 5. This cut-off was chosen considering the miRNA transcriptome's small size and the fact that a single miRNA can target multiple RNA transcripts. With this procedure, 10 different modules of EigenmiRNA were identified (Fig. 12).

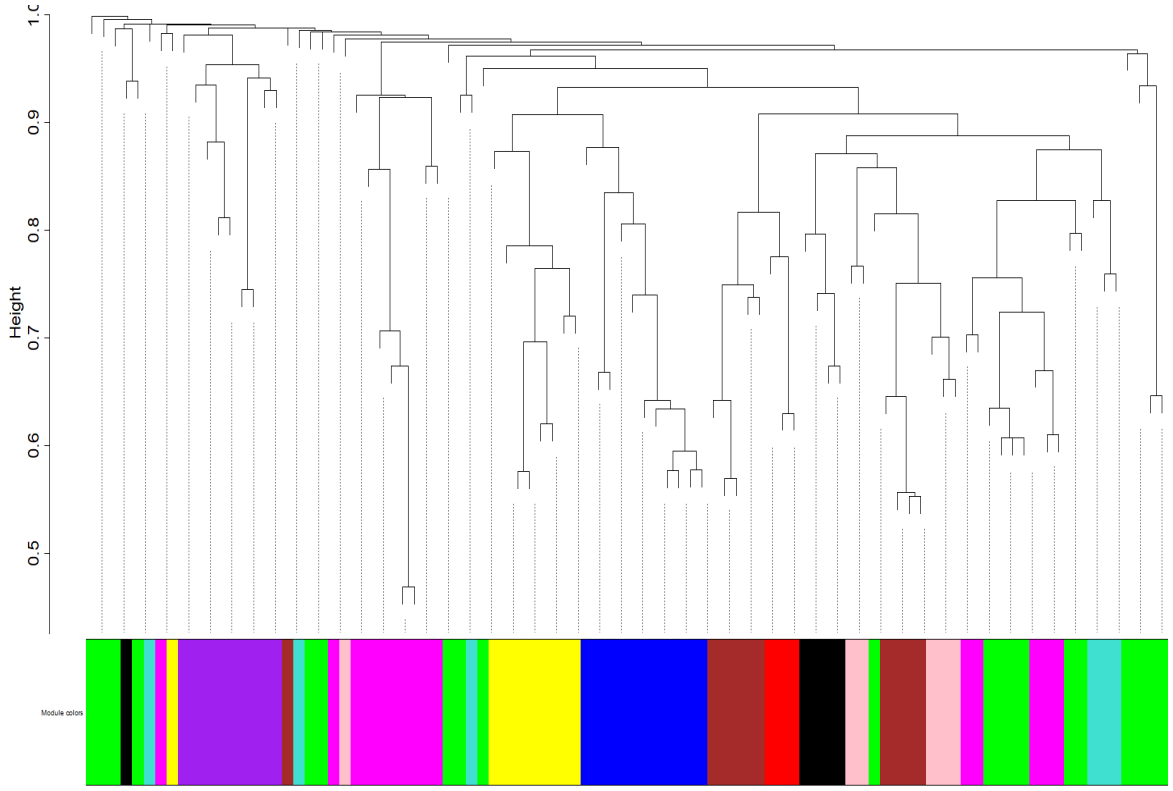

Figure 12. miRNA Clustering dendrogram and module color of co-expression genes, with dissimilarity based on topological overlap, together with assigned module colors for porcine liver transcriptome. Correlated miRNA were grouped into colored modules identified through the Dynamic Tree Cut function. Each leaf, which is a short vertical line, corresponds to a specific miRNA. Branches of the dendrogram group together densely interconnected highly co-expressed miRNAs.

The size of miRNA modules ranges from a minimum of 3 miRNA of the red module to the 20 miRNAs of the Green module. (Table 24).

Table 24. Number of miRNAs included in each module

Module	**N° of miRNAs**
Black	5
Blue	11
Brown	10
Green	20
Magenta	15
Pink	6
Purple	9
Red	3
Turquoise	6
Yellow	9

4.2.7. Correlation between modules and investigated phenotypic trait and Quantification of the trait-associated modules

A total of 37 porcine phenotypic trait (Table 23) were investigated in the WGCNA analysis. The absolute value of the correlation of paired miRNAs was used to define the trait-associated gene co-expression network. The gene expression similarity matrix was converted into and an adjacency matrix, based on the criterion of approximate scale-free topology, to define the strength between connected miRNAs transcripts.

In this analysis, the trait-associated modules that are significantly associated with the measured phenotypic traits were identified. Since we already have a summary profile (eigengene) for each module, we simply correlate eigengenes with external traits and look for the most significant associations. The resulting color-coded table representing the trait-associated MEMs is shown in Figure 13. The analysis identifies the several significant trait-associated modules, with weighted values of the investigated porcine phenotypic trait.

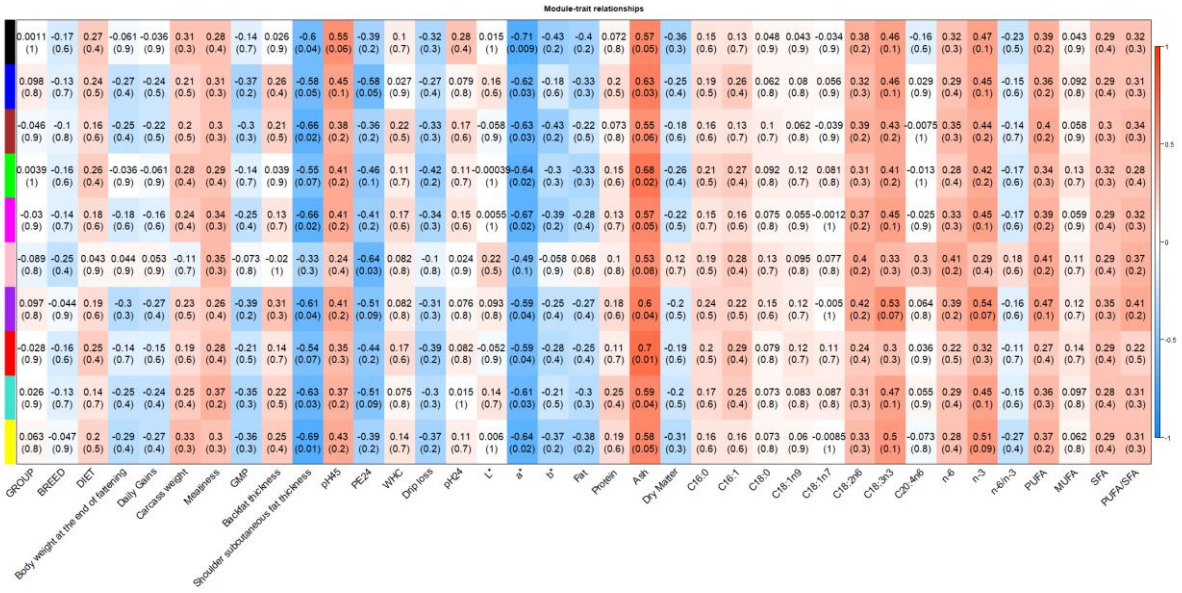

Figure 13. Heatmap of module-trait relationships: The relationships of identified clusters and phenotypic trait. Each row in the table corresponds to a module and each column to a phenotypic trait. Numbers in the table report the correlations scores between module and traits, with the p-values of the correlations in parentheses. The table is color-coded by correlation according to the color legend on the right, Blue indicates a negative correlation while Red a positive one.

Modules with p-value ≤ 0.05 were classified as statistically significant for the trait. In results 4 traits were discovered with significant modules. Shoulder subcutaneous fat thickness which is in correlation with 7 modules (black, blue, brown, magenta, purple, turquoise and yellow). The strongest correlation for this trait was present with the yellow module (cor = -0.69, p-value = 0.01). Next trait with strong, statistically significant correlation with modules, was a*. The trait was correlated with 9 modules (black, blue, brown, green, magenta, purple, red, turquoise, and yellow). The strongest correlation was observed with the black module (cor = -0.71, p-value = 0.009). Ash was the next trait with significant correlation with modules. It was positively correlated with 8 modules (black, blue, green, magenta, purple, red, turquoise, yellow), where the strongest correlation was with red module (cor = 0.7, p-value = 0.01). The last trait with significant correlation observed was PE24 (Conductivity 24 hours postmortem). It was correlated with 2 modules (blue, pink). The strongest correlation was with pink module (cor = -0.64, p-value = 0.03).

4.2.7.1. Expression profile of detected modules

The more detailed insight into the miRNAs clustered into the trait correlated modules was obtained with expression heatmap of miRNAs in specific clusters. The heatmaps were generated for all modules grouped, for every trait with its' significantly correlated modules grouped and for every module separately.

To generate the heatmaps, R function heatmap.2 was used. Expression data were centered and scaled by the rows which represents the miRNA and columns represents the sample id. Furthermore, the dendrogram to represent the distance were generated and are visible in the heatmap. Dendrogram represents Euclidean distance between rows and columns.

Heatmap with all detected module (Fig. 13), shows the close distance between samples 4R3_PxD_treat (Group II), 2R1_PxD_treat (Group II) and 3R1_P_ctrl (Group III) with relatively high expression of miRNA in the modules. Samples 4R1_PxD_ctrl (Group I), 1R2_PxD_ctrl (Group I), 20R3_P_treat (Group IV), 21R2_PxD_treat (Group II) and 3R2_PxD_ctrl (Group I) characterize relatively low expression of miRNA in all modules. Small distance was also observed between 32R3_P_ctrl (Group III), 1R1_PxD_ctrl (Group I), 30R2_PxD_ctrl (Group I) and 9R3_P_treat (Group IV) with mixed, highly and low expressed miRNAs.

Heatmaps with the modules correlated with Shoulder subcutaneous fat thickness (Fig. 15), a* (Fig. 16), Ash (Fig. 17) traits have similar Euclidean distance between samples. The samples distance based on the expression of genes from modules correlated with PE24 trait (Fig. 18) differs from the dendrogram from figure 14. The higher distance of 3R1_P_ctrl sample from the 4R3_PxD_treat, 2R1_PxD_treat samples were observed. The rest of samples are characterized with the similar distance comparing to the distance calculated for all the miRNAs.

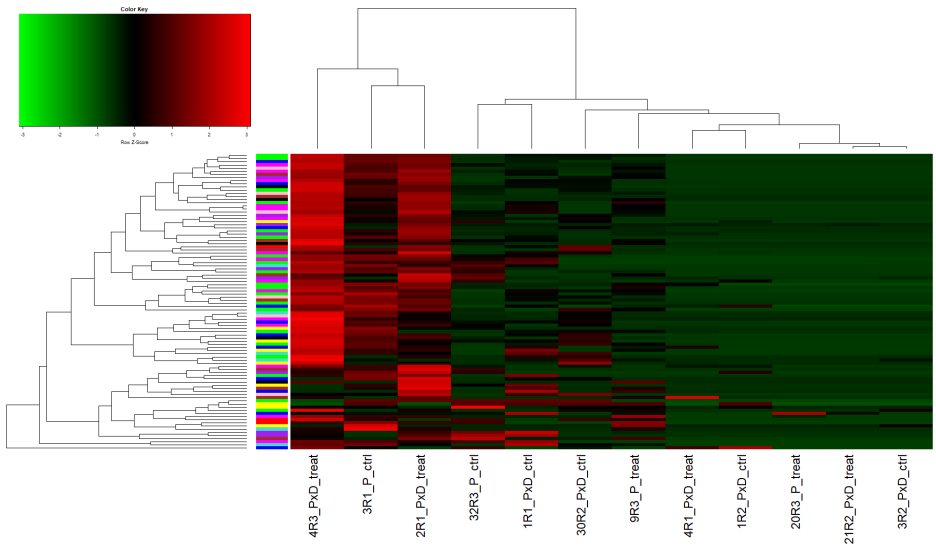

Figure 14. Expression heatmap of all detected modules. The greener color the lower expression while the redder color the higher expression. Columns represent samples. On top the dendrogram based on euclidian distance of samples miRNA expression profile. On the bottom sample ids. Rows represent miRNAs. On the left, dendrogram

based on Euclidean distance of miRNAs expression and the color which symbolize the module membership of miRNA.

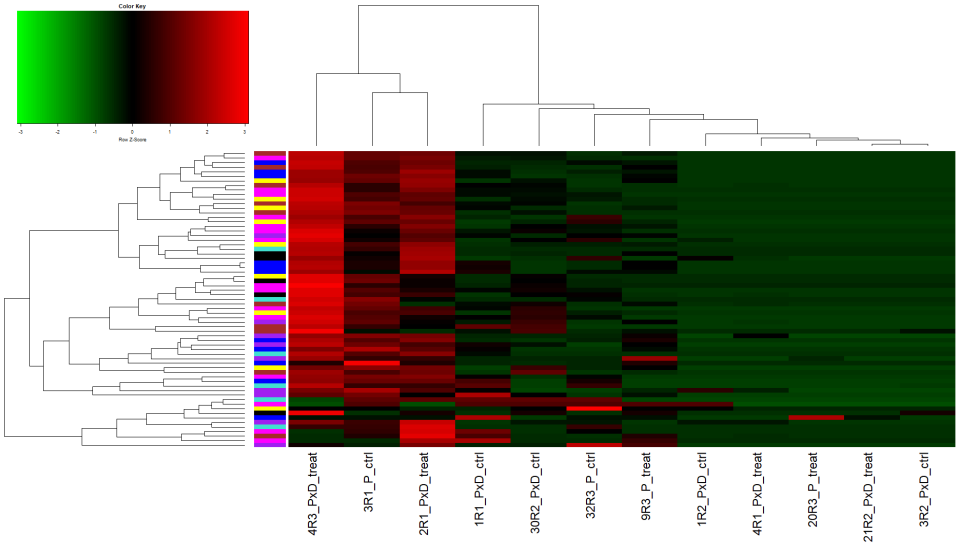

Figure 15. Expression heatmap of modules significantly correlated with the **Shoulder subcutaneous fat thickness** trait. The greener color the lower expression while the redder color the higher expression. Columns represent samples. On top the dendrogram based on euclidian distance of samples miRNA expression profile. On the bottom sample ids. Rows represent miRNAs. On the left, dendrogram based on euclidian distance of miRNAs expression and the color which symbolize the module membership of miRNA.

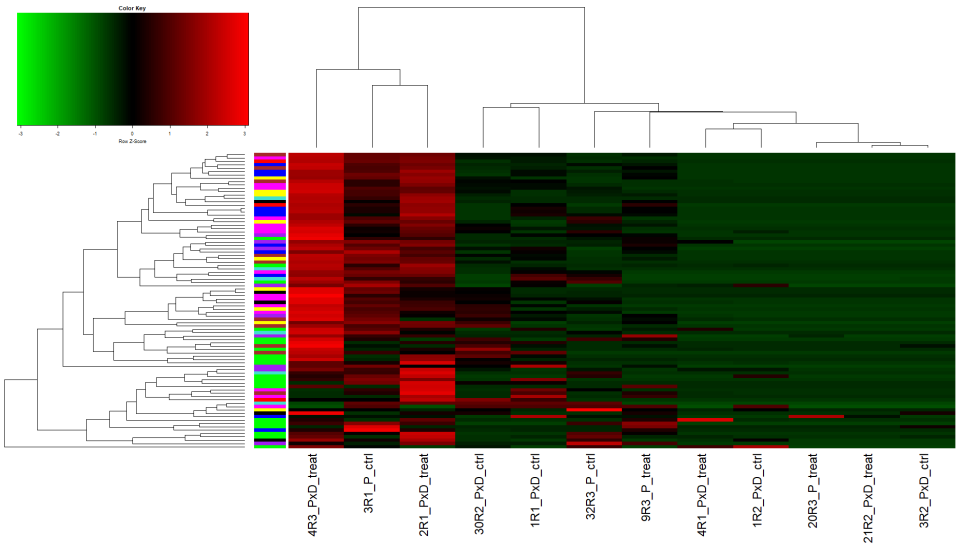

Figure 16. Expression heatmap of modules significantly correlated with the **a*** trait. The greener color the lower expression while the redder color the higher expression. Columns represent samples. On top the dendrogram based on euclidian distance of samples miRNA expression profile. On the bottom sample ids. Rows represent miRNAs. On the left, dendrogram based on euclidian distance of miRNAs expression and the color which symbolize the module membership of miRNA.

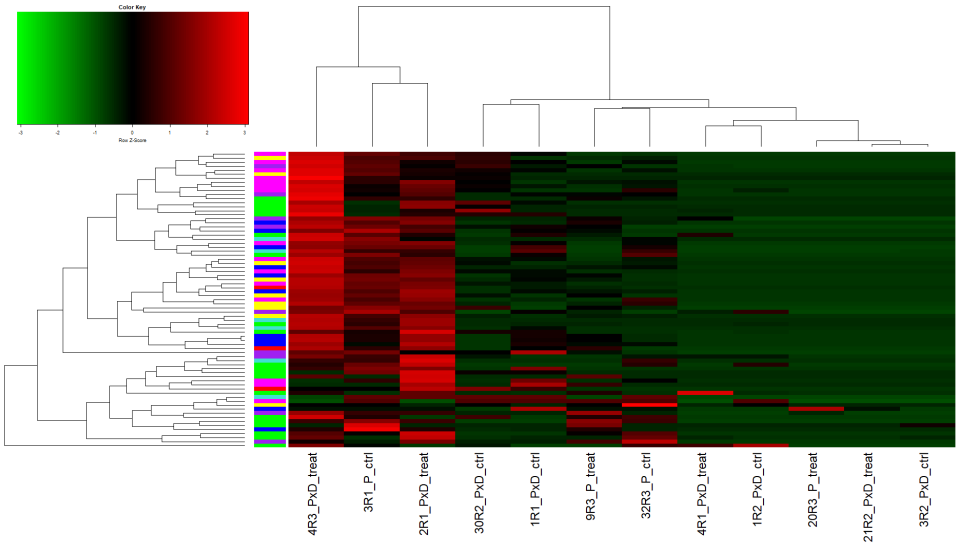

Figure 17. Expression heatmap of modules significantly correlated with the **Ash** trait. The greener color the lower expression while the redder color the higher expression. Columns represent samples. On top the dendrogram based on euclidian distance of samples miRNA expression profile. On the bottom sample ids. Rows represent miRNAs. On the left, dendrogram based on euclidian distance of miRNAs expression and the color which symbolize the module membership of miRNA.

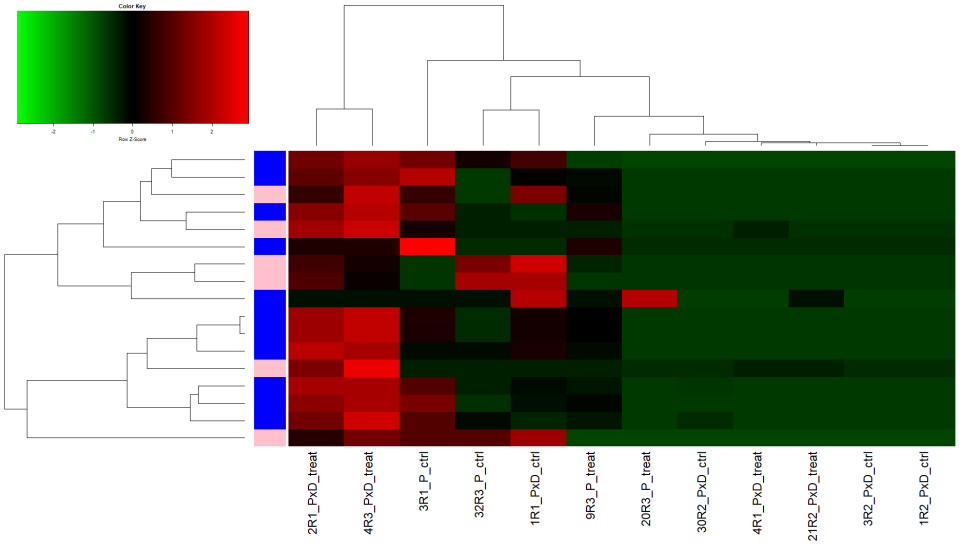

Figure 18. Expression heatmap of modules significantly correlated with the **PE24** trait. The greener color the lower expression while the redder color the higher expression. Columns represent samples. On top the dendrogram based on euclidian distance of samples miRNA expression profile. On the bottom sample ids. Rows represent miRNAs. On the left, dendrogram based on euclidian distance of miRNAs expression and the color which symbolize the module membership of miRNA.

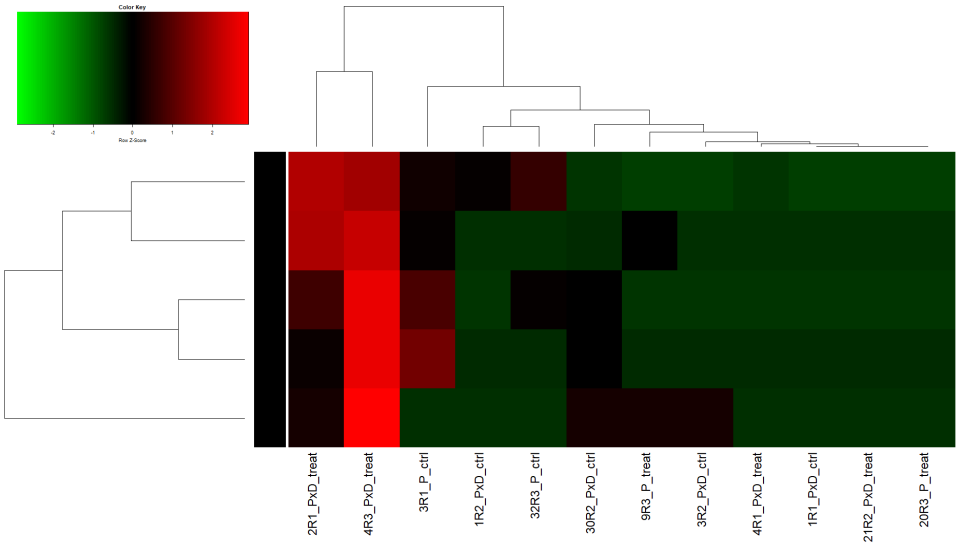

Figure 19. Expression heatmap of black module. The greener color the lower expression while the redder color the higher expression. Columns represent samples. On top the dendrogram based on euclidian distance of samples miRNA expression profile. On the bottom sample ids. Rows represent miRNAs. On the left, dendrogram based on euclidian distance of miRNAs expression and the color which symbolize the module membership of miRNA.

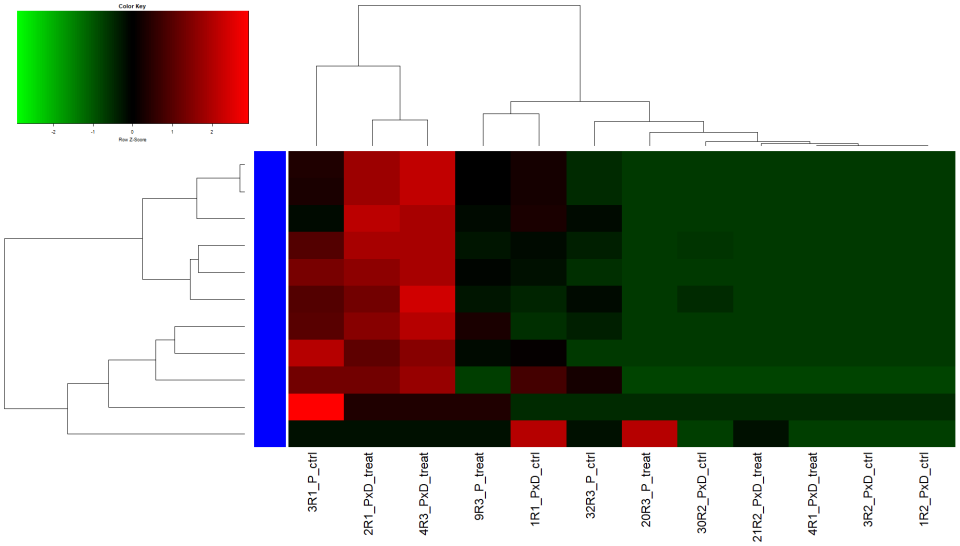

Figure 20. Expression heatmap of blue module. The greener color the lower expression while the redder color the higher expression. Columns represent samples. On top the dendrogram based on euclidian distance of samples miRNA expression profile. On the bottom sample ids. Rows represent miRNAs. On the left, dendrogram based on euclidian distance of miRNAs expression and the color which symbolize the module membership of miRNA.

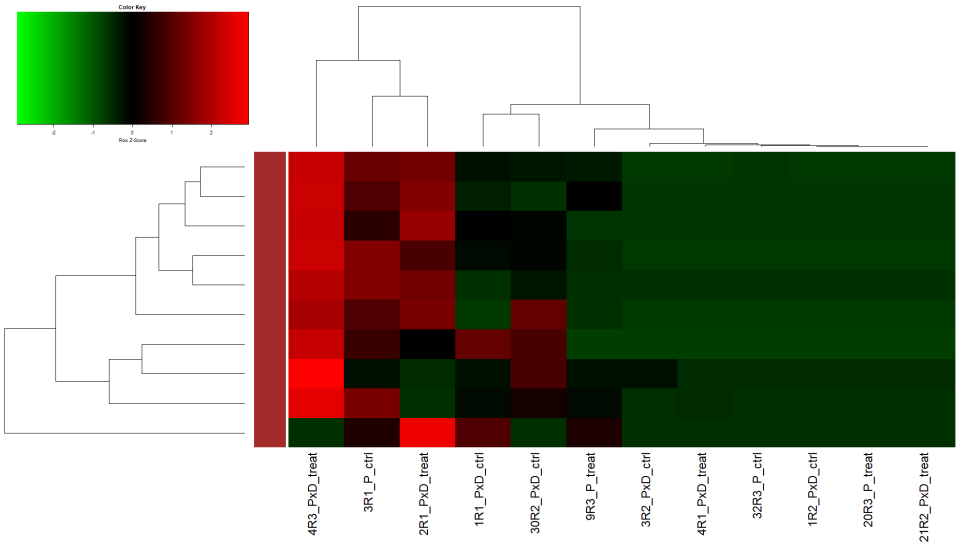

Figure 21. Expression heatmap of brown module. The greener color the lower expression while the redder color the higher expression. Columns represent samples. On top the dendrogram based on euclidian distance of samples miRNA expression profile. On the bottom sample ids. Rows represent miRNAs. On the left, dendrogram based on euclidian distance of miRNAs expression and the color which symbolize the module membership of miRNA.

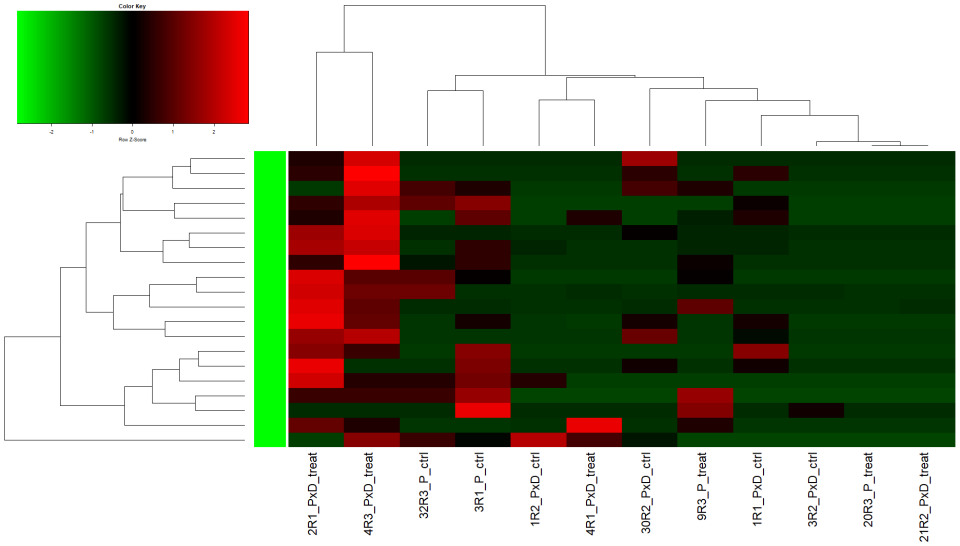

Figure 22. Expression heatmap of green module. The greener color the lower expression while the redder color the higher expression. Columns represent samples. On top the dendrogram based on euclidian distance of samples miRNA expression profile. On the bottom sample ids. Rows represent miRNAs. On the left, dendrogram based on euclidian distance of miRNAs expression and the color which symbolize the module membership of miRNA.

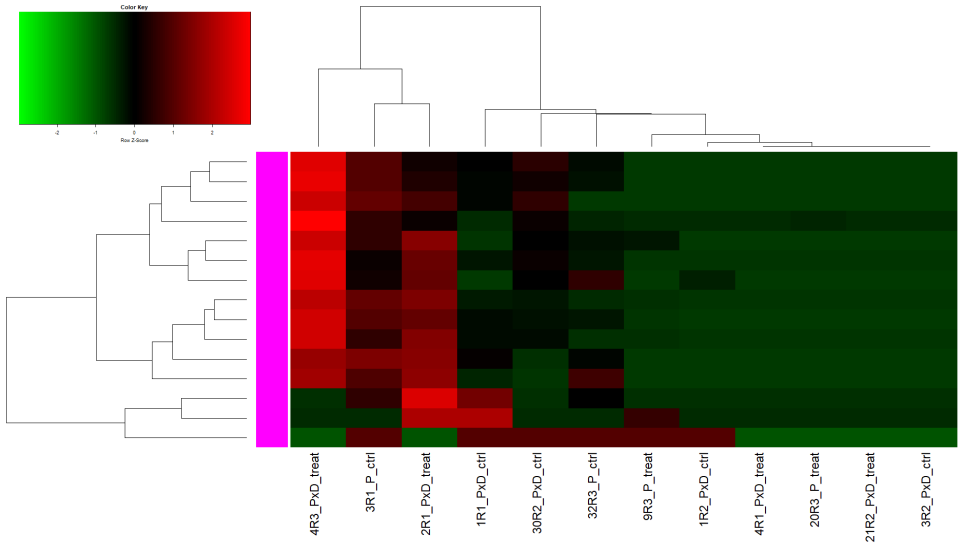

Figure 23. Expression heatmap of magenta module. The greener color the lower expression while the redder color the higher expression. Columns represent samples. On top the dendrogram based on euclidian distance of samples miRNA expression profile. On the bottom sample ids. Rows represent miRNAs. On the left, dendrogram based on euclidian distance of miRNAs expression and the color which symbolize the module membership of miRNA.

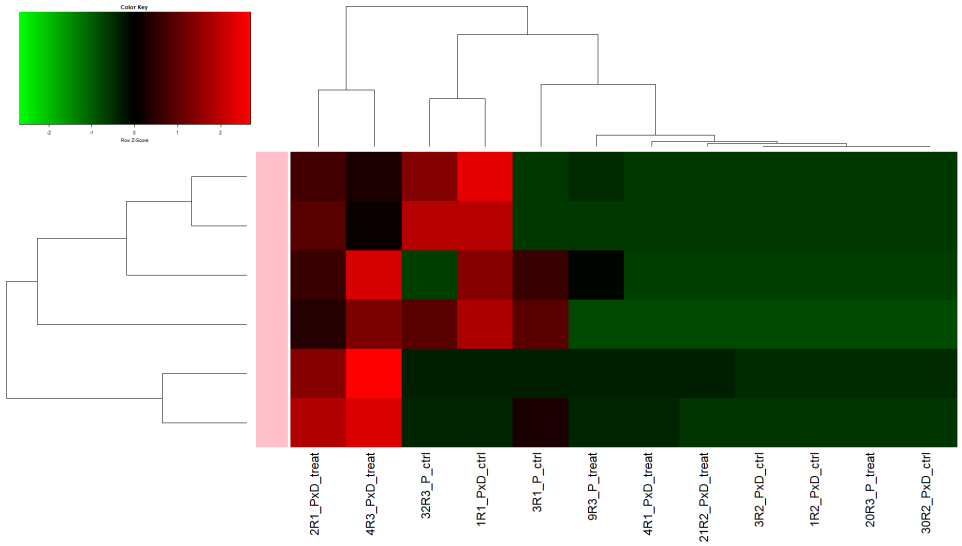

Figure 24. Expression heatmap of pink module. The greener color the lower expression while the redder color the higher expression. Columns represent samples. On top the dendrogram based on euclidian distance of samples miRNA expression profile. On the bottom sample ids. Rows represent miRNAs. On the left, dendrogram based on euclidian distance of miRNAs expression and the color which symbolize the module membership of miRNA.

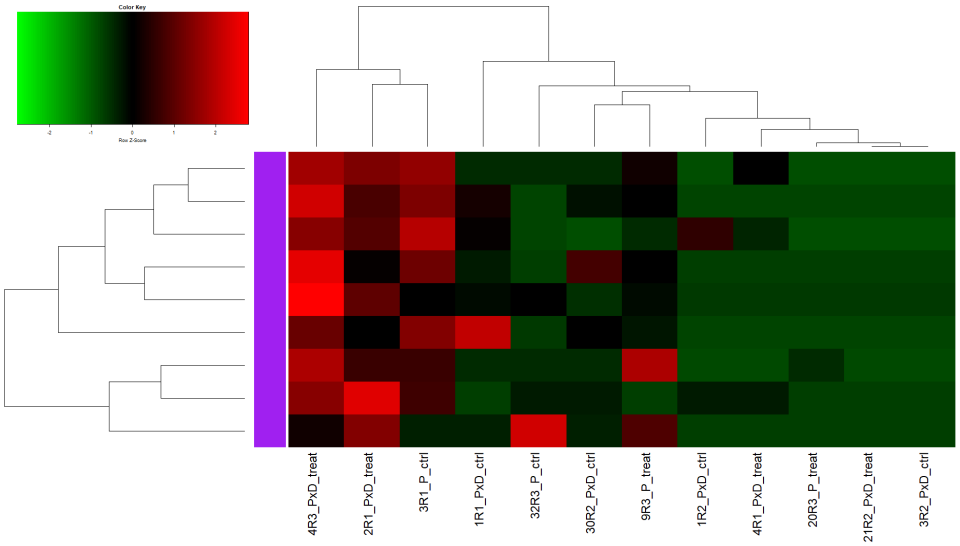

Figure 25. Expression heatmap of purple module. The greener color the lower expression while the redder color the higher expression. Columns represent samples. On top the dendrogram based on euclidian distance of samples miRNA expression profile. On the bottom sample ids. Rows represent miRNAs. On the left, dendrogram based on euclidian distance of miRNAs expression and the color which symbolize the module membership of miRNA.

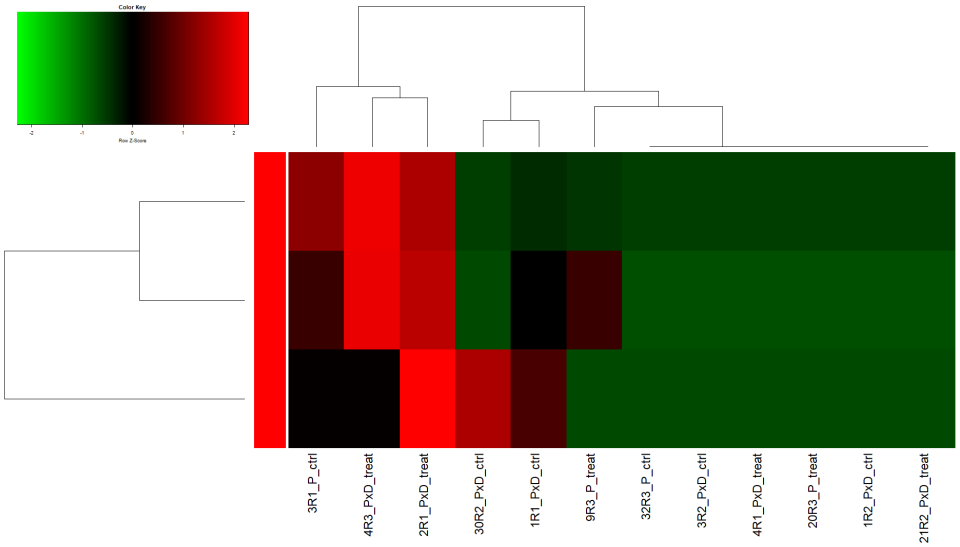

Figure 26. Expression heatmap of red module. The greener color the lower expression while the redder color the higher expression. Columns represent samples. On top the dendrogram based on euclidian distance of samples miRNA expression profile. On the bottom sample ids. Rows represent miRNAs. On the left, dendrogram based on euclidian distance of miRNAs expression and the color which symbolize the module membership of miRNA.

4.2.8. Identification of trait-associated miRNA genes of significance (GS) affected by PUFAs diets in PL an PLxDuroc pigs

Intra-modular analysis for MEM (Module membership of miRNA) was carried out to identify the relationship between the miRNA and the investigated porcine phenotypic trait. Four phenotypic traits affected by PUFAs diets in PL and PLxDuroc pigs were identified, viz., a*, shoulder subcutaneous fat thickness, conductivity 24 hours post mortem (PE24), and Ashes, respectively. Trait-wise, a total of 9, 7, 2 and 8 trait-associated significant modules affected by PUFAs diets in PL and PLxDuroc pigs were identified representing four traits.

4.2.8.1. Identification of trait-associated modules for a* trait, affected by PUFAs diets in PL an PLxDuroc pigs

The correlation between the MEM and the miRNA expression profile for a* trait identified nine modules (Figures 27-35 and Tables 25-33).

In Black module, the correlation between the MEM and the miRNA expression profile for A asterisk trait identified five porcine miRNAs: ssc-miR-142-3p, ssc-miR-204, ssc-miR-30a-3p, ssc-let-7c, and ssc-miR-21-5p respectively (Fig. 26 and Table 25).

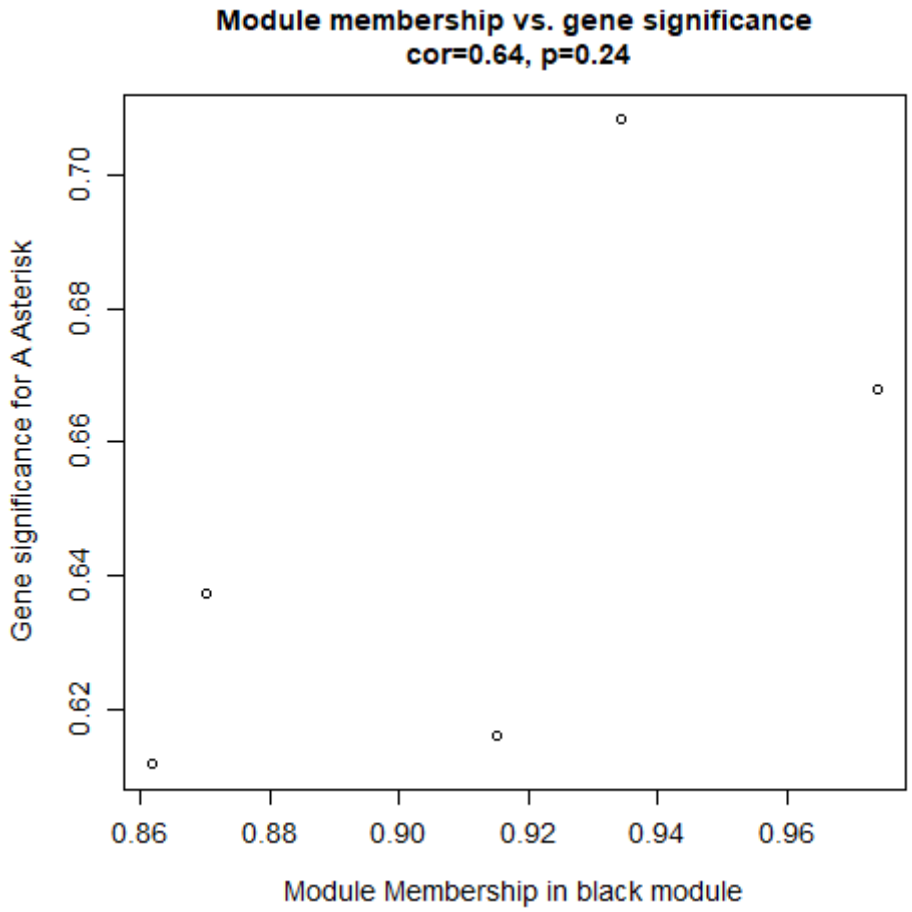

Figure 27. Intra-modular analysis for MEM (black module). The figure shows the scatter plot of GS (y-axis) vs. MM (x-axis) for phenotypic trait **A asterisk** (a*) in MEM black. The **GS** is the absolute value describing the relationship between the miRNA and the phenotypic trait a*, while the **MM** describes the correlation between the MEM and the miRNA expression profile.

Table 25. Intra-modular analysis for phenotypic trait a*. Identification trait-associated miRNA in black module.

SN	**Ensembl**	**Module**	**p.GS**	**GS**
1	ssc-miR-142-3p	black	0.034526086	-0.611739192
2	ssc-miR-204	black	0.025793242	-0.637352009
3	ssc-miR-30a-3p	black	0.03292799	-0.616046046
4	ssc-let-7c	black	0.009938651	-0.708290887
5	ssc-miR-21-5p	black	0.017595916	-0.667972486

In blue module, the correlation between the MEM and the miRNA expression profile for A asterisk trait identified 11 porcine miRNAs: ssc-miR-10387, ssc-miR-425-5p, ssc-miR-191, ssc-miR-199a-5p, ssc-miR-29a-3p, ssc-miR-122-5p, ssc-miR-26a, ssc-miR-199a-3p, ssc-miR-199b-3p, ssc-miR-186-5p, ssc-miR-22-3p, respectively. (Fig. 27 and Table 26).

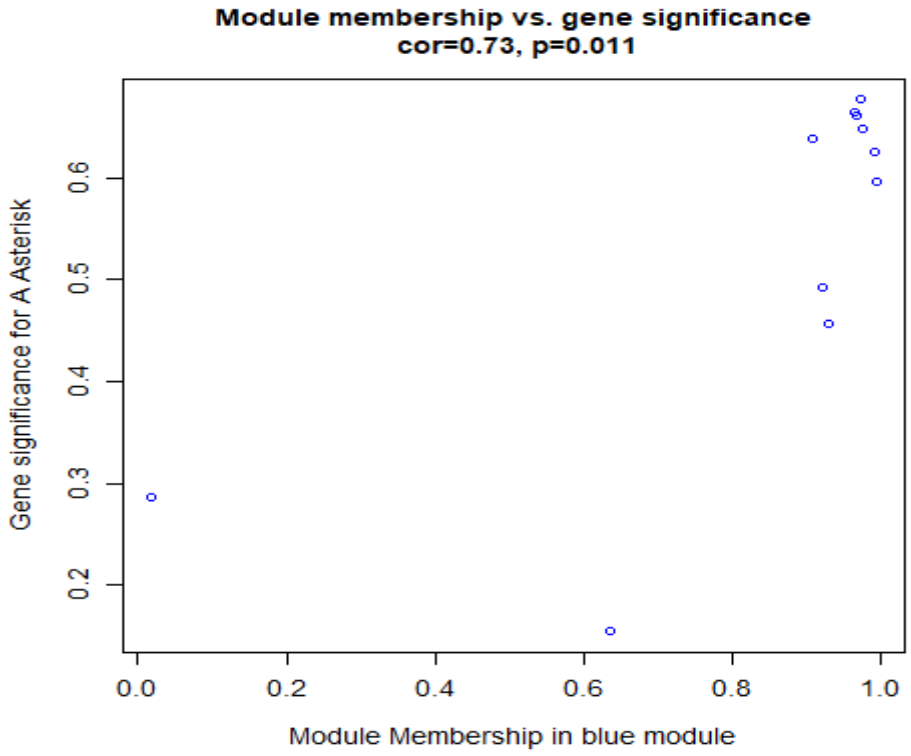

Figure 28. Intra-modular analysis for MEM (blue module). The figure shows the scatter plot of GS (y-axis) vs. MM (x-axis) for phenotypic trait a*in MEM blue. The **GS** is the absolute value describing the relationship between the miRNA and the phenotypic trait a*, while the **MM** describes the correlation between the MEM and the miRNA expression profile.

Table 26. Intra-modular analysis for phenotypic trait a*. Identification trait-associated miRNA in blue module.

SN	**Ensembl**	**Module**	**p.GS**	**GS**
1	ssc-miR-10387	blue	0.366441598	-0.286604413
2	ssc-miR-425-5p	blue	0.631533442	-0.154542872
3	ssc-miR-191	blue	0.13598342	-0.456269538
4	ssc-miR-199a-5p	blue	0.103605674	-0.49275477
5	ssc-miR-29a-3p	blue	0.025544861	-0.638166763
6	ssc-miR-122-5p	blue	0.040702564	-0.596321818
7	ssc-miR-26a	blue	0.029651781	-0.625367784
8	ssc-miR-199a-3p	blue	0.019305955	-0.660834878
9	ssc-miR-199b-3p	blue	0.018195073	-0.665416029
10	ssc-miR-186-5p	blue	0.022416419	-0.648957589
11	ssc-miR-22-3p	blue	0.015564346	-0.677147117

In brown module, the correlation between the MEM and the miRNA expression profile for A asterisk trait identified 10 porcine miRNA: ssc-miR-125a, ssc-miR-486, ssc-miR-423-3p, ssc-miR-181b6, ssc-miR-140-3p, ssc-miR-28-3p, ssc-miR-151-3p, ssc-miR-148a-3p, ssc-miR-26b-5p, ssc-miR-30a-5p, respectively. (Fig. 28 and Table 27)

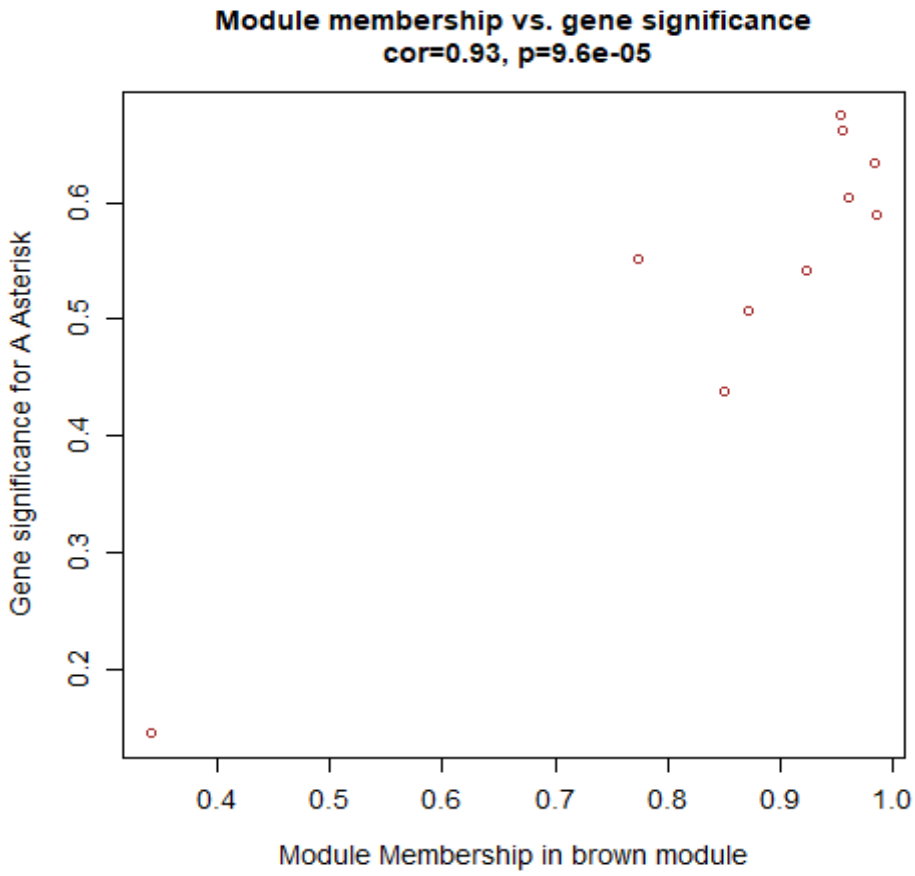

Figure 29. Intra-modular analysis for MEM (Brown module). The figure shows the scatter plot of GS (y-axis) vs. MM (x-axis) for phenotypic trait a*in MEM brown. The **GS** is the absolute value describing the relationship between the miRNA and the phenotypic trait a*, while the **MM** describes the correlation between the MEM and the miRNA expression profile.

Table 27. Intra-modular analysis for phenotypic trait a*. Identification trait-associated miRNA in brown module.

SN	**Ensembl**	**Module**	**p.GS**	**GS**
1	ssc-miR-125a	brown	0.654101506	-0.144503977
2	ssc-miR-486	brown	0.15477077	-0.437653617
3	ssc-miR-423-3p	brown	0.062632933	-0.55223593
4	ssc-miR-181b	brown	0.092592808	-0.506883309
5	ssc-miR-140-3p	brown	0.069192977	-0.541203943
6	ssc-miR-28-3p	brown	0.043596652	-0.589667089
7	ssc-miR-151-3p	brown	0.037383665	-0.604380864
8	ssc-miR-148a-3p	brown	0.026710103	-0.634392741
9	ssc-miR-26b-5p	brown	0.018943348	-0.662308517
10	ssc-miR-30a-5p	brown	0.016073785	-0.674767401

In green module, the correlation between the MEM and the miRNA expression profile for A asterisk trait identified 20 porcine miRNAs: ssc-miR-7142-3p, ssc-miR-127, ssc-miR-100, ssc-miR-10b, ssc-miR-374a-5p, ssc-miR-146a-5p, ssc-miR-320, ssc-let-7d-5p, ssc-miR-340, ssc-miR-122-3p, ssc-miR-24-3p, ssc-miR-374a-3p, ssc-miR-7134-3p, ssc-miR-423-5p, ssc-miR-375, ssc-miR-10383, ssc-miR-15a, ssc-miR-107, ssc-miR-148b-3p, and ssc-let-7e respectively. (Fig. 29 and Table 28).

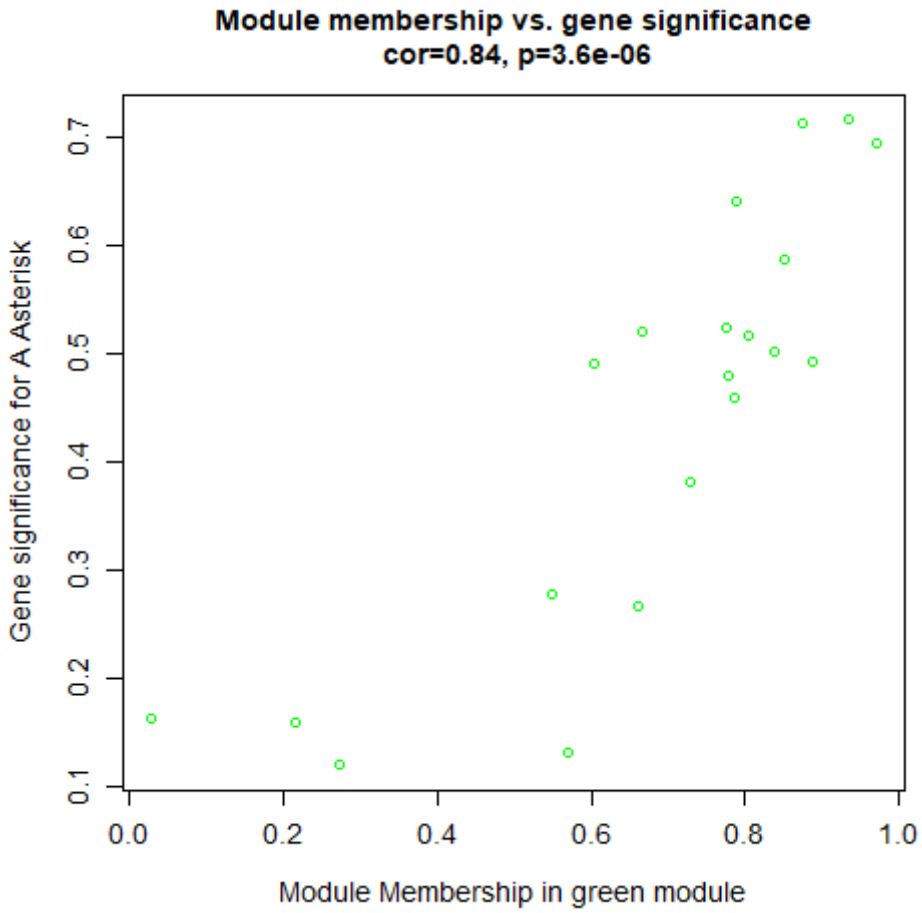

Figure 30. Intra-modular analysis for MEM (Green module). The figure shows the scatter plot of GS (y-axis) vs. MM (x-axis) for phenotypic trait a*in MEM green. The **GS** is the absolute value describing the relationship between the miRNA and the phenotypic trait a*, while the **MM** describes the correlation between the MEM and the miRNA expression profile.

Table 28. Intra-modular analysis for phenotypic trait a*. Identification trait-associated miRNA in green module.

SN	**Ensembl**	**Module**	**p.GS**	**GS**
1	ssc-miR-7142-3p	green	0.614398636	0.162250613
2	ssc-miR-127	green	0.711337401	0.119546706
3	ssc-miR-100	green	0.686422526	-0.130328818
4	ssc-miR-10b	green	0.623298587	-0.158237519
5	ssc-miR-374a-5p	green	0.383695746	-0.276844251

6	ssc-miR-146a-5p	green	0.40378785	-0.265758905
7	ssc-miR-320	green	0.221818318	-0.380940931
8	ssc-let-7d-5p	green	0.079643197	-0.525029918
9	ssc-miR-340	green	0.085803095	-0.516166579
10	ssc-miR-122-3p	green	0.095714591	-0.50276876
11	ssc-miR-24-3p	green	0.104198779	-0.492022994
12	ssc-miR-374a-3p	green	0.105227753	-0.490759997
13	ssc-miR-7134-3p	green	0.082484246	-0.520886146
14	ssc-miR-423-5p	green	0.114019185	-0.48028958
15	ssc-miR-375	green	0.044230137	-0.588252448
16	ssc-miR-10383	green	0.133018367	-0.45935647
17	ssc-miR-15a	green	0.024791945	-0.640672134
18	ssc-miR-107	green	0.008728864	-0.716652408
19	ssc-miR-148b-3p	green	0.01221033	-0.694447235
20	ssc-let-7e	green	0.009240335	-0.713018056

In magenta module, the correlation between the MEM and the miRNA expression profile for A asterisk trait identified 15 porcine miRNAs: ssc-miR-10390, ssc-miR-99b, ssc-miR-542-3p, ssc-miR-142-5p, ssc-miR-30e-5p, ssc-miR-92a, ssc-miR-103, ssc-let-7i-5p, ssc-miR-222, ssc-miR-192, ssc-miR-98, ssc-let-7a, ssc-miR-101, ssc-miR-221-3p, and ssc-miR-30d respectively. (Fig. 30 and Table 29)

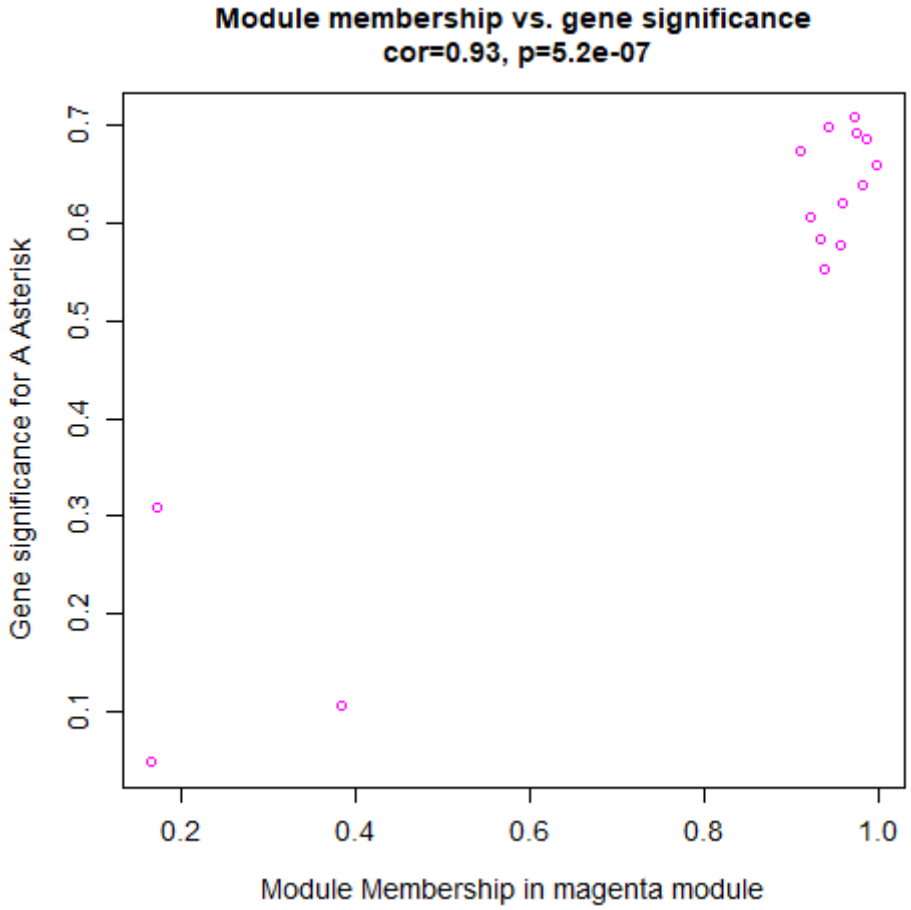

Figure 31: Intra-modular analysis for MEM (Magenta module). The figure shows the scatter plot of GS (y-axis) vs. MM (x-axis) for phenotypic trait a*in MEM magenta. The **GS** is the absolute value describing the relationship between the miRNA and the phenotypic trait a*, while the **MM** describes the correlation between the MEM and the miRNA expression profile.

Table 29. Intra-modular analysis for phenotypic trait a*. Identification trait-associated miRNA in magenta module.

SN	**Ensembl**	**Module**	**p.GS**	**GS**
1	ssc-miR-10390	magenta	0.880393846	-0.04875607
2	ssc-miR-99b	magenta	0.742026153	-0.106418063
3	ssc-miR-542-3p	magenta	0.32675432	0.310019415
4	ssc-miR-142-5p	magenta	0.062229855	-0.552939379
5	ssc-miR-30e-5p	magenta	0.037000288	-0.605344209
6	ssc-miR-92a	magenta	0.046871237	-0.582504284

7	ssc-miR-103	magenta	0.049516065	-0.576972519
8	ssc-let-7i-5p	magenta	0.03136874	-0.620395175
9	ssc-miR-222	magenta	0.016169428	-0.674326838
10	ssc-miR-192	magenta	0.025623568	-0.637907967
11	ssc-miR-98	magenta	0.011713458	-0.697300513
12	ssc-let-7a	magenta	0.019926706	-0.658358451
13	ssc-miR-101	magenta	0.013776206	-0.685983522
14	ssc-miR-221-3p	magenta	0.010064819	-0.707463404
15	ssc-miR-30d	magenta	0.012588669	-0.692331802

In purple module, the correlation between the MEM and the miRNA expression profile for A asterisk trait identified 9 porcine miRNAs: ssc-miR-125b, ssc-miR-451, ssc-miR-10a-5p, ssc-miR-23a, ssc-miR-23b, ssc-miR-151-5p, ssc-miR-143-3p, ssc-miR-215, and ssc-miR-126-3p respectively. (Fig. 31 and Table 30)

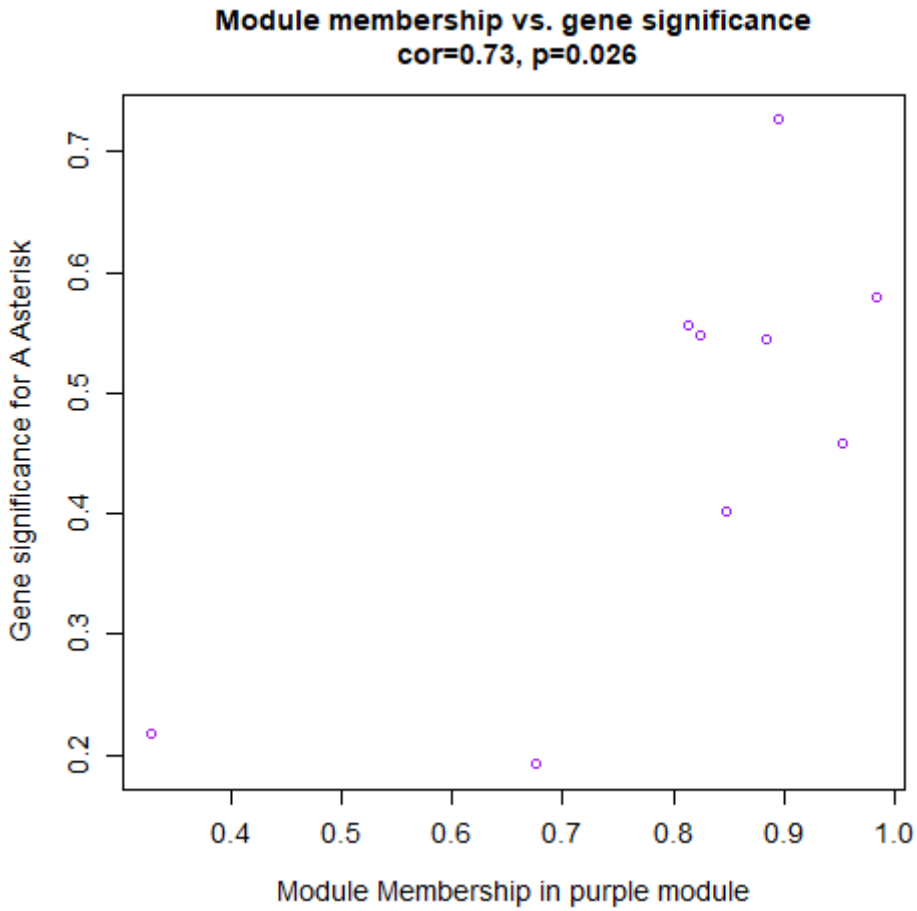

Figure 32. Intra-modular analysis for MEM (Purple module). The figure shows the scatter plot of GS (y-axis) vs. MM (x-axis) for phenotypic trait a*in MEM purple. The **GS** is the absolute value describing the relationship between the miRNA and the phenotypic trait a*, while the **MM** describes the correlation between the MEM and the miRNA expression profile.

Table 30. Intra-modular analysis for phenotypic trait a*. Identification trait-associated miRNA in purple module.

SN	**Ensembl**	**Module**	**p.GS**	**GS**
1	ssc-miR-125b	purple	0.496423587	-0.217834702
2	ssc-miR-451	purple	0.548872448	-0.192517193
3	ssc-miR-10a-5p	purple	0.195491246	-0.401741017
4	ssc-miR-23a	purple	0.060265579	-0.556413419
5	ssc-miR-23b	purple	0.065248488	-0.547745843
6	ssc-miR-151-5p	purple	0.133536969	-0.458813352
7	ssc-miR-143-3p	purple	0.066693127	-0.545319034
8	ssc-miR-215	purple	0.048169213	-0.579762797
9	ssc-miR-126-3p	purple	0.007461755	-0.726396812

In red module, the correlation between the MEM and the miRNA expression profile for A asterisk trait identified 3 porcine miRNAs: ssc-miR-142-3p, ssc-miR-204, ssc-miR-30a-3p, ssc-let-7c, and ssc-miR-21-5p, respectively. (Fig. 32 and Table 31)

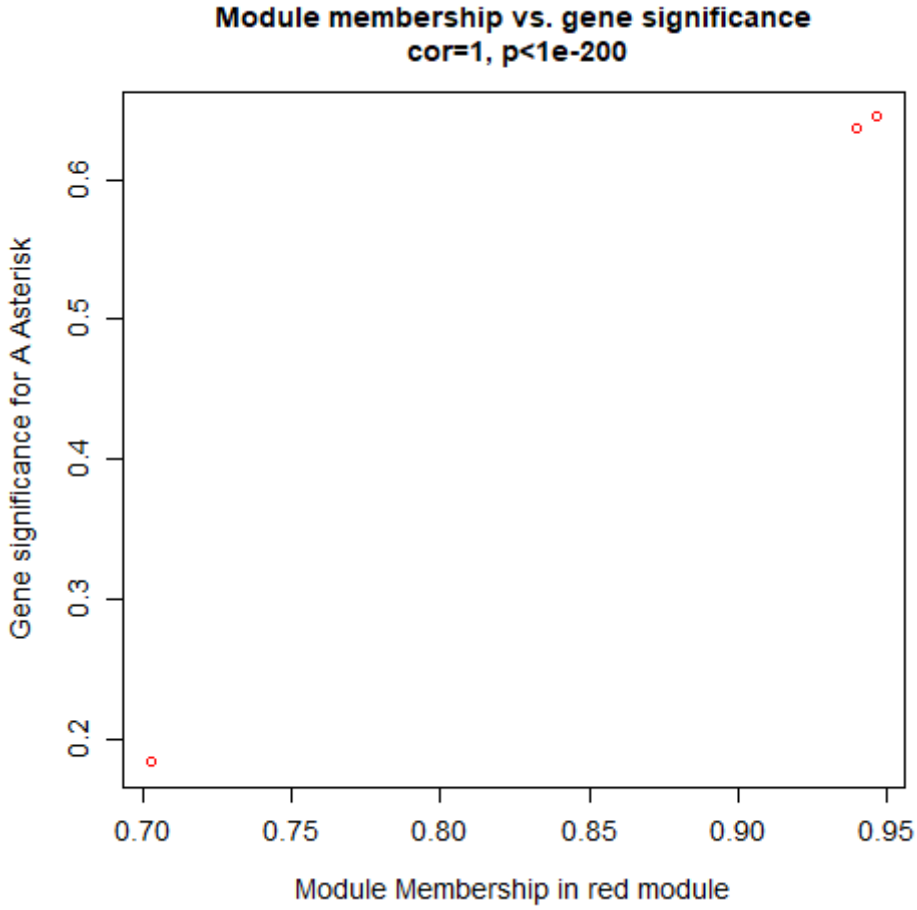

Figure 33. Intra-modular analysis for MEM (Red module). The figure shows the scatter plot of GS (y-axis) vs. MM (x-axis) for phenotypic trait a*in MEM red. The **GS** is the absolute value describing the relationship between the miRNA and the phenotypic trait a*, while the **MM** describes the correlation between the MEM and the miRNA expression profile.

Table 31. Intra-modular analysis for phenotypic trait a*. Identification trait-associated miRNA in red module.

SN	**Ensembl**	**Module**	**p.GS**	**GS**
1	ssc-miR-27a	red	0.567574527	-0.183739199
2	ssc-miR-148a-5p	red	0.023662707	-0.644535284
3	ssc-let-7g	red	0.02588081	-0.637066116

In turquoise module, the correlation between the MEM and the miRNA expression profile for A asterisk trait identified 6 porcine miRNAs: ssc-miR-146b, ssc-miR-1285, ssc-miR-182, ssc-miR-92b-3p, ssc-miR-181c, and ssc-miR-130a, respectively. (Fig.33 and Table 32)

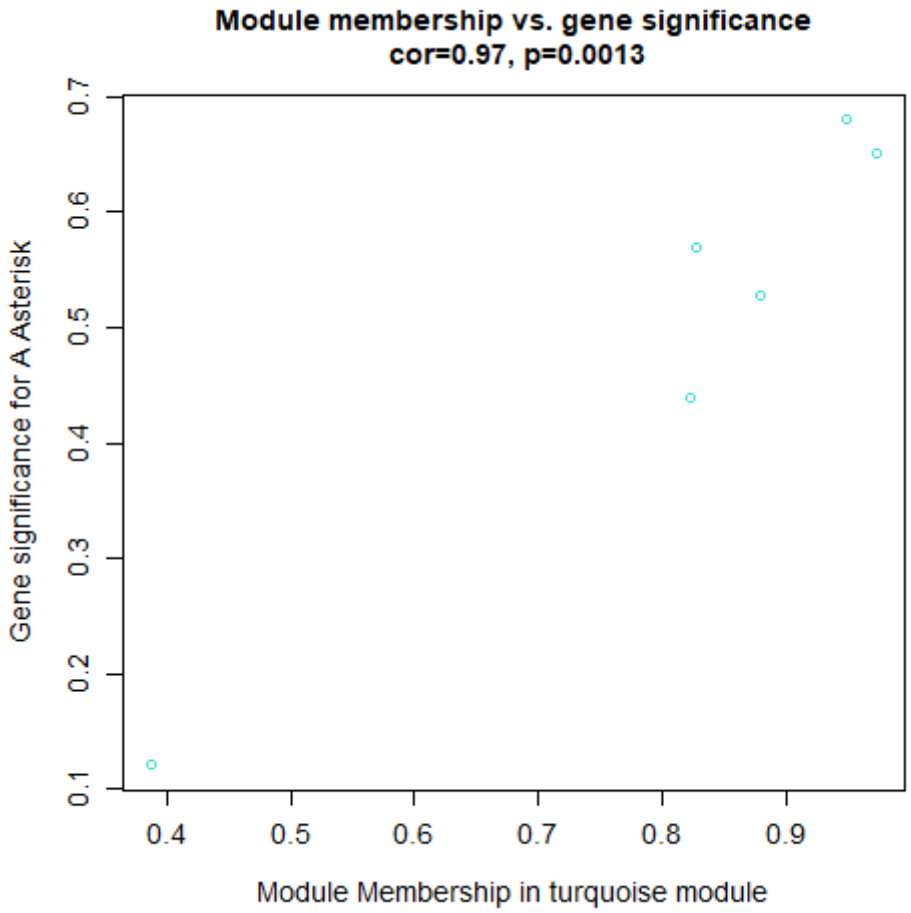

Figure 34. Intra-modular analysis for MEM (Turquoise module). The figure shows the scatter plot of GS (y-axis) vs. MM (x-axis) for phenotypic trait a*in MEM turquoise. The **GS** is the absolute value describing the relationship between the miRNA and the phenotypic trait a*, while the **MM** describes the correlation between the MEM and the miRNA expression profile.

Table 32. Intra-modular analysis for phenotypic trait a*. Identification trait-associated miRNA in turquoise module.

SN	**Ensembl**	**Module**	**p.GS**	**GS**
1	ssc-miR-146b	turquoise	0.708306339	0.120852203
2	ssc-miR-1285	turquoise	0.152538336	-0.439786932
3	ssc-miR-182	turquoise	0.077468917	-0.528269763
4	ssc-miR-92b-3p	turquoise	0.053635035	-0.568757039
5	ssc-miR-181c	turquoise	0.021907784	-0.650813888
6	ssc-miR-130a	turquoise	0.014989988	-0.679899867

In yellow module, the correlation between the MEM and the miRNA expression profile for A asterisk trait identified 9 porcine miRNAs: ssc-miR-874, ssc-miR-16, ssc-miR-30c-5p, ssc-miR-126-5p, ssc-miR-194a-5p, ssc-miR-378, ssc-let-7f-5p, ssc-miR-27b-3p, and ssc-miR-181a respectively. (Fig. 34 and Table 33)

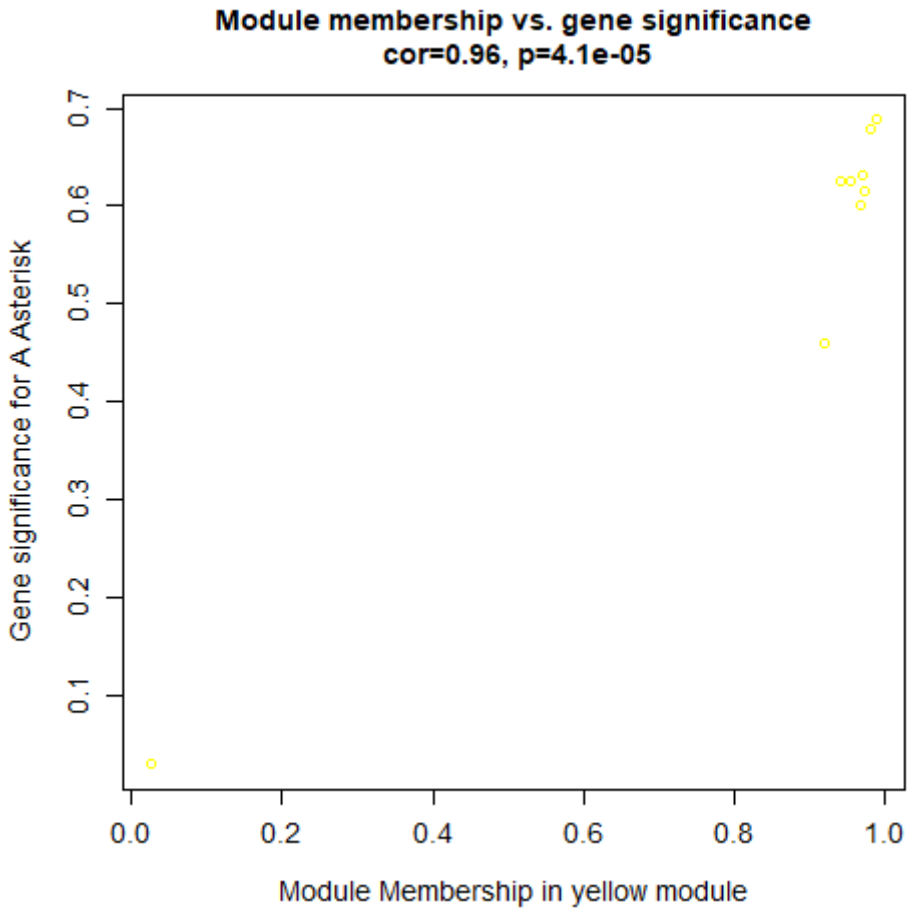

Figure 35. Intra-modular analysis for MEM (Yellow module). The figure shows the scatter plot of GS (y-axis) vs. MM (x-axis) for phenotypic trait a*in MEM yellow. The **GS** is the absolute value describing the relationship between the miRNA and the phenotypic trait a*, while the **MM** describes the correlation between the MEM and the miRNA expression profile.

Table 33. Intra-modular analysis for phenotypic trait a*. Identification trait-associated miRNA in yellow module.

SN	**Ensembl**	**Module**	**p.GS**	**GS**
1	ssc-miR-874	yellow	0.928062366	0.029265194
2	ssc-miR-16	yellow	0.132980065	-0.459396638
3	ssc-miR-30c-5p	yellow	0.038772273	-0.600949439
4	ssc-miR-126-5p	yellow	0.033554506	-0.614340117
5	ssc-miR-194a-5p	yellow	0.029843529	-0.624802331
6	ssc-miR-378	yellow	0.029330412	-0.626321408
7	ssc-let-7f-5p	yellow	0.027355682	-0.632352856
8	ssc-miR-27b-3p	yellow	0.015152669	-0.679112404
9	ssc-miR-181a	yellow	0.013385266	-0.688027102

4.2.8.2. Identification of trait associated modules for shoulder subcutaneous fat thickness trait, affected by PUFAs diets in PL and PLxDuroc pigs

The correlation between the MEM and the miRNA expression profile for shoulder subcutaneous fat thickness trait identified seven modules (Fig. 35-41 and Tables 34-40).

In black module, the correlation between the MEM and the miRNA expression profile for shoulder subcutaneous fat thickness trait identified 5 porcine miRNAs: ssc-miR-30a-3p, ssc-miR-21-5p, ssc-miR-204, ssc-let-7c, and ssc-miR-142-3p, respectively. (Fig. 35 and Table 34).

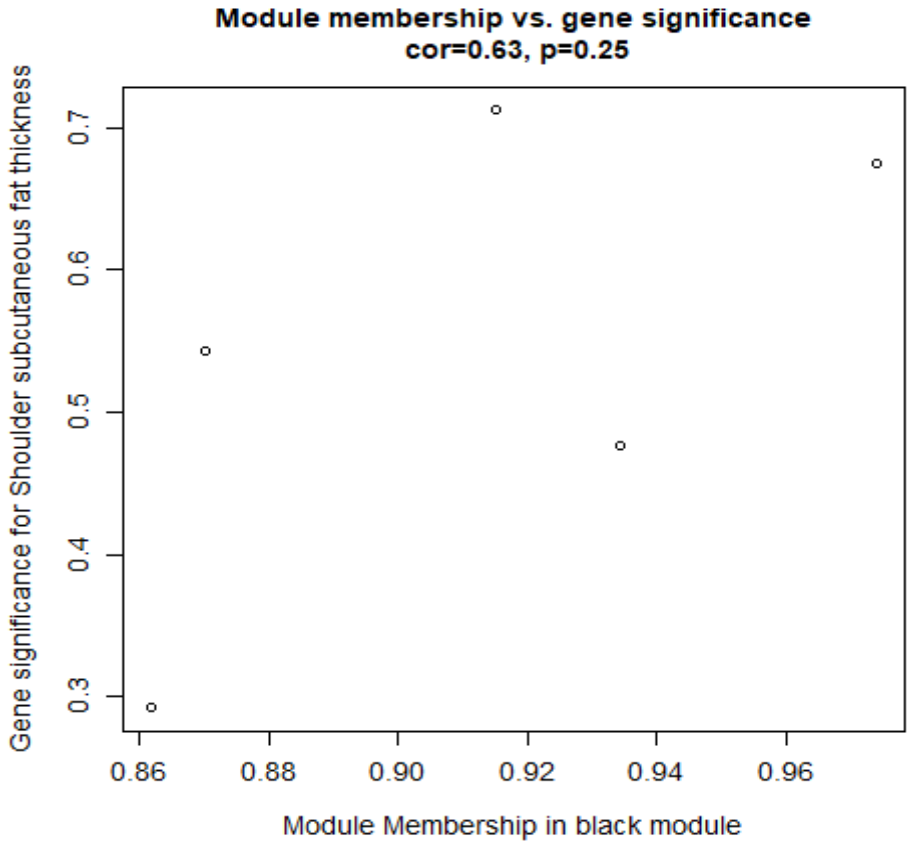

Figure 36: Intra-modular analysis for MEM (black module). The figure shows the scatter plot of GS (y-axis) vs. MM (x-axis) for phenotypic trait shoulder subcutaneous fat thickness in MEM black. The **GS** is the absolute value describing the relationship between the miRNA and the phenotypic trait shoulder subcutaneous fat thickness, while the **MM** describes the correlation between the MEM and the miRNA expression profile.

Table 34. Intra-modular analysis for phenotypic trait shoulder subcutaneous fat thickness. Identification trait-associated miRNA in black module.

SN	**Ensembl**	**Module**	**p.GS**	**GS**
1	ssc-miR-30a-3p	black	0.009365987	-0.712148271
2	ssc-miR-21-5p	black	0.015933205	-0.675418476
3	ssc-miR-204	black	0.067966849	-0.543209271
4	ssc-let-7c	black	0.117054996	-0.476798461
5	ssc-miR-142-3p	black	0.356226989	-0.292496064

In blue module, the correlation between the MEM and the miRNA expression profile for shoulder subcutaneous fat thickness trait identified 11 porcine miRNAs: ssc-miR-191, ssc-miR-22-3p, ssc-miR-122-5p, ssc-miR-26a, ssc-miR-199a-5p, ssc-miR-186-5p, ssc-miR-425-5p, ssc-miR-199b-3p, ssc-miR-199a-3p, ssc-miR-29a-3p, and ssc-miR-10387 respectively. (Fig. 36 and Table 35).

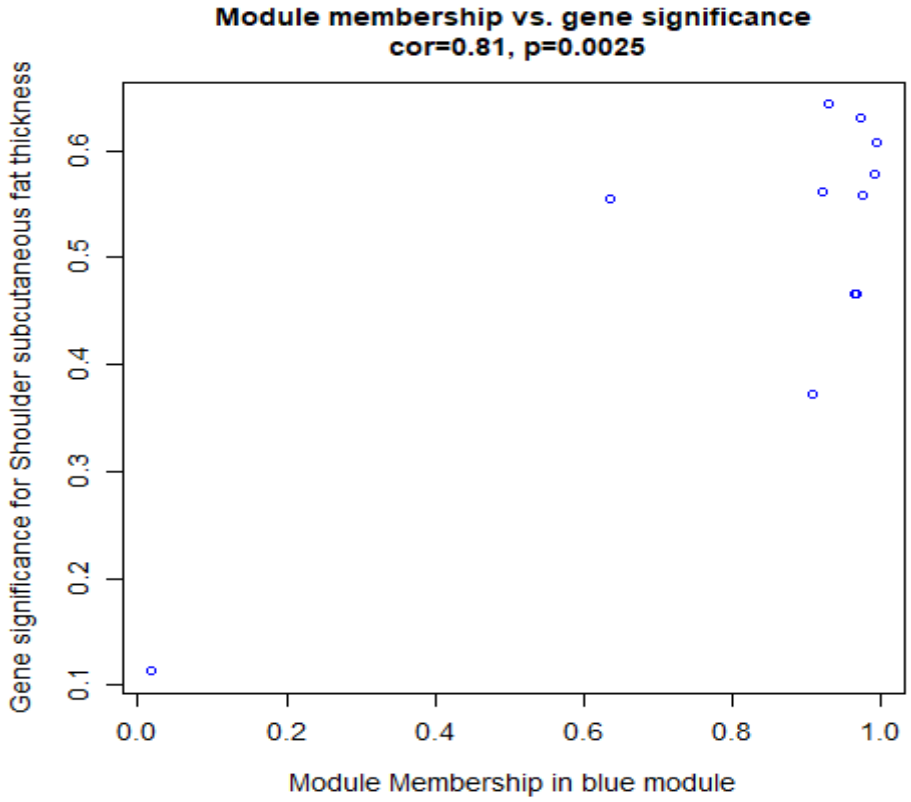

Figure 37: Intra-modular analysis for MEM (blue module). The figure shows the scatter plot of GS (y-axis) vs. MM (x-axis) for phenotypic trait shoulder subcutaneous fat thickness in MEM blue. The **GS** is the absolute value describing the relationship between the miRNA and the phenotypic trait shoulder subcutaneous fat thickness, while the **MM** describes the correlation between the MEM and the miRNA expression profile.

Table 35. Intra-modular analysis for phenotypic trait shoulder subcutaneous fat thickness. Identification trait-associated miRNA in blue module.

SN	**Ensembl**	**Module**	**p.GS**	**GS**
1	ssc-miR-10387	blue	0.024125932	-0.642934732
2	ssc-miR-425-5p	blue	0.028163008	-0.629850247
3	ssc-miR-191	blue	0.036189611	-0.607404955
4	ssc-miR-199a-5p	blue	0.049065825	-0.577899275
5	ssc-miR-29a-3p	blue	0.057733322	-0.561010127
6	ssc-miR-122-5p	blue	0.059700908	-0.557426633
7	ssc-miR-26a	blue	0.061466123	-0.554280952
8	ssc-miR-199a-3p	blue	0.126337938	-0.466479346
9	ssc-miR-199b-3p	blue	0.126927787	-0.465840685
10	ssc-miR-186-5p	blue	0.233182911	-0.372424044
11	ssc-miR-22-3p	blue	0.725406709	-0.113508231

In brown module, the correlation between the MEM and the miRNA expression profile for shoulder subcutaneous fat thickness trait identified 10 porcine miRNAs: ssc-miR-151-3p, ssc-miR-28-3p, ssc-miR-140-3p, ssc-miR-148a-3p, ssc-miR-181b, ssc-miR-30a-5p, ssc-miR-26b-5p, ssc-miR-486, ssc-miR-423-3p, and ssc-miR-125a respectively. (Fig. 37 and Table 36)

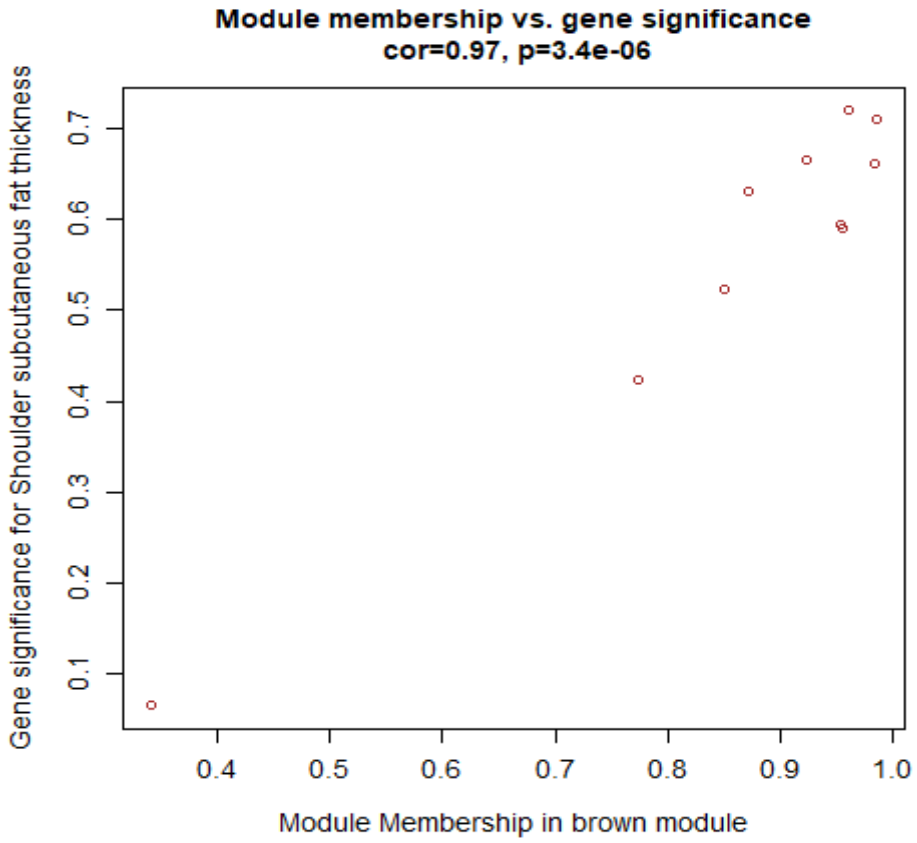

Figure 38. Intra-modular analysis for MEM (Brown module). The figure shows the scatter plot of GS (y-axis) vs. MM (x-axis) for phenotypic trait shoulder subcutaneous fat thickness in MEM brown. The **GS** is the absolute value describing the relationship between the miRNA and the phenotypic trait shoulder subcutaneous fat thickness, while the **MM** describes the correlation between the MEM and the miRNA expression profile.

Table 36. Intra-modular analysis for phenotypic trait shoulder subcutaneous fat thickness. Identification trait-associated miRNA in brown module.

SN	**Ensembl**	**Module**	**p.GS**	**GS**
1	ssc-miR-151-3p	brown	0.008311209	-0.719740027
2	ssc-miR-28-3p	brown	0.00968923	-0.709950034
3	ssc-miR-140-3p	brown	0.018061827	-0.665979161
4	ssc-miR-148a-3p	brown	0.019370689	-0.660573932
5	ssc-miR-181b	brown	0.027695796	-0.631292129
6	ssc-miR-30a-5p	brown	0.04131304	-0.594890795
7	ssc-miR-26b-5p	brown	0.043256598	-0.590432471
8	ssc-miR-486	brown	0.081116041	-0.522869385
9	ssc-miR-423-3p	brown	0.170551945	-0.423103198
10	ssc-miR-125a	brown	0.840867923	-0.065028448

In magenta module, the correlation between the MEM and the miRNA expression profile for shoulder subcutaneous fat thickness trait identified 15 porcine miRNAs: ssc-miR-103, ssc-miR-192, ssc-let-7i-5p, ssc-miR-92a, ssc-let-7a, ssc-miR-142-5p, ssc-miR-222, ssc-miR-101, ssc-miR-30d, ssc-miR-30e-5p, ssc-miR-98, ssc-miR-221-3p, ssc-miR-10390, ssc-miR-99b, and ssc-miR-542-3p, respectively. (Fig. 38 and Table 37).

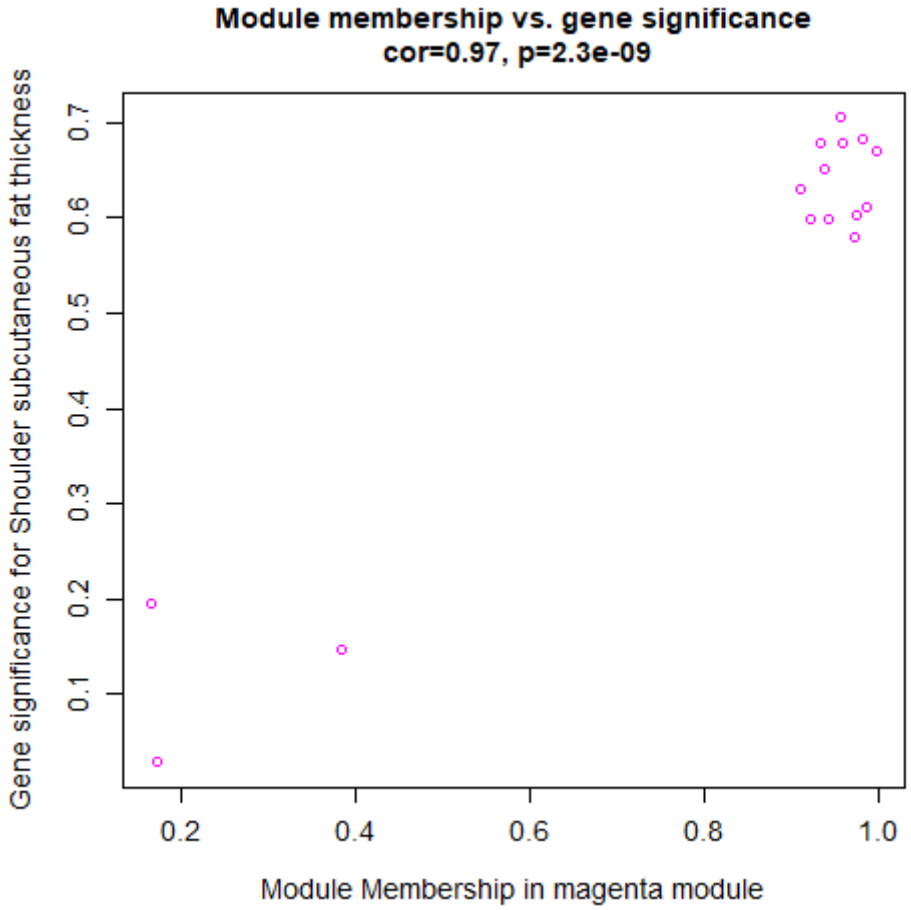

Figure 39. Intra-modular analysis for MEM (Magenta module). The figure shows the scatter plot of GS (y-axis) vs. MM (x-axis) for phenotypic trait shoulder subcutaneous fat thickness in MEM magenta. The **GS** is the absolute value describing the relationship between the miRNA and the phenotypic trait shoulder subcutaneous fat thickness, while the **MM** describes the correlation between the MEM and the miRNA expression profile.

Table 37. Intra-modular analysis for phenotypic trait shoulder subcutaneous fat thickness. Identification trait-associated miRNA in magenta module.

SN	**Ensembl**	**Module**	**p.GS**	**GS**
1	ssc-miR-103	magenta	0.01046956	-0.704859933
2	ssc-miR-192	magenta	0.014641211	-0.681609603
3	ssc-let-7i-5p	magenta	0.015392268	-0.677963878
4	ssc-miR-92a	magenta	0.015420967	-0.677827196
5	ssc-let-7a	magenta	0.016981789	-0.670659961

6	ssc-miR-142-5p	magenta	0.021907089	-0.650816446
7	ssc-miR-222	magenta	0.02839583	-0.629138162
8	ssc-miR-101	magenta	0.034942138	-0.610641424
9	ssc-miR-30d	magenta	0.038355189	-0.601970778
10	ssc-miR-30e-5p	magenta	0.039719499	-0.598658611
11	ssc-miR-98	magenta	0.039835542	-0.598380646
12	ssc-miR-221-3p	magenta	0.048669306	-0.578720421
13	ssc-miR-10390	magenta	0.544802726	0.194443581
14	ssc-miR-99b	magenta	0.65027118	-0.146199214
15	ssc-miR-542-3p	magenta	0.928677706	-0.0290143

In purple module, the correlation between the MEM and the miRNA expression profile for shoulder subcutaneous fat thickness trait identified 9 porcine miRNAs: ssc-miR-10a-5p, ssc-miR-143-3p, ssc-miR-215, ssc-miR-23b, ssc-miR-151-5p, ssc-miR-126-3p, ssc-miR-451, ssc-miR-23a, and ssc-miR-125b, respectively. (Fig. 39 and Table 38).

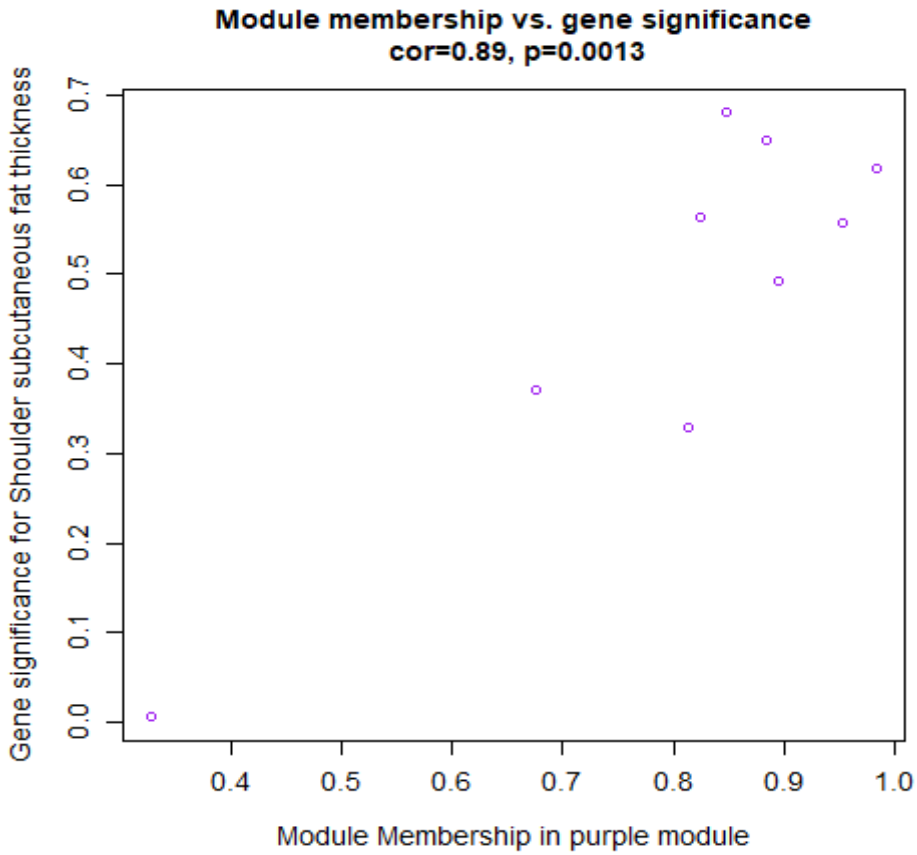

Figure 40. Intra-modular analysis for MEM (Purple). The figure shows the scatter plot of GS (y-axis) vs. MM (x-axis) for phenotypic trait shoulder subcutaneous fat thickness in MEM purple. The **GS** is the absolute value describing the relationship between the miRNA and the phenotypic trait shoulder subcutaneous fat thickness, while the **MM** describes the correlation between the MEM and the miRNA expression profile.

Table 38. Intra-modular analysis for phenotypic trait shoulder subcutaneous fat thickness. Identification trait-associated miRNA in purple module.

SN	**Ensembl**	**Module**	**p.GS**	**GS**
1	ssc-miR-10a-5p	purple	0.014990356	-0.679898078
2	ssc-miR-143-3p	purple	0.022445695	-0.648851678
3	ssc-miR-215	purple	0.032376456	-0.617567173
4	ssc-miR-23b	purple	0.05675669	-0.562820495
5	ssc-miR-151-5p	purple	0.060356335	-0.556251187
6	ssc-miR-126-3p	purple	0.103861677	-0.492438571
7	ssc-miR-451	purple	0.236180871	-0.370218815
8	ssc-miR-23a	purple	0.297247491	-0.328450977
9	ssc-miR-125b	purple	0.984406952	0.006336562

In turquoise module, the correlation between the MEM and the miRNA expression profile for shoulder subcutaneous fat thickness trait identified 6 porcine miRNAs: ssc-miR-92b-3p, ssc-miR-181c, ssc-miR-130a, ssc-miR-182, ssc-miR-1285, and ssc-miR-146b, respectively. (Fig.40 and Table 39).

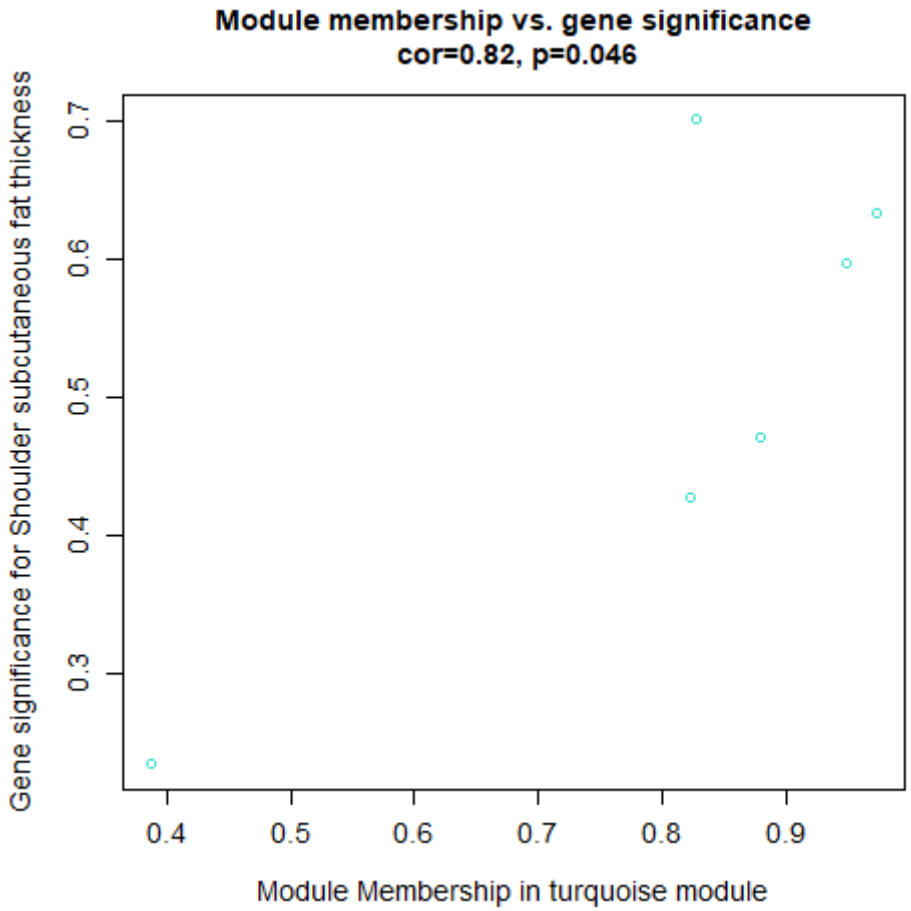

Figure 41. Intra-modular analysis for MEM (Turquoise module). The figure shows the scatter plot of GS (y-axis) vs. MM (x-axis) for phenotypic trait shoulder subcutaneous fat thickness in MEM turquoise. The **GS** is the absolute value describing the relationship between the miRNA and the phenotypic trait shoulder subcutaneous fat thickness, while the **MM** describes the correlation between the MEM and the miRNA expression profile.

Table 39. Intra-modular analysis for phenotypic trait shoulder subcutaneous fat thickness. Identification trait-associated miRNA in turquoise module.

SN	**Ensembl**	**Module**	**p.GS**	**GS**
1	ssc-miR-146b	turquoise	0.011046821	-0.701273269
2	ssc-miR-1285	turquoise	0.026811785	-0.634069101
3	ssc-miR-182	turquoise	0.040247206	-0.597399182
4	ssc-miR-92b-3p	turquoise	0.121819035	-0.471438159
5	ssc-miR-181c	turquoise	0.165368849	-0.427784396
6	ssc-miR-130a	turquoise	0.464511463	-0.23382345

In yellow module, the correlation between the MEM and the miRNA expression profile for shoulder subcutaneous fat thickness trait identified 9 porcine miRNAs: ssc-miR-378, ssc-let-7f-5p, ssc-miR-181a, ssc-miR-126-5p, ssc-miR-16, ssc-miR-194a-5p, ssc-miR-27b-3p, ssc-miR-30c-5p, and ssc-miR-874, respectively. (Fig. 41 and Table 40).

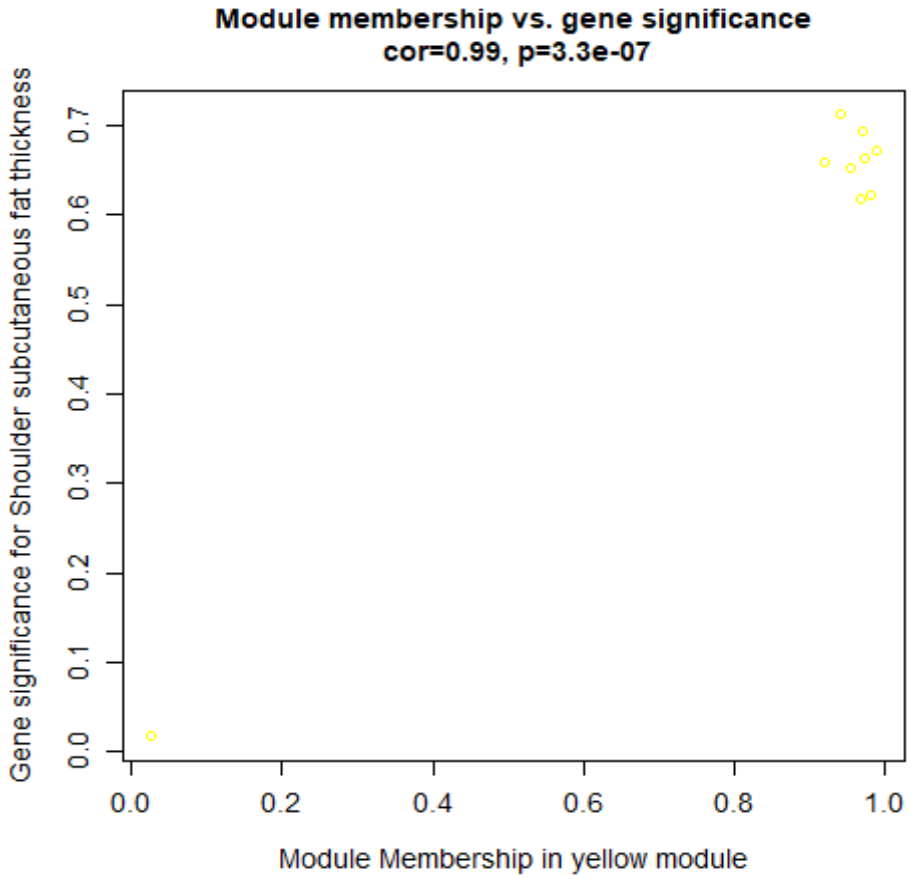

Figure 42. Intra-modular analysis for MEM (yellow module). The figure shows the scatter plot of GS (y-axis) vs. MM (x-axis) for phenotypic trait shoulder subcutaneous fat thickness in MEM yellow. The **GS** is the absolute value describing the relationship between the miRNA and the phenotypic trait shoulder subcutaneous fat thickness, while the **MM** describes the correlation between the MEM and the miRNA expression profile.

Table 40. Intra-modular analysis for phenotypic trait shoulder subcutaneous fat thickness. Identification trait-associated miRNA in yellow module.

SN	**Ensembl**	**Module**	**p.GS**	**GS**
1	ssc-miR-378	yellow	0.009304947	-0.712569708
2	ssc-let-7f-5p	yellow	0.012273438	-0.694091035
3	ssc-miR-181a	yellow	0.016768607	-0.67160954
4	ssc-miR-126-5p	yellow	0.018575802	-0.663823441
5	ssc-miR-16	yellow	0.019645279	-0.659474087
6	ssc-miR-194a-5p	yellow	0.021613357	-0.6519028
7	ssc-miR-27b-3p	yellow	0.030262221	-0.623576669
8	ssc-miR-30c-5p	yellow	0.032373612	-0.617575066
9	ssc-miR-874	yellow	0.958103475	-0.017031205

4.2.8.3. Identification of trait associated modules for Conductivity 24 hours postmortem (PE24) trait, affected by PUFAs diets in PL and PLxDuroc pigs

The correlation between the MEM and the miRNA expression profile for Conductivity 24 hours postmortem (PE24) trait identified only two modules (Figure 43-44 and Table 41-42).

In blue module, the correlation between the MEM and the miRNA expression profile for Conductivity 24 hours post mortem (PE24) trait identified 11 porcine miRNAs: ssc-miR-199a-5p, ssc-miR-199a-3p, ssc-miR-199b-3p, ssc-miR-29a-3p, ssc-miR-186-5p, ssc-miR-122-5p, ssc-miR-26a, ssc-miR-191, ssc-miR-22-3p, ssc-miR-425-5p, and ssc-miR-10387 respectively. (Fig. 42 and Table 41).

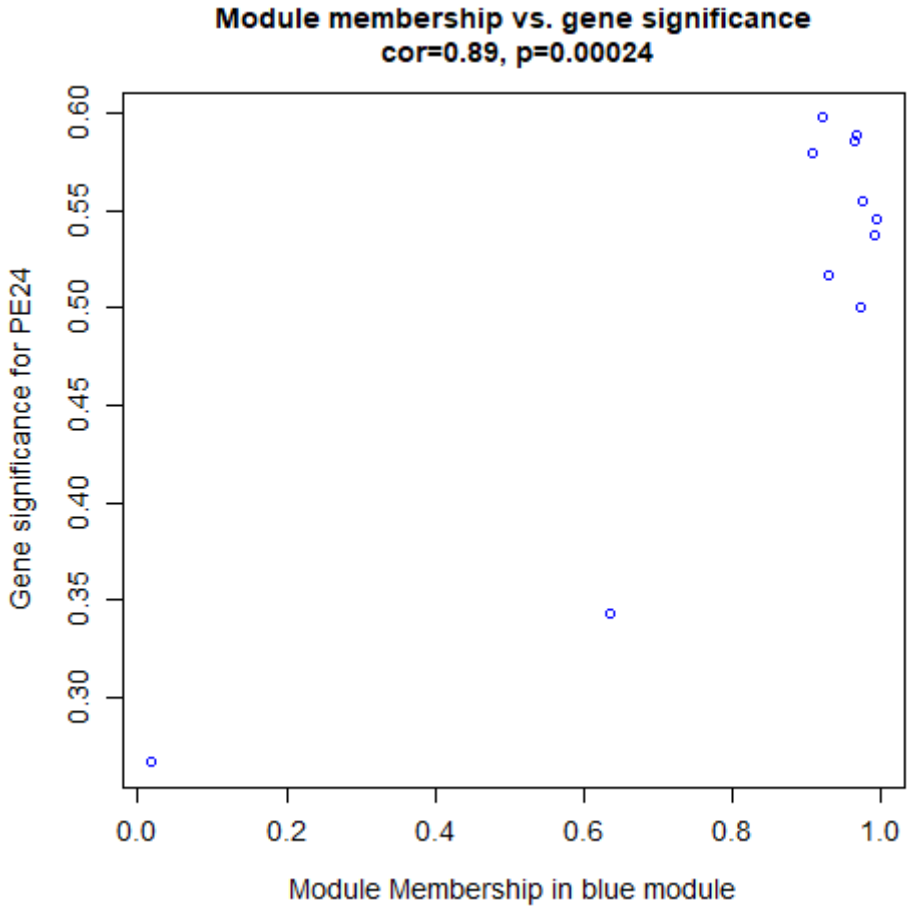

Figure 43. Intra-modular analysis for MEM (blue module). The figure shows the scatter plot of GS (y-axis) vs. MM (x-axis) for phenotypic trait Conductivity 24 hours postmortem (PE24) in MEM blue. The **GS** is the absolute value describing the relationship between the miRNA and the phenotypic trait Conductivity 24 hours postmortem (PE24), while the **MM** describes the correlation between the MEM and the miRNA expression profile.

Table 41. Intra-modular analysis for phenotypic trait Conductivity 24 hours postmortem (PE24). Identification trait-associated miRNA in blue module.

SN	**Ensembl**	**Module**	**p.GS**	**GS**
1	ssc-miR-199a-5p	blue	0.040219059	-0.597466061
2	ssc-miR-199a-3p	blue	0.043915251	-0.588953817
3	ssc-miR-199b-3p	blue	0.045342948	-0.585801726
4	ssc-miR-29a-3p	blue	0.048354014	-0.579376721
5	ssc-miR-186-5p	blue	0.061212417	-0.55472917
6	ssc-miR-122-5p	blue	0.066485011	-0.545666388
7	ssc-miR-26a	blue	0.071633127	-0.537284733
8	ssc-miR-191	blue	0.085103763	-0.517150625
9	ssc-miR-22-3p	blue	0.097325726	-0.500680466
10	ssc-miR-425-5p	blue	0.274192548	-0.343579417
11	ssc-miR-10387	blue	0.401664631	-0.266916914

In pink module, the correlation between the MEM and the miRNA expression profile for Conductivity 24 hours postmortem (PE24) trait identified 6 porcine miRNAs: ssc-miR-30b-5p, ssc-miR-30e-3p, ssc-miR-99a-5p, ssc-miR-19b, ssc-miR-339, and ssc-miR-339-5p respectively. (Fig. 43 and Table 42).

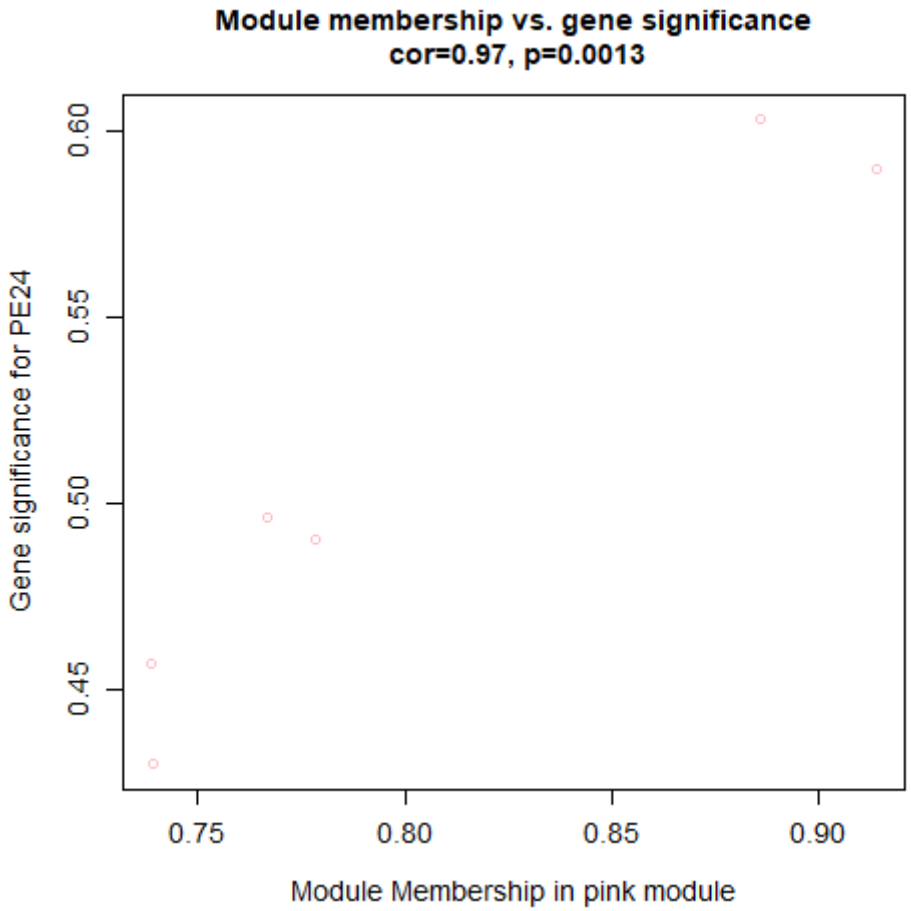

Figure 44. Intra-modular analysis for MEM (Pink module). The figure shows the scatter plot of GS (y-axis) vs. MM (x-axis) for phenotypic trait Conductivity 24 hours postmortem (PE24) in MEM pink. The **GS** is the absolute value describing the relationship between the miRNA and the phenotypic trait Conductivity 24 hours postmortem (PE24), while the **MM** describes the correlation between the MEM and the miRNA expression profile.

Table 42. Intra-modular analysis for phenotypic trait Conductivity 24 hours postmortem (PE24). Identification trait-associated miRNA in pink module.

SN	**Ensembl**	**Module**	**p.GS**	**GS**
1	ssc-miR-30b-5p	pink	0.081547887	-0.522240974
2	ssc-miR-30e-3p	pink	0.138630005	-0.453550799
3	ssc-miR-99a-5p	pink	0.191080269	-0.405390679
4	ssc-miR-19b	pink	0.261705572	-0.35207853
5	ssc-miR-339	pink	0.766216014	0.096174188
6	ssc-miR-339-5p	pink	0.816095063	0.075295913

4.2.8.4. Identification of trait associated modules for Ashes trait, affected by PUFAs diets in PL and PLxDuroc pigs

The correlation between the MEM and the miRNA expression profile for Ashes trait identified eight modules (Fig. 44-51 and Table 43-50).

In black module, the correlation between the MEM and the miRNA expression profile for Ashes trait identified 5 porcine miRNAs: ssc-let-7c, ssc-miR-204, ssc-miR-21-5p, ssc-miR-30a-3p, and ssc-miR-142-3p, respectively. (Fig. 44 and Table 43).

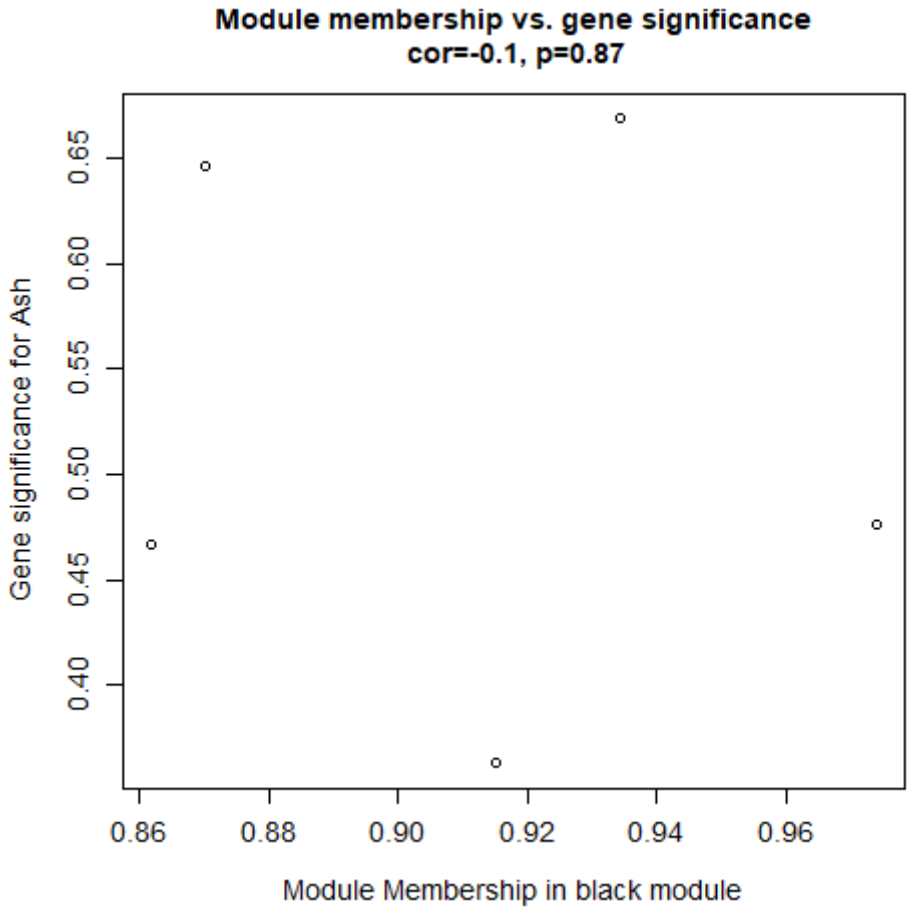

Figure 45. Intra-modular analysis for MEM (Black module). The figure shows the scatter plot of GS (y-axis) vs. MM (x-axis) for phenotypic trait ashes in MEM black. The **GS** is the absolute value describing the relationship between the miRNA and the phenotypic trait ashes.

Table 43. Intra-modular analysis for phenotypic trait ashes. Identification trait-associated miRNA in black module.

SN	**Ensembl**	**Module**	**p.GS**	**GS**
1	ssc-let-7c	black	0.124625278	-0.468344851
2	ssc-miR-204	black	0.245931885	-0.363158849
3	ssc-miR-21-5p	black	0.272858221	-0.344476819
4	ssc-miR-30a-3p	black	0.33125619	-0.307289105
5	ssc-miR-142-3p	black	0.346512992	-0.298182567

In blue module, the correlation between the MEM and the miRNA expression profile for Ashes trait identified 10 porcine miRNAs: ssc-miR-199a-3p, ssc-miR-199b-3p, ssc-miR-26a, ssc-miR-186-5p, ssc-miR-122-5p, ssc-miR-22-3p, ssc-miR-199a-5p, ssc-miR-191, ssc-miR-425-5p, and ssc-miR-10387 respectively. (Fig. 45 and Table 44)

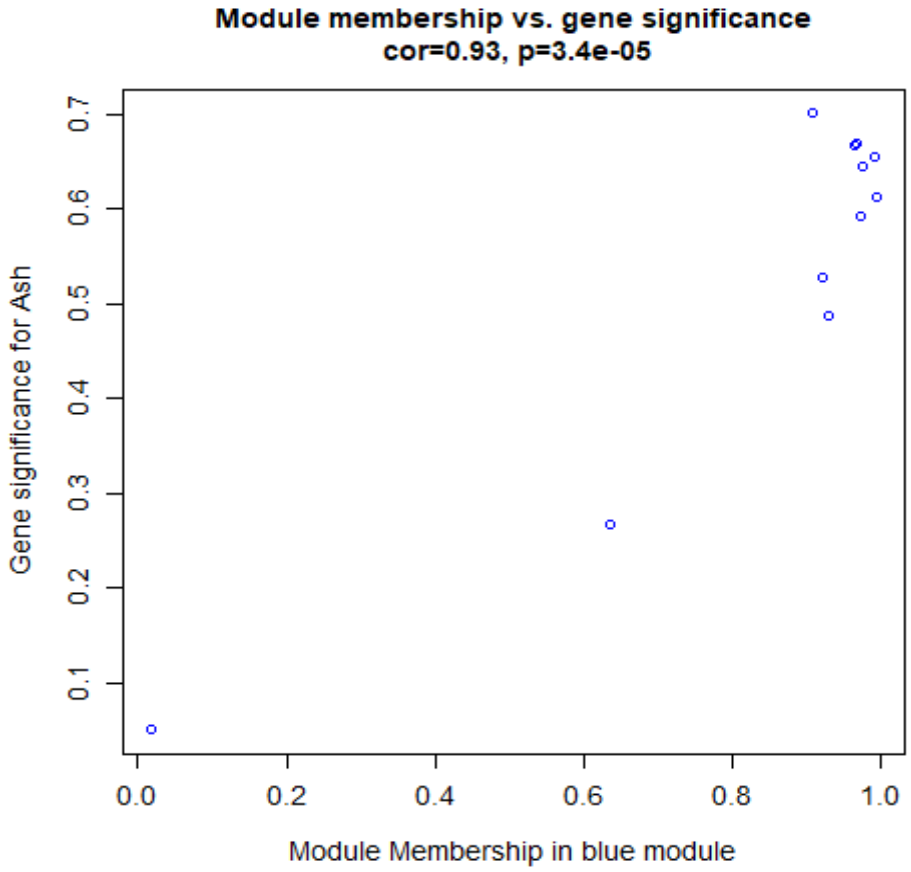

Figure 46. Intra-modular analysis for MEM (Blue module). The figure shows the scatter plot of GS (y-axis) vs. MM (x-axis) for phenotypic trait ashes in MEM blue. The **GS** is the absolute value describing the relationship between the miRNA and the phenotypic trait ashes.

Table 44. Intra-modular analysis for phenotypic trait ashes. Identification trait-associated miRNA in blue module.

SN	**Ensembl**	**Module**	**p.GS**	**GS**
1	ssc-miR-199a-3p	blue	0.017373041	0.668939729
2	ssc-miR-199b-3p	blue	0.017728166	0.667402779
3	ssc-miR-26a	blue	0.020928264	0.654479058
4	ssc-miR-186-5p	blue	0.02363066	0.644646854
5	ssc-miR-122-5p	blue	0.034109896	0.612846836
6	ssc-miR-22-3p	blue	0.042599447	0.591923728
7	ssc-miR-199a-5p	blue	0.078032064	0.527424734
8	ssc-miR-191	blue	0.107693913	0.487766048
9	ssc-miR-425-5p	blue	0.402040762	0.266711546
10	ssc-miR-10387	blue	0.877092617	0.050110715

In green module, the correlation between the MEM and the miRNA expression profile for Ashes trait identified 20 porcine miRNAs: ssc-miR-10383, ssc-miR-374a-5p, ssc-miR-423-5p, ssc-miR-146a-5p, ssc-miR-122-3p, ssc-let-7e, ssc-let-7d-5p, ssc-miR-148b-3p, ssc-miR-340, ssc-miR-107, ssc-miR-127, ssc-miR-24-3p, ssc-miR-7142-3p, ssc-miR-320, ssc-miR-15a, ssc-miR-100, ssc-miR-10b, ssc-miR-374a-3p, ssc-miR-7134-3p, and ssc-miR-375 respectively. (Fig. 46 and Table 45).

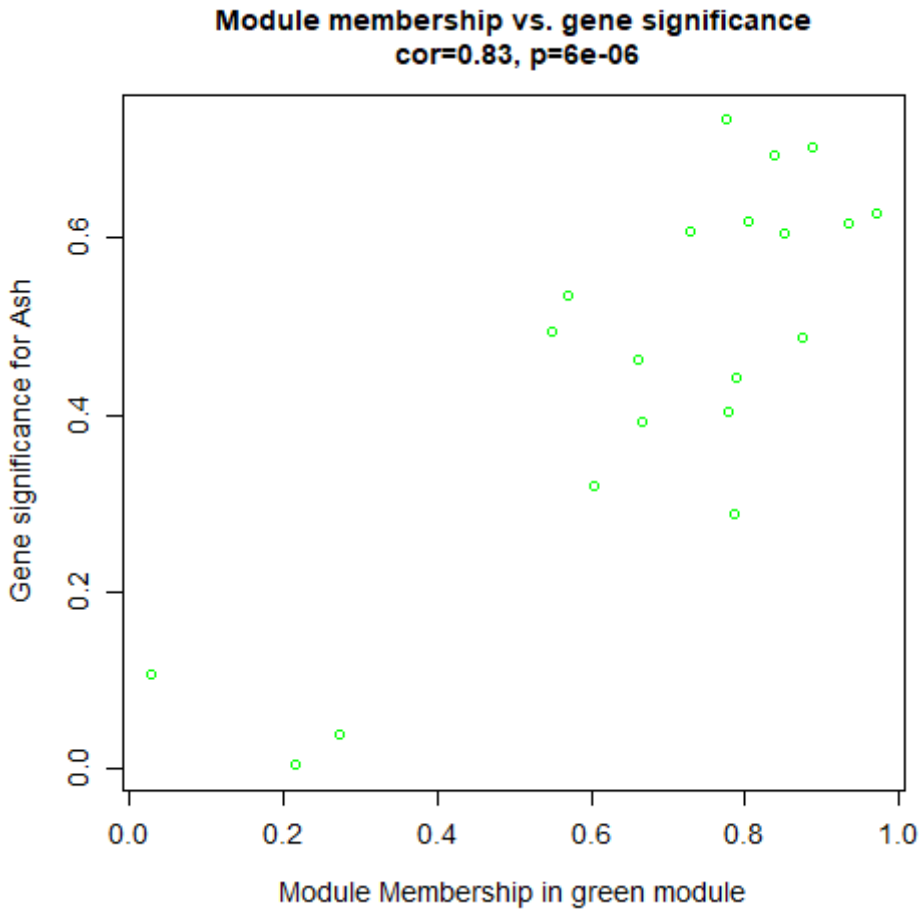

Figure 47. Intra-modular analysis for MEM (Green module). The figure shows the scatter plot of GS (y-axis) vs. MM (x-axis) for phenotypic trait ashes in MEM green. The **GS** is the absolute value describing the relationship between the miRNA and the phenotypic trait ashes.

Table 45. Intra-modular analysis for phenotypic trait ashes. Identification trait-associated miRNA in green module.

SN	**Ensembl**	**Module**	**p.GS**	**GS**
1	ssc-miR-10383	green	0.058701855	-0.559235724
2	ssc-miR-374a-5p	green	0.059468843	-0.557844968
3	ssc-miR-423-5p	green	0.07122336	-0.537936391
4	ssc-miR-146a-5p	green	0.08160238	-0.522161838
5	ssc-miR-122-3p	green	0.089296596	-0.511330467
6	ssc-let-7e	green	0.11286941	-0.481627816
7	ssc-let-7d-5p	green	0.119249156	-0.474312203

8	ssc-miR-148b-3p	green	0.139228368	-0.452940786
9	ssc-miR-340	green	0.150838973	-0.441424247
10	ssc-miR-107	green	0.310392827	-0.320120019
11	ssc-miR-127	green	0.314406915	-0.317615319
12	ssc-miR-24-3p	green	0.3146928	-0.317437609
13	ssc-miR-7142-3p	green	0.371822298	-0.283535549
14	ssc-miR-320	green	0.408758391	-0.263059873
15	ssc-miR-15a	green	0.418298974	-0.257924818
16	ssc-miR-100	green	0.505615308	-0.213316494
17	ssc-miR-10b	green	0.547281168	0.193269709
18	ssc-miR-374a-3p	green	0.555826351	-0.189239228
19	ssc-miR-7134-3p	green	0.738433865	0.107946837
20	ssc-miR-375	green	0.755613903	-0.100653399

In magenta module, the correlation between the MEM and the miRNA expression profile for Ashes trait identified 15 miRNAs: ssc-miR-142-5p, ssc-miR-30e-5p, ssc-miR-10390, ssc-let-7a, ssc-miR-99b, ssc-miR-192, ssc-miR-101, ssc-miR-30d, ssc-miR-221-3p, ssc-miR-98, ssc-let-7i-5p, ssc-miR-222, ssc-miR-92a, ssc-miR-103, ssc-miR-542-3p, respectively (Fig.47 and Table 46).

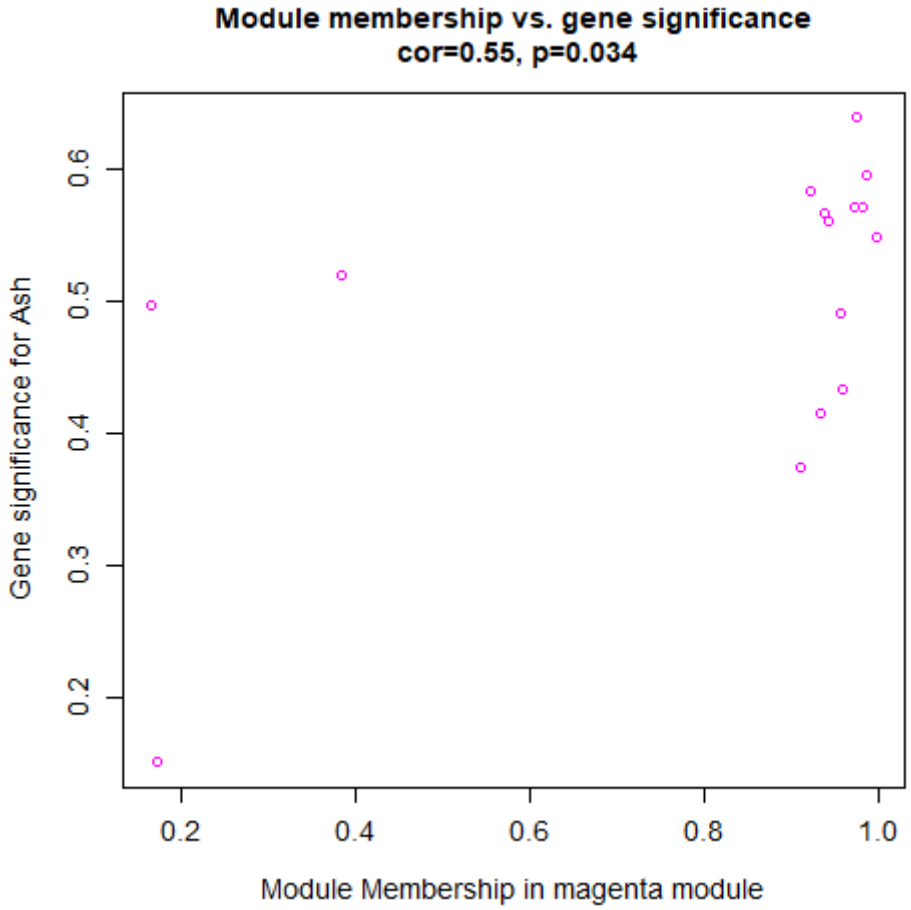

Figure 48. Intra-modular analysis for MEM (Magenta module). The figure shows the scatter plot of GS (y-axis) vs. MM (x-axis) for phenotypic trait ashes in MEM magenta. The **GS** is the absolute value describing the relationship between the miRNA and the phenotypic trait ashes.

Table 46. Intra-modular analysis for phenotypic trait ashes. Identification trait-associated miRNA in magenta module.

SN	**Ensembl**	**Module**	**p.GS**	**GS**
1	ssc-miR-142-5p	magenta	0.086033597	-0.515843426
2	ssc-miR-30e-5p	magenta	0.09087084	-0.509192971
3	ssc-miR-10390	magenta	0.13018842	-0.462344722
4	ssc-let-7a	magenta	0.16450193	-0.428576367
5	ssc-miR-99b	magenta	0.166842006	-0.42644459
6	ssc-miR-192	magenta	0.171506997	-0.422250441
7	ssc-miR-101	magenta	0.183093322	-0.412134086
8	ssc-miR-30d	magenta	0.195980752	-0.401339138
9	ssc-miR-221-3p	magenta	0.267751945	-0.347934572

10	ssc-miR-98	magenta	0.290680057	-0.332690581
11	ssc-let-7i-5p	magenta	0.293257283	-0.331020483
12	ssc-miR-222	magenta	0.397045525	-0.269446905
13	ssc-miR-92a	magenta	0.408904668	-0.262980693
14	ssc-miR-103	magenta	0.428506575	-0.252494509
15	ssc-miR-542-3p	magenta	0.526053759	0.203397681

In purple module, the correlation between the MEM and the miRNA expression profile for Ashes trait identified 9 porcine miRNAs: ssc-miR-23a, ssc-miR-151-5p, ssc-miR-126-3p, ssc-miR-215, ssc-miR-125b, ssc-miR-451, ssc-miR-23b, ssc-miR-10a-5p, and ssc-miR-143-3p, respectively (Fig. 48 and Table 47).

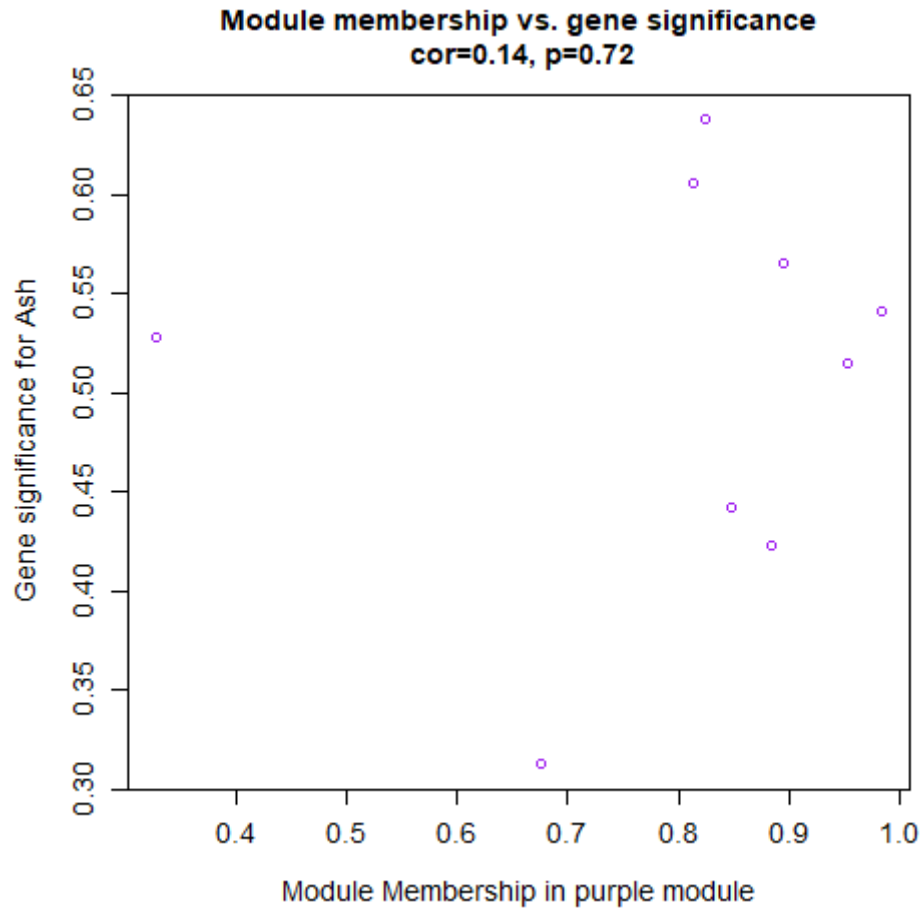

Figure 49. Intra-modular analysis for MEM (Purple module). The figure shows the scatter plot of GS (y-axis) vs. MM (x-axis) for phenotypic trait ashes in MEM purple. The **GS** is the absolute value describing the relationship between the miRNA and the phenotypic trait ashes.

Table 47. Intra-modular analysis for phenotypic trait ashes. Identification trait-associated miRNA in purple module.

SN	**Ensembl**	**Module**	**p.GS**	**GS**
1	ssc-miR-23a	purple	0.060326201	-0.556305034
2	ssc-miR-151-5p	purple	0.070860508	-0.538515592
3	ssc-miR-126-3p	purple	0.084383157	-0.518170359
4	ssc-miR-215	purple	0.112311912	-0.48227994
5	ssc-miR-125b	purple	0.15292772	-0.439413408
6	ssc-miR-451	purple	0.179203787	-0.415484338
7	ssc-miR-23b	purple	0.27071331	-0.345924683
8	ssc-miR-10a-5p	purple	0.284701782	-0.33659717
9	ssc-miR-143-3p	purple	0.503258409	-0.214471524

In red module, the correlation between the MEM and the miRNA expression profile for Ashes trait identified 3 porcine miRNAs: ssc-miR-148a-5p, ssc-let-7g, and ssc-miR-27a, respectively (Fig.49 and Table 48).

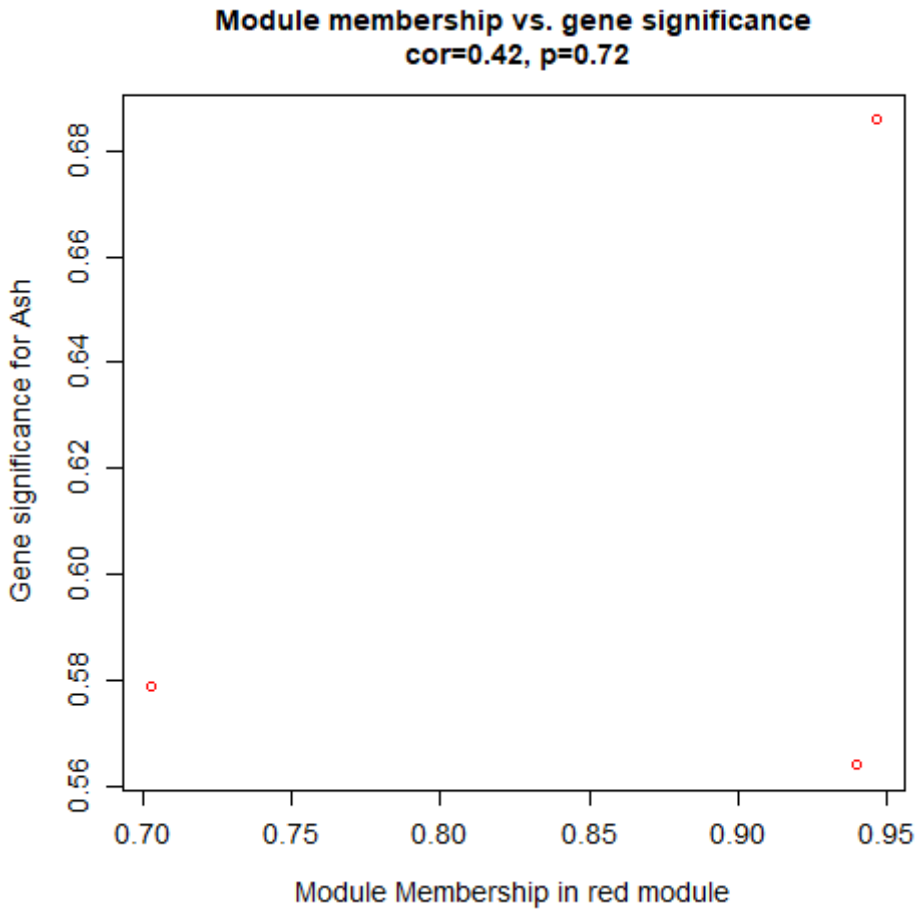

Figure 50. Intra-modular analysis for MEM (Red module). The figure shows the scatter plot of GS (y-axis) vs. MM (x-axis) for phenotypic trait ashes in MEM red. The **GS** is the absolute value describing the relationship between the miRNA and the phenotypic trait ashes.

Table 48. Intra-modular analysis for phenotypic trait ashes. Identification trait-associated miRNA in red module.

SN	**Ensembl**	**Module**	**p.GS**	**GS**
77	ssc-miR-148a-5p	red	0.042538266	-0.59206339
78	ssc-let-7g	red	0.119987995	-0.473481784
79	ssc-miR-27a	red	0.982634191	0.007057051

In turquoise module, the correlation between the MEM and the miRNA expression profile for Ashes trait identified 6 porcine miRNAs: ssc-miR-182, ssc-miR-181c, ssc-miR-130a, ssc-miR-1285, ssc-miR-92b-3p, and ssc-miR-146b, respectively (Fig. 50 and Table 49).

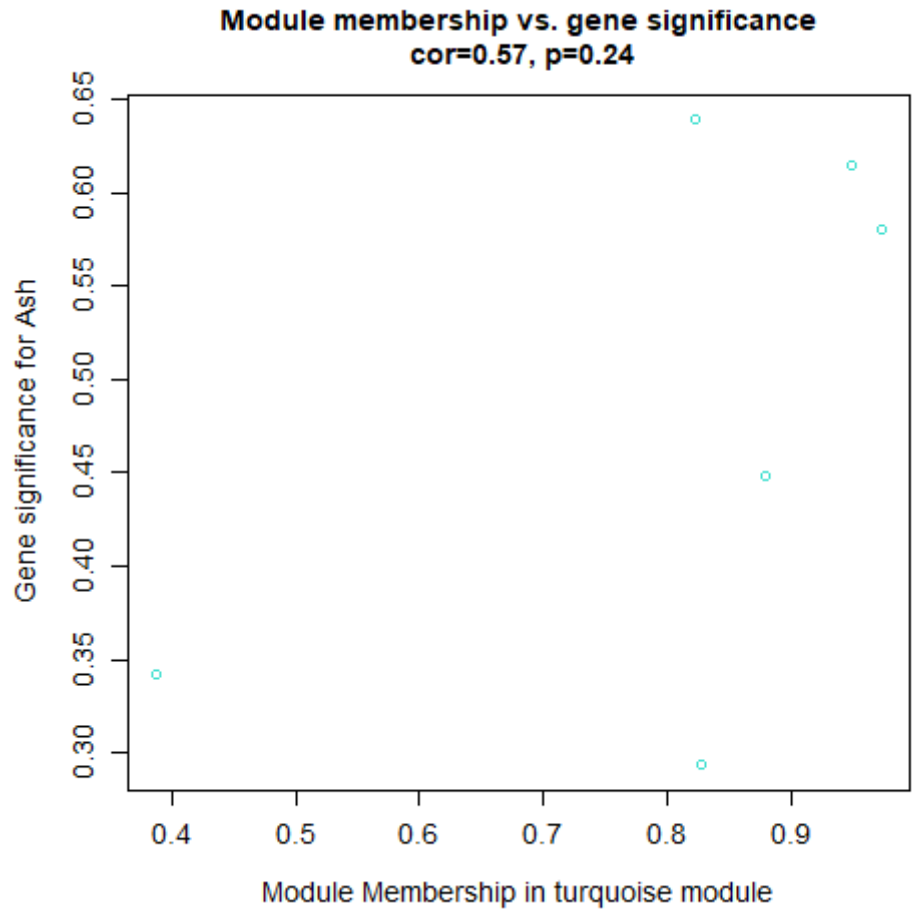

Figure 51. Intra-modular analysis for MEM (Turquoise module). The figure shows the scatter plot of GS (y-axis) vs. MM (x-axis) for phenotypic trait ashes in MEM turquoise. The **GS** is the absolute value describing the relationship between the miRNA and the phenotypic trait ashes.

Table 49. Intra-modular analysis for phenotypic trait ashes. Identification trait-associated miRNA in turquoise module.

SN	**Ensembl**	**Module**	**p.GS**	**GS**
1	ssc-miR-182	turquoise	0.040230046	-0.597439952
2	ssc-miR-181c	turquoise	0.10977179	-0.485278644
3	ssc-miR-130a	turquoise	0.145743069	-0.446406062
4	ssc-miR-1285	turquoise	0.163323676	-0.429656999
5	ssc-miR-92b-3p	turquoise	0.212753505	-0.387924353
6	ssc-miR-146b	turquoise	0.831635793	-0.068847932

In yellow module, the correlation between the MEM and the miRNA expression profile for Ashes trait identified 9 miRNAs: ssc-miR-126-5p, ssc-miR-194a-5p, ssc-miR-27b-3p, ssc-miR-30c-5p, ssc-miR-181a, ssc-miR-378, ssc-miR-16, ssc-let-7f-5p, and ssc-miR-874, respectively (Fig. 51 and Table 50).

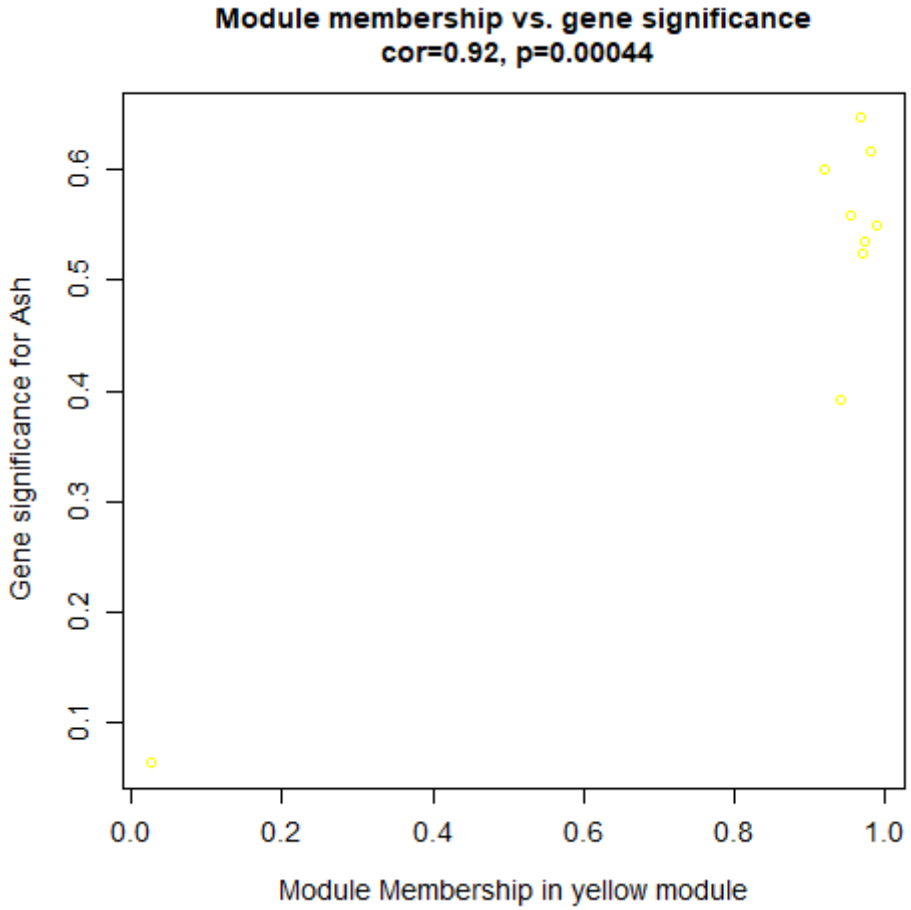

Figure 52. Intra-modular analysis for MEM (Yellow module). The figure shows the scatter plot of GS (y-axis) vs. MM (x-axis) for phenotypic trait ashes in MEM yellow. The **GS** is the absolute value describing the relationship between the miRNA and the phenotypic trait ashes.

Table 50. Intra-modular analysis for phenotypic trait ashes. Identification trait-associated miRNA in yellow module.

SN	**Ensembl**	**Module**	**p.GS**	**GS**
1	ssc-miR-126-5p	yellow	0.09894793	-0.498601117
2	ssc-miR-194a-5p	yellow	0.118964474	-0.474633075
3	ssc-miR-27b-3p	yellow	0.136582952	-0.45565068
4	ssc-miR-30c-5p	yellow	0.163640731	-0.429365729
5	ssc-miR-181a	yellow	0.221490266	-0.381190624
6	ssc-miR-378	yellow	0.365101085	-0.287372633
7	ssc-miR-16	yellow	0.454746408	-0.238816978
8	ssc-let-7f-5p	yellow	0.467529368	-0.232290175
9	ssc-miR-874	yellow	0.819795854	-0.073758219

4.3. Mapping of the fixed target genes of miRNA pig

The python script designed for the mapping fixed target genes of miRNA pig was utilized for the complete WGCNA analysis of miRNA liver transcriptome of PL purebred and PLxDuroc crossbred pigs.

The list of target genes for porcine miRNA was downloaded from the miRDB.org database (https://mirdb.org/). The miRDB is an online database with miRNA target predictions. Database hosts predicted miRNA targets for five species: human, mouse, rat, dog and chicken **(Liu W et. al, 2019)**.

The target genes with target score greater than 90 were classified as significant. A total of 94 miRNA with the module membership established during WGCNA analysis. The obtained result revealed that a total of 44 miRNAs (out of 94 miRNA) had a 6719 statistically significant target genes with the target score > 90.

The highest number of target genes were found in ssc-miR-30e-5p (520) which is a member of the magenta module. The second highest number of target genes were found for the ssc-miR-30b-5p and ssc-miR-30c-5p (518 each) from modules pink and yellow, respectively. The lowest number of target genes were found for ssc-miR-126-3p and ssc-miR-423-3p (1 each) from modules purple and brown, respectively.

Table 51. Number of target genes found for miRNA with target score > 90.

miRNA	Number of target genes	module
ssc-miR-30e-5p	520	magenta
ssc-miR-30b-5p	518	pink
ssc-miR-30c-5p	518	yellow
ssc-miR-30a-5p	517	brown
ssc-miR-27b-3p	326	yellow
ssc-miR-26b-5p	322	brown
ssc-miR-92b-3p	312	turquoise
ssc-miR-186-5p	285	blue
ssc-miR-126-5p	283	yellow
ssc-miR-29a-3p	252	blue
ssc-miR-148a-3p	211	brown
ssc-miR-148b-3p	211	green
ssc-miR-374a-5p	186	green
ssc-let-7i-5p	184	magenta
ssc-let-7f-5p	181	yellow
ssc-miR-30e-3p	162	pink

ssc-miR-30a-3p	161	black
ssc-miR-107	148	green
ssc-let-7d-5p	146	green
ssc-miR-24-3p	143	green
ssc-miR-142-5p	141	magenta
ssc-miR-143-3p	91	purple
ssc-miR-199a-5p	86	blue
ssc-miR-199a-3p	81	blue
ssc-miR-199b-3p	81	blue
ssc-miR-221-3p	80	magenta
ssc-miR-142-3p	73	black
ssc-miR-21-5p	72	black
ssc-miR-22-3p	60	blue
ssc-miR-374a-3p	54	green
ssc-miR-140-3p	49	brown
ssc-miR-423-5p	38	green
ssc-miR-542-3p	38	magenta
ssc-miR-146a-5p	35	green
ssc-miR-122-5p	34	blue
ssc-miR-10a-5p	30	purple
ssc-miR-148a-5p	27	red
ssc-miR-339-5p	20	pink
ssc-miR-425-5p	18	blue
ssc-miR-28-3p	14	brown
ssc-miR-99a-5p	7	pink
ssc-miR-122-3p	2	green
ssc-miR-126-3p	1	purple
ssc-miR-423-3p	1	brown

Target genes were grouped by the module of its miRNAs target. miRNAs from the yellow module had the highest number of target genes (1308), brown module miRNAs identified 1114 genes, and green and magenta modules miRNAs targets 963 genes each. The lowest number of target genes were present in the red module (27).

Table 52. Number of target genes with target score > 90 identified for miRNAs in each of the modules.

Module	Number of target genes
Yellow	1308
Brown	1114
Green	963
Magenta	963
Blue	897
Pink	707
Turquoise	312
Black	306
Purple	122
Red	27

Table 53. The highest target gene score for miRNAs from black module

miRNA	Target Gene	Target Score	module
ssc-miR-30a-3p	PCLO	99.8725051981171	black
ssc-miR-30a-3p	NUFIP2	99.7764011073975	black
ssc-miR-30a-3p	CDC73	99.6234578884547	black
ssc-miR-142-3p	TASOR2	99.616660325564	black
ssc-miR-30a-3p	ZEB2	99.526955288982	black

Table 54. The highest target gene score for miRNAs from blue module

miRNA	Target Gene	Target Score	module
ssc-miR-29a-3p	TET3	99.9994760552698	blue
ssc-miR-186-5p	TBL1XR1	99.9855216659122	blue
ssc-miR-186-5p	GABRA4	99.9746693277311	blue
ssc-miR-186-5p	STK17B	99.9742948949727	blue
ssc-miR-22-3p	GRM5	99.9270382681564	blue

Table 55. The highest target gene score for miRNAs from brown module

miRNA	Target Gene	Target Score	module
ssc-miR-30a-5p	CELSR3	99.998490412936	brown
ssc-miR-30a-5p	PPARGC1B	99.9829001483369	brown
ssc-miR-30a-5p	WDR7	99.9536578864795	brown
ssc-miR-30a-5p	STOX2	99.9306249844605	brown
ssc-miR-30a-5p	ANKRA2	99.8285694902398	brown

Table 56. The highest target gene score for miRNAs from green module

miRNA	Target Gene	Target Score	module
ssc-miR-107	DICER1	99.9830481731394	green
ssc-let-7d-5p	TRIM71	99.9620105034215	green
ssc-miR-146a-5p	TRAF6	99.9583778416227	green
ssc-let-7d-5p	HMGA2	99.9464199196979	green
ssc-miR-374a-5p	PRDM11	99.9019803393543	green

Table 57. The highest target gene score for miRNAs from magenta module

miRNA	Target Gene	Target Score	module
ssc-miR-30e-5p	CELSR3	99.998490412936	magenta
ssc-let-7i-5p	TRIM71	99.9837730009893	magenta
ssc-miR-30e-5p	PPARGC1B	99.9829001483369	magenta
ssc-miR-30e-5p	WDR7	99.9536578864795	magenta
ssc-let-7i-5p	HMGA2	99.9502531848861	magenta

Table 58. The highest target gene score for miRNAs from pink module

miRNA	Target Gene	Target Score	module
ssc-miR-30b-5p	CELSR3	99.998490412936	pink
ssc-miR-30b-5p	PPARGC1B	99.9829001483369	pink
ssc-miR-30b-5p	WDR7	99.9536578864795	pink
ssc-miR-30b-5p	STOX2	99.9306249844605	pink
ssc-miR-30e-3p	PCLO	99.8725051981171	pink

Table 59. The highest target gene score for miRNAs from purple module

miRNA	Target Gene	Target Score	module
ssc-miR-143-3p	ABL2	99.4866669688238	purple
ssc-miR-143-3p	DENND1B	99.1801630196855	purple
ssc-miR-143-3p	ABL2	99.0902856466229	purple
ssc-miR-143-3p	VASH1	99.0834705051181	purple
ssc-miR-10a-5p	CADM2	98.88699985084	purple

Table 60. The highest target gene score for miRNAs from red module

miRNA	Target Gene	Target Score	module
ssc-miR-148a-5p	FAM169A	99.2989908804394	red
ssc-miR-148a-5p	GSR	97.0207929388	red
ssc-miR-148a-5p	ZFP42	96.6976333192	red
ssc-miR-148a-5p	PHTF2	96.5165090438856	red
ssc-miR-148a-5p	SIX4	96.2874152912125	red

Table 61. The highest target gene score for miRNAs from turquoise module

miRNA	Target Gene	Target Score	module
ssc-miR-92b-3p	CD69	99.9846637529554	turquoise
ssc-miR-92b-3p	MAN2A1	99.9084233380634	turquoise
ssc-miR-92b-3p	SLC12A5	99.7980543780163	turquoise
ssc-miR-92b-3p	FBXW7	99.66863766777	turquoise
ssc-miR-92b-3p	SLC12A5	99.6523443307826	turquoise

Table 62. The highest target gene score for miRNAs from yellow module

miRNA	Target Gene	Target Score	module
ssc-miR-126-5p	DENND1B	99.9999999806704	yellow
ssc-miR-126-5p	FAM168A	99.9999992954528	yellow
ssc-miR-126-5p	GRIK2	99.999997669618	yellow
ssc-miR-126-5p	RFX4	99.9999894463683	yellow
ssc-miR-126-5p	GNE	99.9998900518947	yellow

4.4. Biological gene networks and pathways analysis of trait-specific co-expressed miRNAs target genes in PL and PLxDuroc pigs using Cytoscape ClueGo

The biological functions of target genes discovered for every trait-specific module were evaluated using the ClueGO application of Cytoscape. The target genes were grouped according to its miRNA module membership. For every trait-specific module, the GO/pathway analysis were performed using the GO-BiologicalProcess-EBI-UniProt-GOA database for human genes. Every functional network and pathway with the p-value < 0.05 after Bonferroni correction were discarded from the analysis. Gene pathways were generated for target genes from nine trait-specific miRNAs' modules black, blue, brown, green, magenta, pink, purple, turquoise, yellow. Target genes of miRNAs from the module red did not have the statistically significant pathway.

4.4.1. Identification of miRNAs' target genes representing biological gene networks and GO/Pathways for the trait-specific black module affected by PUFAs diet in PL and PLxDuroc pigs

Identification of miRNA target genes associated with GO/pathway terms affected by PUFAs diet in PL and PLxDuroc pigs for trait-associated black module: ClueGO analysis identified 38 GO/pathway specific terms associated with black module miRNAs' target genes affected by PUFAs diet in PL and PLxDuroc pigs (Fig. 52): namely, regulation of epithelial cell differentiation, Cellular response to insulin-like growth factor stimulus, Positive regulation of Wnt signaling pathway, Sebaceous gland development, tau-protein kinase activity, Regulation of metallo-endopeptidase activity, mesenchyme development, mesenchymal cell differentiation, Response to interleukin-1, Cellular response to interleukin-1, Intracellular receptor signaling pathway, Intracellular steroid hormone receptor signaling pathway, Regulation of intracellular steroid hormone receptor signaling pathway, Negative regulation of locomotion, Negative regulation of cellular component movement, Negative regulation of cell motility, Muscle tissue development, Muscle organ development, Striated muscle tissue development, Myoblast differentiation, Heart valve development, Positive regulation of Notch signaling pathway, Semi-lunar valve development, Aortic valve development, MAP kinase activity, Regulation of MAP kinase activity, Regulation of protein serine/threonine kinase activity, Positive regulation of MAP kinase activity, Positive regulation of protein serine/threonine kinase activity, Positive regulation of nuclear-transcribed mRNA poly(A) tail shortening, Negative regulation of cellular amide metabolic process, Negative regulation of

translation, Positive regulation of mRNA metabolic process, Positive regulation of mRNA catabolic process, Regulation of nuclear-transcribed mRNA catabolic process, deadanylation-dependant decay, Nuclear-transcribed mRNA poly(A) tail shortening, Positive regulation of nuclear-transcribed mRNA catabolic process, deadenylation-dependency, Regulation of nuclear-transcribed mRNA poly(A) tail shortening.

4.4.2. Identification of functional groups affected by PUFAs diet in PL and PLxDuroc pigs for trait-associated black module

ClueGO analysis identified 14 functional groups for the trait-associated black-module miRNAs' target genes affected by PUFAs diet in PL and PLxDuroc pigs: namely: regulation of epithelial cell differentiation, cellular response to insulin-like growth factor stimulus, positive regulation of Wnt signaling pathway, sebaceous gland development, tau-protein kinase activity, regulation of metalloendopeptidase activity, mesenchymal cell differentiation and development, cellular response to interleukin-1, regulation of intracellular steroid hormone receptor signaling pathway, negative regulation of cell motility and cellular component movement, muscle organ development, heart valve development and myoblast differentiation, regulation of protein serine/threonine and MAP kinase activity, and regulation of mRNA catabolic metabolic process respectively (Fig. 53).

Finally, the distribution of all 38 module-specific GO/pathways specific terms, represented in the 14 functional group networks were visualized in Figure 54.

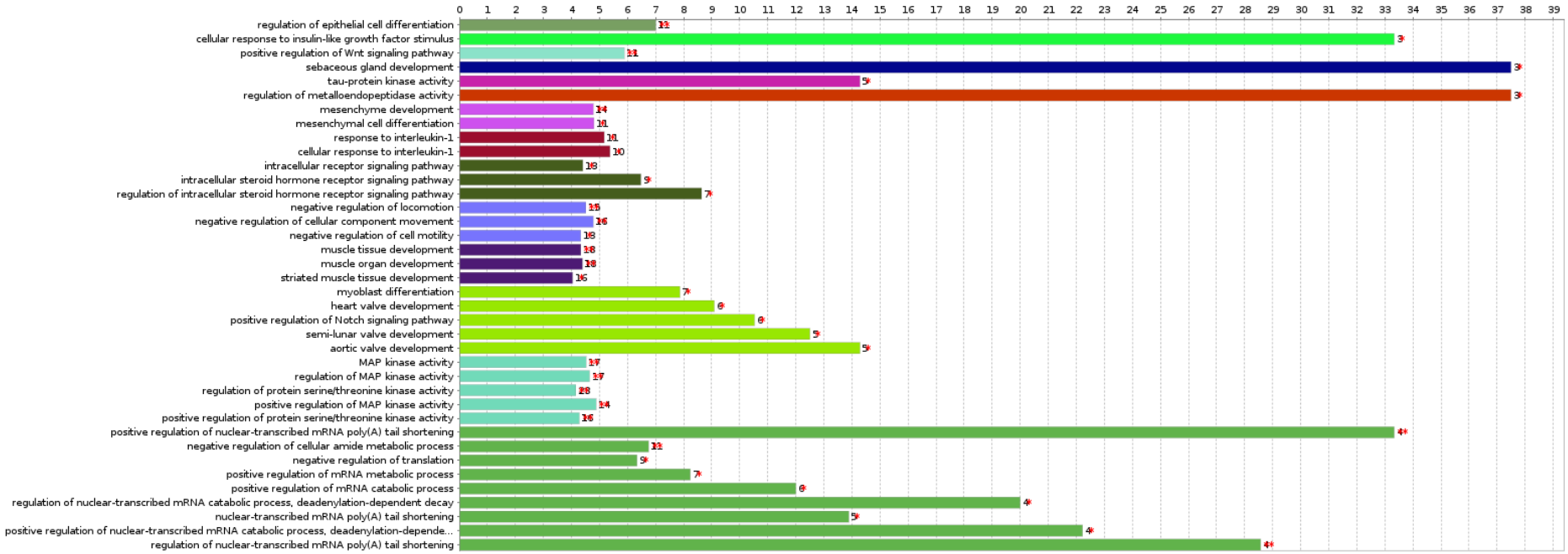

Figure 53. ClueGO analysis of black module miRNAs' target genes: The Figure shows the **GO/pathway terms** specific for black module miRNAs' target genes. The bars represent the number of genes associated with the terms. The percentage of genes per term is shown as bar label.

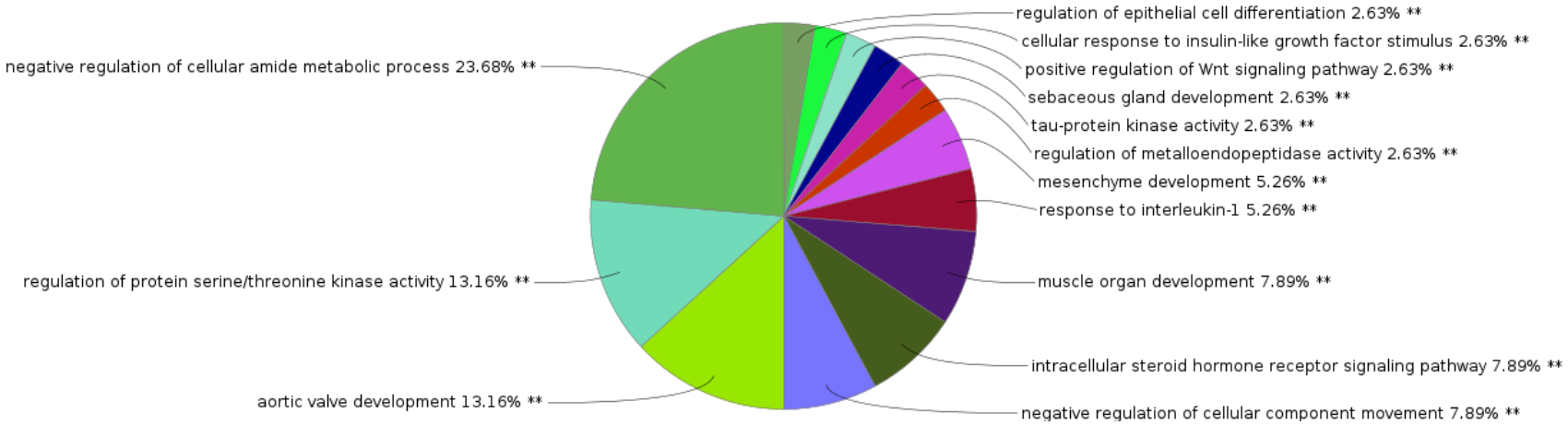

Figure 54. ClueGO analysis of black module miRNAs' target genes: The Figure shows an overview chart with **functional groups** including specific terms for black module miRNAs' target genes.

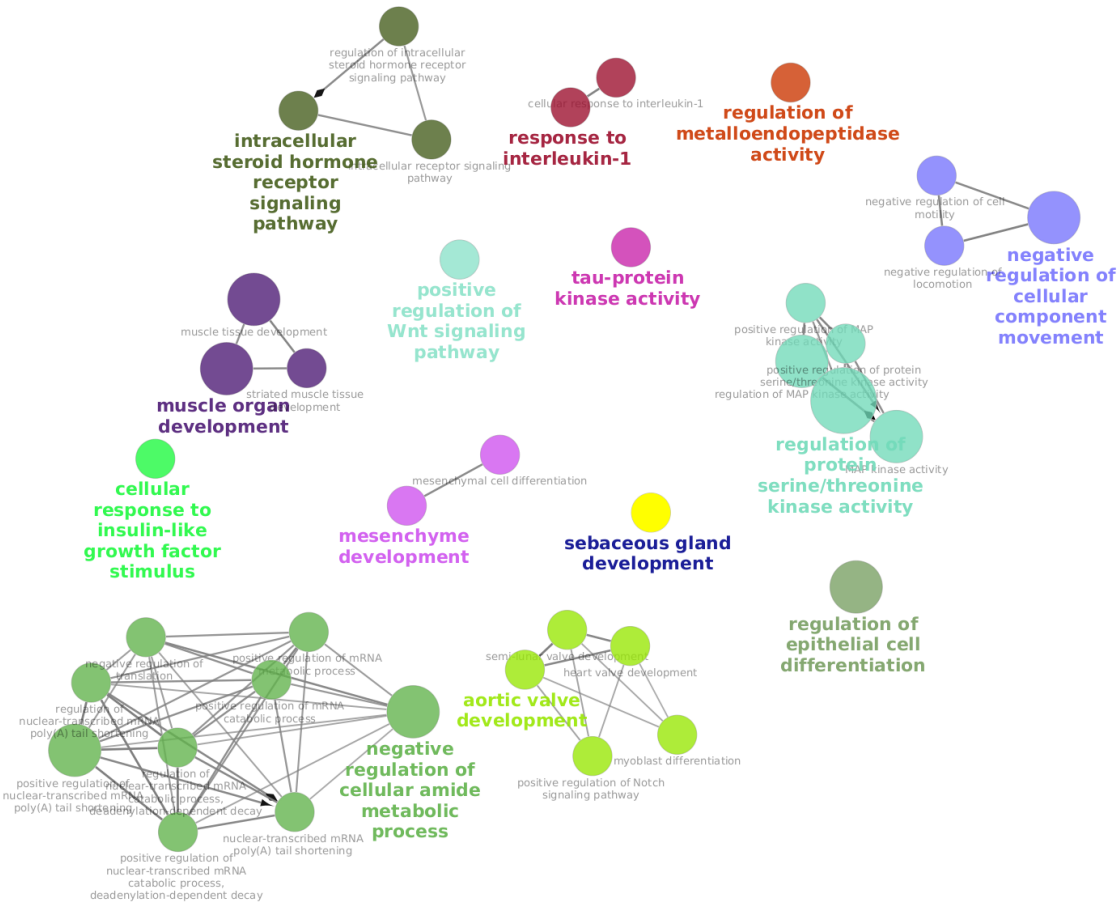

Figure 55. The distribution of all pathway terms (for black module miRNAs' target genes) visualized on the network. The Figure shows the functionally grouped network with terms as nodes (hubs) linked based on their kappa score level (≥0.3) and p-value after Bonferroni correction < 0.05, where only the label of the most significant term per group is shown. The node size represents the term enrichment significance. Node color represents the functional groups.

4.4.3. Identification of miRNAs' target genes representing biological gene networks and GO/pathways for the trait-specific blue module affected by PUFAs diet in PL and PLxDuroc pigs

Identification of miRNA target genes associated with GO/pathway terms affected by PUFAs diet in PL and PLxDuroc pigs for trait-associated blue module: ClueGO analysis identified 57 GO/pathway specific terms associated with blue module miRNAs' target genes affected by PUFAs diet in PL and PLxDuroc pigs (Fig. 55), namely: Regulation of cellular process, Homophilic cell adhesion via plasma membrane adhesion molecules, connective tissue development, Skeletal system development, Response to growth factor, Cellular response to growth factor stimulus, Regulation of cell communication, Regulation of signal transduction, Intracellular signal transduction, Extracellular structure organization, Extracellular matrix organization, Collagen fibril organization, Multicellular organism development, Anatomical structure morphogenesis, Regulation of developmental process, Tissue development, Cell development, System development, Regulation of multi-cellular organismal development, Animal organ development, Nervous system development, Circulatory system development, Positive regulation of biological process, Negative regulation of biological process, Regulation of metabolic process, Positive regulation of metabolic process, Positive regulation of cellular process, Negative regulation of cellular process, Regulation of biosynthetic process, Regulation of cellular metabolic process, Cellular macromolecule metabolic process, Regulation of nitrogen compound metabolic process, Regulation of macromolecule metabolic process, Regulation of primary metabolic process, Negative regulation of biosynthetic process, Positive regulation of macromolecule metabolic process, Positive regulation of cellular metabolic process, Negative regulation of nitrogen compound metabolic process, Positive regulation of nitrogen compound metabolic process, Regulation of macromolecule biosynthetic process, Regulation of nucleobase-containing compound metabolic process, Chromatin organization, Positive regulation of gene expression, Positive regulation of nucleobase-containing compound metabolic process, Regulation of RNA metabolic process, Regulation of cellular macromolecule biosynthetic process, Positive regulation of RNA metabolic process, Negative regulation of cellular macromolecule biosynthetic process, Regulation of RNA biosynthetic process, Transcription, DNA-templated, Nucleic acid-templated transcription, Regulation of transcription, DNA-templated, Regulation of nucleic acid-templated transcription, Transcription by RNA polymerase II, Negative regulation of transcription, DNA-templated,

Positive regulation of transcription, DNA-templated, Regulation of transcription by RNA polymerase II.

4.4.4. Identification of functional groups affected by PUFAs diet in PL and PLxDuroc pigs for trait-associated blue module

ClueGO analysis identified 8 functional groups for the trait-associated blue-module miRNAs' target genes affected by PUFAs diet in PL and PLxDuroc pigs: namely: regulation of cellular process, homophilic cell adhesion via plasma membrane adhesion molecules, connective tissue and skeletal system development, cellular response to growth factor stimulus, intracellular signal transduction, extracellular structure organization, animal organ development and regulation of multicellular organismal development, and regulation of RNA biosynthetic and metabolic process respectively (Fig. 56).

Finally, the distribution of all 57 module-specific GO/pathways specific terms, represented in the 8 functional group networks were visualized in Figure 57.

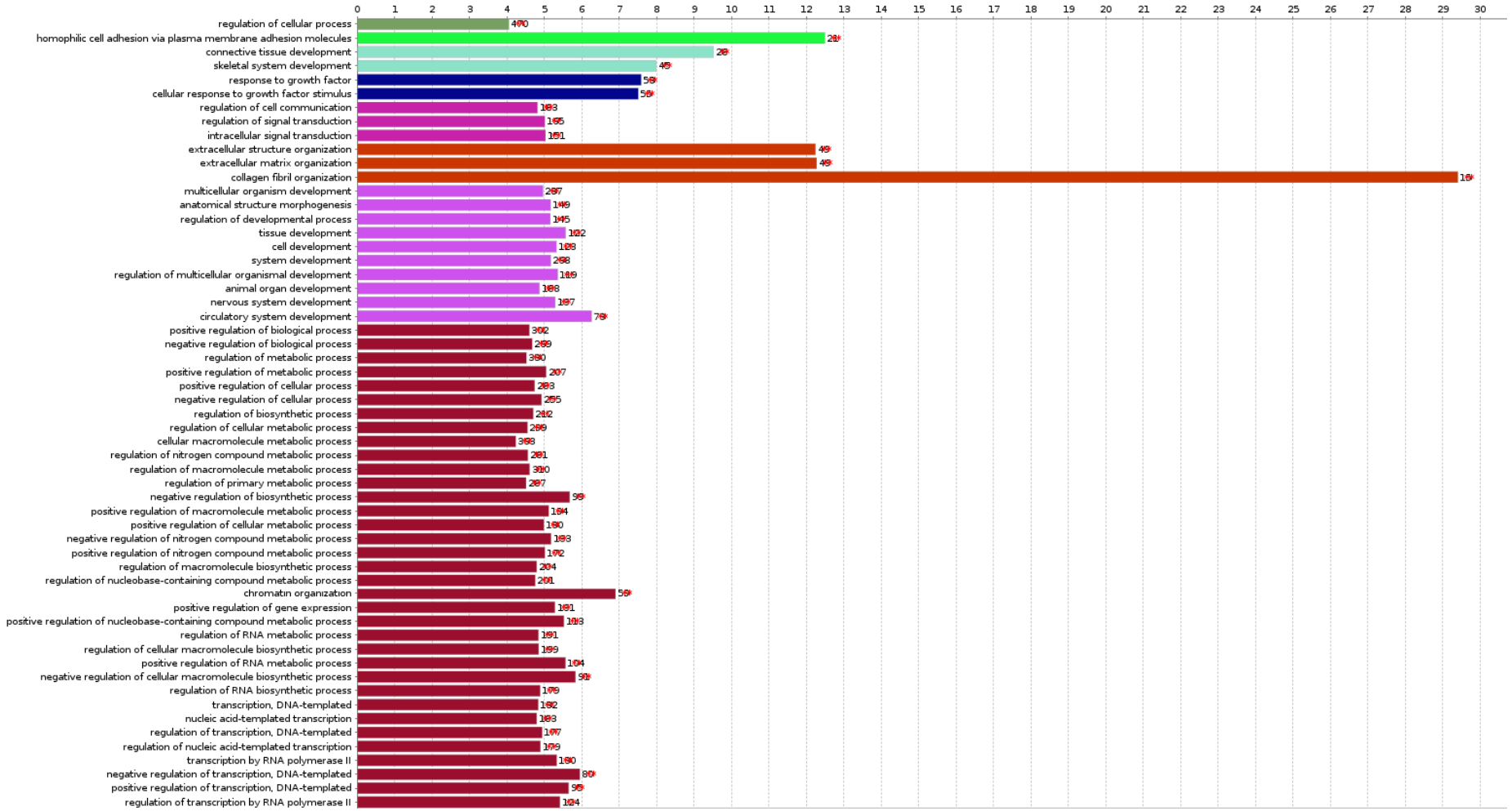

Figure 56. ClueGO analysis of blue module miRNAs' target genes: The Figure shows the GO/pathway terms specific for black module miRNAs' target genes. The bars represent the number of genes associated with the terms. The percentage of genes per term is shown as bar label.

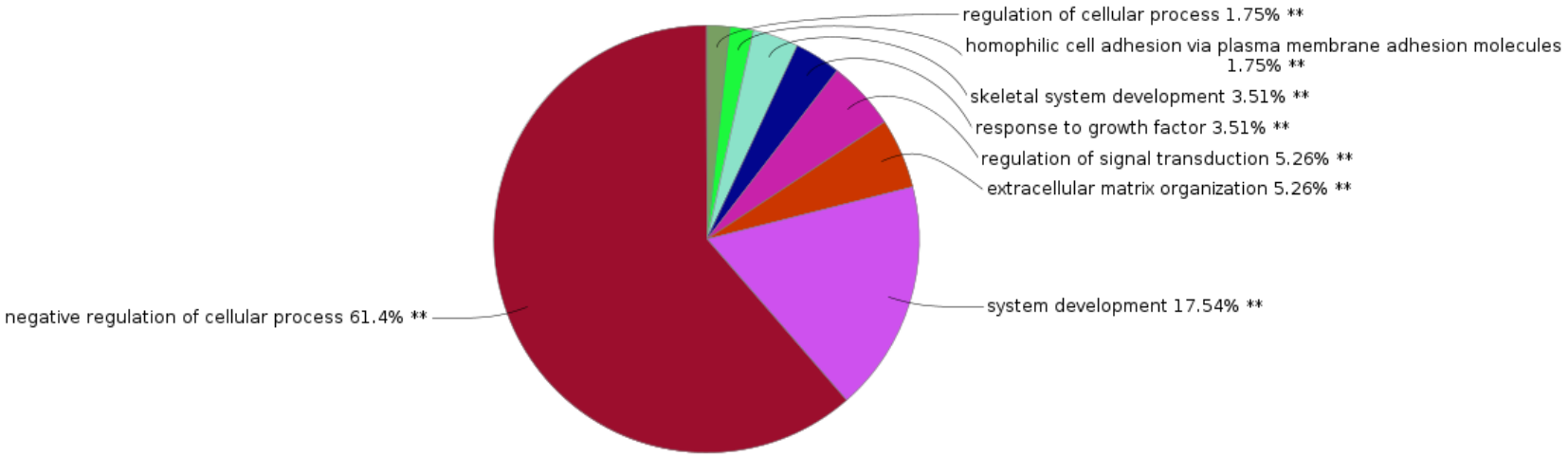

Figure 57. ClueGO analysis of blue module miRNAs' target genes: The Figure shows an overview chart with functional groups including specific terms for black module miRNAs' target genes.

Figure 58. The distribution of all pathway terms (for blue module miRNAs' target genes) visualized on the network. The Figure shows the functionally grouped network with terms as nodes (hubs) linked based on their kappa score level (≥0.3) and p-value after Bonferroni correction < 0.05, where only the label of the most significant term per group is shown. The node size represents the term enrichment significance. Node color represents the functional groups.

4.4.5. Identification of miRNAs' target genes representing biological gene networks and GO/pathways for the trait-specific brown module affected by PUFAs diet in PL and PLxDuroc pigs

Identification of miRNA target genes associated with GO/pathway terms affected by PUFAs diet in PL and PLxDuroc pigs for trait-associated brown module: ClueGO analysis identified 88 GO/pathway specific terms associated with brown module miRNAs' target genes affected by PUFAs diet in PL and PLxDuroc pigs (Fig. 58): namely,

Cellular response to endogenous stimulus, Wnt signaling pathway, calcium modulating pathway, Cellular component organization, Regulation of cellular component organization, Organelle organization, Cell projection organization, Positive regulation of cellular component organization, Plasma membrane bounded cell projection organization, Anatomical structure morphogenesis, Regulation of developmental process, Regulation of multicellular organismal process, Cell morphogenesis, Regulation of anatomical structure morphogenesis, Regulation of multicellular organismal development, Circulatory system development, Cardiovascular system development, Vasculature development, Blood vessel development, Blood vessel morphogenesis, Multicellular organism development, Anatomical structure morphogenesis, Regulation of developmental process, Regulation of multicellular organismal process, Cell differentiation, Cell morphogenesis, Regulation of anatomical structure morphogenesis, Cellular component morphogenesis, Regulation of cell differentiation, Cell development, System development, Regulation of cellular component organization, Regulation of multicellular organismal development, Cell projection organization, Cell morphogenesis involved in differentiation, Nervous system development, Cell part morphogenesis, Circulatory system development, Neurogenesis, Cell projection morphogenesis, Plasma membrane bounded cell projection organization, Generation of neurons, Plasma membrane bounded cell projection morphogenesis, Neuron differentiation, Neuron development, Neuron projection development, Cell morphogenesis involved in neuron differentiation, Neuron projection morphogenesis, Axonogenesis, Positive regulation of biological process, Negative regulation of biological process, Regulation of metabolic process, Regulation of signaling, Regulation of cellular process, negative regulation of metabolic process, Positive regulation of metabolic process, Macromolecule metabolic process, Positive regulation of cellular process, Negative regulation of cellular process, Regulation of cell communication, Protein metabolic process, Regulation of cellular metabolic process, Cellular macromolecule metabolic process, Regulation of nitrogen compound metabolic process, Regulation of macromolecule metabolic

process, Regulation of primary metabolic process, Regulation of signal transduction, Positive regulation of macromolecule metabolic process, Negative regulation of macromolecule metabolic process, Negative regulation of cellular metabolic process, Positive regulation of cellular metabolic process, Intracellular signal transduction, Macromolecule modification, Negative regulation of nitrogen compound metabolic process, Positive regulation of nitrogen compound metabolic process, Regulation of gene expression, Regulation of nucleusbase-containing compound metabolic process, Protein modification process, Cellular protein metabolic process, Regulation of protein metabolic process, Positive regulation of gene expression, Regulation of cellular protein metabolic process, Cellular protein modification process, Regulation of RNA metabolic process, Regulation of protein modification process, Protein phosphorylation, Peptidyl-amino acid modification, Protein serine/threonine kinase activity, Regulation of transcription by RNA polymerase II.

4.4.6. Identification of functional groups affected by PUFAs diet in PL and PLxDuroc pigs for trait-associated brown module

ClueGO analysis identified 6 functional groups for the trait-associated brown-module miRNAs' target genes affected by PUFAs diet in PL and PLxDuroc pigs: namely: cellular response to endogenous stimulus, Wnt signaling pathway, calcium modulating pathway, regulation of cellular component and organelle organization, regulation of multicellular organismal development, cell morphogenesis involved in differentiation, and regulation of cellular protein metabolic process (Figure 59). Finally, the distribution of all 88 module-specific GO/pathways specific terms, represented in the 6 functional group networks were visualized in Figure 60.

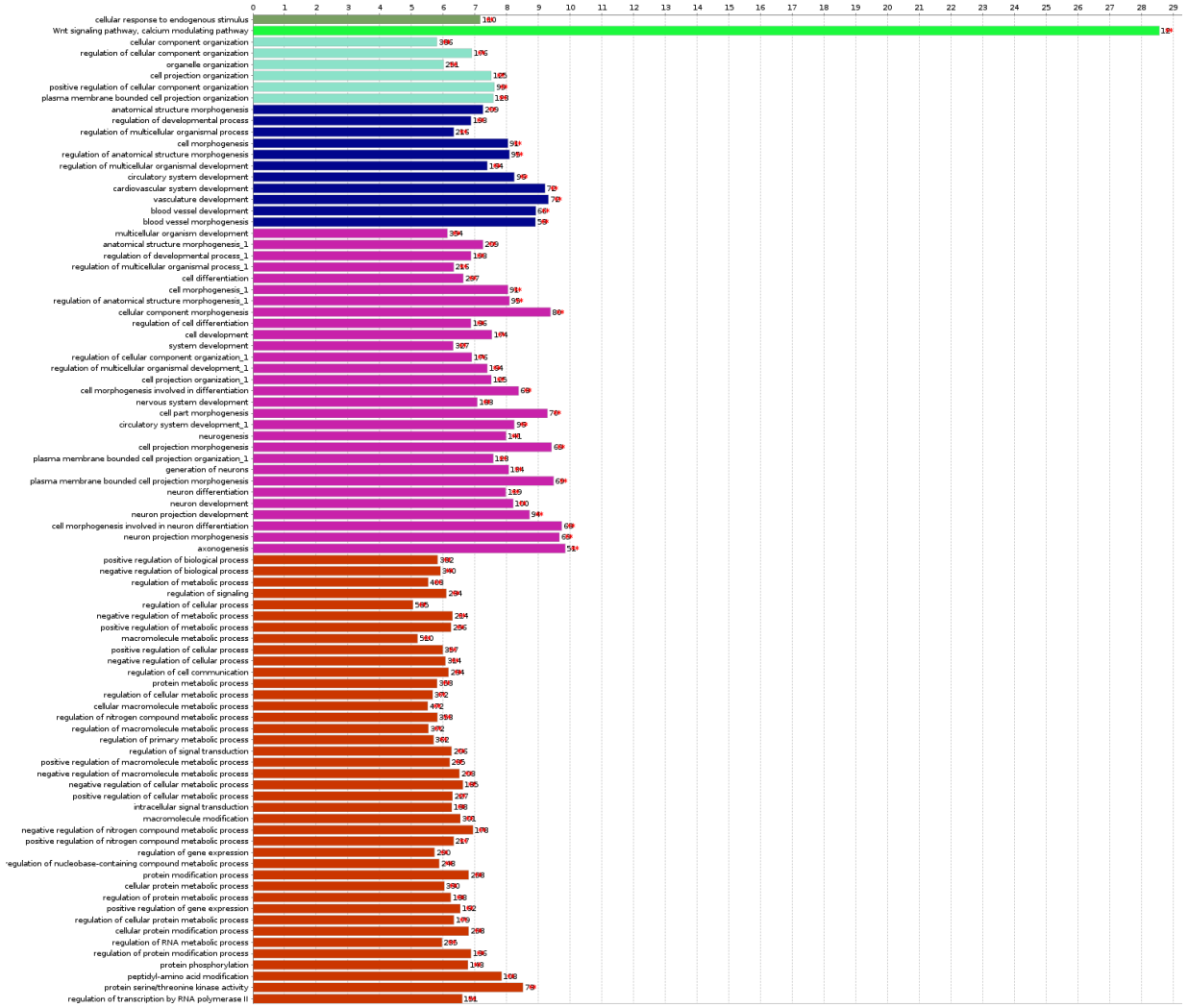

Figure 59. ClueGO analysis of brown module miRNAs' target genes: The Figure shows the GO/pathway terms specific for black module miRNAs' target genes. The bars represent the number of genes associated with the terms. The percentage of genes per term is shown as bar label.

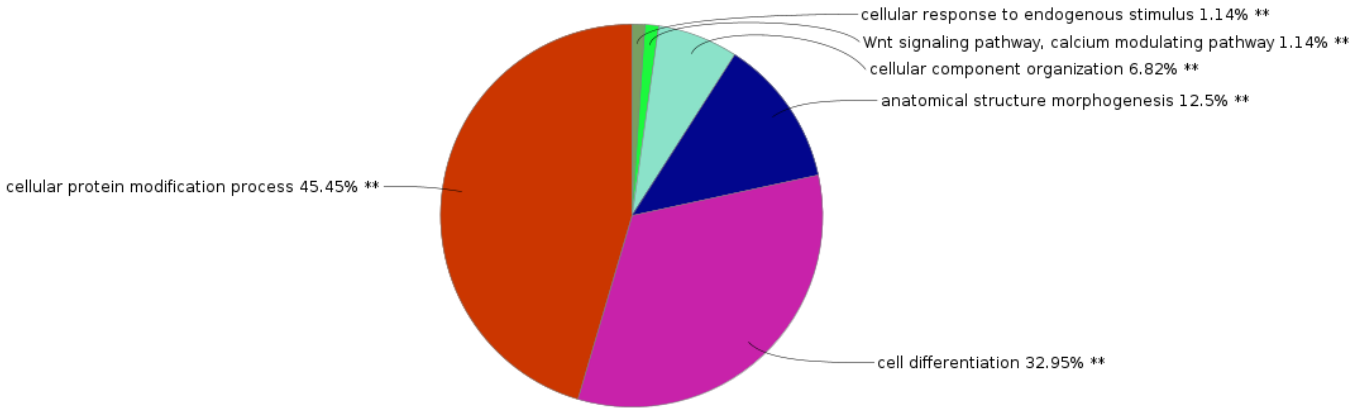

Figure 60. ClueGO analysis of brown module miRNAs' target genes: The Figure shows an overview chart with functional groups including specific terms for black module miRNAs' target genes.

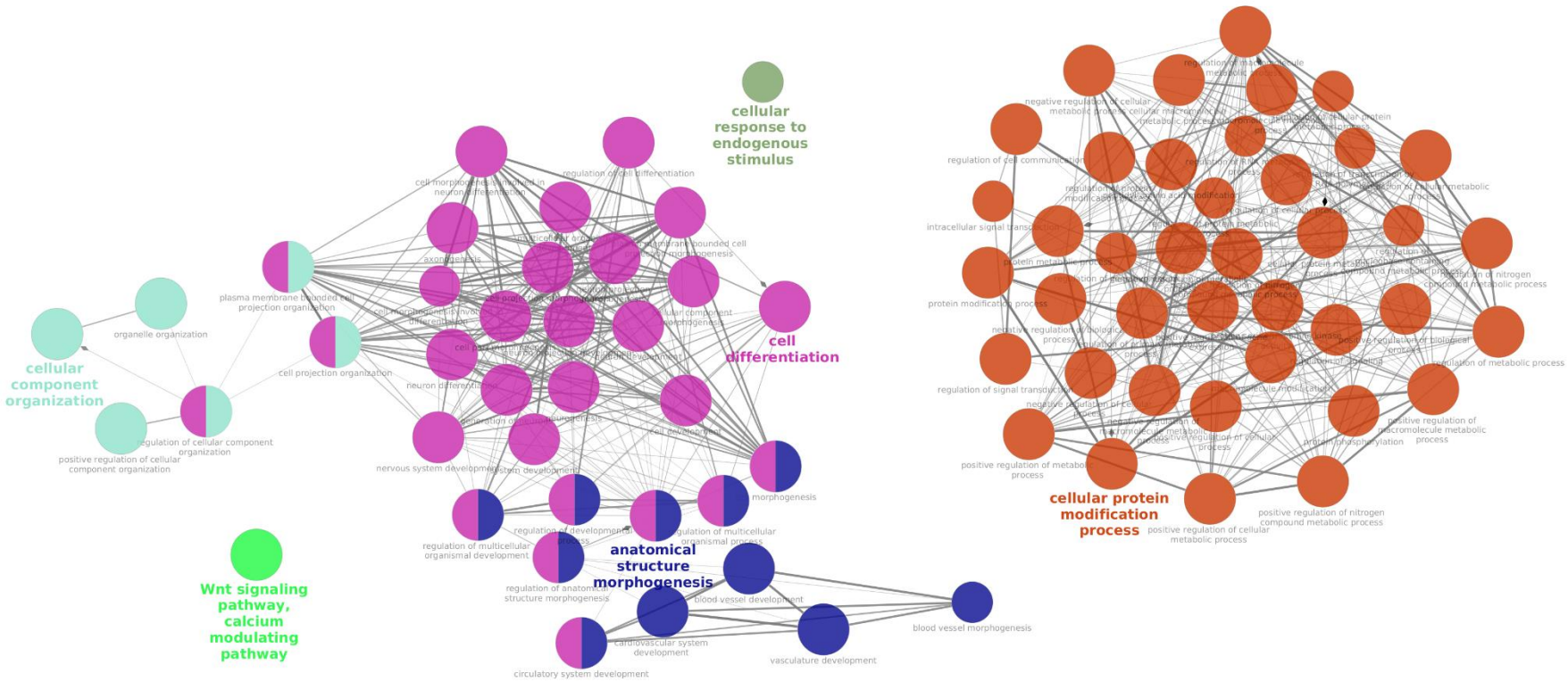

Figure 61. The distribution of all pathway terms (for brown module miRNAs' target genes) visualized on the network. The Figure shows the functionally grouped network with terms as nodes (hubs) linked based on their kappa score level (≥0.3) and p-value after Bonferroni correction < 0.05, where only the label of the most significant term per group is shown. The node size represents the term enrichment significance. Node color represents the functional groups.

4.4.7. Identification of miRNAs' target genes representing biological gene networks and GO/pathways for the trait-specific green module affected by PUFAs diet in PL and PLxDuroc

Identification of miRNA target genes associated with GO/pathway terms affected by PUFAs diet in PL and PLxDuroc pigs for trait-associated green module: ClueGO analysis identified 90 GO/pathway specific terms associated with green module miRNAs' target genes affected by PUFAs diet in PL and PLxDuroc pigs (Fig. 61), namely: Regulation of cellular process, Regulation of signaling, Regulation of response to stimulus, Regulation of cell communication, Regulation of signal transduction, Regulation of protein modification process, Anatomical structure morphogenesis, Regulation of developmental process, Embryo development, Regulation of anatomical structure morphogenesis, Tube development, Regulation of multicellular organismal development, Tube morphogenesis, Circulatory system development, Epithelial tube morphogenesis, Positive regulation of biological process, Negative regulation of biological process, Regulation of metabolic process, Negative regulation of metabolic process, Positive regulation of metabolic process, Macromolecule metabolic process, Positive regulation of cellular process, Negative regulation of cellular process, Regulation of cellular metabolic process, Cellular macromolecule metabolic process, Regulation of nitrogen compound metabolic process, Regulation of macromolecule metabolic process, Regulation of primary metabolic process, Macromolecule biosynthetic process, Negative regulation of biosynthetic process, Regulation of signal transduction, Positive regulation of macromolecule metabolic process, Negative regulation of cellular metabolic process, Positive regulation of cellular metabolic process, Macromolecule modification, Negative regulation of nitrogen compound metabolic process, Positive regulation of nitrogen compound metabolic process, Protein modification process, Negative regulation of macromolecule biosynthetic process, Positive regulation of gene expression, Negative regulation of cellular biosynthetic process, Regulation of cellular protein metabolic process, Cellular protein modification process, Regulation of protein modification process, Negative regulation of cellular macromolecule biosynthetic process, Transcription by RNA polymerase I, Protein serine/threonine kinase activity, Regulation of transcription by RNA polymerase I. Multicellular organism development, Anatomical structure morphogenesis, Regulation of developmental process, Regulation of multicellular organismal process, Cell differentiation, Negative regulation of multicellular organismal process, Head development, cell morphogenesis, Regulation of anatomical structure morphogenesis, Cellular component morphogenesis, Tube development,

Regulation of cell differentiation, Cell development, System development, Regulation of cellular component organization, Regulation of multicellular organismal development, Cell projection organization, Tube morphogenesis, Animal organ development, nervous system development, Regulation of cell projection organization, Cell part morphogenesis, Regulation of cell development, Circulatory system development, Central nervous system development, Neurogenesis, Positive regulation of cell projection organization, Cell projection morphogenesis, Regulation of nervous system development, Plasma membrane bounded cell projection organization, Brain development, Regulation of plasma membrane bounded cell projection organization, Generation of neurons, Plasma membrane bounded cell projection morphogenesis, Neuron differentiation, Neuron development, Regulation of neurogenesis, Positive regulation of neurogenesis, Neuron projection development, Positive regulation of neuron differentiation, Regulation of neuron projection development.

4.4.8. Identification of functional groups affected PUFAs diet in PL and PLxDuroc pigs for trait-associated green module

ClueGO analysis identified 5 functional groups for the trait-associated green-module miRNAs' target genes affected by PUFAs diet in PL and PLxDuroc pigs: namely: Regulation of cellular process, regulation of cell communication and signal transduction, regulation of anatomical structure morphogenesis and developmental process, regulation of macromolecule biosynthetic and metabolic process, and animal organ development & regulation of cellular component morphogenesis (Fig. 62).

Finally, the distribution of all 90 module-specific GO/pathways specific terms, represented in the 5 functional group networks were visualized in Figure 63.

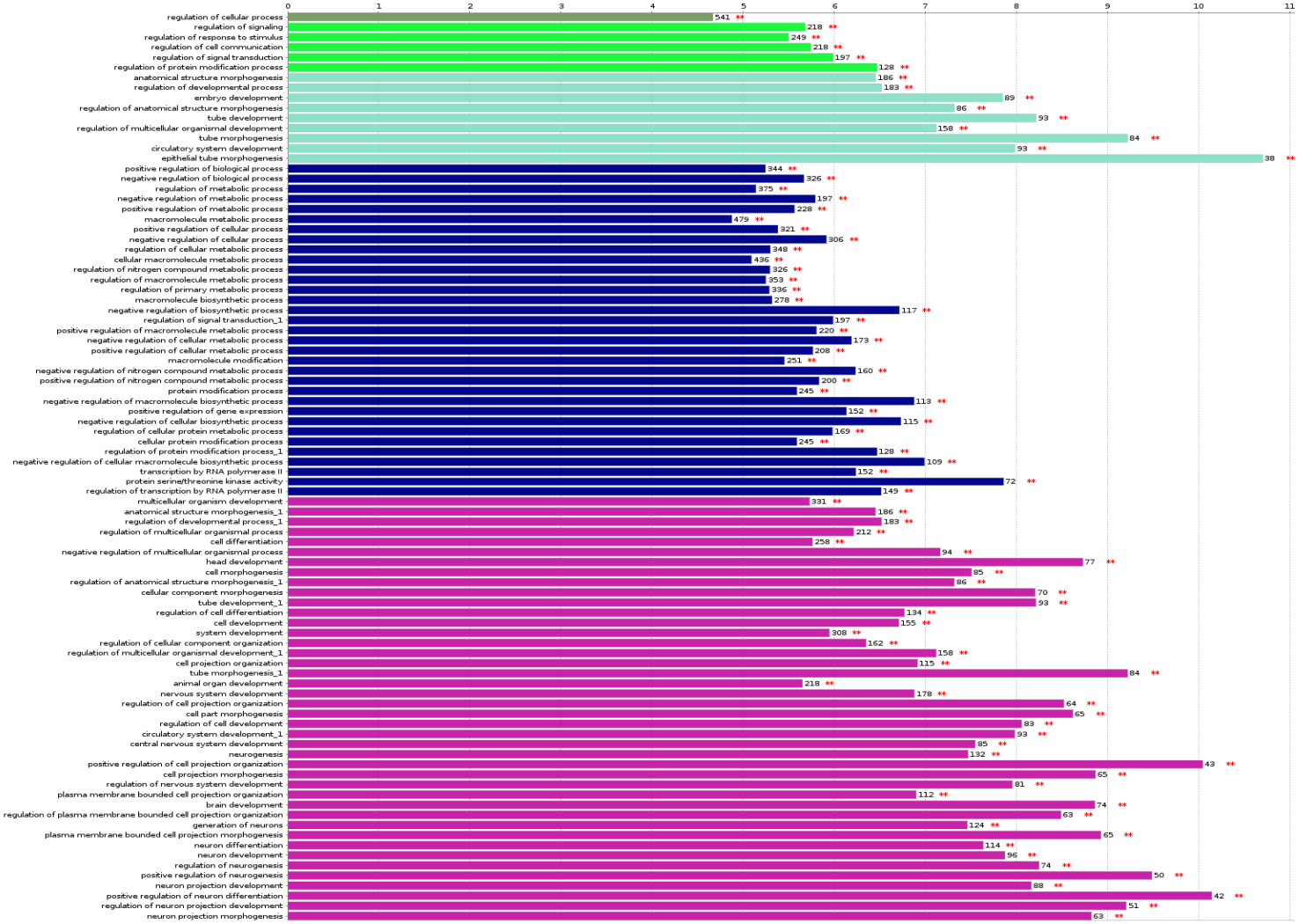

Figure 62. ClueGO analysis of green module miRNAs' target genes: The Figure shows the GO/pathway terms specific for black module miRNAs' target genes. The bars represent the number of genes associated with the terms. The percentage of genes per term is shown as bar label.

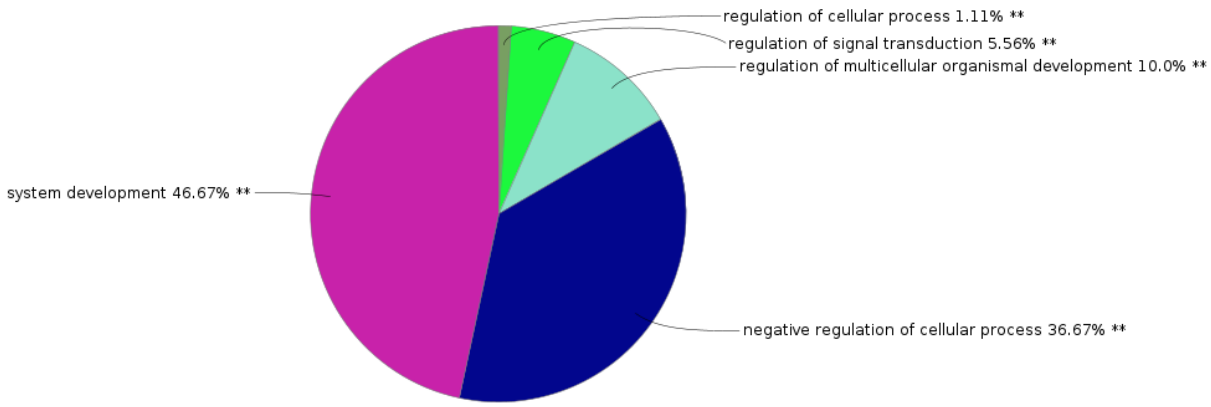

Figure 63. ClueGO analysis of green module miRNAs' target genes: The Figure shows an overview chart with functional groups including specific terms for black module miRNAs' target genes.

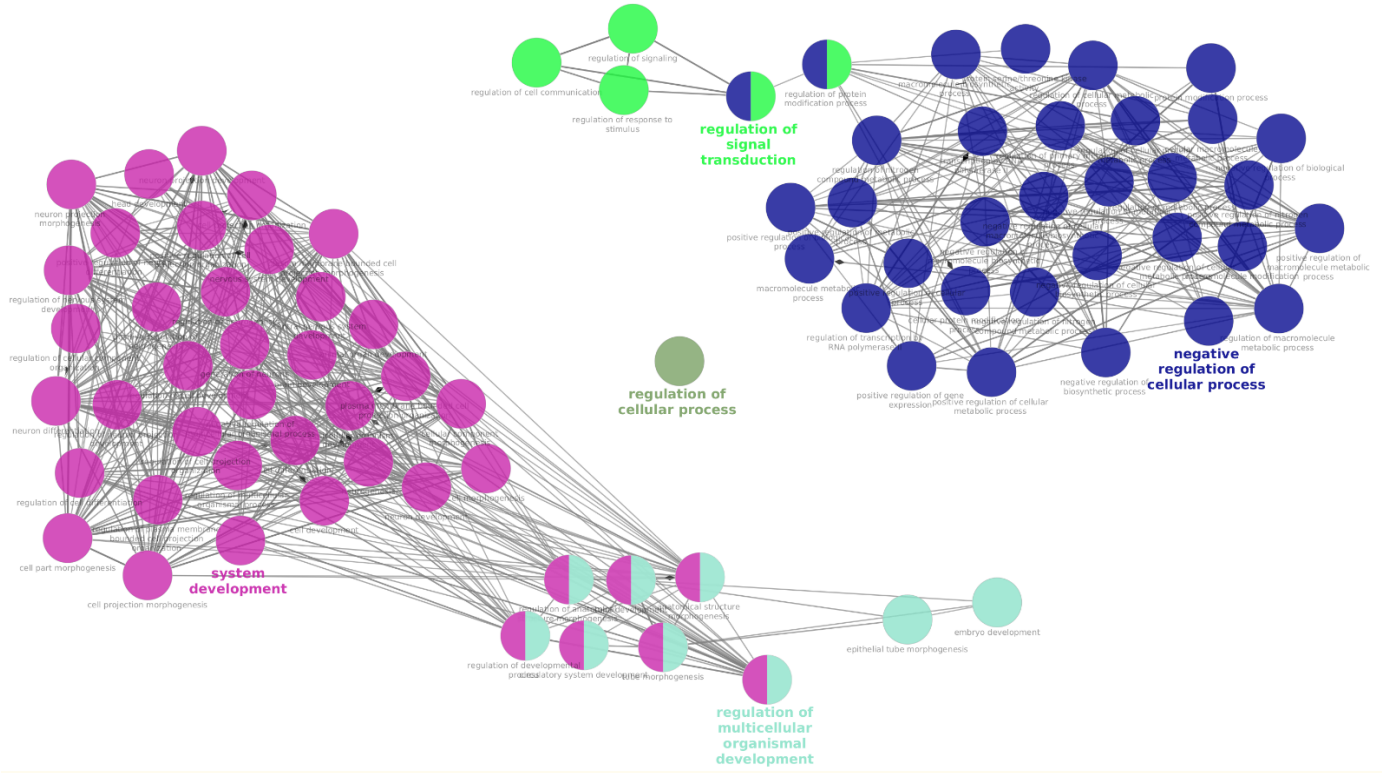

Figure 64. The distribution of all pathway terms (for green module miRNAs' target genes) visualized on the network. The Figure shows the functionally grouped network with terms as nodes (hubs) linked based on their kappa score level (≥0.3) and p-value after Bonferroni correction < 0.05, where only the label of the most significant term per group is shown. The node size represents the term enrichment significance. Node color represents the functional groups.

4.4.9. Identification of miRNAs' target genes representing biological gene networks and GO/pathways for the trait specific magenta module affected by PUFAs diet in PL and PLxDuroc pigs

Identification of miRNA target genes associated with GO/pathway terms affected by PUFAs diet in PL and PLxDuroc pigs for trait-associated magenta module: ClueGO analysis identified 57 GO/pathway specific terms associated with magenta module miRNAs' target genes affected by PUFAs diet in PL and PLxDuroc pigs (Fig. 64), namely: Cellular component organization, Anatomical structure morphogenesis, Regulation of developmental process, Embryo development, Regulation of multicellular organismal development, Tube morphogenesis, Circulatory system development, Cardiovascular system development, Vasculature development, Blood vessel development, Blood vessel morphogenesis, Multicellular organism development, Anatomical structure morphogenesis, Regulation of developmental process, Regulation of multicellular organismal process, Cell differentiation, Regulation of cell differentiation, Cell development, System development, Regulation of multicellular organismal development, Cell projection organization, Tube morphogenesis, Nervous system development, Circulatory system development, Neurogenesis, Cardiovascular system development, Plasma membrane bounded cell projection organization, Vasculature development, Generation of neurons, neuron differentiation, Neuron development, Neuron projection development, Positive regulation of biological process, Negative regulation of biological process, Regulation of metabolic process, Regulation of cellular process, Positive regulation of metabolic process, Macromolecule metabolic process, Positive regulation of cellular process, Negative regulation of cellar process, Protein metabolic process, Regulation of cellular metabolic process, Cellular macromolecule metabolic process, Regulation of nitrogen compound metabolic process, Regulation of macromolecule metabolic process, Regulation of primary metabolic process, Positive regulation of macromolecule metabolic process, Positive regulation of cellular metabolic process, Macromolecule modification, Positive regulation of nitrogen compound metabolic process, Regulation of nucleobase-containing compound metabolic process, Protein modification process, Cellular protein metabolic process, Cellular protein modification process, Regulation of RNA metabolic process, Regulation of protein modification process, Positive regulation of RNA metabolic process.

4.4.10. Identification of functional groups affected by PUFAs diet in PL and PLxDuroc pigs for trait-associated magenta module

ClueGO analysis identified 4 functional groups for the trait-associated magenta-module miRNAs' target genes affected by PUFAs diet in PL and PLxDuroc pigs: namely: Cellular component organization, regulation of multicellular organismal development, regulation of cell development and differentiation, and regulation of cellular and macromolecule metabolic process (Fig. 65).,

Finally, the distribution of all 57 module-specific GO/pathways specific terms, represented in the 4 functional group networks were visualized in Figure 66.

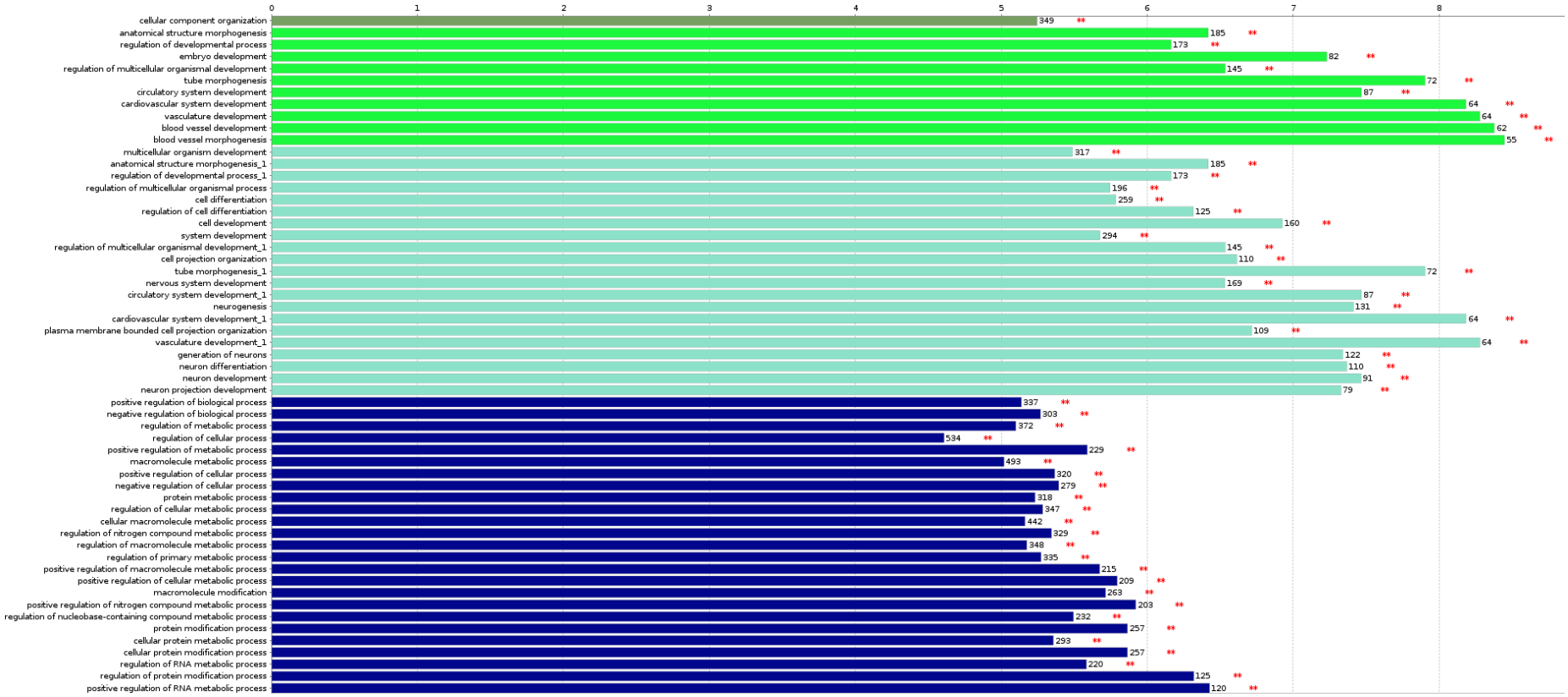

Figure 65. ClueGO analysis of magenta module miRNAs' target genes: The Figure shows the GO/pathway terms specific for black module miRNAs' target genes. The bars represent the number of genes associated with the terms. The percentage of genes per term is shown as bar label.

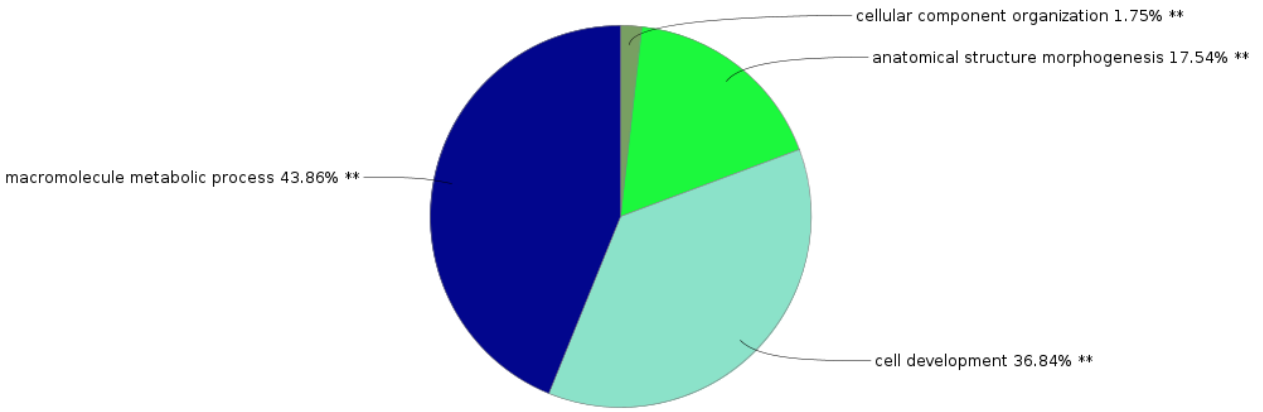

Figure 66. ClueGO analysis of magenta module miRNAs' target genes: The Figure shows an overview chart with functional groups including specific terms for black module miRNAs' target genes.

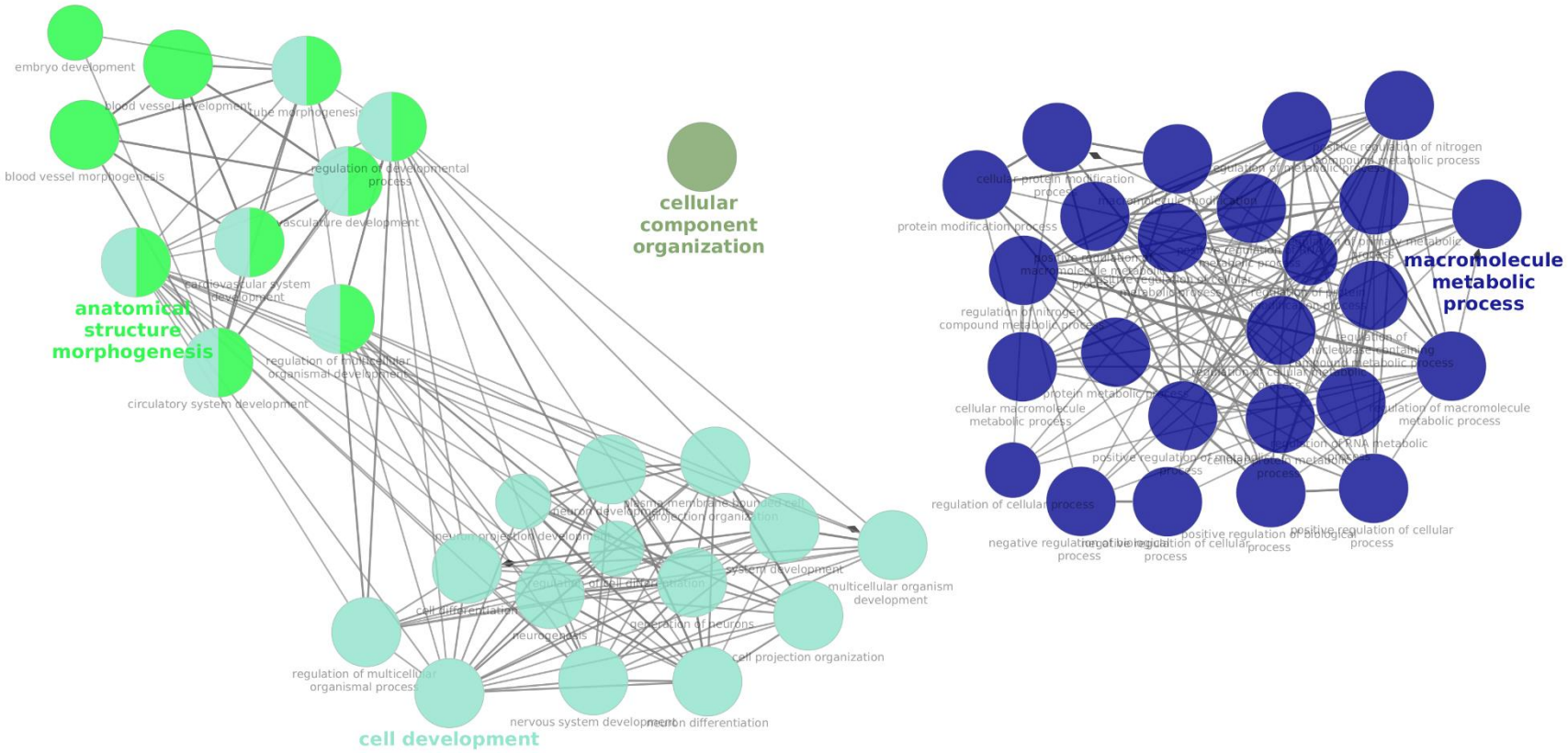

Figure 67. The distribution of all pathway terms (for magenta module miRNAs' target genes) visualized on the network. The Figure shows the functionally grouped network with terms as nodes (hubs) linked based on their kappa score level (≥0.3) and p-value after Bonferroni correction < 0.05, where only the label of the most significant term per group is shown. The node size represents the term enrichment significance. Node color represents the functional groups.

4.4.11. Identification of miRNAs' target genes representing biological gene networks and GO/pathways for the trait-specific pink module affected by PUFAs diet in PL and PLxDuroc pigs

Identification of miRNA target genes associated with GO/pathway terms affected by PUFAs diet in PL and PLxDuroc pigs for trait-associated pink module: ClueGO analysis identified 54 GO/pathway specific terms associated with pink module miRNAs' target genes affected by PUFAs diet in PL and PLxDuroc pigs (Fig. 67), namely: Positive regulation of cell death, Regulation of keratinocyte migration, Muscle tissue development, Positive regulation of catabolic process, Positive regulation of cellular catabolic process, Protein modification process, cellular protein modification process, Response to leukemia inhibitory factor, Cellular response to leukemia inhibitory Factor, Immune system development, Hematopoietic or lymphoid organ development, Hemopoiesis, Myeloid cell differentiation, Anatomical structure morphogenesis, Regulation of developmental process, Cell differentiation, Cellular component morphogenesis, Regulation of cell differentiation, cell development, cell part morphogenesis, Neurogenesis, cell projection morphogenesis, Generation of neurons, Plasma membrane bounded cell projection morphogenesis, Neuron differentiation, Neuron development, Neuron projection development, Cell morphogenesis involved in neuron differentiation, Neuron projection morphogenesis, Axon development, Axonogenesis, Positive regulation of metabolic process, Positive regulation of biosynthetic process, positive regulation of macromolecule metabolic process, Positive regulation of cellular metabolic process, Negative regulation of nitrogen compound metabolic process, Positive regulation of nitrogen compound metabolic process, Regulation of nucleobase-containing compound metabolic process, positive regulation of macromolecule biosynthetic process, Negative regulation of macromolecule biosynthetic process, Positive regulation of gene expression, Negative regulation of cellular biosynthetic process, Positive regulation of nucleobase -containing compound metabolic process, Regulation of RNA metabolic process, RNA biosynthetic process, Positive regulation of RNA metabolic process, Negative regulation of cellular macromolecule biosynthetic process, Nucleic acid-templated transcription, Positive regulation of RNA biosynthetic process, Transcription by RNA polymerase II, Positive regulation of transcription, DNA-templated, Positive regulation of nucleic acid-templated transcription, Regulation of transcription by RIVA polymerase I, Positive regulation of transcription by RNA polymerase I.

4.4.12. Identification of functional groups affected by PUFAs diet in PL and PLxDuroc pigs for trait-associated pink module

ClueGO analysis identified 9 functional groups for the trait-associated pink-module miRNAs' target genes affected by PUFAs diet in PL and PLxDuroc pigs: namely: positive regulation of cell death, regulation of keratinocyte migration, muscle tissue development, positive regulation of cellular catabolic process, cellular protein modification process, cellular response to leukemia inhibitory factor, hematopoietic or lymphoid organ development, cellular component morphogenesis & regulation of developmental process, and regulation of macromolecule biosynthetic and metabolic process, respectively (Fig. 68).

Finally, the distribution of all 54 module-specific GO/pathways specific terms, represented in the 9 functional group networks were visualized in Figure 69.

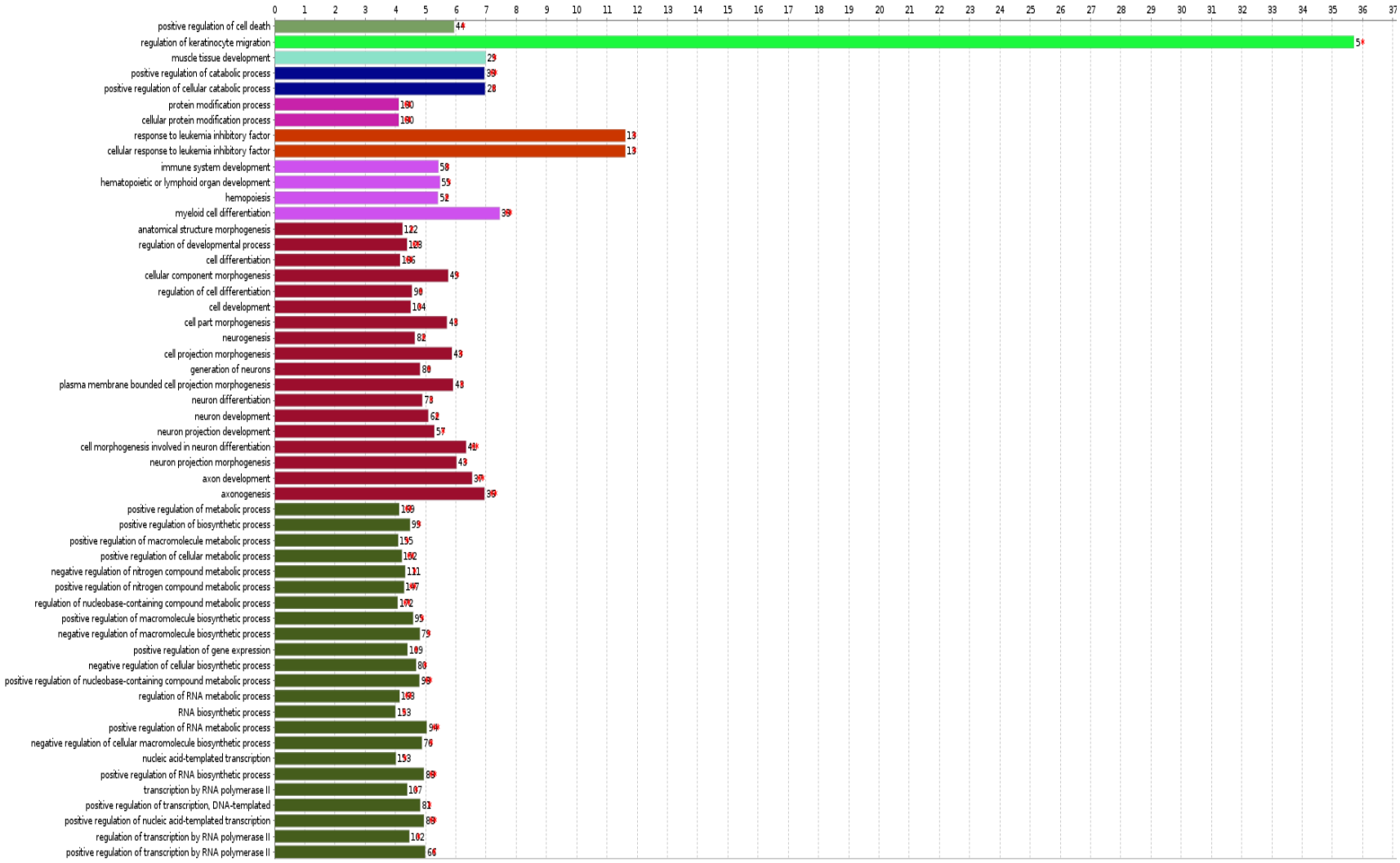

Figure 68. ClueGO analysis of pink module miRNAs' target genes: The Figure shows the GO/pathway terms specific for black module miRNAs' target genes. The bars represent the number of genes associated with the terms. The percentage of genes per term is shown as bar label.

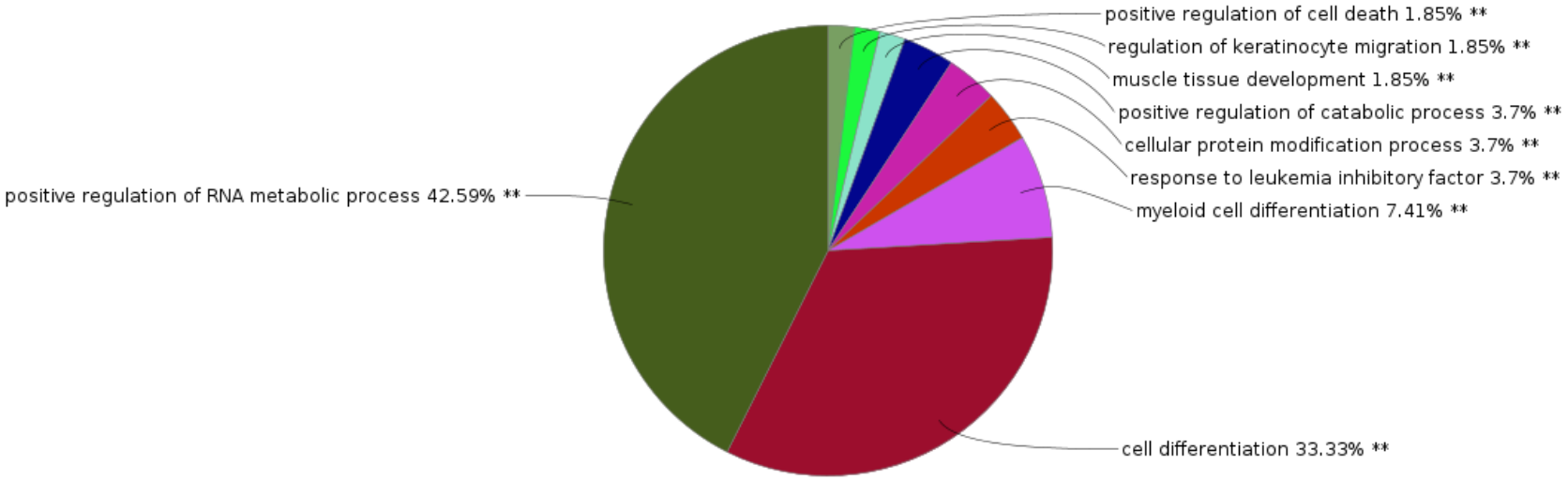

Figure 69. ClueGO analysis of pink module miRNAs' target genes: The Figure shows an overview chart with functional groups including specific terms for black module miRNAs' target genes.

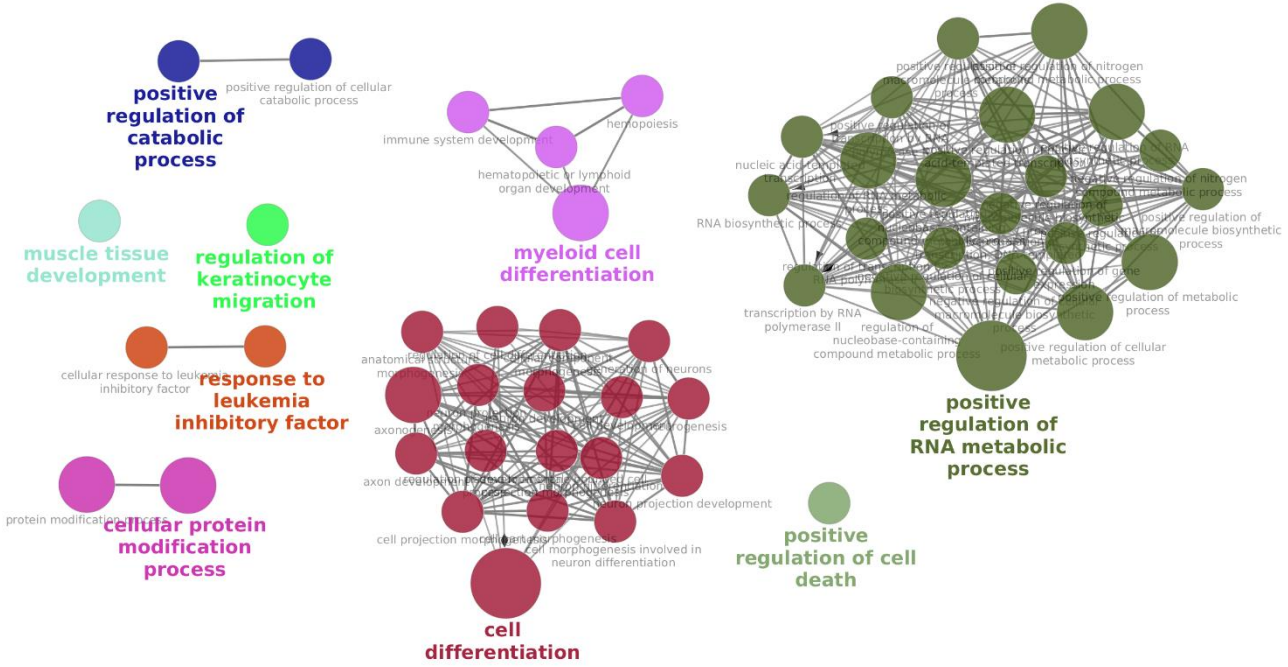

Figure 70. The distribution of all pathway terms (for pink module miRNAs' target genes) visualized on the network. The Figure shows the functionally grouped network with terms as nodes (hubs) linked based on their kappa score level (≥0.3) and p-value after Bonferroni correction < 0.05, where only the label of the most significant term per group is shown. The node size represents the term enrichment significance. Node color represents the functional groups.

4.4.13. Identification of miRNAs' target genes representing biological gene networks and GO/pathways for the trait-specific purple module affected by PUFAs diet in PL and PLxDuroc pigs

Identification of miRNA target genes associated with GO/pathway terms affected by PUFAs diet in PL and PLxDuroc pigs for trait-associated purple module: ClueGO analysis identified 16 GO/pathway specific terms associated with purple module miRNAs' target genes affected by PUFAs diet in PL and PLxDuroc pigs (Fig. 70), namely: Activation of MAPKK activity, Endoplasmic reticulum organization, Neuroblast proliferation, Rac protein signal transduction, Skeletal muscle cell differentiation, Positive regulation of fat cell differentiation, Positive regulation of oxidoreductase activity, Regulation of cell aging, Cellar senescence, Regulation of cellular senescence, Astrocyte development, Regulation of muscle tissue development, Negative regulation of muscle tissue development, Positive regulation of muscle tissue development, Positive regulation of muscle organ development, Positive regulation of striated muscle tissue development.

4.4.14. Identification of functional groups affected by PUFAs diet in PL and PLxDuroc pig for trait-associated purple module

ClueGO analysis identified 9 functional groups for the trait-associated purple-module miRNAs' target genes affected by PUFAs diet in PL and PLxDuroc pigs: namely: activation of MAPKK activity, endoplasmic reticulum organization, neuroblast proliferation, Rac protein signal transduction, skeletal muscle cell differentiation, positive regulation of fat cell differentiation, positive regulation of oxidoreductase activity, regulation of cellular senescence & cell aging, and regulation of muscle tissue development respectively (Fig. 71).

Finally, the distribution of all 16 module-specific GO/pathways specific terms, represented in the 9 functional group networks were visualized in Figure 72.

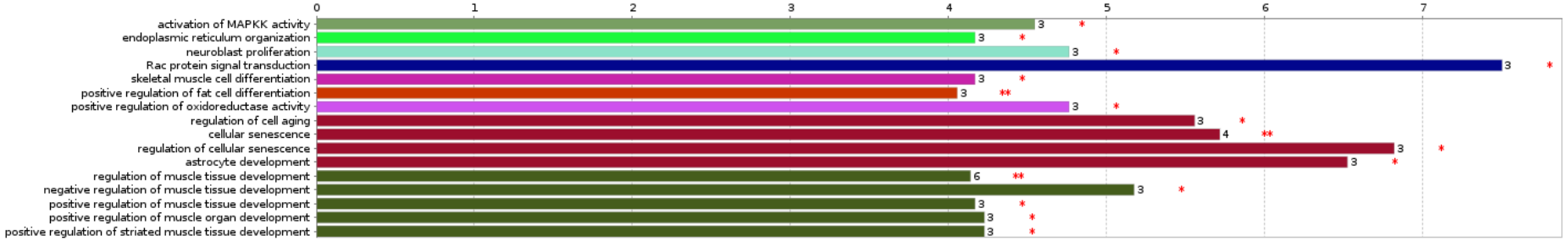

Figure 71. ClueGO analysis of purple module miRNAs' target genes: The Figure shows the GO/pathway terms specific for black module miRNAs' target genes. The bars represent the number of genes associated with the terms. The percentage of genes per term is shown as bar label.

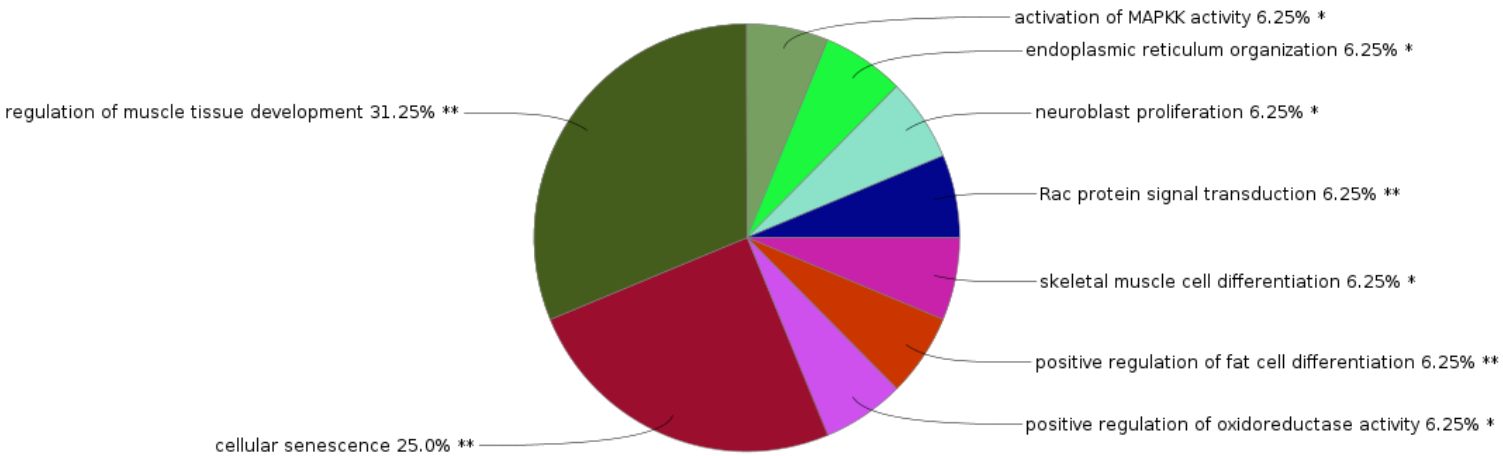

Figure 72. ClueGO analysis of purple module miRNAs' target genes: The Figure shows an overview chart with functional groups including specific terms for black module miRNAs' target genes.

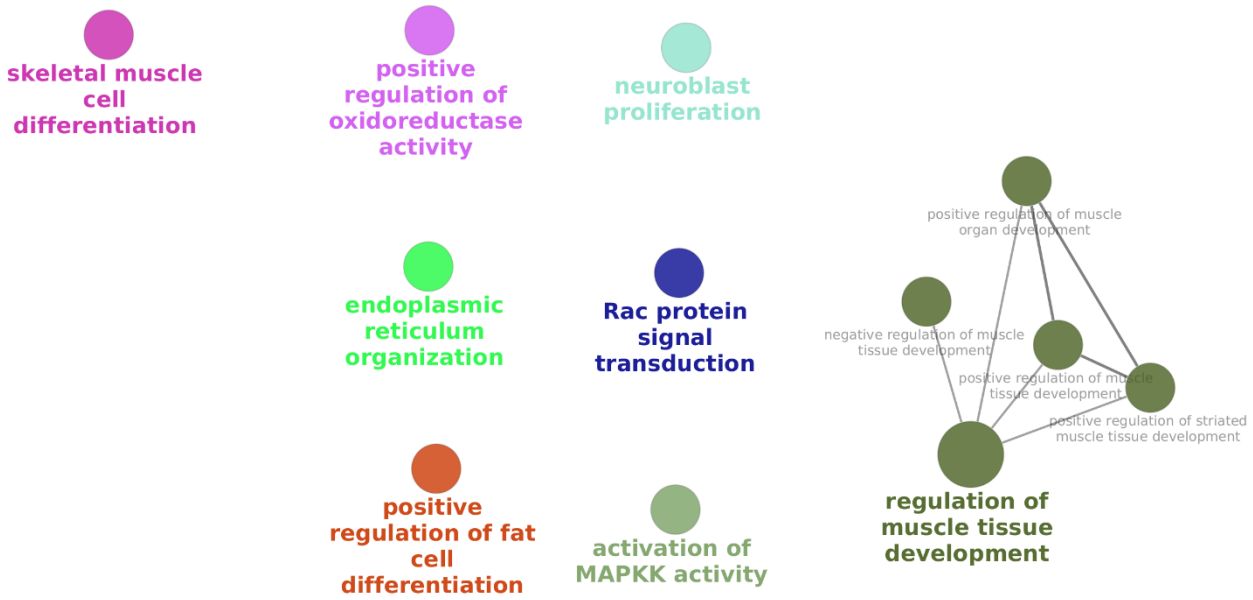

Figure 73. The distribution of all pathway terms (for purple module miRNAs' target genes) visualized on the network. The Figure shows the functionally grouped network with terms as nodes (hubs) linked based on their kappa score level (≥0.3) and p-value after Bonferroni correction < 0.05, where only the label of the most significant term per group is shown. The node size represents the term enrichment significance. Node color represents the functional groups.

4.4.15. Identification of miRNAs' target genes representing biological gene networks and GO/pathways for the trait-specific turquoise module affected by PUFAs diet in PL and PLxDuroc pigs

Identification of miRNA target genes associated with GO/pathway terms affected by PUFAs diet in PL and PLxDuroc pigs for trait-associated turquoise module: ClueGO analysis identified 14 GO/pathway specific terms associated with turquoise module miRNAs' target genes affected by PUFAs diet in PL and PLxDuroc pigs (Fig. 73), namely: Positive regulation of ubiquitin-protein transferase activity, Phosphatidylinositol bisphosphate phosphatase activity, Regulation of nuclear-transcribed mRNA catabolic process, deadenylation-dependent decay, Regulation of nuclear-transcribed mRNA poly(A) tail shortening, odontogenesis, Odontogenesis of dentin-containing tooth, Intermediate filament bundle assembly, Neurofilament bundle assembly, Post-embryonic development, Post-embryonic animal morphogenesis, Post-embryonic animal organ development, Sympathetic nervous system development, Cardiac ventricle formation, Noradrenergic neuron differentiation.

4.4.16. Identification of functional groups affected by PUFAs diet in PL and PLxDuroc pigs for trait-associated turquoise module

ClueGO analysis identified 7 functional groups for the trait-associated turquoise-module miRNAs' target genes affected by PUFAs diet in PL and PLxDuroc pigs: namely: positive regulation of ubiquitin-protein transferase activity, phosphatidylinositol bisphosphate phosphatase activity, regulation of nuclear-transcribed mRNA catabolic process and deadenylation-dependent decay, odontogenesis, neurofilament and intermediate bundle assembly, post-embryonic animal morphogenesis and organ development, and sympathetic nervous system development, respectively (Fig. 74).

Finally, the distribution of all 14 module-specific GO/pathways specific terms, represented in the 7 functional group networks were visualized in Figure 75.

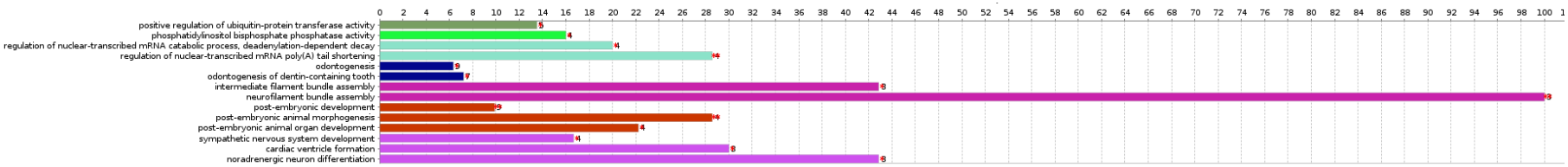

Figure 74. ClueGO analysis of turquoise module miRNAs' target genes: The Figure shows the GO/pathway terms specific for black module miRNAs' target genes. The bars represent the number of genes associated with the terms. The percentage of genes per term is shown as bar label.

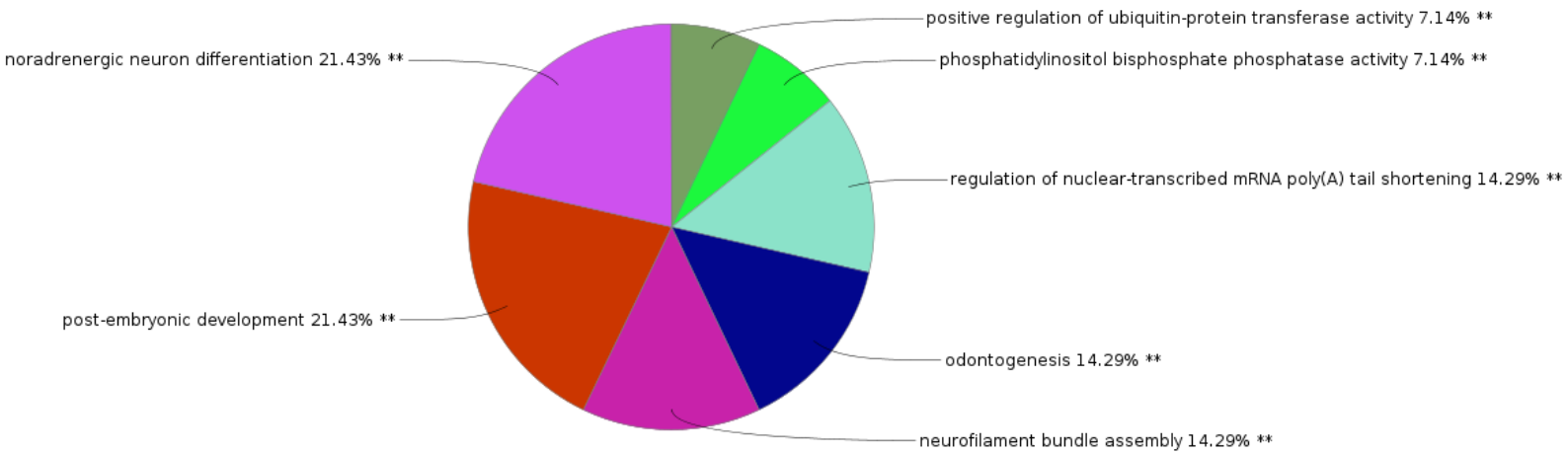

Figure 75. ClueGO analysis of turquoise module miRNAs' target genes: The Figure shows an overview chart with functional groups including specific terms for black module miRNAs' target genes.

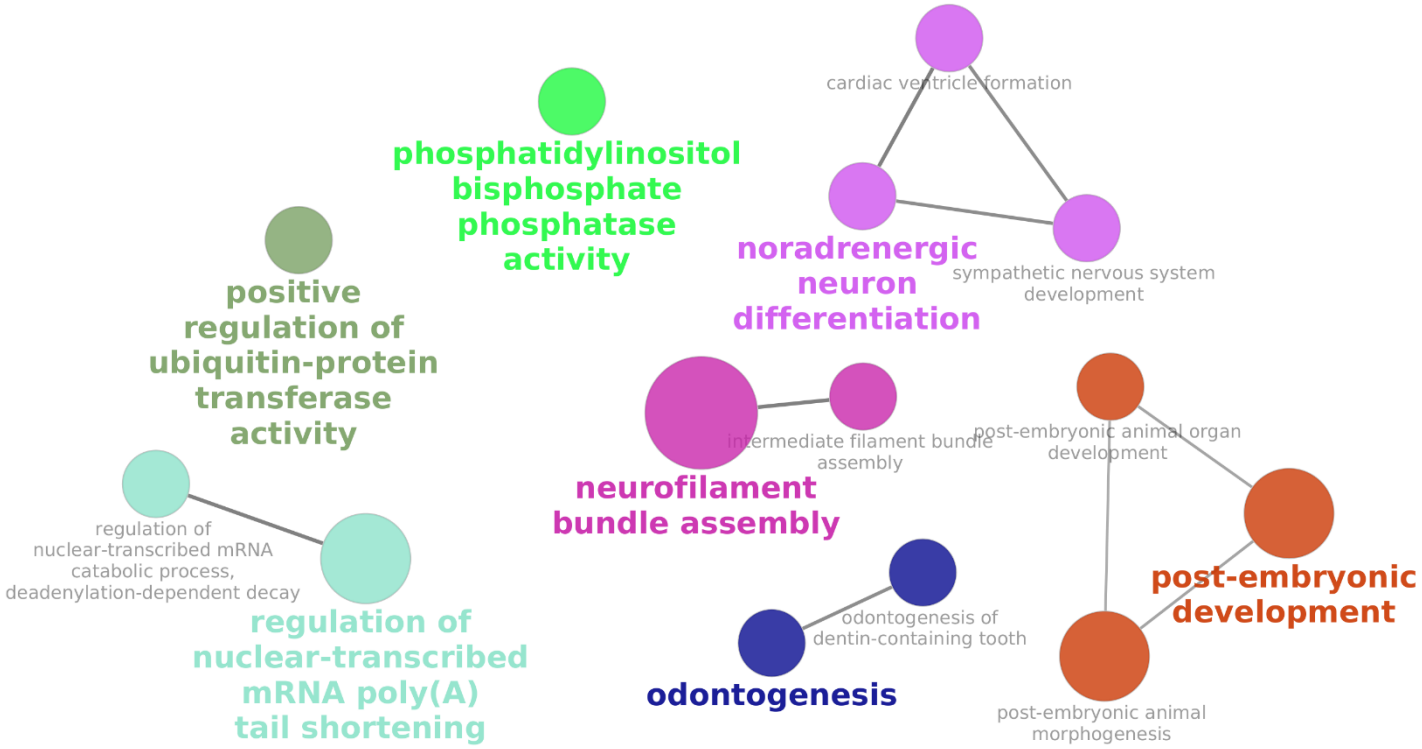

Figure 76. The distribution of all pathway terms (for turquoise module miRNAs' target genes) visualized on the network. The Figure shows the functionally grouped network with terms as nodes (hubs) linked based on their kappa score level (≥0.3) and p-value after Bonferroni correction < 0.05, where only the label of the most significant term per group is shown. The node size represents the term enrichment significance. Node color represents the functional groups.

4.4.17. Identification of miRNAs' target genes representing biological gene networks and GO/pathways for the trait-specific yellow module affected by PUFAs diet in PL and PLxDuroc pigs

Identification of miRNA target genes associated with GO/pathway terms affected by PUFAs diet in PL and PLxDuroc pigs for trait-associated yellow module: ClueGO analysis identified 78 GO/pathway specific terms associated with yellow module miRNAs' target genes affected by PUFAs diet in PL and PLxDuroc pigs (Fig. 76), namely: Protein serine/threonine/tyrosine kinase activity, Regulation of trans-synaptic signaling, Modulation of chemical synaptic transmission, Regulation of signaling, Regulation of cell communication, Regulation of signal transduction, Intracellular signal transduction, Multicellular organism development, Anatomical structure morphogenesis, Regulation of developmental process, Cell differentiation, Cell morphogenesis, Cell development, System development, Regulation of multicellular organismal development, Nervous system development, Neurogenesis, Generation of neurons, Neuron differentiation, Neuron development, Regulation of metabolic process, Macromolecule metabolic process, Cellular biosynthetic process, Organonitrogen compound metabolic process, Organic substance biosynthetic process, Protein metabolic process, Regulation of cellular metabolic process, Cellular macromolecule metabolic process, Regulation of nitrogen compound metabolic process, Regulation of macromolecule metabolic process, Regulation of primary metabolic process, Macromolecule biosynthetic process, Macromolecule modification, Regulation of macromolecule biosynthetic process, Cellular macromolecule biosynthetic process, Protein modification process, Cellular protein metabolic process, Cellular protein modification process, Regulation of cellular macromolecule biosynthetic process, Positive regulation of biological process, Negative regulation of biological process, Regulation of metabolic process, Regulation of cellular process, Macromolecule metabolic process, Cellular biosynthetic process, Positive regulation of cellular process, Negative regulation of cellular process, Organic substance biosynthetic process, Regulation of biosynthetic process, Regulation of cellular metabolic process, Cellular macromolecule metabolic process, Regulation of nitrogen compound metabolic process, Regulation of macromolecule metabolic process, Regulation of primary metabolic process, Macromolecule biosynthetic process, Positive regulation of macromolecule metabolic process, Positive regulation of cellular metabolic process, Positive regulation of nitrogen compound metabolic process, Regulation of macromolecule biosynthetic process, Regulation of nucleobase-containing compound metabolic process, Regulation of cellular biosynthetic

process, Cellular macromolecule biosynthetic process, Regulation of RNA metabolic process, Regulation of cellular macromolecule biosynthetic process, DNA biosynthetic process, Positive regulation of RNA metabolic process, Regulation of RNA biosynthetic process, Transcription by DNA-templated, nucleic acid-templated transcription, Positive regulation of RNA biosynthetic process, Regulation of transcription, DNA-templated, Regulation of nuclei acid-templated transcription, Transcription by RNA polymerase I, Positive regulation of transcription, DNA-templated, Positive regulation of nucleic acid-templated transcription, DNA-binding transcription factor activity, Regulation of transcription by RNA polymerase I, DNA-binding transcription factor activity, RNA polymerase II-specific.

4.4.18. Identification of functional groups affected by PUFAs diet in PL and PLxDuroc pigs for trait-associated yellow module

ClueGO analysis identified 6 functional groups for the trait-associated yellow-module miRNAs' target genes affected by PUFAs diet in PL and PLxDuroc pigs: namely: protein serine/threonine/tyrosine kinase activity, regulation of trans-synaptic signaling, regulation of signal transduction and cell communication, regulation of cell morphogenesis and multicellular organismal development, regulation of cellular macromolecule biosynthetic process, and regulation of RNA biosynthetic and cellular metabolic process, respectively (Fig. 77).

Finally, the distribution of all 78 module-specific GO/pathways specific terms, represented in the 6 functional group networks were visualized in Figure 78.

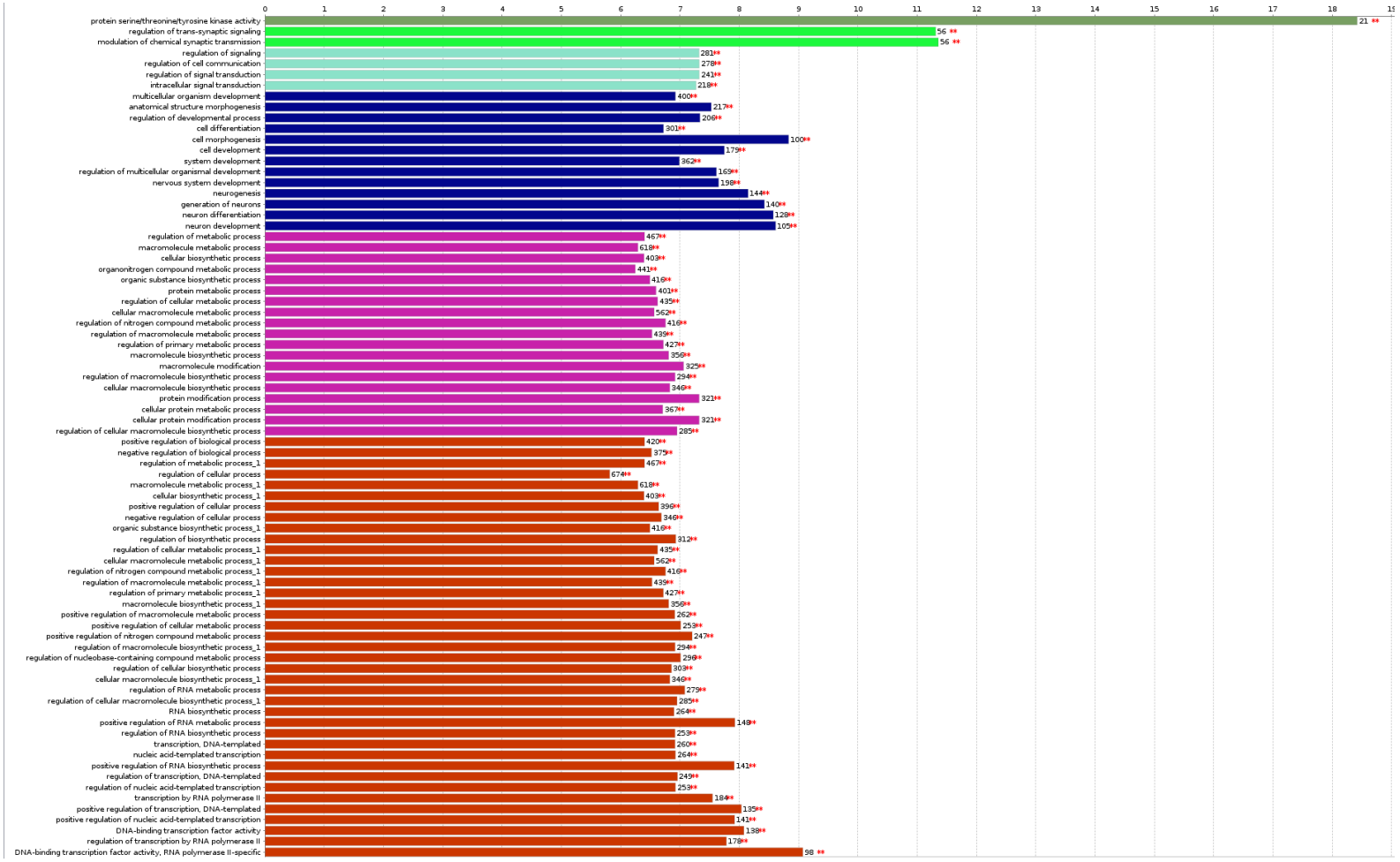

Figure 77. ClueGO analysis of yellow module miRNAs' target genes: The Figure shows the GO/pathway terms specific for black module miRNAs' target genes. The bars represent the number of genes associated with the terms. The percentage of genes per term is shown as bar label.

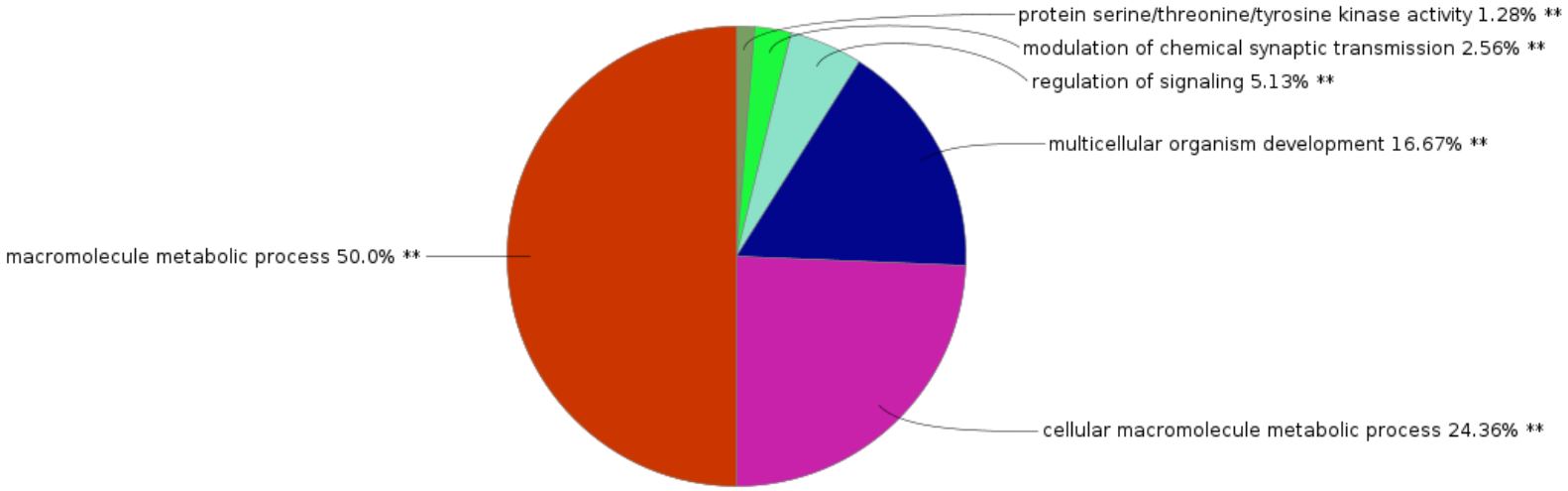

Figure 78. ClueGO analysis of yellow module miRNAs' target genes: The Figure shows an overview chart with functional groups including specific terms for black module miRNAs' target genes.

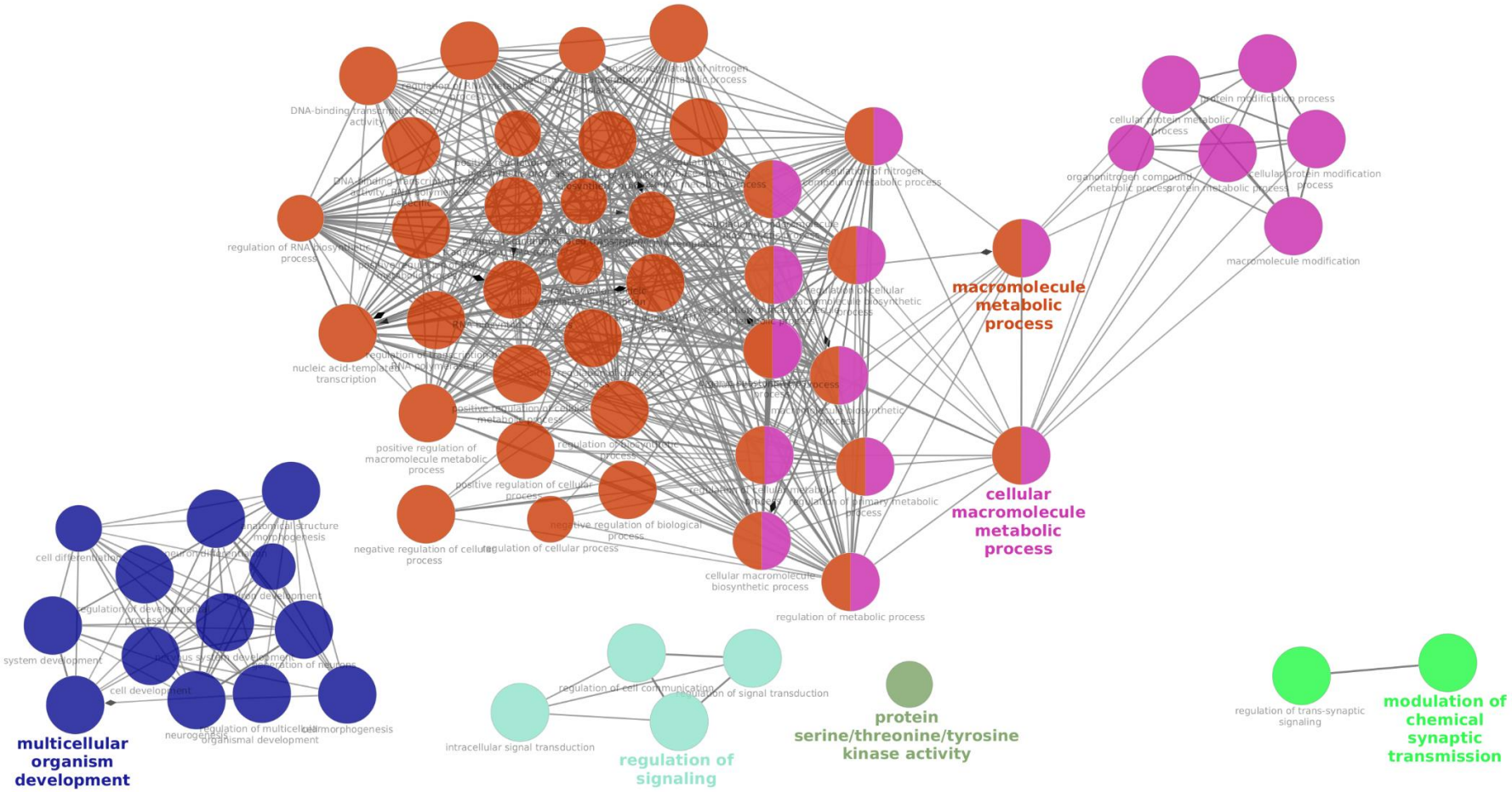

Figure 79. The distribution of all pathway terms (for yellow module miRNAs' target genes) visualized on the network. The Figure shows the functionally grouped network with terms as nodes (hubs) linked based on their kappa score level (≥0.3) and p-value after Bonferroni correction < 0.05, where only the label of the most significant term per group is shown. The node size represents the term enrichment significance. Node color represents the functional groups.

5. Discussion

The research based on the dietary effects of PUFAs and in particular omega-3 and omega-6 PUFAs has been growing substantially in the past few years **(Szostak, et al. 2016, Ogluska et al. 2017, Shrestha et al. 2020, Lin et al. 2019, Zhang et al. 2019)**. As an important essential dietary constituents, omega-3 and omega 6 PUFAs play wide-range of important roles in lipidomic and biophysical homeostasis improving membrane fluidity to maintain cellular fitness **(Levental et al. 2020)**, in critical illness and being precursors of anti-inflammatory derivatives **(Molfino et al. 2017, Zarate et al. 2017)**, fetal programming **(Shrestha et al. 2020),** direct differentiation of the membrane phenotype in mesenchymal stem cells to potentiate osteogenesis **(Levental et al. 2017)**, breast cancer **(Zanoaga et al. 2016)**, metabolic syndrome in adults **(Mirmiran et al. 2016)**, Increases the Risk for Obesity **(Simopoulos 2016)**, disorders of lipids metabolism **(Jacometo et al. 2014)** and triglyceride metabolism in liver through disturbances in omega-6/omega-3 fatty acids ratio in western diet, are closely related to prevalence of obesity **(Simopoulos 2016)** or obesity related diseases like type II diabetes, cardiovascular diseases **(Bowen et al. 2016)** or more and more common cases of nonalcoholic fatty liver disease **(Jump et al. 2018)**. As outlined in this dissertation, dietary PUFAs play significant roles in liver physiology, viz., by removal of cholesterol excess from hepatocytes, protection from excessive release of FFA from TG, enhancement of catabolic processes in β-oxidation or counteraction of liver steatosis presumably through pathways **(Terracciano et al. 2018)**. In this Ph.D. dissertation, the functional miRNA gene expression analysis was performed with the DE-miRNA analysis and WGCNA co-expression gene network analysis in investigated purebred and crossbred pigs. Both analyses in the PL purebred and PLxDuroc crossbred pigs were conducted to reveal the specific effect of dietary PUFAs on hepatic MiRNA gene expression depending on the breed of pigs, which are characterized by distinct fatness and growth traits. In pig breeding in Poland, both purebred and crossbred pigs are commonly used in commercial farms for meat production. The PL breed is the most commonly occurring pig breed in Poland. In Poland, PL is used as a maternal line and Duroc as a paternal line in production crossbreeding. Duroc is often used as an additional genetic component, because of high intramuscular fat (IMF), which is responsible for improving the quality of meat and higher technological value for production and sensory value for consumers. The major difference between the two selected breeds concerns fatness. The crossbred PLxDuroc is characterized by a higher content of MUFA in IMF and higher content of SFA in back fat in comparison to PL, which is known as a relatively lean pig, characterized by less fatness. These characteristics and

differences between investigated purebred and crossbred pigs in fatness are interesting subjects to investigate because of their different metabolism. The dissertation study is based on investigating the dietary effect of fatty acid metabolism, therefore the best choice for the analyzed organ was the liver. Furthermore, we can investigate not only the major mechanism influenced by omega fatty acids on metabolism, but additionally indicate the breed-specific differences in pigs fed with PUFAs diets. Moreover, this study is relevant also for human studies, as an animal model to explain the different predisposition factors to obesity or the ability to lipid storage. In humans, despite the same diet and lifestyle, some people are more prone to obesity than others, because of different metabolism in the global human population.

5.1. Discussion on DE-miRNA analysis:

In the DE-miRNA NGS experiments, we performed six breed-and-diet-specific comparisons of porcine hepatic miRNA profiles to identify putative DE-miRNA biomarkers. In past studies, numerous miRNAs classified as known and unknown as novel biomarkers in metabolic tissues such as the porcine liver, adipose, and skeletal muscle were identified **(Liang et al. 2019)**. In our study in all six DE-miRNA comparisons, large sets of breed-and-diet-specific putative DE-miRNA biomarkers were identified and were further filtered to show the most commonly sheared putative DE-miRNA in all six comparisons (Table 63).

Table 63. The highest target gene score for miRNAs from pink module.

Shared Comparison number	Number of shared genes	Identification of commonly shared hepatic DE miRNA in pigs
II, III, IV, V	3	ssc-let-7f-1 ENSSSCT00000020276.4 ssc-mir-143
II, IV, V	1	ENSSSCT00000047143.1
II, IV, VI	1	ENSSSCT00000040180.1
II, V, VI	1	ENSSSCT00000019672.1
III, IV, V	2	ssc-mir-22 ssc-mir-101-2
III, V, VI	3	ENSSSCT00000050925.1 ENSSSCT00000063905.1 ENSSSCT00000062826.1
I, III	2	ssc-mir-103-2 ENSSSCT00000039582.1
I, IV	1	ENSSSCT00000048121.1
II, IV	1	ssc-let-7f-2

III, V	9	ssc-mir-27b ssc-mir-133a-1 ssc-mir-148a ENSSSCT00000063347.1 ssc-mir-142 ssc-mir-26a ssc-mir-122 ENSSSCT00000039099.1 ENSSSCT00000051609.1
III, VI	3	ENSSSCT00000024894.2 ENSSSCT00000019668.1 ENSSSCT00000049859.1
IV, V	3	ssc-mir-378-2 ssc-mir-21 ssc-mir-26b
IV, VI	11	ENSSSCT00000056706.1 ENSSSCT00000019680.1 ENSSSCT00000039323.3 ENSSSCT00000053008.1 ENSSSCT00000057520.3 ENSSSCT00000037189.3 ENSSSCT00000037621.3 ENSSSCT00000064915.1 ENSSSCT00000037492.1 ENSSSCT00000049986.3 ENSSSCT00000049792.1
I	9	ENSSSCT00000056391.1 ssc-mir-10a ssc-mir-141 ENSSSCT00000039714.1 ENSSSCT00000038143.1 ENSSSCT00000044507.1 ENSSSCT00000054955.1 ENSSSCT00000041574.1 ENSSSCT00000043911.1
II	3	ENSSSCT00000019666.3 ENSSSCT00000055613.1 ENSSSCT00000046577.1
III	32	ENSSSCT00000029616.2 ssc-mir-126 ENSSSCT00000019657.1 ENSSSCT00000042113.1 ssc-mir-194a ENSSSCT00000046107.1 ssc-mir-425 ENSSSCT00000046476.3 ssc-mir-30a

		microRNA let-7g ENSSSCT00000050810.1 ENSSSCT00000040236.3 ssc-mir-30d ssc-mir-215 ssc-mir-30c-1 ENSSSCT00000039872.1 ENSSSCT00000043456.1 ENSSSCT00000039038.1 ENSSSCT00000022223.2 ENSSSCT00000056553.1 ssc-mir-16-1 ssc-let-7d ssc-let-7i ENSSSCT00000040324.1 ssc-mir-151a ENSSSCT00000046058.1 ENSSSCT00000019663.3 ssc-mir-191 ENSSSCT00000023227.2 ssc-mir-28 ssc-mir-186
IV	21	ENSSSCT00000039452.1 ENSSSCT00000044673.1 ENSSSCT00000042978.1 ENSSSCT00000045294.1 ENSSSCT00000052705.1 ENSSSCT00000029220.2 ENSSSCT00000039920.1 ENSSSCT00000020341.2 ssc-mir-221 ENSSSCT00000049975.1 ENSSSCT00000064785.1 ENSSSCT00000059464.1 ENSSSCT00000053796.1 ssc-let-7a-1 ssc-mir-181a-2 ENSSSCT00000041574.2 ENSSSCT00000019662.1 ENSSSCT00000044072.1 ENSSSCT00000020179.3 ENSSSCT00000056393.1 ENSSSCT00000060513.1
V	5	ENSSSCT00000050260.2 ssc-let-7a-2 ssc-mir-30e ssc-mir-451

		ENSSSCT00000059159.1
VI	11	ENSSSCT00000059046.3 ENSSSCT00000057013.1 ENSSSCT00000020968.2 ssc-mir-214 ENSSSCT00000051559.1 ENSSSCT00000025229.2 ENSSSCT00000043594.1 ssc-mir-181a-1 ENSSSCT00000043491.1 ENSSSCT00000025078.2 ENSSSCT00000055228.3

In the first comparison study, we identified the novel 13 breed-specific hepatic DE-miRNA ($p \leq 0.05$) that were differentially expressed in crossbred pigs fed with a standard (control) diet and supplementary diet enriched with omega-6 and omega-3 PUFAs. In this comparison, the 5 upregulated and 10 downregulated breed-specific DE-miRNA can be considered as the potential candidate miRNA genes identified in crossbred PLxDuroc pigs (Table 3 – 5). Most of these identified breed-and-diet-specific hepatic DE-miRNA can be suggested as novel hepatic miRNA biomarkers, as they are not reported in previous studies. However, in a recent study **(Xu et al. 2022)**, a hypoxic stress-related ssc-mir-141 was identified as a potential biomarker involved in the mechanism underlying the hypoxia adaptation of Tibetan pigs. Identified ssc-miR-141 miRNA was mainly enriched in mitogen-activated protein kinase (MAPK), autophagy-animal, and Ras signalling pathways. In other studies, porcine ssc-miR-103 miRNA was identified as: a potential biomarker of potent activator LPS-stimulated PBMCs in porcine immune system **(Zhang et al. 2020)**, and a potential biomarker for tooth morphogenesis during early development in miniature pigs **(Li et al. 2015)**.

In the second comparison study, we identified the 10 diet-specific hepatic DE-miRNA ($p \leq 0.05$) that were differentially expressed in both purebred and crossbred fed with a standard (control) diet. In this comparison, the 21 upregulated and 21 downregulated diet-specific DE-miRNAs can be considered as the potential candidate genes associated with control diets fed to the purebred and crossbred pigs. Most of these identified hepatic DE-miRNA (Table 6 – 8) can be suggested as novel hepatic miRNA biomarkers, as they are not reported in previous studies. However, some of the studies identified the DE-miRNA biomarkers expressed in other porcine tissues. For example, i) study of Ding et al. (2022) identified miR-143-3p as a crucial miRNA biomarker in early porcine pregnancy, where it regulates the function of PTr2 cells during

porcine embryo implantation, ii) study of Zhong et al. (2020) identified ssc-miR-143-3p (MIR143) as an apoptosis factor in porcine granulosa cells, and study of Ye et al. (2012) reported ssc-miR-143 as most highly expressed and new resistance biomarkers for E. coli F18 infection, when they compared the resistance to E. coli F18 between local Chinese and exotic pig breeds.

In the third comparison study, we identified the **54 diet-and-breed-specific** hepatic DE-miRNA ($p \leq 0.05$) that were differentially expressed in the control diet of crossbred and PUFAs diet of purebred pigs. In this comparison, the 29 upregulated and 64 downregulated diet-and-breed-specific DE-miRNAs can be considered as the potential candidate genes associated with the control diet of crossbred and PUFAs diet of purebred pigs (Table 9 – 12). Most of these identified hepatic DE-miRNA can be suggested as novel hepatic miRNA biomarkers, as they are not reported in previous studies. However, the ssc-miR-16 miRNA identified in our study was also identified as a potential miRNA toxicity biomarker in another study by **Segura-Wang et al. (2021)**, by investigating the dietary effect of deoxynivalenol (DON) exposures in porcine liver, and jejunum tissues. However, using RT-PCR, study **Timoneda et al. (2012)** of investigated the stability of ten miRNAs (Ssc-let-7a, Ssc-miR-103, Ssc-miR-17-3p, Hsa-miR-25, Hsa-miR-93, Ssc-miR-106a, Ssc-miR-191, Ssc-miR-16, Ssc-miR-26a and Ssc-miR-17-5p) in different tissues (skeletal muscle, kidney, liver, ovary and uterus) and different pig breeds (Iberian, Landrace, Large White, Meishan and Vietnamese). Study concluded that the porcine miR-93 was the most stable miRNA. According to tissues, the let-7a was the most stable in skeletal muscle and ovary, miR-17-5p in kidney, miR-26a in liver and miR-103 in uterus, respectively. Moreover, the study of Liang et al. (2019) identified that the ssc-miR-129-5p, ssc-miR-30 and ssc-miR-150 DE-miRNA biomarkers are involved in porcine adipose tissue function.

In the fourth comparison study, we identified the **56** breed-specific hepatic DE-miRNA ($p \leq 0.05$) that were differentially expressed in the control diet of purebred and PUFAs diet of crossbred pigs. In this comparison, the 16 upregulated and 26 downregulated breed-specific DE-miRNAs can be considered as the potential candidate genes associated with the control diet of purebred and PUFA diet of crossbred pigs (Table 13 – 15). Most of these identified hepatic DE-miRNA are belonging to small nucleolar RNA SNORD families (Small nucleolar RNA SNORD24, Small nucleolar RNA SNORD27, Small nucleolar RNA SNORD30, Small nucleolar RNA SNORD58, Small nucleolar RNA SNORD96 etc.). In literature, the Small nucleolar RNA SNORD family has been identified as a candidate diagnostic biomarker for

Alzheimer's disease **(Fitz et al. 2021)**, and Prader-Willi syndrome **(Cavaille 2017)**, as an endogenous spliceosome and alternative splicing (AS) biomarker of numerous human diseases including cancer **(Sperling 2019)**, and the dual function in rRNA modification and alternative pre-RNA splicing **(Falaleeva et al. 2017)**.

In the fifth comparison study, we identified the **27** breed-specific hepatic DE-miRNA ($p \leq 0.05$) that were differentially expressed in both purebred and crossbred pigs fed with PUFAs diet. In this comparison, the 15 upregulated and 22 downregulated breed-specific DE-miRNAs can be considered as the potential candidate genes associated with purebred and crossbred pigs fed with PUFA diets. (Table 16 – 18). Most of the identified hepatic DE-miRNA can be suggested as novel hepatic miRNA biomarkers, as they are not reported in previous studies. However, two miRNA biomarkers namely, ssc-let-7a and ssc-miR451 identified in this comparison were also reported in different transcriptome studies in the pig. For example, a very recent study by Truong et al. (2023) identified ssc-let-7a, along with ssc-miR-130b-3p, ssc-let-7a, and ssc-let-7c as the candidate miRNA biomarker for the African swine fever virus-infected pigs. In another recent study, the integrated analysis on differentially expressed (DE) mRNAs and miRNAs in the *Longissimus dorsi (*LD) muscle between Laiwu pigs (LW, fat-type pigs) and commercial Duroc × Landrace × Yorkshire pigs (DLY, lean-type pigs) identified two network modules: between five upregulated mRNA genes (*GALNT15*, *FKBP5*, *PPARGC1A, LOC110258214,* and *LOC110258215*) and six downregulated miRNA genes (*ssc-let-7a*, *ssc-miR190-3p, ssc-miR356-5p*, *ssc-miR573-5p*, *ssc-miR204-5p* and *ssc-miR-10383*), and between three downregulated DE mRNA genes (*IFRD1, LOC110258600,* and *LOC102158401*) and six upregulated DE miRNA genes (*ssc-miR1379-3p*, *ssc-miR1379-5p*, *ssc-miR397-5p, ssc-miR1358-5p*, *ssc-miR299-5p,* and *ssc-miR1156-5p*) in LW pigs (Zhang et al. 2022). In past several studies (Zhu et al. 2022, Jang and Lee 2021, Gan et al. 2020, and Kiss et al. 2020) reported the ssc-miR451 as a candidate biomarker expressed in different porcine tissues. For example, a study by Zhu et al. (2022) revealed that there was essentially no change in the expression of ssc-miR-451, ssc-miR-1285, and ssc-miR-486 in the cis infusion or joint infusion kidney groups, and their expression was significantly down-regulated over time in the trans-infusion kidney group. Studies conclude that specific miRNA markers, such as miR-451, may play a negative regulatory role in cell metabolism following the perfusion of kidney transplants using different methods. A study by Jang and Lee 2021, identified ssc-miR-451 as a weaning-associated differentially expressed miRNA during the suckling-to-weaning transition in pigs. Another study by Gan et al. (2020) revealed that inhibition of ssc-miR-451 promoted

adipogenic differentiation and regulated the lipid deposition and fatty acid composition by targeting ACACA, and ssc-miR-451 to improve pork quality. Finally, a study by Kiss et al. (2020) found that ssc-miR-451 was associated with cardiopulmonary bypass, cardiac arrest, and subsequent myocardial ischemia/reperfusion by investigating the effects of cardiopulmonary bypass and temperature of cardioplegic arrest on myocardial miRNA profile in pigs' left ventricular tissue.

In the sixth comparison study, we identified the **34** breed-specific hepatic DE-miRNA ($p \leq 0.05$) that were differentially expressed in PLxDuroc crossbred pigs fed with control vs PUFAs diets. In this comparison, the 13 upregulated and 27 downregulated breed-specific DE-miRNAs can be considered as the potential candidate genes associated with PLxDuroc crossbred pigs fed with PUFA diet. (Table 19 – 21). Most of these identified hepatic DE-miRNA can be suggested as novel hepatic miRNA biomarkers, as they are not reported in previous studies. In previous studies **(Jiao et al. 2018)**, the ssc-miR-214 miRNA was identified as a potential miRNA biomarker for Notch signaling in porcine satellite cells (PSCs) and skeletal muscle development **(Jiao et al. 2018)**, and also as a weaning-associated differentially expressed miRNA during the suckling-to-weaning transition in pigs **(Jang and Lee 2021).**

5.2. Discussion on WGCNA analysis:

In the WGCNA experiments, we performed the co-expression analysis by identifying the trait-associated hub miRNA genes of the porcine liver. Using the WGCNA R script, nine trait-associated modules with p-value ≤ 0.05 were identified as statistically significant for the trait affected by PUFAs diets in PL and PLxDuroc pigs. As a result, **four traits** were identified with significant modules: i) The shoulder subcutaneous fat thickness ii) meat color (a*), iii) Conductivity 24 hours postmortem (PE24). and iv) ash, respectively. The intra-modular analysis for MEM (modules in color) was carried out to identify the relationship between the miRNA and the identified porcine phenotypic trait. Trait-wise, a total of 9,7, 2, and 8 trait-associated significant modules affected by PUFAs diets in PL and PLxDuroc pigs were identified representing four traits. In general, a total of 63 significant (p-value ≤ 0.05) porcine hepatic miRNAs were identified representing nine trait-associated modules (Table 24). These identified trait-associated miRNAs can be suggested as novel hepatic miRNA biomarkers, as they are not reported in previous studies. However, previous numerous studies identified these putative miRNA biomarkers by investigating other transcriptomes including porcine liver, and

the phenotypic traits, particularly the porcine growth and development, meat quality, health, and reproduction. (Table 64).

Table 64. List of significantly trait-correlated modules putative porcine hepatic miRNA hub genes identified in this study, and list of references which were identified these porcine miRNAs in the liver and other tissues (skeletal muscle, adipose, tumour etc).

Significantly trait-correlated module	Identified miRNA hub genes in trait-associated modules	References *References mentioned in discussion section
Black	ssc-miR-142-3p, ssc-miR-30a-3p, ssc-miR-21-5p	**Su et al. (2017)*, Kiss et al. (2020)*, Mármol-Sánchez et al. (2020)*,** Hua et al. (2020), Tang et al. (2022), Li et al. (2021), Wang et al. (202), Xu et al. (2020)
Blue	ssc-miR-425-5p, ssc-miR-199a-5p, ssc-miR-29a-3p, ssc-miR-122-5p, ssc-miR-199a-3p, ssc-miR-199b-3p, ssc-miR-186-5p, ssc-miR-22-3p	**Davoli et al. (2018)*, Liao et al. (2022)*,Marmol-Sanchez et al. (2020)*,** Swain et al. (2021), Gao et al. (2022) Godia et al. (2020) Yang et al. (2022) Li et al. (2018)
Brown	ssc-miR-486, ssc-miR-423-3p, ssc-miR-181b, ssc-miR-140-3p, ssc-miR-28-3p, ssc-miR-151-3p, ssc-miR-148a-3p, ssc-miR-26b-5p, ssc-miR-30a-5p	**Zhang et al. (2022)*, Zhu et al. (2022)*,** Zhang et al. (2018) Zuo et al. (2015) Ding et al. (2020) Xie et al. (2010) Marmol-Sanchez et al. (2020) Zhang et al. (2020)
Green	ssc-miR-7142-3p, ssc-miR-127, ssc-miR-10b, ssc-miR-374a-5p, ssc-miR-146a-5p, ssc-let-7d-5p, ssc-miR-340, ssc-miR-122-3p, ssc-miR-24-3p, ssc-miR-374a-3p, ssc-miR-7134-3p, ssc-miR-423-5p, ssc-miR-15a, ssc-miR-148b-3p	**Segura-Wang et al. (2021)*, Daza et al. (2017)*, Stachowiak et al. (2017)*,** Li et al. (2015) Li et al. (2019) Kiss et al. (2020) Huang et al. (2019) Zhang et al. (2015) Swain et al. (2021) Zhang et al. (2014) Truong et al. (2023) Wang et al. (2017) Liu et al. (2022) Ding et al. (2020) Zhang et al. (2022) Brogaard et al. (2018)
Magenta	ssc-miR-99b, ssc-miR-542-3p, ssc-miR-142-5p, ssc-miR-30e-5p, ssc-miR-92a, ssc-miR-103, ssc-let-7i-5p, ssc-let-7a, ssc-miR-101, ssc-miR-221-3p	**Oczkowicz et al.(2022)*, Jang et al. (2021)*** Sun et al. (2021) Grenier et al. (2019) Zhang et al. (2016) Qianqian et al. (2021) Zhang et al. (2022) Ding et al. (2020) Zhang et al. (2015) Zuo et al. (2015) Cordoba et al. (2015) Zhang et al. (2020) Timoneda et al. (2012) Wang et al. (2015) Li et al. (2015)

		Hua et al. (2021) Zhang et al. (2022a) Truong et al. (2023) Song et al. (2020) Zhang et al. (2015)
Pink	ssc-miR-339, ssc-miR-339-5p, ssc-miR-19b, ssc-miR-99a-5p, ssc-miR-30e-3p, ssc-miR-30b-5p	**Feng et al. (2022)*, Jia et al. (2012)*** Zhang et al. (2019) Kiss et al. (2020) Mármol-Sánchez et al. (2020)
Purple	ssc-miR-125b, ssc-miR-10a-5p, ssc-miR-151-5p, ssc-miR-143-3p, ssc-miR-126-3p	**Jang et al. (2021)*, Li et al. (2019)*** Xie et al. (2010) Chen et al. (2017) Kaczmarek et al. (2021) Timoneda et al. (2013) Fleming et al. (2019) Kiss et al. (2020) Ding et al. (2020) Qianqian et al. (2021) Li et al. (2017) Zuo et al. (2015) Zhong et al. (2020) Stachowiak et al. (2017)
Red	ssc-miR-148a-5p, ssc-let-7g	**Biamonte et al. (2019)*** Wang et al. (2022)
Turquoise	ssc-miR-146b, ssc-miR-1285, ssc-miR-92b-3p, ssc-miR-181c	**Tao et al. (2013)*, Tao et al. (2017)*** Oczkowicz et al. (2022) Zhang et al. (2016) Davoli et al. (2018) Stachowiak et al. (2017) Sun et al. (2020) Jang et al. (2021) Alvarez-Rodriguez et al. (2020) Zhu et al. (2022) Wang et al. (2022)
Yellow	ssc-miR-16, ssc-miR-30c-5p, ssc-miR-126-5p, ssc-miR-194a-5p, ssc-miR-378, ssc-let-7f-5p, ssc-miR-27b-3p, ssc-miR-181a	**Jiang et al. (2021**)*, **Zhang et al. (2019)*,** Timoneda et al. (2012) Wang et al. (2015) Segura-Wang et al. (2021) Godia et al. (2020) Zuo et al. (2015) Yang et al. (2022) Hou et al. (2012) Daza et al. (2017) Hua et al. (2020) Ye et al. (2012) Lian et al. (2012)

***References mentioned in discussion section**

5.2.1. Identification of the trait-associated miRNA hub genes, and the metabolic pathways in the trait-specific black module

In the trait-associated black module, our study identified putative porcine hepatic miRNA: ssc-miR-142-3p, ssc-miR-30a-3p, ssc-miR-21-5p, respectively. Previous studies conducted in the myocardial tissue of Coronary microembolization infected pigs revealed that the expression of ssc-miR-92b-5p, ssc-miR-491, ssc-miR-874, ssc-miR-425-3p, ssc-miR-376a-5p, ssc-miR-370, ssc-miR-30c-3p, ssc-miR-493-5p and ssc-miR-323 was significantly increased, whereas the

expression of ssc-miR-136 and ssc-miR-142-3p was significantly decreased. However, the GO and KEGG pathway analysis indicated that the target genes of these miRNAs are mainly associated with cell proliferation, apoptosis, necrosis, inflammation, and fibrosis. **(Su et al. 2017)**. Using the myocardial tissue, Kiss et al. (2020) investigated the effects of cardiopulmonary bypass and temperature of cardioplegic arrest on myocardial miRNA profile in pigs' left ventricular tissue and found ssc-miR-451 was differently expressed between STH2-warm and STH2-cold cardioplegia and the cardiopulmonary bypass and temperature of cardioplegic solution significantly affected the expression of miR-451 miRNAs in left ventricular tissue. **(Kiss et al. 2020).**

In another study on porcine *gluteus medius* muscle, ssc-miR-148a-3p, ssc-miR-22-3p and ssc-miR-1 DE-miRNAs were identified which play key roles in the regulation of glucose and lipid metabolism. The study concludes that seven miRNAs (ssc-miR-148a-3p, **ssc**-miR-151-3p, ssc-miR-30a-3p, ssc-miR-30e-3p, ssc-miR-421-5p, ssc-miR-493-5p, and ssc-miR-503) which putatively interact with the PDK4 mRNA, one of the master regulators of glucose utilization and fatty acid oxidation **(Mármol-Sánchez et al. 2020).** In our study, the identified ssc-miR-21 is a well-known biomarker that plays a significant role in the pathogenesis of inflammatory diseases. A previous study showed that elevated ssc-miR-21-5p (miR-21) levels in porcine circovirus type 2 (PCV2) infected porcine kidney 15 (PK-15) cells causing postweaning multisystemic wasting syndrome (PMWS) and other PCV-associated diseases (PCVADs). The study also found that miR-21 overexpression induced the NF-κB pathway along with inflammation in cells exposed to PCV2. **(Li et al. 2021).**

5.2.2. Identification of the trait-associated miRNA hub genes, and the metabolic pathways in the trait-specific blue modules

In the trait-associated blue module, our study identified putative porcine hepatic miRNA: ssc-miR-425-5p, ssc-miR-199a-5p, ssc-miR-29a-3p, ssc-miR-122-5p, ssc-miR-199a-3p, ssc-miR-199b-3p, ssc-miR-186-5p, ssc-miR-22-3p, respectively.

By investigating the divergent backfat deposition trait in Italian Large White pig backfat tissue, Davoli et al. (2018) detected 31 significant DE-miRNAs: 14 up-regulated (including ssc-miR-132, ssc-miR-146b, ssc-miR-221-5p, ssc-miR-365-5p and the miRNA ssc-moR-21-5p) and 17 down-regulated (including ssc-miR-136, ssc-miR-195, ssc-miR-199a-5p and ssc-miR-335), and numerous miRNAs and mRNAs network were found that were expressed from backfat-related pig QTL **(Davoli et al. 2018).**

A previous study by Liao et al. (2022) identified the most significantly down-regulated ssc-miR-122-5p and ssc-miR-192 miRNAs in porcine adipose tissue affected by feed efficiency in pigs. Furthermore, the GO and KEGG analyses indicated that these miRNAs were significantly related to lipid metabolism, and these miRNAs modulated FE by regulating lipid metabolism.

In another previous study by Mármol-Sánchez et al. (2020) investigated the porcine gluteus medius muscle miRNA expression before and after food intake in gilts. Feeding experiment identified ssc-miR-148a-3p, ssc-miR-22-3p and ssc-miR-1, which play key roles in the regulation of glucose and lipid metabolism. Moreover, the co-expression network analyses revealed several miRNAs that putatively interact with mRNAs playing key metabolic roles and that also showed differential expression before and after feeding **(Mármol-Sánchez et al. 2020).**

5.2.3. Identification of the trait-associated miRNA hub genes, and the metabolic pathways in the trait-specific brown modules

In the trait-associated brown module, our study identified putative porcine hepatic miRNA: ssc-miR-486, ssc-miR-423-3p, ssc-miR-181b, ssc-miR-140-3p, ssc-miR-28-3p, ssc-miR-151-3p, ssc-miR-148a-3p, ssc-miR-26b-5p, ssc-miR-30a-5p, respectively.

A previous study by Zhang et al. 2022 investigated the regulatory functions of miRNAs in the subcutaneous adipose tissue of Laiwu (LW) and Large White (LY) pig breeds. The study identified 39 known miRNAs and 56 novel miRNAs significantly DE-miRNA LW and LY pig breeds. The Gene Ontology and KEGG pathways analysis identified predicted miRNAs that were involved in several fat-associated pathways, such as the peroxisome proliferator-activated receptor (PPAR), mitogen-activated protein kinases (MAPK) and Wnt signaling pathways. Additionally, ssc-miR-133a-3p, ssc-miR-486 and ssc-miR-1 biomarkers had a great impact on the development of porcine subcutaneous fat through the PPAR signaling pathway **(Zhang et al. 2022).**

A study by Zuo et al. 2022 investigated the skeletal muscle fibre types during porcine growth to help understand the miRNA regulation mechanism of fibre differentiation. The study identified that ssc-miR-1 and ssc-miR-133 belonging to the MyomiRs, which control muscle myosin content, myofibre identity, and muscle performance. However, the overexpression and inhibition of ssc-miR-143-3p in porcine skeletal muscle satellite cells induced the increase and reduction of the slow muscle fibre gene and protein (MYH7), indicating that miR-143 activity regulated muscle fibre differentiated in skeletal muscle **(Zuo et al. 2022).**

5.2.4. Identification of the trait-associated miRNA hub genes, and the metabolic pathways in the trait-specific green modules

In the trait-associated green module, our study identified putative porcine hepatic miRNA: ssc-miR-7142-3p, ssc-miR-127, ssc-miR-10b, ssc-miR-374a-5p, ssc-miR-146a-5p, ssc-let-7d-5p, ssc-miR-340, ssc-miR-122-3p, ssc-miR-24-3p, ssc-miR-374a-3p, ssc-miR-7134-3p, ssc-miR-423-5p, ssc-miR-15a, ssc-miR-148b-3p, respectively.

In a previous study, the dietary effect of deoxynivalenol (DON) in the porcine liver and jejunum transcriptome was investigated **(Segura-Wang et al. 2021)**. The miRNA expression profiling result revealed that ssc-miR-10b is downregulated in the liver of DON-exposed pigs. Furthermore, the identified predicted microRNA target genes showed enrichment of several pathways including PIK3-AKT, Wnt/β-catenin, and adherents junctions**. (Segura-Wang et al. 2021)**. In another miRNA expression profiling study **(Daza et al. 2017)** using the *longissimus dorsi* (LD) muscle of Duroc × Pietrain resource population, the most abundant identified miRNAs were ssc-miR-1, ssc-miR-133a-3p, ssc-miR-378, ssc-miR-206, and ssc-miR-10b in pig skeletal muscle. In a similar transcriptome study, Zhang et al. (2015) identified ssc-miR-146a-5p and ssc-miR-221-5p miRNAs significantly upregulated in LPS-challenged pig skeletal muscle.

Using a pig model study by Stachowiak et al. (2017), pigs carrying a mutation in the adenomatous polyposis coli tumour suppressor (APC^{1311}, orthologous to human APC^{1309}) were fed with a normal pig diet were investigated. The study identified ssc-let-7e, ssc-miR-98, ssc-miR-146a-5p, ssc-miR-146b, ssc-miR-183 and ssc-miR-196a overexpressed miRNA and low-expressed ssc-miR-126-3p miRNA in high-grade intraepithelial dysplastic polyps **(Stachowiak et al. 2017).**

5.2.5. Identification of the trait-associated miRNA hub genes, and the metabolic pathways in the trait-specific magenta modules

In the trait-associated magenta module, our study identified putative porcine hepatic miRNA: ssc-miR-99b, ssc-miR-542-3p, ssc-miR-142-5p, ssc-miR-30e-5p, ssc-miR-92a, ssc-miR-103, ssc-let-7i-5p, ssc-let-7a, ssc-miR-101, ssc-miR-221-3p, respectively.

Previous studies by Oczkowicz et al. 2022, showed that various sources of fat (rapeseed oil, beef tallow, coconut oil) and different amounts of cDDGS (corn Dried Distilled Grains with Solubles) affects the miRNA profile in pig fat-the main source of circulating miRNAs. Obtained

results revealed that observed the highest number of differentially expressed miRNAs in the samples from animals that were fed with coconut oil in the diet compared to all other treatments. On the contrary, cDDGS appeared to have little effect on miRNA expression. The study proposed a subset of diet-related, adipose-specific, conservative miRNAs among mammals, namely: ssc-miR-99b, ssc-miR-4334-3p, ssc-miR-146b, ssc-miR-23a **(Oczkowicz et al. 2022).**

In another study, the miRNA expression profiling in the small intestine of pigs before weaning (BW), 1 week after weaning (1W), and 2 weeks after weaning (2W) was investigated to identify weaning-associated differentially expressed miRNAs (Jang and Lee, 2021). The study identified 133 candidate targets for miR-196a using a target prediction database. However, the gene ontology and Kyoto Encyclopedia of Genes and Genomes (KEGG) pathway analyses identified the target genes were associated with 19 biological processes, 4 cellular components, 8 molecular functions, and 7 KEGG pathways, including anterior/posterior pattern specification as well as cancer, PI3K-Akt, MAPK, GnRH, and neurotrophin signaling pathways (**Jang and Lee, 2021**).

5.2.6. Identification of the trait-associated miRNA hub genes, and the metabolic pathways in the trait-specific pink modules

In the trait-associated pink module, our study identified putative porcine hepatic miRNA: ssc-miR-339, ssc-miR-339-5p, ssc-miR-19b, ssc-miR-99a-5p, ssc-miR-30e-3p, ssc-miR-30b-5p, respectively.

In a study by Feng et al. (2022), the miRNA and circRNA profiles in the regulation of intramuscular and subcutaneous adipose tissue of Laiwu pig were Investigated. Study identified 265 differentially expressed circRNAs, of which 187 up-regulated circRNA and 78 down-regulated circRNA in IMF. Subsequently, study found that DEcircRNA's host genes were mainly involved in GO terms (including cellular response to fatty acids, lysophosphatidic acid acyltransferase activity, R-SMAD binding, etc.) and signaling pathways (fatty acid biosynthesis, Citrate cycle, TGF- β Signal pathway) related to adipogenesis, differentiation and lipid metabolism. Moreover, the functional annotation of indirect target genes and protein network analysis, study found that circRNA_06424 affects the expression of PPARD, MMP9, UBA7 and other indirect target genes by competitively binding to miRNAs such as ssc-miR-339-5p, ssc-miR-744 and ssc-miR-328, and participates in PPAR signaling pathway, Wnt signaling pathway, unsaturated fatty acid and other signaling pathways, resulting in the difference of fat deposition between IMF and SCF. **(Feng et al. 2022).**

In another study, the dietary effect of standard-protein or low-protein diets throughout gestation in primiparous, purebred Meishan sows were investigated to analyse the hepatic G6PC expression in both male and female newborn pigs. Study found that identified ssc-miR-339-5p and ssc-miR-532-3p, targeting the G6PC 3' untranslated region were significantly upregulated by the low protein diet only in females. Study suggested that a maternal low protein diet during pregnancy causes hepatic activation of G6PC gene expression in male pigs, which possibly contributes to adult-onset hyperglycemia. **(Jia et al. 2012).**

5.2.7. Identification of the trait-associated miRNA hub genes, and the metabolic pathways in the trait-specific purple modules

In the trait-associated purple module, our study identified putative porcine hepatic miRNA: ssc-miR-125b, ssc-miR-10a-5p, ssc-miR-151-5p, ssc-miR-143-3p, ssc-miR-126-3p, respectively.

Previous study by Jang and Lee (2021) investigated the miRNA expression profiling in the small intestine of pigs before weaning (BW), and after weaning (1 Week, 2 week) to identify weaning-associated differentially expressed miRNAs. Study identified 38 DE miRNAs with varying expression levels among BW, 1W, and 2W. Study also identified the classified expression patterns of miRNAs, namely ssc-miR-196a and ssc-miR-451 represent pattern 1, ssc-miR-499-5p represents pattern 2, ssc-miR-7135-3p and ssc-miR-144 represent pattern 3, and the Eleven miRNAs (ssc-miR-542-3p, ssc-miR-214, ssc-miR-758, ssc-miR-4331, ssc-miR-105-1, ssc-miR-1285, ssc-miR-10a-5p, ssc-miR-4332, ssc-miR-503, ssc-miR-6782-3p, and ssc-miR-424-5p) represent pattern 4, respectively. Moreover, the gene ontology and Kyoto Encyclopedia of Genes and Genomes (KEGG) pathway analyses revealed that the target genes were associated with 19 biological processes, 4 cellular components, 8 molecular functions, and 7 KEGG pathways, including anterior/posterior pattern specification as well as the cancer, PI3K-Akt, MAPK, GnRH, and neurotrophin signaling pathways **(Jang and Lee 2021).**

In another study by Li et al. (2019), the miRNAs expression profile in porcine alveolar macrophages after Toxoplasma gondii infection identified 81 DE miRNAs, including 36 novel miRNAs and 45 mature miRNAs. The putative ssc-miR-127 and ssc-miR-143-3p were predicted to regulate nitric oxide synthase 1 (NOS1) and nitric oxide synthase 3 (NOS3), respectively. A KEGG enrichment analysis identified predicted target genes that were involved in multiple signaling pathways, including FcγR-mediated phagocytosis, the AMPK signaling pathway, the mTOR signaling pathway, and the FcγRI signaling pathway **(Li et al. 2019).**

5.2.8. Identification of the trait-associated miRNA hub genes, and the metabolic pathways in the trait-specific red modules

In the trait-associated red module, our study identified putative porcine hepatic miRNA: ssc-miR-148a-5p and ssc-let-7g.

In trait-associated red modules, few miRNA biomarkers were identified. The identified miRNA let-7 miRNA family members have the known function as tumor suppressors and might be used to disable EOC tumor progression and chemoresistance to cis-platinum-based chemotherapy **(Biamonte et al. 2019).** Study revealed that ectopic overexpression of let-7g in OVCAR3 and HEY-A8 epithelial ovarian cancer (EOC) cells induced i) a down-regulation of c-Myc and cyclin-D2 thus promoting cell cycle arrest, ii) a reduction of Vimentin, Snail and Slug thus counteracting the progression of epithelial to mesenchymal transition, iii) a chemosensitization to cis-platinum treatment. The study concluded that decreased expression of let-7g could serve as a tissue and serum biomarker able to predict the chemo-resistant features of EOC patients.

5.2.9. Identification of the trait-associated miRNA hub genes, and the metabolic pathways in the trait-specific turquoise modules

In the trait-associated turquoise module, our study identified putative porcine hepatic miRNA: ssc-miR-146b, ssc-miR-1285, ssc-miR-92b-3p, ssc-miR-181c, respectively. In past, Tao and Xu (2013) investigated the porcine miRNA transcriptome of the small intestine during weaning stress in weaning pigs at 1, 4, and 7 d after weaning (libraries W1, W4, and W7, respectively) and from suckling pigs on the same days as the weaning pigs (libraries S1, S4 and S7, respectively). The study identified 16 DE miRNAs by comparing the W1 and S1; 98 DE miRNAs by comparing W4 and S4 (ssc-mir-146b had the largest difference); and 22 DE miRNAs by comparing W7 and S7. **(Tao and Xu 2013)**. In a later year study, Tao et al. (2017) confirmed that over-expression of miR-146b plays a significant regulatory role in the intestinal epithelial cell viability, proliferation, and apoptosis in pigs.

5.2.10. Identification of the trait-associated miRNA hub genes, and the metabolic pathways in the trait-specific yellow modules

In the trait-associated yellow module, our study identified putative porcine hepatic miRNA: ssc-miR-16, ssc-miR-30c-5p, ssc-miR-126-5p, ssc-miR-194a-5p, ssc-miR-378, ssc-let-7f-5p, ssc-miR-27b-3p, ssc-miR-181a, respectively.

A recent study by Jiang et al. (2021) constructed the whole genome-wide miRNA expression profiles of porcine fast-twitch muscle [biceps femoris (Bf)] and slow-twitch muscle [soleus (Sol)], and identified hundreds of miRNAs, including four skeletal muscle-highly expressed miRNAs, ssc-miR-378, ssc-let-7f, ssc-miR-26a, and ssc-miR-27b-3p. Moreover, the study identified 63 DE miRNAs between biceps femoris vs. soleus, of skeletal muscle fiber types.

In past, Zhang et al. 2019 investigated the dietary effects of resveratrol supplementation on growth performance, meat quality, serum lipid profiles, intramuscular fat (IMF) deposition, and the expression levels of several lipid metabolism-related miRNAs and genes in growing-finishing crossbred pigs (Duroc × Landrace × Yorkshire) fed either with a basal diet (CON) or basal diet containing 600 mg/kg resveratrol (RES). Study revealed that dietary resveratrol supplementation increased the IMF content in longissimus dorsi ($P < 0.05$), up-regulated mRNA abundances of peroxisome proliferator-activated receptor γ, fatty acid synthase, acetyl-CoA carboxylase, and lipoprotein lipase ($P < 0.05$), while downregulated mRNA abundances of carnitine palmitoyl transferase-1, sirtuin 1, and peroxisome proliferator-activated receptor α ($P < 0.05$) in LM. Moreover, resveratrol enhanced ($P < 0.05$) the expression of ssc-miR-181a, ssc-miR-370, and ssc-miR-21 and reduced ($P < 0.05$) the expression of ssc-miR-27a in longissimus dorsi. These results concluded that dietary resveratrol supplementation significantly improved IMF content and decreased serum lipids levels, which might be related with the changes in ssc-miR-181a, ssc-miR-370, ssc-miR-21, ssc-miR-27a and their downstream genes expression **(Zhang et al 2019).**

6. Conclusions

1) Study generated 12 hepatic microRNA gene expression profile FASTq data sets of the PL purebred and the PLxDuroc crossbred, based on the significant relationship with traits, diets and breeds, allowing for further investigation of the relations between miRNA expression profile and porcine phenotypic traits.
2) The study allowed for identifying a large set of diet-specific/breed-specific differentially expressed microRNA (DE miRNA) gene transcripts within PL purebred and PLxDuroc crossbred. The identified discovered novel DE-miRNAs show that the PUFA diet affects the expression profile of miRNAs in purebred and crossbred pigs.
3) The study identified 10 modules with co-expressed miRNAs in the porcine liver transcriptome. It shows that both investigated breeds in each dietary group miRNA expression profiles are characterized by the strong interconnection between miRNAs, which are highly co-expressed with each other.
4) The study identified phenotypic traits correlated with co-expressed miRNAs. Detected modules are significantly correlated with PE24, meat color, shoulder subcutaneous fat thickness, and ash traits. However, there were no trait-specific modules identified. Therefore, the identified miRNAs from significant modules of mentioned phenotypic traits can be considered as predicted miRNA genes associated with PE24, meat color, shoulder subcutaneous fat thickness, and ashes. However, confirmation of this needs further investigation to validate their potential functionality.
5) Among all trait-correlated modules, target for co-expressed miRNAs were identified. The identified co-expressed miRNA affects the phenotypic traits probably by specific functional pathways by regulating the expression of its' target genes.
6) The study identified the genes of significance in each module for each significantly correlated trait. Results concluded that the higher the number of module membership for miRNA, the higher the gene's significance. Therefore, the identified miRNA genes with the highest module membership are strongly predicted miRNA genes for the investigated traits.
7) Study Identified the hepatic miRNA target genes expression networks and metabolic pathways in trait-specific modules affected by PUFAs diets in PL and PLxDuroc pigs, which could play a significant role in biological functions such as: i) muscle organ development, ii) different cellular processes and developments, iii) system development, iv) metabolic processes, v) muscle tissue development.

7. References

1. Al-Khalaifah H. "*Modulatory Effect of Dietary Polyunsaturated Fatty Acids on Immunity, Represented by Phagocytic Activity.*" Front. Vet. Sci. (**2020**).
2. Almeida V. V., Silva J. P. M., Schinckel A. P., Meira A. N., Moreira G. C. M., Gomes J. D., Poleti M. D., Dargelio M. D. B., Patinho I., Contreras-Castillo C. J., Coutinho L. L., Mourão G. B., Reecy J. M., Koltes D., Serão N. V. L., Regitano L. C. A., Fukumasu H., Brustolini A. P. L., Alencar S. M., Filho A. L., Cesar A. S. M. *"Effects of increasing dietary oil inclusion from different sources on growth performance, carcass and meat quality traits, and fatty acid profile in genetically lean immunocastrated male pigs."* Livest. Sci. (**2021**)
3. Alvarez-Rodriguez M., Martinez C., Wright D., Barranco I., Roca J., Rodriguez-Martinez H. *"The Transcriptome of Pig Spermatozoa, and Its Role in Fertility."* Int J Mol Sci. **(2020)**; 21(5):1572.
4. Ambros V. "The functions of animal microRNAs. Nature. (**2004**); 431:350–355.
5. Anders S., Huber W., *"Differential expression analysis for sequence count data."* Genome Biology (**2010**); 11.
6. Ayuso M., Fernández A., Núñez Y., Benítez R., Isabel B., Barragán C., Fernandez A. I., Rey A. I., Fedrano J. F., Canovas A., Gonzales-Bulnes A., Lopez-Bote C., Ovilo C. *"Comparative analysis of muscle transcriptome between pig genotypes identifies genes and regulatory mechanisms associated to growth, fatness and metabolism."* PLoS One. (**2015**).
7. Azorín-Ortuño M., Yáñez-Gascón M. J., González-Sarrías A., Larrosa M., Vallejo F., Pallarés F. J., et al. *"Effects of long-term consumption of low doses of resveratrol on diet-induced mild hypercholesterolemia in pigs: A transcriptomic approach to disease prevention."* J Nutr Biochem. (**2012**);23: 829–837.
8. Baker, E. J., Miles, E. A., Burdge, G. C., Yaqoob, P., Calder, P. C. *"Metabolism and functional effects of plant-derived omega-3 fatty acids in humans."* Prog. Lipid Res. (**2016**).
9. Barrel D., Dimmer E., Huntley R. P., Binns D., O'Donovan C., Apweiler R. *"The GOA database in 2009—an integrated Gene Ontology Annotation resource"* Nucleic Acids Res. (**2009**); 37:D396–D403.
10. Bartel D. P. *"MicroRNAs: Genomics, biogenesis, mechanism, and function."* Cell. (**2004**); 116:281–297.

11. Bassols, A., Costa, C., Eckersall, P. D., Osada, J., Sabri`a, J., Tibau, J. *"The pig as an animal model for human pathologies: a proteomics perspective."* Proteom. Clin. Appl. (**2014**)
12. Bee G. *"Dietary conjugated linoleic acids affect tissue lipid composition but not de novo lipogenesis in finishing pigs."* Anim Res. (**2001**) 50:383–399.
13. Benítez R., Núñez Y., Óvilo C. *"Nutrigenomics in farm animals."* J Invest Genomics. (**2017**); 4:1.
14. Biamonte F., Santamaria G., Sacco A. *"MicroRNA let-7g acts as tumor suppressor and predictive biomarker for chemoresistance in human epithelial ovarian cancer."* Sci Rep **(2019)**; 9:5668.
15. Bindea G., Mlecnik B., Hackl H., Charoentong P., Tosolini M., Kirilovsky A., Fridman W. H., Pages F., Trajanoski Z., Galon J. *"ClueGO: a Cytoscape plug-in to decipher functionally grouped gene ontology and pathway annotation networks"* Bioinformatics (**2009**).
16. Bork C. S., Veno S. K., Lasota A. N., Lundbye-Christensen S., Schmidt E. B. "*Marine and plant-based n-3 PUFA and atherosclerotic cardiovascular disease.*" Proc. Nutr. Soc. 79 (**2020**).
17. Bowen K. J., Harris W. S., Kris-Etherton P. M. *"Omega-3 Fatty Acids and Cardiovascular Disease: Are There Benefits?"* Curr Treat Options Cardiovasc Med. **(2016)**.
18. Brogaard L., Larsen L. E., Heegaard P. M. H., Anthon C., Gorodkin J., Dürrwald R., Skovgaard K. *"IFN-λ and microRNAs are important modulators of the pulmonary innate immune response against influenza A (H1N2) infection in pigs."* PLoS One. **(2018)**; 13(4).
19. Brown J., Pirrung M., McCue L. A. *"FQC Dashboard: integrates FastQC results into a web-based, interactive, and extensible FASTQ quality control tool."* Bioinformatics. (**2017**); 19:3137-3139.
20. Burgess T. A., Robich M. P., Chu L. M., Bianchi C., Sellke F. W. *"Improving glucose metabolism with resveratrol in a swine model of metabolic syndrome through alteration of signaling pathways in the liver and skeletal muscle.*" Archives of Surgery. (**2011**); 146:556–564.
21. Caiyan Ma Z., Heng L. *"Low n-6/n-3 PUFA ratio improves inflammation and myocardial ischemic reperfusion injury."* Biochem Cell Biol. (**2019**) 97:621–9.

22. Carrington J. C., Ambros V. *"Role of microRNAs in plant and animal development."* Science. (**2003**); 301:336–338.
23. Caterina, R.De. "*n–3 fatty acids in cardiovascular disease."* N. Engl. J. Med. (**2011**)
24. Cavaillé J. *"Box C/D small nucleolar RNA genes and the Prader-Willi syndrome: a complex interplay."* Wiley Interdiscip Rev RNA. **(2017)**.
25. Chen X., Che D., Zhang P., Li X., Yuan Q., Liu T., Guo J., Feng T., Wu L., Liao M., He Z., Zeng W. *"Profiling of miRNAs in porcine germ cells during spermatogenesis."* Reproduction. **(2017)**; 154(6):789-798
26. Christine E., Scott D., Murray S. F., et al. "*miR-122 regulation of lipid metabolism revealed by in vivo antisense targeting."* Cell Metab. (**2006**); 3:87–98.
27. Corino C., Di Giancamillo A., Rossi R., Domeneghini C. *"Dietary conjugated linoleic acid affects morphofunctional and chemical aspects of subcutaneous adipose tissue in heavy pigs."* J Nutr. (**2005**) 135:1444–1450.
28. Couet C., Delarue J., Ritz P., Antoine J. M., Lamisse F. *"Effect of dietary fish oil on body fat mass and basal oxidation in healthy adults."* Inter J Obesity. (**1997**) 21:637–43.
29. Córdoba S., Balcells I., Castelló A., Ovilo C., Noguera J. L., Timoneda O., Sánchez A. *"Endometrial gene expression profile of pregnant sows with extreme phenotypes for reproductive efficiency."* Sci Rep. **(2015)**; 5:14416.
30. Dabadie, H., Peuchant, E., Bernard, M., Leruyet, P., Mendy, F. "*Moderate intake of myristic acid in sn-2 position has beneficial lipidic effects and enhances DHA of cholesteryl esters in an interventional study."* J. Nutr. Biochem. 16. (**2005**)
31. Davoli R., Gaffo E., Zappaterra M., Bortoluzzi S., Zambonelli P. *"Identification of differentially expressed small RNAs and prediction of target genes in Italian Large White pigs with divergent backfat deposition."* Anim Genet. **(2018)**; 49(3):205-214.
32. Dayrit, F.M. "*The properties of lauric acid and their significance in coconut oil*." J. Am. Oil Chem. Soc. 92 (**2015**).
33. Daza K. R., Steibel J. P., Velez-Irizarry D., Raney N. E., Bates R. O., Ernst C. W. *"Profiling and characterization of a longissimus dorsi muscle microRNA dataset from an F2 Duroc × Pietrain pig resource population."* Genom Data. **(2017)**; 13:50-53.
34. De Groote D., Van Belleghem K., Devire J., Van Brussel W., Mukaneza A., Amininejad L. *"Effect of the intake of resveratrol, resveratrol phosphate, and catechin-rich grape seed extract on markers of oxidative stress and gene expression in adult obese subjects."* Ann Nutr Metab. (**2012**);61: 15–24.

35. Ding H., Liu M., Zhou C., You X., Su T., Yang Y., Xu D. *"Integrated analysis of miRNA and mRNA expression profiles in testes of Duroc and Meishan boars."* BMC Genomics. **(2020)**; 21(1):686.
36. Ding Y., Hu Q., Gan J., Zang X., Gu T., Wu Z., Cai G., Hong L. *"Effect of miR-143-3p from Extracellular Vesicles of Porcine Uterine Luminal Fluid on Porcine Trophoblast Cells."* Animals (Basel). **(2022)**.
37. Doreau, M., Chilliard, Y. "*Digestion and metabolism of dietary fat in farm animals."* Br. J. Nutr. (**1997);** 78
38. Duran-Montgé P., Theil P. K., Lauridsen C., Esteve-Garcia E. *"Fat metabolism is regulated by altered gene expression of lipogenic enzymes and regulatory factors in liver and adipose tissue but not in semimembranosus muscle of pigs during the fattening period.*" Animal. (**2009**); 3:1580–1590.
39. Ebrahimi M., Rajion M. A., Jafari S., Jahromi M. F., Oskoueian E., Qurni Sazili A., *"Effects of dietary n-6: n-3 polyunsaturated fatty acid ratios on meat quality, carcass characteristics, tissue fatty acid profiles, and expression of lipogenic genes in growing goats."* Plos One. (**2018**).
40. Elmadfa, M. Kornsteiner. "*Dietary fat intake - a global perspective*" Ann. Nutr. Metab. (**2009**).
41. Esau C., Davis S., Murray S. F., Yu X. X., Pandey S. K., et al. "*miR-122 regulation of lipid metabolism revealed by in vivo antisense targeting."* Cell Metab. (**2006**); 3:87–98.
42. Eshak, E. S., Yamagishi K., and H. Iso. *"Dietary fat and risk of cardiovascular disease."*. Encyclopedia of Cardiovascular Research and Medicine (**2018**); 60-89.
43. Eun Kyung L., Jeong L. M., Kotb A., et al. "*miR-130 suppresses adipogenesis by inhibiting peroxisome proliferator-activated receptor gamma expression".* Mol Cell Biol. (**2011**); 31:626–38.
44. Falaleeva M., Pages A., Matuszek Z., Hidmi S., Agranat-Tamir L., Korotkov K., Nevo Y., Eyras E., Sperling R., Stamm S. *"Dual function of C/D box small nucleolar RNAs in rRNA modification and alternative pre-mRNA splicing."* Proc Natl Acad Sci U S A. **(2016)**.
45. Fam B. C., Joannides C. N., Andrikopoulos S. *"The liver: Key in regulating appetite and body weight. Adipocyte.*" (**2012**); 1:259–264.
46. Fanalli, S. L., da Silva, B. P. M., Petry, B., Santana, M. H. D. A., Polizel, G. H. G., Antunes, R. C., Cesar, A. S. "*Dietary fatty acids applied to pig production and their relation to the biological processes: A review.*" Livestock Science, (**2022**); 265

47. Feng H., Yousuf S., Liu T., Zhang X., Huang W., Li A., Xie L., Miao X. *"Global miRNA, lncRNA, and mRNA Transcriptome Profiling of Endometrial Epithelial Cells Reveals Genes Related to Porcine Reproductive Failure Caused by Porcine Reproductive and Respiratory Syndrome Virus."* Sci Rep. **(2022)**; 12(1):16542.
48. Fiesel A., Gessner D. K., Most E., Eder K. *"Effects of dietary polyphenol-rich plant products from grape or hop on pro-inflammatory gene expression in the intestine, nutrient digestibility and faecal microbiota of weaned pigs."* BMC Vet Res. (**2014**);10: 196.
49. Fitz N. F., Wang J., Kamboh M. I., Koldamova R., Lefterov I. *"Small nucleolar RNAs in plasma extracellular vesicles and their discriminatory power as diagnostic biomarkers of Alzheimer's disease."* Neurobiol Dis. **(2021)**.
50. Fleming D. S., Miller L. C. *"Differentially Expressed MiRNAs and tRNA Genes Affect Host Homeostasis During Highly Pathogenic Porcine Reproductive and Respiratory Syndrome Virus Infections in Young Pigs."* Front Genet. **(2019)**; 10:691
51. Frayn K.N., Arner P., Yki-Järvinen H. "*Fatty acid metabolism in adipose tissue, muscle and liver in health and disease.*" Essays in Biochemistry. (**2006**); 42:89–103.
52. Friedlander M. R., Mackowiak S. D., Li N., Chen W., Rajewsky N. *"miRDeep2 accurately identifies known and hundreds of novel microRNA genes in seven animal clades"* Nucleic Acids Research (**2012**); 40:37-52.
53. Gan M., Shen L., Fan Y., Tan Y., Liu L., Chen L., Zhao Y., Niu L., Tang G., Li Q., Xu X., Zhang T., Li X., Zhang S., Zhu L. *"ssc-miR-451 Regulates Porcine Primary Adipocyte Differentiation by Targeting ACACA."* Animals (Basel). **(2020)**.
54. Gao Q. X., Song D. J., Jin L. *"Effect of dietary n-6/n-3 polyunsaturated fatty acid ratio on animal health and product quality."* Chinese J Anim Nutr. (**2013**) 25:1429–36.
55. Gao X., Yang Q., Zhang S., Huang X., Yan Z., Wang P., Gun S. *"LncRNA ALDB-898 modulates intestinal epithelial cell damage caused by Clostridium perfringens type C in piglet by regulating ssc-miR-122-5p/OCLN signaling."* Mol Immunol. **(2022)**.
56. Gessner D. K., Bonarius M., Most E., Fiesel A., Eder K. *"Effects of polyphenol-rich plant products from grape or hop as feed supplements on the expression of inflammatory, antioxidative, cytoprotective and endoplasmic reticulum stress-related genes and the antioxidative status in the liver of piglets."* J Anim Physiol Anim Nutr. (**2017**);101: e185–e194.
57. Gòdia M., Reverter A., González-Prendes R., Ramayo-Caldas Y., Castelló A., Rodríguez-Gil J. E., Sánchez A., Clop A. *"A systems biology framework integrating*

GWAS and RNA-seq to shed light on the molecular basis of sperm quality in swine." Genet Sel Evol. **(2020)**; 52(1):72

58. Grenier B., Hackl M., Skalicky S., Thamhesl M., Moll W. D., Berrios R., Schatzmayr G., Nagl V. *"MicroRNAs in porcine uterus and serum are affected by zearalenone and represent a new target for mycotoxin biomarker discovery."* Sci Rep. **(2019)**.
59. Grifith-Jones S., Saini H. K., van Dongen S., Enright A. J., *"miRBase: tools for microRNA genomics."* Nucleic Acids Research (**2007**); 36: D154-D158.
60. Herrera-Uribe J., Zaldívar-López S., Aguilar C., Entrenas-García C., Bautista R., Claros M. G., Garrido J.J. *"Study of microRNA expression in Salmonella Typhimurium-infected porcine ileum reveals miR-194a-5p as an important regulator of the TLR4-mediated inflammatory response."* Vet. Res. (**2022**).
61. Hill J. O., Peters J. C., Lin D., Yakubu F., Greene H., Swift L. *"Lipid accumulation and body fat distribution is influenced by type of dietary fat fed to rats."* Inter J Obesity. (**1993**) 17:223–6.
62. Horvath S., Dong J. *"Geometric Interpretation of Gene Coexpression Network Analysis"* PLoS Computational Biology (**2008**); 4.
63. Horvath S., Zhang B., Carlson M., Lu K., Zhu S., Felciano R., Laurance M., Zhao W., Shu Q., Lee Y., Scheck A., Liau L., Wu H., Geschwind D., Febbo P., Kornblum H., Cloughesy T., Nelson S., Mischel P. *"Analysis of Oncogenic Signaling Networks in Glioblastoma Identifies ASPM as a Novel Molecular Target."* Proc Natl Acad Sci (**2006**); 103:17402–17407.
64. Hou X., Tang Z., Liu H., Wang N., Ju H., Li K. *"Discovery of MicroRNAs associated with myogenesis by deep sequencing of serial developmental skeletal muscles in pigs."* PLoS One. **(2012)**; 7(12):e52123.
65. Houpt K. A., Houpt T. R., Pond W. G. *"The pig as a model for the study of obesity and of control of food intake: a review."* The Yale journal of biology and medicine. (**1979**); 52:307.
66. Hu M., Kuang R., Guo Y., Ma R., Hou Y., Xu Y., Qi X., Wang D., Zhou H., Xiong Y., et al. *"Epigenomics analysis of miRNA cis-regulatory elements in pig muscle and fat tissues."* Genomics. (**2022**).
67. Hua R., Wang Y., Lian W., Li W., Xi Y., Xue S., Kang T., Lei M. *"Small RNA-seq analysis of extracellular vesicles from porcine uterine flushing fluids during peri-implantation."* Gene. **(2021)**; 766:145117.

68. Hua R., Zhang X., Li W., Lian W., Liu Q., Gao D., Wang Y., Lei M. *"Ssc-miR-21-5p regulates endometrial epithelial cell proliferation, apoptosis and migration via the PDCD4/AKT pathway."* J Cell Sci. **(2020)**.

69. Huang J. C., et al. *"Using expression profiling data to identify human microRNA targets."* Nature methods. (**2007**); 4:1045–1049.

70. Huang T., Huang X., Chen W., Yin J., Shi B., Wang F., Feng W., Yao M. *"MicroRNA responses associated with Salmonella enterica serovar typhimurium challenge in peripheral blood: effects of miR-146a and IFN-γ in regulation of fecal bacteria shedding counts in pig."* BMC Vet Res. **(2019)**; 15(1):195

71. Hussain T., Tan B., Yin Y., Blachier F., Tossou M.C.B. and Rahu N. *"Oxidative stress and inflammation: what polyphenols can do for us?"* Oxid Med Cell Lon. (**2016**).

72. Ito M., Adachi-Akahane S. "*Inter-organ communication in the regulation of lipid metabolism: focusing on the network between the liver, intestine, and heart.*" Journal of Pharmacological Sciences. (**2013**);123(4):312–317

73. Jacometo C. B., Schmitt E., Pfeifer L. F., Schneider A., Bado F., da Rosa F. T., Halfen S., Del Pino F. A., Loor J. J., Corrêa M. N., Dionello N. J. *"Linoleic and α-linolenic fatty acid consumption over three generations exert cumulative regulation of hepatic expression of genes related to lipid metabolism."* Genes Nutr. **(2014)**.

74. Jang H. J., Lee S. I. *"MicroRNA expression profiling during the suckling-to-weaning transition in pigs."* J Anim Sci Technol. **(2021)**; 63(4):854-863.

75. Jia C., Kong X., Koltes J. E., Gou X., Yang S., Yan D., Lu S., Wei Z. "*Gene Co-Expression Network Analysis Unraveling Transcriptional Regulation of High-Altitude Adaptation of Tibetan Pig."* PLoS One. (**2016**).

76. Jiang A., Yin D., Zhang L., Li B, Li R, Zhang X, Zhang Z, Liu H, Kim K, Wu W. *"Parsing the microRNA genetics basis regulating skeletal muscle fiber types and meat quality traits in pigs."* Anim Genet. **(2021)**; 52(3):292-303.

77. Jiang Z. Y., Zhong W. J., Zheng C. T., Yang L., Jiang S. Q. *"Conjugated linoleic acid differentially regulates fat deposition in back fat and longissimus muscle of finishing pigs."* J Anim Sci. (**2010**) 88:1694–1705.

78. Jiao Y., Huang B., Chen Y., Hong G., Xu J., Hu C., Wang C. *"Integrated Analyses Reveal Overexpressed Notch1 Promoting Porcine Satellite Cells' Proliferation through Regulating the Cell Cycle."* Int J Mol Sci. **(2018)**.

79. Juarez M.; Dugan M. E. R.; Aldai N.; Aalhus J. L.; Patience J. F.; Zijlstra R. T.; Beaulieu A. D. *"Feeding co-extruded flaxseed to pigs: Effect of duration and feeding level on*

growth performance and back fat fatty acid composition of grower-finisher pigs." Meat Sci. (**2010**), 84, 578–584.

80. Jump D. B., Lytle K. A., Depner C. M., Tripathy S. *"Omega-3 polyunsaturated fatty acids as a treatment strategy for nonalcoholic fatty liver disease."* Pharmacol Ther. **(2018)**.
81. Kaczmarek M. M., Reliszko Z. P., Szuszkiewicz J., Nitkiewicz A., Guzewska M. M., Myszczynski K., Romaniewicz M., Sikora M., Kajko M., Heifetz Y. *"Profiling circulating microRNAs in the serum of pregnant and non-pregnant pigs reveals a plethora of reproductive status-dependent microRNAs."* Animal. **(2021)**; 15(4):100182.
82. Kawęcka M., Jacyno E., Matysiak B., Kołodziej-Skalska A., Pietruszka A. *"Effects of selenium and vitamin E supplementation on selenium distribution and meat quality of pigs."* Acta Agric Scand (**2013**);63: 194–200.
83. Kim Y. A., Keogh J. B., Clifton P. M. "*Polyphenols and glycémie control."* Nutrients. (**2016**);8.
84. Kiss A., Heber S., Kramer A. M., Hackl M., Skalicky S., Hallström S., Podesser B. K., Santer D. *"MicroRNA Expression Profile Changes after Cardiopulmonary Bypass and Ischemia/Reperfusion-Injury in a Porcine Model of Cardioplegic Arrest."* Diagnostics (Basel). **(2020)**; 10(4):240.
85. Kozomara A., Grifith-Jones S. *"miRBase: integrating microRNA annotation and deep-sequencing data"* Nucleic Acids Research. (**2010**); 39: D152-D157.
86. Lahučký R., Bahelka I., Novotná K.& Vašíčková K. *"Effects of dietary vitamin E and vitamin C supplementation on the level of α-tocopherol and L-ascorbic acid in muscle and on the antioxidative status and meat quality of pigs."* Czech J Anim Sci. (**2005**);50: 175–184.
87. Langfelder P., Horvath S. *"WGCNA: an R package for weighted correlation network analysis"* BMC Bioinformatics (**2008**); 9.
88. Levental K. R., Malmberg E., Symons J. L., Fan Y. Y., Chapkin R. S., Ernst R., Levental I. *"Lipidomic and biophysical homeostasis of mammalian membranes counteracts dietary lipid perturbations to maintain cellular fitness."* Nat Commun. **(2020);** 11(1):1339.
89. Levental K. R., Surma M. A., Skinkle A. D., Lorent J. H., Zhou Y., Klose C., Chang J. T., Hancock J. F., Levental I. *"ω-3 polyunsaturated fatty acids direct differentiation of the membrane phenotype in mesenchymal stem cells to potentiate osteogenesis."* Sci Adv. **(2017)**.

90. Li A., Li Y., Song T., Wang F., Liu D., Fan Z., Cheng S., Zhang C., Wang J., He J., Wang S. *"Identification of differential microRNA expression during tooth morphogenesis in the heterodont dentition of miniature pigs, SusScrofa."* BMC Dev Biol. **(2015)**; 15:51
91. Li C., Sun Y., Jiang C., Cao H., Zeng W., Zhang X., Li Z., He Q. *"Porcine circovirus type 2 infection activates NF-κB pathway and cellular inflammatory responses through circPDCD4/miR-21/PDCD4 axis in porcine kidney 15 cell."* Virus Res. **(2021)**.
92. Li H., Chen X., Guan L., Qi Q., Shu G., Jiang Q., Yuan L., Xi Q., Zhang Y. *"MiRNA-181a regulates adipogenesis by targeting tumor necrosis factor-α (TNF-α) in the porcine model."* Plos One. (**2013**).
93. Li H., Zhang M., Zheng E. *"Comprehensive miRNA expression profiles in the ilea of Lawsonia intracellularis-infected pigs."* J Vet Med Sci. **(2017)**; 79(2):282-289
94. Li R., Sun Q., Jia Y., Cong R., Ni Y., Yang X., Jiang Z., Zhao R. *"Coordinated miRNA/mRNA Expression Profiles for Understanding Breed-Specific Metabolic Characters of Liver between Erhualian and Large White Pigs."* Plos One. (**2012**); 7:2778–2802.
95. Li S., Yang J., Wang L., Du F., Zhao J., Fang R. *"Expression profile of microRNAs in porcine alveolar macrophages after Toxoplasma gondii infection."* Parasit Vectors. **(2019)**; 12(1):65.
96. Li W., Xi Y., Xue S., Wang Y., Wu L., Liu H., Lei M. *"Sequence analysis of microRNAs during pre-implantation between Meishan and Yorkshire pigs."* Gene. **(2018)**.
97. Li Z., Fuscoe J. C., Chen T. "*MicroRNAs and their predicted target messenger RNAs are deregulated by exposure to a carcinogenic dose of comfrey in rat liver.*" Environ Mol Mutagen. (**2011**); 52:469–478.
98. Lian C., Sun B., Niu S., Yang R., Liu B., Lu C., Meng J., Qiu Z., Zhang L., Zhao Z. *"A comparative profile of the microRNA transcriptome in immature and mature porcine testes using Solexa deep sequencing."* FEBS J. **(2012)** ;279(6):964-75
99. Liang Y., Wang Y., Ma L., Zhong Z., Yang X., Tao X., Chen X., He Z., Yang Y., Zeng K., Kang R., Gong J., Ying S., Lei Y., Pang J., Lv X., Gu Y. *"Comparison of microRNAs in adipose and muscle tissue from seven indigenous Chinese breeds and Yorkshire pigs."* Anim Genet. **(2019)**.
100. Liao M., Ren Z., Miao Y. *"Identification of Differentially Expressed miRNAs in Porcine Adipose Tissues and Evaluation of Their Effects on Feed Efficiency."* Genes (Basel). **(2022)**.

101. Lin C. R., Chu T. M., Luo A., Huang S. J., Chou H. Y., Lu M. W., Wu J. L. *"Omega-3 polyunsaturated fatty acids suppress metastatic features of human cholangiocarcinoma cells by suppressing twist."* J Nutr Biochem. **(2019)**; 74:108245.
102. Lipiński K., Mazur M., Antoszkiewicz Z., Purwin C. *"Polyphenols in monogastric nutrition—A review."* Ann Anim Sci. (**2017**);17: 41–58.
103. Liu F., Cottrell J. J., Furness J. B., Rivera L. R., Kelly F. W., Wijesiriwardana U., et al. *"Selenium and vitamin E together improve intestinal epithelial barrier function and alleviate oxidative stress in heat-stressed pigs."* Exp Physiol. (**2016**);101: 801–810.
104. Liu W., Wang X. *"Prediction of functional microRNA targets by integrative modeling of microRNA binding and target expression data"* Genome Biology (**2019**); 20.
105. Liu Z., Xie Y., Guo J., Su X., Zhao C., Zhang C., Qin Q., Dai D., Tuo Y., Li Z., Wu D., Li J. *"Comparison of porcine milk microRNA expression in milk exosomes versus whole swine milk and prediction of target genes."* Arch Anim Breed. **(2022)**; 65(1):37-46.
106. Lo L., McLaren D., McKeith F., Fernando R., Novakofski J. *"Genetic analyses of growth, real-time ultrasound, carcass, and pork quality traits in Duroc and Landrace pigs: II. Heritabilities and correlations."* Journal of animal science. (**1992**); 70:2387–2396.
107. Lonergan S. M., Huff-Lonergan E., Rowe L. J., Kuhlers D. L., Jungst S. B. *"Selection for lean growth efficiency in Duroc pigs influences pork quality."* J Anim Sci. (**2001**); 2075-85.
108. Love M. I., Huber W., Anders S., *"Moderated estimation of fold change and dispersion for RNA-seq data with DESeq2"* Genome Biology (**2014**); 15.
109. Lund A. H. *"miR-10 in development and cancer."* Cell Death Differ. (**2010**); 17:209–214.
110. Lunney, J.K. *"Advances in swine biomedical model genomics."* Int. J. Biol. Sci. (**2007**)
111. M.H. Moghadasian, F. Shahidi. "*Fatty Acids"*. Int. Encycl. Public Heal. (**2017**); 114-122.
112. Mármol-Sánchez E., Ramayo-Caldas Y., Quintanilla R., Cardoso T. F., González-Prendes R., Tibau J., Amills M. *"Co-expression network analysis predicts a key role of microRNAs in the adaptation of the porcine skeletal muscle to nutrient supply."* J Anim Sci Biotechnol. **(2020)**.
113. McDaneld T. G., Smith T. P., Doumit M. E., Miles J. R., Coutinho L. L., et al. *"MicroRNA transcriptome profiles during swine skeletal muscle development."* BMC Genomics. (**2009**); 10:77.

114. McKenna L. B., Schug J., Vourekas A., McKenna J. B., Bramswig N. C., et al. *"MicroRNAs control intestinal epithelial differentiation, architecture, and barrier function."* Gastroenterology (**2010**); 139: 1654–1664.
115. Meng S. X., Yi-Yang H. U., Feng Q. *"Application of microRNA in prevention and treatment of nonalcoholic fatty liver disease with traditional Chinese medicine."* Chin J Tradit Chin Med Pharm. (**2014**); 29:806–9.
116. Michelle A., Mary S., Chick J. M., Galuppo B. T., Feldstein A. E, Bridget P. "Low ω-6 to ω-3 PUFA Ratio (n-6:n-3 PUFA) diet to treat fatty liver disease in obese youth." J Nutrition. (**2020**) 150:2314–21.
117. Mirmiran P., Hosseinpour-Niazi S., Naderi Z, Bahadoran Z., Sadeghi M., Azizi F. "*Association between interaction and ratio of ω-3 and ω-6 polyunsaturated fatty acid and the metabolic syndrome in adults."* Nutrition. **(2012)**.
118. Molfino A., Amabile M. I., Monti M., Muscaritoli M. *"Omega-3 Polyunsaturated Fatty Acids in Critical Illness: Anti-Inflammatory, Proresolving, or Both?"* Oxid Med Cell Longev. **(2017)**; 5987082.
119. Monsma, C.C., Ney, D.M. *"Interrelationship of stearic acid content and triacylglycerol composition of lard, beef tallow and cocoa butter in rats.".* Lipids 28. (**1993**).
120. Morel P. C. H., Leong J., Nuijten W. G. M., Purchas R. W., Wilkinson B. H. P. *"Effect of lipid type on growth performance, meat quality and the content of long chain n − 3 fatty acids in pork meat."* Meat Sci. (**2013**); 95: 151–159.
121. Muñoz M., García-Casco J. M., Caraballo C., Fernández-Barroso M. A., Sánchez-Esquiliche F., Gómez F., et al. *"Identification of candidate genes and regulatory factors underlying intramuscular fat content through longissimus dorsi transcriptome analyses in heavy Iberian pigs."* Front Genet. (2018).
122. Muñoz R., Estany J., Tor M., Doran O. *"Hepatic lipogenic enzyme expression in pigs is affected by selection for decreased backfat thickness at constant intramuscular fat content."* Meat science. (**2013**); 93:746–751.
123. Nakanishi N. *"The up-regulation of microRNA-335 is associated with lipid metabolism in liver and white adipose tissue of genetically obese mice."* Biochemical and Biophysical Research Communications. (**2009**); 385:492.
124. Newman R. E., Bryden W. L., Fleck E., Ashes J. R., Buttemer W. A., Storlien L. H. *"Dietary n-3 and n-6 fatty acids alter avian metabolism: metabolism and abdominal fat deposition."* Bri J Nutr. (**2002**) 88:11

125. Niculita P., Popa M. E., Ghidurus M., Turtoi M. *"Effect of vitamin e in swine diet on animal growth performance and meat quality parameters."* Polish J Food Nutr Sci. (**2007**);57: 125–130.
126. Nürnberg K.; Nürnberg G.; Priepke A.; Dannenberger D. *"Sea buckthorn pomace supplementation in the finishing diets of pigs - are there effects on meat quality and muscle fatty acids?"*. Arch. Anim. Breed. (**2015**), 58, 107–113.
127. Oczkowicz M., Pawlina-Tyszko K., Świątkiewicz M., Szmatoła T. *"Feeding pigs with coconut oil affects their adipose miRNA profile."* Mol Biol Rep. **(2022)**; 49(7):6919-6929.
128. Oczkowicz M., Świątkiewicz M., Ropka-Molik K., Gurgul A., Żukowski K. *"Effects of different sources of fat in the diet of pigs on the liver transcriptome estimated by RNA-seq."* Ann of Anim Sci. (**2016**);16: 1073–1090.
129. Ogłuszka M., Szostak A., Te Pas M. F. W., Poławska E., Urbański P., Blicharski T., Pareek C. S., Juszczuk-Kubiak E., Dunkelberger J. R., Horbańczuk J. O., Pierzchała M. *"A porcine gluteus medius muscle genome-wide transcriptome analysis: dietary effects of omega-6 and omega-3 fatty acids on biological mechanisms."* Genes Nutr. **(2017);** 31.
130. Oh D. Y., Talukdar S., Bae E. J., Imamura T., Morinaga H., Fan W. Q., et al. *"GPR120 Is an Omega-3 Fatty Acid Receptor Mediating Potent Anti-inflammatory and Insulin-Sensitizing Effects."* Cell. 2010;142: 687–698.
131. Pan, Z., Yao, Y., Yin, H., Cai, Z., Wang, Y., Bai, L., Kern, C., Halstead, M., Chanthavixay, G., Nares, T., Wimmers, K., Sahana, G., Su, G., Lund, M.S., Fredholm, M., Karlskov-Mortensen, P., Ernst, C.W., Ross, P., Tuggle, C.K., Fang, L., Zhou, H., *"Pig genome functional annotation enhances the biological interpretation of complex traits and human disease."* Nat. Commun. (**2021**); 12
132. Panov A., Orynbayeva Z., Vavilin V., Lyakhovich V. "*Fatty acids in energy metabolism of the central nervous system."* BioMed Research International. (**2014**)
133. Peng Y., Xiang H., Chen C., et al. "*MiR-224 impairs adipocyte early differentiation and regulates fatty acid metabolism."* Int J Biochem Cell B. (**2013**); 45:1585–93.
134. Petrovic, S., Arsic, A. "*Fatty acids: fatty acids*". Encyclopedia of Food and Health (**2016**); 623–631.
135. Pieszka M., Szczurek P., Bederska-Łojewska D., Migdał W., Pieszka M., Gogol P., et al. *"The effect of dietary supplementation with dried fruit and vegetable pomaces on*

production parameters and meat quality in fattening pigs." Meat Sci. (**2017**);126: 1–10.

136. Qianqian Z., Wei X., Chuang L., Zhenliang C., Qiaoli W., Mingzhi L., Longyan W., Rui B., Jianhui T., Junjie L., Shiqiao W. *"MicroRNAs are potential regulators of the timed artificial insemination effect in gilt endometrium."* Anim Reprod Sci. **(2021)**; 233:106837
137. Qun L., Zhanguo G., Alarcon R. M., Jianping Y., Zhong Y. "*A role of miR-27 in the regulation of adipogenesis."* FEBS J. (**2009**); 276:2348–58.
138. Rauw W., Kanis E., Noordhuizen-Stassen E., Grommers F. *"Undesirable side effects of selection for high production efficiency in farm animals: a review."* Livestock Production Science. (**1998**); 56:15–33.
139. Realini C. E.; Duran-Montge P.; Lizardo R.; Gispert M.; Oliver M. A.; Esteve-Garcia E. *"Effect of source of dietary fat on pig performance, carcass characteristics and carcass fat content, distribution and fatty acid composition."* Meat Sci. (**2010**), 85, 606–612.
140. Schmid A., Collomb M., Sieber R., Bee G. *"Conjugated linoleic acid in meat and meat products: A review."* Meat Sci. (**2006**) 73:29–41.
141. Schook, L.B., Collares, T.V., Darfour-Oduro, K.A., De, A.K., Rund, L.A., Schachtschneider, K.M., Seixas, F.K. *"Unraveling the swine genome: implications for human health."* Annu. Rev. Anim. Biosci. (**2015**); 3
142. Segura-Wang M., Grenier B., Ilic S., Ruczizka U., Dippel M., Bünger M., Hackl M. *"MicroRNA Expression Profiling in Porcine Liver, Jejunum and Serum upon Dietary DON Exposure Reveals Candidate Toxicity Biomarkers."* Nagl V.Int J Mol Sci. **(2021)**; 22(21):12043.
143. Segura-Wang M., Grenier B., Ilic S., Ruczizka U., Dippel M., Bünger M., Hackl M., Nagl V. *"MicroRNA Expression Profiling in Porcine Liver, Jejunum and Serum upon Dietary DON Exposure Reveals Candidate Toxicity Biomarkers."* Int J Mol Sci. **(2021)**.
144. Sharda T., Kalpana G. "*miR-122 is a unique molecule with great potential in diagnosis, prognosis of liver disease, and therapy both as miRNA mimic and antimir.*" Curr Gene Ther. (**2015**); 15:142–50.
145. Shen L., Gan M., Chen L., Zhao Y., Niu L., Tang G., Jiang Y., Zhang T., Zhang S., Zhu L. *"miR-152 targets pyruvate kinase to regulate the glycolytic activity of pig skeletal muscles and affects pork quality."* Meat Sci. (**2022**);185

146. Shivdasani R. A. *"MicroRNAs: regulators of gene expression and cell differentiation."* Blood. (**2006**); 108:3646–3653.
147. Shrestha N., Holland O. J., Kent N. L., Perkins A. V., McAinch A. J., Cuffe J. S. M., Hryciw D. H. *"Maternal High Linoleic Acid Alters Placental Fatty Acid Composition."* Nutrients. **(2020)**; 23.
148. Simopoulos A. P. *"An Increase in the Omega-6/Omega-3 Fatty Acid Ratio Increases the Risk for Obesity."* Nutrients. **(2016)**.
149. Simopoulos A.P. "*n-3 fatty acids and human health: defining strategies for public policy*." Lipids. (**2001**); 36.
150. Skugor A.; Kjos N. P.; Sundaram A. Y. M.; Mydland L. T.; Ånestad R.; Tauson A. H.; Overland M. *"Effects of long-term feeding of rapeseed meal on skeletal muscle transcriptome, production efficiency and meat quality traits in Norwegian Landrace growing-finishing pigs."* PLoS One (**2019**), 14
151. Sobol M., Skiba G., Raj S. *"Effect of n-3 polyunsaturated fatty acid intake on its deposition in the body of growing-finishing pigs."* Anim Feed Sci and Tech. (**2015**) 208:107–18.
152. Soneson C., Love M. I., Robinson M. I., *"Differential analyses for RNA-seq: transcript-level estimates improve gene-level inferences"* F1000Res. (**2015**); 4.
153. Song J., Sun H., Sun H., Jiang Z., Zhu J., Wang C., Gao W., Wang T., Pu J., Sun Y., Yuan H. Y., Liu J. *"Swine MicroRNAs ssc-miR-221-3p and ssc-miR-222 Restrict the Cross-Species Infection of Avian Influenza Virus."* J Virol. **(2020)**; 94(23):e01700-20.
154. Souza C. S., Moreira J. A., Silva N.R., Marinho A.L., Costa C.V.S., Souza J.G., Teixeira E.N.M., Aguiar E.M. *"Enrichment diets of pigs with oil blends and its effects on performance, carcass characteristics and fatty acid profile."* Arq. Bras. Med. Vet. e Zootec., (**2020**); 72
155. Sperling R. *"Small non-coding RNA within the endogenous spliceosome and alternative splicing regulation."* Biochim Biophys Acta Gene Regul Mech. **(2019)**.
156. Stachowiak M., Flisikowska T., Bauersachs S., Perleberg C., Pausch H., Switonski M., Kind A., Saur D., Schnieke A., Flisikowski K. *"Altered microRNA profiles during early colon adenoma progression in a porcine model of familial adenomatous polyposis."* Oncotarget. **(2017)**; 8(56):96154-96160
157. Su Q., Li L., Zhao J., Sun Y., Yang H. *"MiRNA Expression Profile of the Myocardial Tissue of Pigs with Coronary Microembolization."* Cell Physiol Biochem. **(2017)**.

158. Sun J., Zhao Y., He J., Zhou Q., El-Ashram S., Yuan S., Chi S., Qin J., Huang Z., Ye M., Huang S., Li Z. *"Small RNA expression patterns in seminal plasma exosomes isolated from semen containing spermatozoa with cytoplasmic droplets versus regular exosomes in boar semen."* Theriogenology. **(2021)**; 176:233-243.
159. Sun Z, Cai D, Yang X, Shang Y, Li X, Jia Y, Yin C, Zou H, Xu Y, Sun Q, Zhang X. *"Stress Response Simulated by Continuous Injection of ACTH Attenuates Lipopolysaccharide-Induced Inflammation in Porcine Adrenal Gland."* Front Vet Sci. **(2020)**; 7:315.
160. Swain T., Deaver C.M., Lewandowski A., Myers M. J. *"Lipopolysaccharide (LPS) induced inflammatory changes to differentially expressed miRNAs of the host inflammatory response."* Vet Immunol Immunopathol. (2021); 237:110267
161. Szostak A., Ogłuszka M., te Pas M. F. W., Poławska E., Urbański P., Juszczuk-Kubiak E., et al. *"Effect of a diet enriched with omega-6 and omega-3 fatty acids on the pig liver transcriptome."* Genes Nutr. (**2016**);11: 9.
162. Tang Q., Zhang Y., Yue L., Ren H., Pan C. *"Ssc-MiR-21-5p and Ssc-MiR-615 Regulates the Proliferation and Apoptosis of Leydig Cells by Targeting SOX5."* Cells. **(2022)**.
163. Tang, Z. et al. *"Integrated analysis of miRNA and mRNA paired expression profiling of prenatal skeletal muscle development in three genotype pigs."* Scientific reports 5 (**2015**).
164. Tao X., Liu S., Men X., Xu Z. *"Over-expression of miR-146b and its regulatory role in intestinal epithelial cell viability, proliferation, and apoptosis in piglets."* Biol Direct. **(2017)**; 12(1):27.
165. Tao X., Xu Z. *"MicroRNA transcriptome in swine small intestine during weaning stress."* PLoS One. **(2013)**; 8(11):e79343.
166. Terracciano A., Stephan Y., Sutin A. R. *"Omega-3 fatty acid: A promising pathway linking personality and health."* J Psychosom Res. **(2018)**.
167. Timoneda O., Balcells I., Córdoba S., Castelló A., Sánchez A. *"Determination of reference microRNAs for relative quantification in porcine tissues."* PLoS One. (2012); 7(9):e44413.
168. Timoneda O., Balcells I., Núñez J. I., Egea R., Vera G., Castelló A., Tomàs A., Sánchez A. *"miRNA expression profile analysis in kidney of different porcine breeds."* PLoS One. **(2013)**; 8(1):e55402.
169. Tretola M.; Maghin F.; Silacci P.; Ampuero S.; Bee G. *"Effect of Supplementing Hydrolysable Tannins to a Grower–Finisher Diet Containing Divergent PUFA Levels*

on Growth Performance, Boar Taint Levels in Back Fat and Intestinal Microbiota of Entire Males." Animals (**2019**), 9,

170. Truong A. D., Kang S., Dang H. V., Hong Y., Vu T. H., Heo J., Chu N. T., Nguyen H. T., Tran H. T. T., Hong Y. H. *"Small RNA sequencing and profiling of serum-derived exosomes from African swine fever virus-infected pigs."* J Anim Sci. **(2023)**.
171. Tummaruk P., Lundeheim N., Einarsson S., Dalin A. M. *"Effect of birth litter size, birth parity number, growth rate, backfat thickness and age at first mating of gilts on their reproductive performance as sows."* Animal Reproduction Science. (**2001**); 66:225–237.
172. Vidal O., Noguera J. L., Amills M., Varona L., Gil M., Jiménez N., Dávalos G., Folch J. M., Sánchez A. *"Identification of carcass and meat quality quantitative trait loci in a Landrace pig population selected for growth and leanness."* J Anim Sci. (**2005**); 293-300.
173. Wang H., Wang J., Sun S., Wang Y., Guo J., Ning C., Yang K., Liu J. F. *"Identification of reference microRNAs for quantitative expression analysis in porcine peripheral blood mononuclear cells treated with polyinosinic-polycytidylic acid."* Int J Immunogenet. **(2015)**; 42(3):217-225.
174. Wang K., Li W., Bai Y., Yang W., Ling Y., Fang M. *"ssc-miR-7134-3p regulates fat accumulation in castrated male pigs by targeting MARK4 gene."* Int J Biol Sci. **(2017)**; 13(2):189-197.
175. Wang L.-Y., Le F., Wang N., Li L., Liu X.-Z., Zheng Y.-M., et al. "*Alteration of fatty acid metabolism in the liver, adipose tissue, and testis of male mice conceived through assisted reproductive technologies: fatty acid metabolism in ART mice*." Lipids in Health and Disease. (**2013**);12(1):5
176. Wang Q., Sun Q., Wang J., Qiu X., Qi R., Huang J. *"Lactobacillus Plantarum 299v Changes miRNA Expression in the Intestines of Piglets and Leads to Downregulation of LITAF by Regulating ssc-miR-450a."* Probiotics Antimicrob Proteins. **(2021)**.
177. Wang T., Li M., Guan J., Li P., Wang H., Guo Y., Shuai S., Li X. *"MicroRNAs miR-27a and miR-143 regulate porcine adipocyte lipid metabolism."* International journal of molecular sciences. (**2011**); 12:7950–7959.
178. Wang Y., Zhou C., Meng F., Hu Q., Ding Y., Wang X., Gu T., Li Z., Wu Z., Hong L., Cai G. *"Ssc-miR-92b-3p Regulates Porcine Trophoblast Cell Proliferation and Migration via the PFKM Gene."* Int. J. Mol. Sci. **(2022)**; 23:16138.

179. WHO 2003. Diet*, "Nutrition and the Prevention of Report of a Joint WHO / FAO"* Expert Consultation; (**2003**); 1–149
180. Wood J. D., Richardson R. I., Nute G. R., Fisher A. V.., Campo M. M., Kasapidou E., et al. *"Effects of fatty acids on meat quality: A review."* Meat Sci. (**2004**);66: 21–32.
181. Wood, J.D., Enser, M., Fisher, A.V., Nute, G.R., Sheard, P.R., Richardson, R.I., Hughes, S. I., Whittington, F.M. "*Fat deposition, fatty acid composition and meat quality: a review."* Meat Sci. (**2008**) 78, 343–358.
182. Xie S. S., Huang T. H., Shen Y., Li X. Y., Zhang X. X., Zhu M. J., Qin H. Y., Zhao S. H. *"Identification and characterization of microRNAs from porcine skeletal muscle."* Anim Genet. **(2010)**; 41(2):179-90.
183. Xie S. S., Li X. Y., Liu T., Cao J. H., Zhong Q., et al. *"Discovery of porcine microRNAs in multiple tissues by a Solexa deep sequencing approach."* PLoS One. (**2011**);6
184. Xu L., Yuan H., Wang Z., Zhao S., Yang Y. *"Ssc-miR-141 Attenuates Hypoxia-Induced Alveolar Type II Epithelial Cell Injury in Tibetan Pigs by Targeting PDCD4."* Genes (Basel). **(2022).**
185. Xu Z., Xie Y., Zhou C., Hu Q., Gu T., Yang J., Zheng E., Huang S., Xu Z., Cai G., Liu D., Wu Z., Hong L. *"Expression Pattern of Seminal Plasma Extracellular Vesicle Small RNAs in Boar Semen."* Front Vet Sci. **(2020)**.
186. Yang Y, Li Y, Yuan H, Liu X, Ren Y, Gao C, Jiao T, Cai Y, Zhao S. *"Characterization of circRNA-miRNA-mRNA networks regulating oxygen utilization in type II alveolar epithelial cells of Tibetan pigs."* Front Mol Biosci. **(2022)**; 9:854250.
187. Ye L., Su X., Wu Z., Zheng X., Wang J., Zi C., Zhu G., Wu S., Bao W. *"Analysis of differential miRNA expression in the duodenum of Escherichia coli F18-sensitive and -resistant weaned piglets."* PLoS One. **(2012)**; 7(8):e43741
188. Yip A. M., Horvath S. *"Gene network interconnectedness and the generalized topological overlap measure"* BMC Bioinformatics (**2007**); 8.
189. Yu L. H. *"The study of influence for dietary n-6/n-3 fatty acid regulation of fatty metabolism and it's molecular mechanism in goose."* Yang Zhou University. (**2012**) 28–9.
190. Yue W., Wenlong Z., Min J., Fenghong H., Fangling D., Tongcheng X. *"Dietary low ratio of n-6/n-3 polyunsaturated fatty acids improve type 2 diabetes mellitus via activating brown adipose tissue in male mice."* J Food Sci. (**2021**) 3:1058–65.

191. Zanoaga O., Jurj A., Raduly L., Cojocneanu-Petric R., Fuentes-Mattei E., Wu O., Braicu C., Gherman C. D., Berindan-Neagoe I. *"Implications of dietary ω-3 and ω-6 polyunsaturated fatty acids in breast cancer."* Exp Ther Med. **(2018).**
192. Zárate R., El Jaber-Vazdekis N., Tejera N., Pérez J. A., Rodríguez C. *"Significance of long chain polyunsaturated fatty acids in human health."* Clin Transl Med. **(2017).**
193. Zhang B., Horvath S. *"A General Framework for Weighted Gene Co-Expression Network Analysis"* Statistical Application in Genetics and Molecular Biology (**2005**).
194. Zhang C., Luo J., Yu B., Zheng P., Huang Z., Mao X., et al. *"Dietary resveratrol supplementation improves meat quality of finishing pigs through changing muscle fiber characteristics and antioxidative status."* Meat Sci. (**2015**);102: 15–21.
195. Zhang H. Z., Chen D. W., He J., Zheng P., Yu J., Mao X. B., Huang Z. Q., Luo Y. H., Luo J. Q., Yu B. *"Long-term dietary resveratrol supplementation decreased serum lipids levels, improved intramuscular fat content, and changed the expression of several lipid metabolism-related miRNAs and genes in growing-finishing pigs"* J Anim Sci. **(2019)**; 97(4):1745-1756
196. Zhang J., Fu S. L., Liu Y., Liu Y. L., Wang W. J. *"Analysis of MicroRNA Expression Profiles in Weaned Pig Skeletal Muscle after Lipopolysaccharide Challenge."* Int J Mol Scie. **(2015);** 16(9):22438-22455.
197. Zhang J., Wang J., Ma C., Wang W., Wang H., Jiang Y. "*Comparative Transcriptomic Analysis of mRNAs, miRNAs and lncRNAs in the Longissimus dorsi Muscles between Fat-Type and Lean-Type Pigs."* Biomolecules. **(2022)**;12(9):1294
198. Zhang J., Xu X., Huang X., Zhu H., Chen H., Wang W., Liu Y. *"Analysis of microRNA expression profiles in porcine PBMCs after LPS stimulation."* Innate Immun. **(2020)**; 26(5):435-446
199. Zhang K., Ge L., Dong S., Liu Y., Wang D., Zhou C., Ma C., Wang Y., Su F., Jiang Y. *"Maternal low-protein diet induces gender-dependent changes in epigenetic regulation of the glucose-6-phosphatase gene in newborn piglet liver."* Front Immunol. **(2019)**; 4;10:1221.
200. Zhang P., Wang L., Li Y., Jiang P., Wang Y., Wang P., Kang L., Wang Y., Sun Y., Jiang Y. "*Identification and characterization of microRNA in the lung tissue of pigs with different susceptibilities to PCV2 infection."* Vet Res. **(2018)**.
201. Zhang R., Neuhoff C., Yang Q., Cinar M. U., Uddin M. J., Tholen E., Schellander K., Tesfaye D. *"Sulforaphane Enhanced Proliferation of Porcine Satellite Cells via Epigenetic Augmentation of SMAD7."* Animals (Basel). **(2022)**.

202. Zhang W., Zhong L., Wang J., Han J. *"Distinct MicroRNA Expression Signatures of Porcine Induced Pluripotent Stem Cells under Mouse and Human ESC Culture Conditions."* PLoS One. 2016; 11(7):e0158655.
203. Zhang X., Huang W., Guo Y., Miao X. *"Integrative Analysis of miRNAs Involved in Fat Deposition in Different Pig Breeds."* Genes (Basel). **(2022)**.
204. Zhong Y., Li L., Chen Z., Diao S., He Y., Zhang Z., Zhang H., Yuan X., Li J. *"MIR143 Inhibits Steroidogenesis and Induces Apoptosis Repressed by H3K27me3 in Granulosa Cells"* Front Cell Dev Biol. **(2020)**; 8:565261
205. Zhu X. H., Han L. X., Zhang R. J., Zhang P., Chen F. G., Yu J., Luo H., Han X. W. *"The functional activity of donor kidneys is negatively regulated by microribonucleic acid-451 in different perfusion methods to inhibit adenosine triphosphate metabolism and the proliferation of HK2 cells."* Bioengineered. **(2022)**; 13(5):12706-12717.
206. Zuo J., Wu F., Liu Y., Xiao J., Xu M., Yu Q., Xia M., He X., Zou S., Tan H., Feng D. *"MicroRNA Transcriptome Profile Analysis in Porcine Muscle and the Effect of miR-143 on the MYH7 Gene and Protein."* PLoS One. **(2015)**; 10(4):e0124873

7.1. Internet sources

1. NCBI GEO – https://www.ncbi.nlm.nih.gov/geo
2. NCBI SRA – https://www.ncbi.nlm.nih.gov/sra
3. Ensembl – https://www.ensembl.org/biomart/martview
4. miRDB – https://mirdb.org/
5. WGCNA Documentation – https://horvath.genetics.ucla.edu/html/CoexpressionNetwork/Rpackages/WGCNA/